

Analysis of pesticides by using GC-EI-MS and GC-DBDI-MS

PhD in Chemistry

Department of Chemistry | School of Chemistry, Food, and Pharmacy

Mona Nawaf Alshammari

October 2024

Abstract

Organic pesticides are chemical compounds used to control pests and diseases that affect plants. Pesticides are hydrocarbon based and usually contain complex combinations of functional groups, heteroatoms and structural types. The organochlorine pesticides feature at least one, but normally many more C-Cl bonds. These pesticides are known to be stable, many incorporating multiple rings some of which are substituted benzene rings; one notorious example is DDT. Organochlorine pesticides have a significant half-life in the environment, which leads to accumulation in agricultural crops. The organophosphate pesticide class contains the phosphate functional group normally as a phosphate ester. This functional group makes them effective inhibitors of the acetylcholine esterase (AChE) enzyme class found in insects. As this enzyme class is critical to human health, organophosphates are known to have toxic effects in humans and animals. The presence of nitrogen in the composition of pesticides gives rise to the organonitrogen pesticide class usually typified by the presence of a carbamate functional group. This class is known to target and disrupt the nerve system of insects and other pests. The Pyrethroids are synthetic insecticides that are of a more traditional hydrocarbon formula, they are a class adapted from natural pyrethroids that cause hyperexcitability in the nerve cells of insects through binding to sodium channels. In the end, as with most 'treatments' combination therapy achieved through the use of multiple pesticides with different biological and physical properties leads to effective control but also serious questions around residual contamination of products entering the human food chain.

Concerns around toxic compounds entering the food chain brings regulation and chemical analysis to the fore. Thus, gas chromatography (GC) with Mass spectrometry (MS) has been found to be particularly suitable for pesticide analysis, especially with modern high-precision instruments. In addition, the flexibility shown by Mass spectrometry (MS) when using different ionisation methods allows for better coverage of a class of molecules that have distinctly different properties. Furthermore, the mass spectrometer can be coupled with gas chromatography allowing the sample components to be separated prior to MS analysis. In light of this, the development of mass spectrometry techniques for analysing a wide range of pesticides is important and will provide a more selective and more accurate methods of detection.

In this work, the effectiveness of the mass spectrometry methodology in pesticide analysis using different devices such as GC-FID, GC-EI-ITQMS, GC-SICRIT-LTQMS, and GC-EI-MSD was evaluated. The emphasis of the study is on the effectiveness of a soft ionization source, recently commercialized (SICRIT) when compared to established electron ionization (EI) methods. The study compares and contrasts the use of SICRIT vs EI across a number of GC-MS setups for the detection and analysis of the organochlorine, organonitrogen, organophosphate and pyrethroid classes.

Declaration

I confirm that this is my own work and the use of all material from other sources has been properly and fully acknowledged.

Signed: Mona Alshammari

Date: 17/10/2024

Acknowledgements

First and foremost, I praise Allah the Most Gracious, the Most Merciful, the Possessor of Great Bounty for His immense blessing, through which I was able to complete this thesis.

I would like to express my deepest appreciation to Dr John McKendrick who supervised my PhD project. I deeply appreciate his guidance and kind cooperation he offered throughout studies. I am very grateful for his support which has been instrumental in achieving this success, and he also gave me constructive advice to complete my thesis. I would also like to thank Mr Nick Michael for training me in the use of instruments and appreciate his assistance in resolving technical issues and troubleshooting of instrumentation during my studies. I am also grateful to Vincent for training me on installing and using SICRIT with GC and LTQMS.

I want to extend my thanks to everyone who offered me support, advice or information that had a great impact on my academic journey. I also want to express my gratitude to my friends in the Chemistry department, especially those who played a significant role in strengthening me and providing me with positive energy.

I am extremely grateful to university of Hail for giving me the opportunity to study for a PhD at the university of Reading.

Words cannot express my gratitude to the Saudi government for providing funding this project. Their support has made my academic journey possible and successful.

I would like to express my deepest gratitude to my beloved husband, Meshari for his emotional and moral support throughout this journey. I sincerely appreciate all the love and dedicated support you have provided me. I am truly grateful to have him by my side.

I dedicate this achievement to my parents, who always wish to see me successful. I also dedicate this success to my children, Sadeem, Shudayyid, and Faisal, who are a huge part of my happiness, optimism and continuous pursuit of my goals.

Table of contents

TABLE OF CONTENTS	V
LIST OF FIGURES	X
LIST OF TABLES	XV
1. INTRODUCTION AND BACKGROUND	1
1.1 HEALTHY FOOD FOR CHILDREN: CHALLENGES AND OPTIONS IN THE ERA OF PESTICIDES.	1
1.2 PESTICIDES	3
1.2.1 <i>Definition of Pesticides</i>	3
1.2.2 <i>Classification of pesticides depending on the chemical composition.</i>	3
1.2.3 <i>Classification of pesticides used in the study.</i>	4
1.2.3.1 Organophosphate Pesticides	4
1.2.3.2 Organochlorine Pesticides	6
1.2.3.3 Organonitrogen Pesticides.....	9
1.2.3.4 Pyrethroids	12
1.2.4 <i>Negative Effects of Pesticides</i>	15
1.2.5 <i>Legislation related to baby food quality.</i>	16
1.3 ANALYTICAL METHODOLOGY	17
1.3.1 <i>Sample preparation</i>	18
1.3.2 <i>Separation and determination</i>	21
1.3.2.1 Gas Chromatography (GC)	21
1.3.3 <i>Mass spectrometry (MS)</i>	27
1.3.3.1 Ion sources	30
1.3.3.1.1 Electron ionization (EI).....	32
1.3.3.1.2 Dielectric barrier discharge ionization (DBDI).....	35
1.3.3.2 Mass Analyzers	51
1.3.3.2.1 The Ion Trap Quadrupole (ITQ) MS.....	51
1.3.3.2.2 Quadrupole Mass Analyzer (QMS).....	52
1.3.3.2.3 Orbitrap Mass Analyzer	55
1.3.3.3 Detector.....	58
1.3.3.4 Computer system.....	59
1.3.4 <i>Method validation</i>	59
1.3.4.1 Range and linearity.....	59
1.3.4.2 Limit of detection (LOD)	60
1.3.4.3 Limit of quantification (LOQ)	61
1.3.4.4 Precision	62
1.3.4.5 Accuracy	63
1.3.4.6 Selectivity	64
1.3.4.7 Matrix effects.....	64
2. MATERIAL AND METHODS	66
2.1 CHEMICALS & SAMPLES	66
2.1.1 <i>Standard solution preparation</i>	66
2.1.2 <i>Baby food samples</i>	66
2.1.3 <i>General Equipment</i>	66
2.2 PREPARATION OF SAMPLES.....	67

2.2.1 QuEChERS Extraction.....	67
2.2.2 Clean-up Procedures	67
2.3. IMPROVING CHROMATOGRAPHIC ANALYSIS METHODOLOGY: DEVELOPMENT OF EXPERIMENTAL CONDITIONS AND EVALUATION OF EFFICIENCY.....	71
2.4 EQUIPMENT.....	74
2.4.1 GC-SICRIT-MS Instrumentation & Setup	74
2.4.2 GC-FID Instrumentation.....	76
2.4.3 GC-ITQMS Instrumentation & Setup.....	77
2.4.4 GC/MSD Instrumentation	78
2.5 METHOD VALIDATION FOR BABY FOOD.....	80
2.5.1 Linearity.....	81
2.5.2. Limit of detection and quantification	81
2.5.3 Precision	82
2.5.4 Accuracy	82
2.5.5 Matrix Effect.....	82
3. QUANTITATIVE ANALYSIS OF ORGANOPHOSPHORUS PESTICIDE RESIDUES IN BABY FOOD BY GAS CHROMATOGRAPHY WITH DIELECTRIC BARRIER DISCHARGE IONIZATION-MASS SPECTROMETRY (GC-DBDI-MS).....	84
3.1 INTRODUCTION	84
3.2 CHROMATOGRAPHIC SEPARATION IN GC-FID, GC-EI-ITQMS, GC-EI-MSD AND GC-SICRIT-LTQMS.....	85
3.3 IONISATION MECHANISM AND MASS SPECTROMETRY RESULTS	92
3.4 FRAGMENTED PESTICIDES	103
3.5 METHOD VALIDATION	105
3.5.1 Linearity.....	106
3.5.2 LOD and LOQ	106
3.5.3 Matrix Effect evaluation of multiple organophosphorus pesticide residues in selected baby food matrices (milk, rice and cereal)	117
3.5.3.1 Matrix effect of organophosphorus pesticides on baby food samples based on GC-MSD	119
3.5.3.2 Matrix effect of organophosphorus pesticides on baby food samples based on GC-SICRIT-LTQMS	121
3.5.3.3 Matrix effect of organophosphorus pesticides on baby food samples based on GC-ITQMS	123
3.5.4 Comparison of matrix effect of organophosphorus pesticides on baby food samples	124
4. QUANTITATIVE ANALYSIS OF ORGANONITROGEN PESTICIDE RESIDUES IN BABY FOOD BY GAS CHROMATOGRAPHY WITH DIELECTRIC BARRIER DISCHARGE IONIZATION-MASS SPECTROMETRY (GC-DBDI-MS).....	131
4.1 INTRODUCTION	131
4.2 CHROMATOGRAPHIC SEPARATION IN GC-FID, GC-EI-ITQMS, GC-EI-MSD AND GC-SICRIT-LTQMS.....	132
4.2.1 Gas Chromatography-Flame Ionisation Detection (GC-FID).....	134
4.2.2 Gas Chromatography-Electron Ionisation Ion Trap Quadrupole Mass Spectrometry (GC-EI-ITQMS).....	135
4.2.3. Gas Chromatography-Soft Ionisation by Chemical Reaction in Transfer and Linear Trap Quadrupole Mass Spectrometry (GC-SICRIT-LTQMS)	136
4.2.4 Gas Chromatography-Electron Ionisation Mass Selective Detection (GC-EI-MSD).....	137
4.3 IONISATION MECHANISM AND MASS SPECTROMETRY RESULTS	138
4.4 FRAGMENTED PESTICIDES	143
4.5 METHOD VALIDATION	146
4.5.1 Linearity.....	147
4.5.2 LOD and LOQ	147
4.5.3 Matrix Effect evaluation of multiple organonitrogen pesticide residues in selected baby food matrices (milk, rice and cereal)	159
4.5.3.1 Matrix effect of organonitrogen pesticides on baby food samples based on GC-MSD.....	162

4.5.3.2 Matrix effect of organonitrogen pesticides on baby food samples based on GC-SICRIT-LTQMS	163
4.5.3.3 Matrix effect of organonitrogen pesticides on baby food samples based on GC-ITQMS.....	164
4.5.4 Comparison of matrix effect of organonitrogen pesticides on baby food samples	165
5. DEVELOPMENT OF GC METHOD FOR SEPARATION AND DETERMINATION OF SELECTED PYRETHROID PESTICIDES	169
5.1 INTRODUCTION	169
5.2 STRUCTURAL CLASSIFICATION AND SEPARATION OF PYRETHROIDS.....	169
5.3 CHROMATOGRAPHIC SEPARATION	173
5.4 LINEARITY, LOD AND LOQ FOR GC-EI-MS	178
5.5 LINEARITY, LOD AND LOQ FOR GC-SICRIT-MS	180
5.6 IONISATION AND FRAGMENTATION BEHAVIOR OF PYRETHROIDS EI AND SICRIT	185
5.7 MATRIX EFFECT EVALUATION OF MULTIPLE PYRETHROIDS PESTICIDE RESIDUES IN SELECTED BABY FOOD MATRICES (MILK, RICE AND CEREAL).....	189
5.8 COMPARISON OF COMPOUNDS PREFERRED FOR ANALYSIS USING EI OR SICRIT	191
6. DETERMINATION OF ORGANOCHLORIN PESTICIDE RESIDUES IN BABY FOOD AND INFANT FORMULA USING GC-MSD	192
6.1 INTRODUCTION	192
6.2 CHROMATOGRAPHIC SEPARATION IN GC-FID, GC-EI-ITQMS, GC-EI-MSD AND GC-SICRIT-LTQMS.....	194
6.3 MASS SPECTROMETRY RESULTS.	200
6.4 METHOD VALIDATION	206
6.4.1 Linearity for GC-EI-ITQMS, GC-EI-MSD and GC-SICRIT-LTQMS.....	206
6.4.2 LOD and LOQ determination for GC-EI-ITQMS, GC-EI-MSD and GC-SICRIT-LTQMS	214
6.5 MATRIX EFFECT BY GC-EI-MSD	216
6.6 METHOD PRECISION AND ACCURACY BY GC-EI-MSD.....	221
7. CONCLUSION AND FUTURE DIRECTIONS	230
8. APPENDIX	233
8.1 STUDIED PESTICIDES.	233
8.2: EXAMPLES OF TOTAL ION CHROMATOGRAM (TIC) OF A SAMPLE BLANK OBTAINED FROM QUECHERS EXTRACTION METHOD AND D-SPE AS CLEAN-UP METHOD	236
8.3 ANALYSIS OF ORGANOCHLORINE PESTICIDES IN NEGATIVE MODE USING GSICRIT-LTQMS	237
8.4 SELECTING THE APPROPRIATE COLUMN FOR PESTICIDE ANALYSIS BY GC-FID, GC-EI-ITQMS, AND GC-SICRIT-LTQMS	238
8.5 CHOOSING THE APPROPRIATE QUECHERS EXTRACTION METHOD	241
8.6 USE DRY N ₂ WHEN ANALYSIS OF PESTICIDES USING GC-SICRIT-LTQMS	242
9. REFERENCES	246

Abbreviations

Abbreviation	Definition
OCPs (OCs)	Organochlorine pesticides
ONPs (ONs)	Organonitrogen pesticides
OPPs (OPs)	Organophosphorus pesticides
SPPs (SPs)	synthetic Pyrethroid pesticides
POPs	persistent organic pollutants
GC-MS	Gas chromatography–mass spectrometry
GC-ITQMS	Gas Chromatography -Ion Trap Quadrupole Mass Spectrometry
GC-FID	Gas Chromatography-Flame Ionization Detection
GC-LTQMS	Gas Chromatography-Linear ion Trap Quadrupole Mass Spectrometry
GCMSD	Gas Chromatography -single Quadrupole Mass Spectrometry
QToF	Quadrupole time-of-flight
EM	electron multipliers
FC	Faraday cups
HPLC	High performance liquid chromatography
GLPC	gas-liquid partition chromatography
SQ	single quadrupole
TQ	triple quadrupole
ECD	Electron Capture Detector
VPC	Vapor-phase chromatography
NPD	Nitrogen-Phosphorus Detection
EI	Electron Ionisation
SICRIT	Soft Ionization by Chemical Reaction in Transfer
CI	chemical ionization
ESI	electrospray ionization
API	atmospheric pressure ionization
APCI	atmospheric pressure chemical ionization
APLI	atmospheric pressure laser ionization
APPI	atmospheric pressure plasma ionization
DBDI	Dielectric barrier discharge ionization
DBD	Dielectric barrier discharge
DC	Direct current
QuEChERS	quick, easy, cheap, effective, rugged, and safe
d-SPE	A dispersive solid-phase extraction

PSA	primary secondary amine
C18-EC	end-capped
LLE	liquid-liquid extraction
SPE	solid phase extraction
SPME	solid phase micro-extraction
DLLME	dispersive liquid-liquid micro-extraction
SDME	single drop micro-extraction
HF-LPME	hollow fiber-liquid phase micro-extraction
CFME	continuous flow micro-extraction
LOD	Limit of detection
LOQ	limit of quantification
ME	Matrix effect
RSD	Relative standard deviation
CV	coefficient of variation
S/N	Signal/Noise
DDT	Dichlorodiphenyltrichloroethane
DDE	Dichlorodiphenyldichloroethylene
DDD	Dichlorodiphenyldichloroethane
HCH	Hexachlorocyclohexane
EDCs	Endocrine disrupting chemicals
PCBs	Polychlorinated biphenyls
PAHs	polycyclic aromatic hydrocarbons
Bn	Billion
GDP	Gross Domestic Product
WWII	World War II
PD	Parkinson's disease
FFDCA	Federal Food, Drug, and Cosmetic Act
FSMA	Food Safety Modernization Act
EU	European Union
SFCA	Safe Food for Canadians Act
FDA	Food and Drugs Act
CFIA	Food Inspection Agency
USEPA	The U.S. Environmental Protection Agency
EWG	Environment Working Group

List of Figures

FIGURE 1.1: BABY FOOD MARKET SIZE 2023-2032.	2
FIGURE 1.2: CLASSIFICATION OF PESTICIDES(INSECTICIDES)DEPENDING ON THE CHEMICAL COMPOSITION.	4
FIGURE 1.3: CLASSIFICATION OF SOME ORGANOPHOSPHATE PESTICIDE BASED ON THEIR STRUCTURE. ..	6
FIGURE 1.4: STRUCTURE OF SOME ORGANOCHLORINES	7
FIGURE 1.5: STRUCTURE OF SOME ORGANONITROGEN.	11
FIGURE 1.6: TYPICAL STRUCTURE OF PYRETHROIDS CLASSIFIED BY TYPES I AND II.	12
FIGURE 1.7: CHEMICAL STRUCTURE OF TYPE I OF PYRETHROID	14
FIGURE 1.8: CHEMICAL STRUCTURE OF TYPE II OF PYRETHROID.	14
FIGURE 1.9: A TYPICAL ANALYTICAL WORKFLOW USED FOR ANALYZING PESTICIDES.	17
FIGURE 1.10: SCHEMATIC REPRESENTATION OF QUECHERS-DSPE STEPS.	20
FIGURE 1.11: SCHEMATIC ILLUSTRATION OF THE BASIC COMPONENTS OF A MASS SPECTROMETER.	30
FIGURE 1.12: SCHEMATIC DIAGRAMS SHOWING THE IONIZATION PROCESS IN ELECTRON IONIZATION.	33
FIGURE 1.13: FLOWCHART DETAILING THE STEP-BY-STEP DBDI ION FORMATION MECHANISM FROM PLASMA GENERATION TO ANALYTE IONIZATION.	44
FIGURE 1.14: FLOWCHART ILLUSTRATING THE SICRIT ION FORMATION MECHANISM, EMPHASIZING THE CONTROLLED IN TRANSFER CHEMICAL REACTIONS THAT ACHIEVE SOFT IONIZATION.	45
FIGURE.1.15: (A) ACTIVE CAPILLARY IONIZATION DBDI,(B) AP-DBD, (C) DBDI.	50
FIGURE 1.16: SCHEMATIC OF A TRAP QUADRUPOLE	52
FIGURE 1.17: QUADRUPOLE MASS ANALYZER SCHEMATIC.	53
FIGURE 1.18: ORBITRAP MASS ANALYZER SCHEMATIC.	55
FIGURE 1.19: SCHEMATIC OF LIT-ORBITRAP	58
FIGURE 2.1: QUECHERS SAMPLE PREPARATION PROCEDURES	70
FIGURE 2.2. GC–MS-TIC SEPARATION CHROMATOGRAM OF ORGANOPHOSPHORUS PESTICIDES (16 COMPOUND), METHOD 1.	73
FIGURE 2.3. GC–MS-TIC SEPARATION CHROMATOGRAM OF ORGANOPHOSPHORUS PESTICIDES (16 COMPOUND), METHOD 2.	73
FIGURE 2.4: DIAGRAM OF THE APPARATUS UTILISED IN THIS INVESTIGATION. LIGHT BLUE ARROWS REPRESENT PASSIVE GAS FLOW, AND DARK BLUE ARROWS REPRESENT ACTIVELY CREATED GAS FLOWS	75

FIGURE 3.1: GC-FID CHROMATOGRAM OF A MIXTURE OF 16 ORGANOPHOSPHORUS PESTICIDES (COMPOUNDS IDENTITY IN TABLE 3.1) AT 10PPM.....	87
FIGURE 3.2: STRUCTURES OF PIRIMIPHOS-METHYL AND FENITROTHION.	88
FIGURE 3.3: GC-EI-ITQ TIC-MS OF A MIXTURE OF 16 ORGANOPHOSPHORUS PESTICIDES (COMPOUNDS IDINTITY IN TABLE 3.1) AT 10PPM.	88
FIGURE 3.4: GC-EI-SQ TIC-MS OF A MIXTURE OF 16 ORGANOPHOSPHORUS PESTICIDES (COMPOUNDS IDINTITY IN TABLE 3.1) AT 10PPM.	90
FIGURE 3.5: GC-SICRIT-LTQ TIC-MS OF A MIXTURE OF 16 ORGANOPHOSPHORUS PESTICIDES (COMPOUNDS IDINTITY IN TABLE 3.1) AT 10PPM.....	91
FIGURE 3.6: EI-MS AND OF SICRIT-MS SPECTRA (POSITIVE IONIZATION MODE) OF DIZAINON (M/Z304.101 (SEE TABLE 3.2) AT 10PPM, ANALYZED BY GC-SICRIT- LTQ ORBITRAP MASS SPECTROMETER AND GC-EI-ITQMS.	99
FIGURE 3.7: EI-MS AND OF SICRIT-MS SPECTRA (POSITIVE IONIZATION MODE) OF ISAZOPHOS (M/Z 313.0416) (SEE TABLE 3.2) AT 10PPM, ANALYZED BY GC-SICRIT- LTQ ORBITRAP MASS SPECTROMETER AND GC-EI-ITQMS.	101
FIGURE 3.8: EI-MS AND OF SICRIT-MS SPECTRA (POSITIVE IONIZATION MODE) OF FENITRTHION (M/Z 277.0173) (SEE TABLE 3.2) AT 10PPM, ANALYZED BY GC-SICRIT- LTQ ORBITRAP MASS SPECTROMETER AND GC-EI-ITQMS.	102
FIGURE 3.9 STRUCTURE OF THE FRAGMENTED PESTICIDES IN GC-SICRIT-LTQMS.....	103
FIGURE 3.10: EI-MS AND OF SICRIT-MS SPECTRA (POSITIVE IONIZATION MODE) OF (A)PHOAMET (B)PHOSALONE (C)AZINPHOS-METHYL (D)AZINPHOS-ETHYL (SEE TABLE 3.2) AT 10PPM, ANALYZED BY GC-SICRIT- LTQ ORBITRAP MASS SPECTROMETER AND GC-EI-ITQMS.	104
FIGURE 3.11: LOD AND LOQ OF ORGANOPHOSPHORUS PESTICIDES IN GC-ITQMS, GC-MSD AND GC-SICRIT-LTQMS	116
FIGURE 3.12: ME% OF ORGANOPHOSPHORUS PESTICIDES IN GC-MSD.....	121
FIGURE 3.13: ME% OF ORGANOPHOSPHORUS PESTICIDES IN GC-SICRIT-LTQMS.	122
FIGURE 3.14: ME% OF ORGANOPHOSPHORUS PESTICIDES IN GC-EI-ITQMS.....	123
FIGURE 3.15:CHROMATOGRAM (A) MILK BLANK,(B) CEREAL BLANK,(C)RICE BLANK, AND (D) STANDARD ORGANOPHOSPHORUS PESTICIDES, WHICH ARE DESCRIBED IN TABLE 4.2 BY USING GC-LTQMS	125
FIGURE 3.16:ME% OF ORGANOPHOSPHORUS PESTICIDES IN GC-SICRIT-LTQMS, AND GC-EI-ITQMS.....	130
FIGURE 4.1: GC-FID CHROMATOGRAM OF A MIXTURE OF 29 ORGANONITROGEN PESTICIDES (COMPOUNDS IDENTITY IN TABLE 4.1) AT 10PPM.....	134
FIGURE 4.2: GC-EI-ITQ TIC-MS OF A MIXTURE OF 29 ORGANONITROGEN PESTICIDES (COMPOUNDS IDENTITY IN TABLE 4.1) AT 10PPM.	135
FIGURE 4.3: GC-SICRIT-LTQ TIC-MS OF A MIXTURE OF 29 ORGANONITROGEN PESTICIDES (COMPOUNDS IDENTITY IN TABLE 4.1) AT 10PPM.	136

FIGURE 4.4: GC-EI-SQ TIC-MS OF A MIXTURE OF 29 ORGANONITROGEN PESTICIDES (COMPOUNDS IDENTITY IN TABLE 4.1) AT 10PPM.	137
FIGURE 4.5: CHEMICAL STRUCTURE OF DIMETHACHLOR, PROPANIL, METHOXYCHLOR, AND FENPROPATHRIN.	138
FIGURE 4.6: EI-MS AND SICRIT-MS SPECTRA (POSITIVE IONIZATION MODE) OF ALLIDOCHLOR (M/Z 2173.06) (SEE TABLE 4.2) AT 10PPM, ANALYZED BY GC-SICRIT- LTQ ORBITRAP MASS SPECTROMETER AND GC-EI-ITQMS.	141
FIGURE 4.7: EI-MS AND SICRIT-MS SPECTRA (POSITIVE IONIZATION MODE) OF CYCLOATE (M/Z 215.13) (SEE TABLE 4.2) AT 10PPM, ANALYZED BY GC-SICRIT- LTQ ORBITRAP MASS SPECTROMETER AND GC-EI-ITQMS.	142
FIGURE 4.8: EI-MS AND SICRIT-MS SPECTRA (POSITIVE IONIZATION MODE) OF ACETOCHLOR (M/Z 269.1182) (SEE TABLE 4.2) AT 10PPM, ANALYZED BY GC-SICRIT- LTQ ORBITRAP MASS SPECTROMETER AND GC-EI-ITQMS.	143
FIGURE 4.9: EI-MS AND SICRIT-MS SPECTRA (POSITIVE IONIZATION MODE) OFALACHLOR (M/Z 269.1182) (SEE TABLE 4.2) AT 10PPM, ANALYZED BY GC-SICRIT- LTQ ORBITRAP MASS SPECTROMETER AND GC-EI-ITQMS.	145
FIGURE 4.10: LOD AND LOQ OF ORGANOPHOSPHORUS PESTICIDES IN GC-ITQMS, GC-MSD, AND GC-SICRIT-LTQMS.	158
FIGURE 4.11: ME% OF ORGANONITROGEN PESTICIDES IN GCMSD.	162
FIGURE 4.12: ME% OF ORGANONITROGEN PESTICIDES IN GC-SICRIT-LTQMS.....	163
FIGURE 4.13:ME% OF ORGANONITROGEN PESTICIDES IN GC-EI-ITQMS.....	164
FIGURE 4.14:CHROMATOGRAM (A) MILK BLANK,(B) CEREAL BLANK,(C)RICE BLANK, AND (D) STANDARD ORGANONITROGEN PESTICIDES, WHICH ARE DESCRIBED IN TABLE 4.2 BY USING GC-LTQMS.....	165
FIGURE 4.15:ME% OF ORGANONITROGEN PESTICIDES IN GC-MSD, GC-ITQMS, AND GC-SICRIT-LTQMS.168	
FIGURE 5.1: GC-FID CHROMATOGRAM OF PYRETHROID PESTICIDES AT 10 μ G/ML. GC-FID CHROMATOGRAM OF A MIXTURE OF 18 PARENT PYRETHROID PESTICIDES WITH THEIR ISOMERS (COMPOUNDS IDENTITY IN TABLE 5.2) AT 10PPM.....	173
FIGURE 5.2: GC-EI-ITQ TIC-MS CHROMATOGRAM OF A MIXTURE OF 18 PARENT PYRETHROID PESTICIDES WITH THEIR ISOMERS (COMPOUNDS IDENTITY IN TABLE 5.2) AT 10PPM.	174
FIGURE 5.3: CHEMICAL STRUCTURE OF DIFFERENT PYRETHROID PESTICIDES (A) TETRAMETHRIN (B)BIFENTHRIN (C)CYPERMETHRIN (D) FLUCYTHRINATE TAU-FLUVALINATE (F) FENVALERATE.	175
FIGURE 5.4: GC-ITQMS CHROMATOGRAM OF PYRETHROID COMPOUNDS AND THEIR ISOMERS	176
FIGURE 5.5: GC-SICRIT-MS CHROMATOGRAM OF A MIXTURE OF PARENT PYRETHROID PESTICIDES WITH THEIR ISOMERS (COMPOUNDS IDENTITY IN TABLE 5.2) AT 10PPM.....	177
FIGURE 5.6: DIFFERENCE IN PYRETHROID CHROMATOGRAPHY BETWEEN GC-EI-MS AND GC-SICRIT-MS	178

FIGURE 5.7: EI-MS AND SICRIT-MS SPECTRA (POSITIVE IONIZATION MODE) ANTHRAQUINONE (M/Z 208.22) (SEE TABLE 5.5) AT 10PPM, ANALYZED BY GC-SICRIT- LTQ ORBITRAP MASS SPECTROMETER AND GC-EI-ITQMS	187
FIGURE 5.8: EXAMPLES OF IONIZATION OF SOME PYRETHROID PESTICIDES USING GC-SICRIT-MS. WHERE: (A) TEFLUTHRIN, (B)TRANSFLUTHRIN, (C) BIOALLETHRIN, AND (D) PHENOTHRIN (SEE TABLE 5.5) AT 10PPM, ANALYZED BY GC-SICRIT- LTQ ORBITRAP MASS SPECTROMETER.	188
FIGURE 5.9: SUMMARY OF SENSITIVITY FOR GC-EI-MS AND GC-SICRIT-MS.....	191
FIGURE 6.1: STRUCTURES OF (A)ENDRIN AND (B)ENDOSULFAN II	195
FIGURE 6.2: GC-FID CHROMATOGRAM OF A MIXTURE OF 40 ORGANOCHLORIN PESTICIDES (COMPOUNDS IDENTITY IN TABLE 6.1) AT 10PPM.....	196
FIGURE 6.3: GC-EI-ITQ TIC-MS CHROMATOGRAM OF A MIXTURE OF 40 ORGANOCHLORIN PESTICIDES (COMPOUNDS IDENTITY IN TABLE 6.1) AT 10PPM.....	197
FIGURE 6.4: GC-EI-MSD CHROMATOGRAM OF A MIXTURE OF 40 ORGANOCHLORIN PESTICIDES (COMPOUNDS IDENTITY IN TABLE 6.1) AT 10PPM.....	198
FIGURE 6.5: CHEMICAL STRUCTURE OF DIFFERENT ORGANOCHLORINE PESTICIDE (A) LINDANE, (B) CHLORDANE, (C) PENTACHLOROBENZENE AND (D) MIREX.	199
FIGURE 6.6: GC-SICRIT-LTQMS CHROMATOGRAM OF ORGANOCHLORIN PESTICIDES (COMPOUNDS IDENTITY IN TABLE 6.1) AT 10PPM.....	200
FIGURE 6.7: EI-MS AND SICRIT-MS SPECTRA (POSITIVE IONIZATION MODE) OF CHLORONEB (M/Z 205.9901) (SEE TABLE 6.2) AT 10PPM, ANALYZED BY GC-SICRIT- LTQ ORBITRAP MASS SPECTROMETER AND GC-EI-ITQMS.	203
FIGURE 6.8: EI-MS AND SICRIT-MS SPECTRA (POSITIVE IONIZATION MODE) OF DICHLOROBENZOPHENONE, 4,4'- (M/Z 249.995) (SEE TABLE 6.2) AT 10PPM, ANALYZED BY GC-SICRIT- LTQ ORBITRAP MASS SPECTROMETER AND GC-EI-ITQMS.	204
FIGURE 6.9: SICRIT-MS SPECTRA (POSITIVE IONIZATION MODE) OF DICHLOROBENZOPHENONE, 4,4'-(M/Z 249.995) AT 10PPM, ANALYZED BY GC-SICRIT- LTQ ORBITRAP MASS SPECTROMETER.....	204
FIGURE 6.10: IONISATION MECHANISM FOR TETRADIFON EI-MS AND SICRIT-MS SPECTRA (POSITIVE IONIZATION MODE) OF TETRADIFON (M/Z 355.8813) (SEE TABLE 6.2) AT 10PPM, ANALYZED BY GC-SICRIT- LTQ ORBITRAP MASS SPECTROMETER AND GC-EI-ITQMS.	205
FIGURE 6.11: LINEARITY OF ORGANOCHLORINE PESTICIDES IN BABY FOOD SAMPLES WHEN DETECTED BY GC-EI-MS	209
FIGURE 6.12: LOD AND LOQ IN DETERMINATION OF ORGANOCHLORINE PESTICIDES DETECTED BY GC-EI-MSD,GC-EI-ITQMS AND GC-SICRIT-MS.....	215
FIGURE 6.13: MATRIC EFFECT OF ORGANOCHLORINE PESTICIDES IN BABY FOOD SAMPLES.	220
FIGURE 6.14: RECOVERY PERCENTAGE OF ORGANOCHLORINE PESTICIDES IN BABY MILK, RICE AND CEREAL.	227
FIGURE 6.15: RSD PERCENTAGE OF ORGANOCHLORINE PESTICIDES IN BABY MILK, RICE AND CEREAL .	236

FIGURE 8.1: EXAMPLE OF TOTAL ION CHROMATOGRAM (TIC) OF A CEREAL BLANK OBTAINED FROM QUECHERS EXTRACTION METHOD AND D-SPE AS CLEAN-UP METHOD	236
FIGURE 8.2: EXAMPLE OF TOTAL ION CHROMATOGRAM (TIC) OF A BABY RICE BLANK OBTAINED FROM QUECHERS EXTRACTION METHOD AND D-SPE AS CLEAN-UP METHOD	236
FIGURE 8.3: EXAMPLE OF TOTAL ION CHROMATOGRAM (TIC) OF A BABY MILK BLANK OBTAINED FROM QUECHERS EXTRACTION METHOD AND D-SPE AS CLEAN-UP METHOD	237
FIGURE 8.4: GC-SICRIT-LTQMS CHROMATOGRAM OF ORGANOCHLORIN PESTICIDES IN NEGATIVE MODE	237
FIGURE 8.5: GC CAPILLARY COLUMN	238
FIGURE 8.6: GC-EI-ITQMS CHROMATOGRAM OF ORGANOPHOSPHORUS PESTICIDES (A) THE STANDARD CHROMATOGRAM USING COLUMN RXI-5HT (B) THE STANDARD CHROMATOGRAM USING COLUMN RXI-5MS	239
FIGURE 8.7: GC-EI-ITQMS CHROMATOGRAM OF ORGANOCHLORINE PESTICIDES (A) THE STANDARD CHROMATOGRAM USING COLUMN RXI-5HT (B) THE STANDARD CHROMATOGRAM USING COLUMN RXI-5MS	239
FIGURE 8.8: GC-EI-ITQMS CHROMATOGRAM OF ORGANONITROGEN PESTICIDES (A) THE STANDARD CHROMATOGRAM USING COLUMN RXI-5HT (B) THE STANDARD CHROMATOGRAM USING COLUMN RXI-5MS	240
FIGURE 8.9: GC-EI-ITQMS CHROMATOGRAM OF PYRETHROID PESTICIDES (A) THE STANDARD CHROMATOGRAM USING COLUMN RXI-5HT (B) THE STANDARD CHROMATOGRAM USING COLUMN RXI-5MS	240
FIGURE 8.10: EXAMPLE OF TOTAL ION CHROMATOGRAM (TIC) OF BLANK BABY MILK (A) OBTAINED FROM AOAC2007 QUECHERS EXTRACTION METHOD (B) OBTAINED FROM ORIGINAL UNBUFFERED QUECHERS EXTRACTION METHOD	241
FIGURE 8.11: GAS CHROMATOGRAPHY OF ORGANONITROGEN PESTICIDES USING GC-SICRIT-LTQMS (A) USING DRY N ₂ (B) USING WET N ₂	242
FIGURE 8.12: PHOTOGRAPH OF SICRIT SETUP (A) USING DRY N ₂ (B) USING WET N ₂	243
FIGURE 8.13: PHOTOGRAPH OF SICRIT CONNECTED TO GC AND LTQMS.	243
FIGURE 8.14: GC-MS-TIC SEPARATION CHROMATOGRAM OF ORGANONITROGEN PESTICIDES (29COMPOUND), METHOD 1.	244
FIGURE 8.15 :GC-MS-TIC SEPARATION CHROMATOGRAM OF ORGANONITROGEN PESTICIDES (92COMPOUND), METHOD 2.	244
FIGURE 8.16: GC-MS-TIC SEPARATION CHROMATOGRAM OF PYRETHROID PESTICIDES (30 PARENT COMPOUNDS AND THEIR ISOMERS), METHOD 1.	245
FIGURE 8.17: GC-MS-TIC SEPARATION CHROMATOGRAM OF PYRETHROID PESTICIDES (30 PARENT COMPOUNDS AND THEIR ISOMERS), METHOD 2.	245

List of Tables

TABLE 1.1: COMPARISON BETWEEN DIFFERENT TECHNIQUES	19
TABLE 1.2: COMPARATIVE FEATURES OF DBDI AND SICRIT ION SOURCES AND THEIR UNDERLYING IONIZATION MECHANISMS	41
TABLE 1.3: SUMMARIZING THE KEY INSTRUMENT ARCHITECTURE DIFFERENCES BETWEEN DBDI AND SICRIT ION SOURCES	46
TABLE 1.4: SUMMARIZING THE DIFFERENCES BETWEEN ITQ AND SQ.....	54
TABLE 2.1: GAS CHROMATOGRAPHY-MASS SPECTROMETRY –(GCMS-TIC) PARAMETERS FOR PESTICIDES ANALYSIS METHODS.....	72
TABLE 2.2: CONDITIONS OF GC-ITQMS INSTRUMENT.....	77
TABLE 2.3: CONDITION OF GC-MSD INSTRUMENT.....	78
TABLE 3.1: COMPOUNDS OBTAINED THROUGH CHROMATOGRAPHY SEPARATION	86
TABLE 3.2: IONISATION MECHANISM AND MASS SPECTROMETRY RESULTS.	98
TABLE 3.3: LOD, LOQ, AND LINEARITY OF ORGANOPHOSPHORUS PESTICIDES IN GC-ITQMS, GC-MSD, AND GC-SICRIT-LTQMS.	107
TABLE 3.4: DESCRIPTIVE STATISTICS FOR LOD OF ITQMS, SQMS, AND LTQMS	108
TABLE 3.5: TEST OF HOMOGENEITY OF VARIANCES FOR LOD.	109
TABLE 3.6: ANOVA RESULTS FOR LOD ACROSS THREE DEVICES.	110
TABLE 3.7: RESULTS OF TUKEY HSD MULTIPLE COMPARISONS FOR LOD.	111
TABLE 3.8: DESCRIPTIVE STATISTICS FOR LOQ OF ITQMS, SQMS, AND LTQMS	112
TABLE 3.9: TEST OF HOMOGENEITY OF VARIANCES FOR LOQ.	113
TABLE 3.10: ANOVA RESULTS FOR LOQ ACROSS THREE DEVICES.....	113
TABLE 3.11: RESULTS OF TUKEY HSD MULTIPLE COMPARISONS FOR LOD.	114
TABLE 3.12: MATRIX EFFECT ON BABY FOOD SAMPLES BASED ON GC-MSD, GC-SICRIT-LTQMS, AND GC-ITQMS.	126
TABLE 4.1: COMPOUNDS OBTAINED THROUGH CHROMATOGRAPHY SEPARATION.	133
TABLE 4.2: IONISATION MECHANISM AND MASS SPECTROMETRY RESULTS.	139
TABLE 4.3: LOD, LOQ, AND LINEARITY OF ORGANONITROGEN PESTICIDES IN GC-ITQMS, GC-MSD, AND GC-SICRIT-LTQMS.	148
TABLE 4.4: DESCRIPTIVE STATISTICS FOR LOD OF ITQMS, SQMS, AND LTQMS	150
TABLE 4.5: TEST OF HOMOGENEITY OF VARIANCES FOR LOD.	151

TABLE 4.6: ANOVA RESULTS FOR LOD ACROSS THREE DEVICES.	151
TABLE 4.7: RESULTS OF TUKEY HSD MULTIPLE COMPARISONS FOR LOD.	152
TABLE 4.8: TUKEY HSDA RESULTS FOR LOD.	153
TABLE 4.9: DESCRIPTIVE STATISTICS FOR LOQ OF ITQMS, SQMS, AND LTQMS.	153
TABLE 4.10: TEST OF HOMOGENEITY OF VARIANCES FOR LOQ.	154
TABLE 4.11: ANOVA RESULTS FOR LOQ ACROSS THREE DEVICES.	155
TABLE 4.12: RESULTS OF TUKEY HSD MULTIPLE COMPARISONS FOR LOD.	155
TABLE 4.13: TUKEY HSD ^A RESULTS FOR LOQ.	156
TABLE 4.14: MATRIX EFFECT ON BABY FOOD SAMPLES BASED ON GC-MSD, GC-SICRIT-LTQMS AND GC-ITQMS.	160
TABLE 4.15: COMPARISON OF ORGANONITROGEN PESTICIDES IN GC-MSD, GC-ITQMS, AND GC-SICRIT-LTQMS.	167
TABLE 5.1: DESCRIPTION OF THE PYRETHROIDS STUDIED AND SUMMARY OF CHROMATOGRAPHY ACHIEVEMENT.	170
TABLE 5.2: SYNTHETIC PYRETHROID COMPOUNDS AND THEIR ISOMERS THAT APPEAR IN GC-EI-MS AND GC-FID.	172
TABLE 5.3: SYNTHETIC PYRETHROID WITH R ² , LOD AND LOQ VALUES USING GC-EI-MS.	179
TABLE 5.4: SYNTHETIC PYRETHROID WITH R ² , LOD AND LOQ VALUES USING GC-SICRIT-MS.	180
TABLE 5.5: DESCRIPTIVE STATISTICS FOR LOQ OF ITQMS AND LTQMS.	181
TABLE 5.6: TEST OF HOMOGENEITY OF VARIANCES FOR LOD.	181
TABLE 5.7: ANOVA RESULTS FOR LOD.	182
TABLE 5.8: DESCRIPTIVE STATISTICS FOR LOQ OF ITQMS, AND LTQMS.	183
TABLE 5.9: TEST OF HOMOGENEITY OF VARIANCES FOR LOQ.	184
TABLE 5.10: ANOVA RESULTS FOR LOQ.	184
TABLE 5.11: IONISATION MECHANISM AND MASS SPECTROMETRY RESULTS.	186
TABLE 5.12: MATRIX EFFECT ON BABY FOOD SAMPLES BASED ON GC-SICRIT-LTQMS AND GC-ITQMS. MATRIX.	189
TABLE 6.1: COMPOUNDS OBTAINED THROUGH CHROMATOGRAPHY SEPARATION IN GC-ITQMS, AND GC-MSD.	193
TABLE 6.2: LIST OF OCP COMPOUNDS ANALYZED, BY GC-EI-MS AND GC-SICRIT-MS.	201

TABLE 6.3: LIMIT OF DETECTION (LOD), LIMIT OF QUANTIFICATION (LOQ), AND LINEARITY (R2) OF ORGANOCHLORINE PESTICIDES IN BABY FOOD SAMPLES.	207
TABLE 6.4: DESCRIPTIVE STATISTICS FOR LOD OF ITQMS,SQMS,AND LTQMS	210
TABLE 6.5: TEST OF HOMOGENEITY OF VARIANCES FOR LOD.	210
TABLE 6.6: ANOVA RESULTS FOR LOD.	211
TABLE 6.7: DESCRIPTIVE STATISTICS FOR LOQ OF ITQMS,SQMS,AND LTQMS.	212
TABLE 6.8: TEST OF HOMOGENEITY OF VARIANCES FOR LOQ.	213
TABLE 6.9: ANOVA RESULTS FOR LOQ.	213
TABLE 6.10: MATRIX EFFECT OF ORGANOCHLORINE PESTICIDES IN BABY FOOD SAMPLES USING GC-MSD	218
TABLE 6.11: RECOVERY AND RELATIVE STANDARD DEVIATION OF ORGANOCHLORINE PESTICIDES IN BABY FOOD SAMPLES.	223
TABLE 8.1. GC MULTI-RESIDUE PESTICIDE KITS GC MULTIRESIDUE PESTICIDE STANDARDS KIT (RESTEK 32562-100 µG/ML EACH IN TOLUENE, 1 ML/AMPUL)	233

1. Introduction and background

1.1 Healthy Food for Children: Challenges and Options in the Era of Pesticides.

Infants are the age group that ranges from birth to two years. At this stage, the child still depends on breastfeeding or formula as the main source of nutrition, and then begins to eat solid foods from approximately six months. Infant foods include a variety of products that are specifically designed to meet their needs. Examples of these foods are: breast milk, formula milk, soft grains, cereal, mashed fruits, mashed vegetables, and others. These foods contain a nutritious formula that meets the developing needs of infants, including proteins, fats, carbohydrates, vitamins, and minerals necessary for their proper growth and development.¹ Recent research emphasizing the growing need for baby food has led to a steady increase in their manufacturing. Nonetheless, worries about these foods being possibly contaminated with chemicals persist.² There are many baby foods made from cereal, meats, fruit and vegetables.³ These foods may be contaminated with pesticides that are frequently used to control plant pests, in addition to mycotoxins that results from fungal growth either naturally during the growing season or after harvest when the crop is stored⁴. therefore, exposure to pesticides may be seen as inevitable due to food consumption.⁴ Although the Directive 2006/141/EC aims to ensure infant and follow-on formulas are virtually free from pesticide residues, minimizing exposure for vulnerable infants. Key provisions include strict Maximum Residue Limits (MRLs), prohibited pesticides, cumulative risk assessment, monitoring and enforcement, and EFSA reviews. The policy is stricter than general food safety standards, with exceptions for certain pesticides. Prohibited pesticides are completely banned in infant food production, and even traces of acutely toxic pesticides are not permitted. Manufacturers must conduct regular pesticide residue testing on raw materials and finished products, and records must be kept for regulatory inspections. The Directive has been replaced by EU Regulation 2016/127 since 2020, maintaining the same strict pesticide rules.

The term pesticide refers to a wide and diverse group of chemical compounds such as insecticides, fungicides and herbicides, since they are routinely used when crops are grown it is possible that they may then be found in the foods produced from the crops, this may then lead to potential health hazards from ingestion.⁵ Many studies and evidence

indicate that pesticides are related to many health conditions, including cancer and dysfunctions of the endocrine and reproductive systems in addition to neurodegenerative diseases because many pesticides act on the nervous system.^{5,6}

To reduce the risk of pesticides in infant foods, parents should choose organic, approved foods that are carefully monitored to ensure that children are not exposed to harmful chemicals. Because proper nutrition of children is one of the most important factors that contribute to their healthy growth and physical and mental development.

Based on data announced by Global Market Insights, the baby food market is expected to grow significantly by 5.4% in the period from 2023 to 2032, while the baby Food Market size in 2022 was USD 88 billion as shown in figure 1.1. Data indicate an increase in demand for healthy and nutritional baby products is due to an increased awareness of the importance of proper nutrition for a child's development and health.⁷

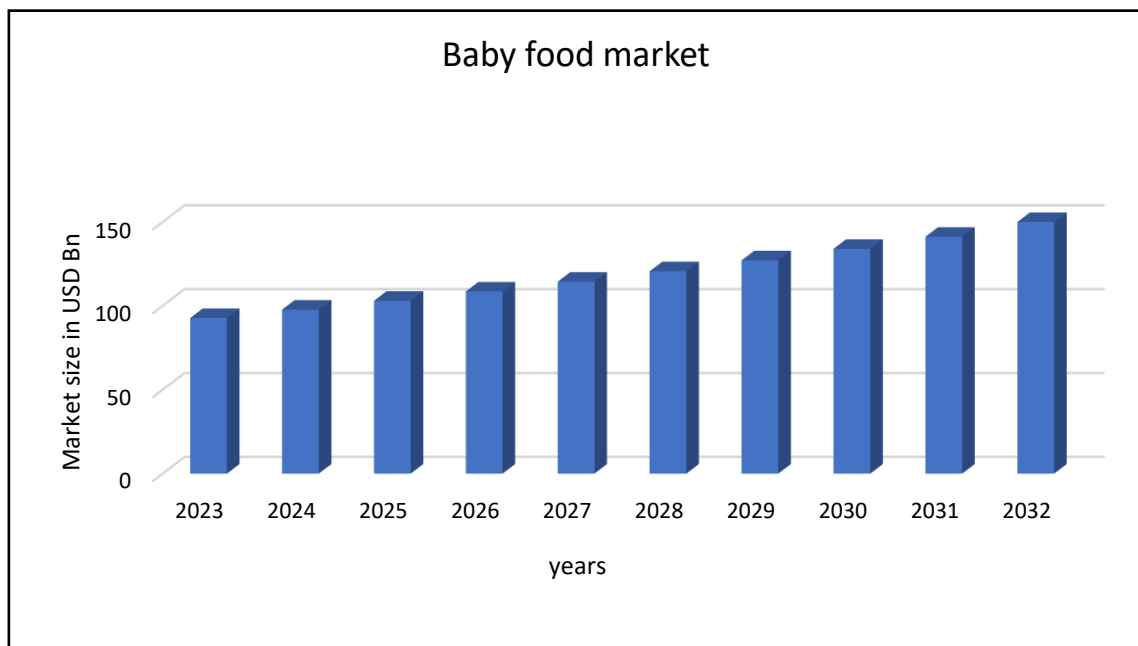


Figure 1.1: Baby food market size 2023-2032.⁷

1.2 Pesticides

1.2.1 Definition of Pesticides

Pesticides are a very heterogeneous group of chemical compounds used for the control of pests hazardistically damaging agricultural productivity, public health, and environmental integrity. Their main function is to inhibit, repel, or destroy organisms considered harmful such as insects, weeds, fungi, and rodents⁸ More generally, pesticides can be grouped according to categories such as insecticides, herbicides, fungicides, and rodenticides, which target specific pest groups or modes of action.

Usage and Impact: The use of pesticides in agriculture has contributed to the dramatic increase in crop yields and helped safeguard crops from pests and other unwanted plant growth. However, such extensive use brings along some challenges; the main issues are seen as environmental pollution by way of pesticide leaching and runoff causing soil and water pollution and the impact on non-target species by way of reduction of beneficial insects and wildlife. The undesired effects are now recognized as serious ecological issues. In addition, the presence of pesticide residues in food has been associated with various health issues, leading to demands for stricter regulatory standards.⁹

1.2.2 Classification of pesticides depending on the chemical composition.

Pesticide is a generic name for a variety of insecticides, herbicides, fungicides, rodenticides, wood preservatives, garden chemicals, and home disinfectants that are used to kill or protect against pests. The physical and chemical characteristics of these pesticides vary from one class to the next. As a result, it is common to categorize pesticides based on their chemical structure and properties and consider them within their respective groupings. Pesticides are generally classified using Drum's three main criteria. These classification criteria are: (i) classification based on pesticide mode of entry, (ii) classification based on pesticide function and the pest organism(s) they kill, and (iii) classification based on pesticide chemical composition.¹⁰

The chemical composition and type of active components are the most popular and practical method of pesticide classification. This type of categorization provides

information about the effectiveness, physical, and chemical aspects of the pesticides. Knowledge of a pesticide's chemical and physical properties is extremely valuable in defining a mode of application, precautions that must be taken during application, and application rate/concentration. Pesticides are categorized into five major classes based on their chemical composition: organochlorines, organophosphorus, organonitrogen, carbamates and pyrethrin, and pyrethroids.¹¹ (Figure 1.2)

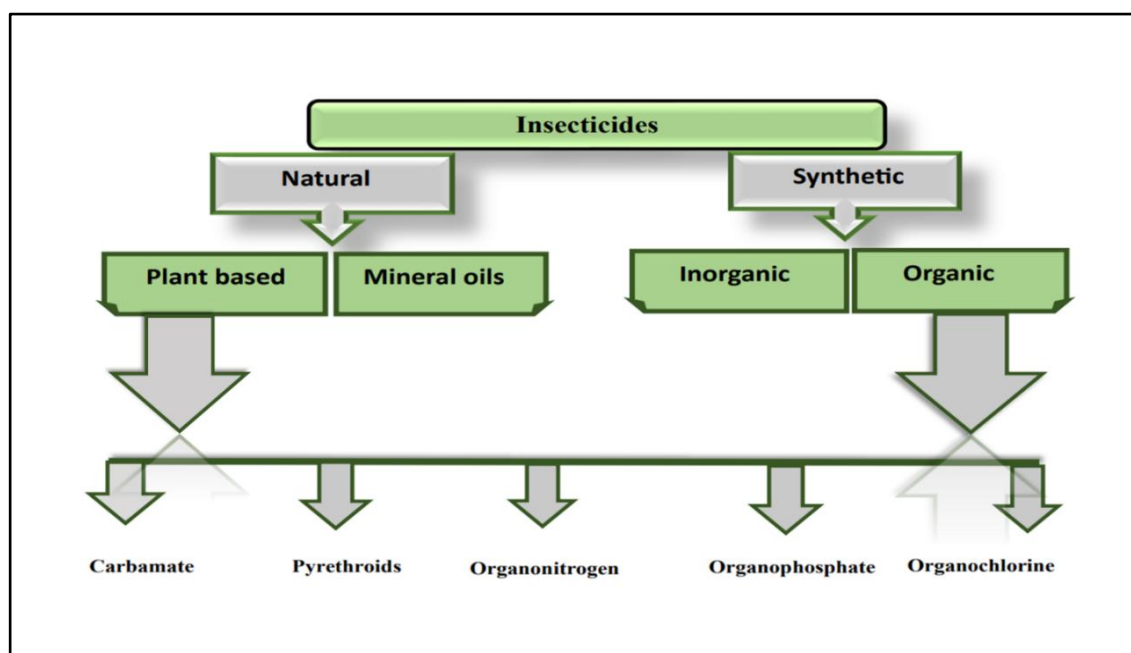


Figure 1.2: Classification of pesticides(insecticides)depending on the chemical composition.

1.2.3 Classification of pesticides used in the study

1.2.3.1 Organophosphate Pesticides

Organophosphate pesticides are considered to be one of the broad-spectrum pesticide classes which control wide range of pests due to their multiple modes of action; most notably the toxic effect of all organophosphates on the central nervous system through inhibition of cholinesterase enzymes. They are known to find their way into biological systems through ingestion, skin contact and inhalation, all of which ultimately lead to nerve poison.¹² These insecticides are biodegradable, have little longstanding environmental impact, and have a slow rate of pest resistance development.

Organophosphate pesticides are more hazardous to vertebrates and invertebrates because they inhibit cholinesterase, resulting in a persistent acetylcholine neurotransmitter interruption. As a result, nerve impulses fail to pass the synapse, resulting in a fast twitching of voluntary muscles and, ultimately, paralysis then death. Some of the widely used organophosphorus insecticides include parathion, malathion, diazinon.⁹ They were among the most extensively used pesticides until the twenty-first century. A total of thirty-six organophosphorus pesticides are approved for use in the United States, and all of them have the potential to induce acute and subacute toxicity in their target organisms.¹³ Organophosphates are employed in agriculture, homes, gardens, and veterinary operations. Over the last decade, some important Organophosphates (OPs) have been phased out including parathion, which is no longer registered for any purpose, and chlorpyrifos, which is no longer registered for residential use.

Although there are minor distinctions within the class, they all have a common mechanism of cholinesterase inhibition and can elicit comparable symptoms. Because they share this mechanism, exposure to the same organophosphate via several pathways, or exposure to numerous organophosphates via multiple routes, may result in substantial cumulative toxicity. However, it is vital to note that these compounds have a wide range of notable symptoms and a large variance in dermal absorption. This is not an uncommon situation, due to use of multiple OPs through cost variation at market, the end result is that accurate identification of the agent(s) is complex and individualized treatment is thus more challenging.¹⁰

Many organophosphates are insecticides that impact on the nervous system by compromising the enzyme that regulates the neurotransmitter concentration. Because of the endurance and toxicity of organochlorines, organophosphate pesticides are frequently utilized in modern agriculture as an alternative to organochlorines for pest management. Organophosphate insecticides are among the top ten most extensively used pesticides worldwide, accounting for more than one-third of all insecticides.¹⁴ OPs are now prevalent in surface natural waterways due to their widespread usage and resistance to natural disintegration and biodegradation.¹⁴ It has been observed that OP residues occur in environmental waterways.¹⁴ However, they are considered highly dangerous substances that interfere essential neurological functions¹⁵ and cause reproductive damage.¹⁶ A published study investigated various organophosphate esters in many different samples of baby food such as cereal and infant formula collected from different

locations in China.¹⁵ Chlorpyrifos and phosalone were also detected in apple-based baby food in the Czech Republic during food safety monitoring between 2001 and 2003.¹⁶

Organophosphate pesticides are synthetic compounds and are usually esters, amides, or thiol derivatives of phosphoric, phosphonic, phosphorothioic, or phosphorothioic acids.¹⁷ The classification of organophosphate pesticides on the basis of their structure is shown in figure 1.3.

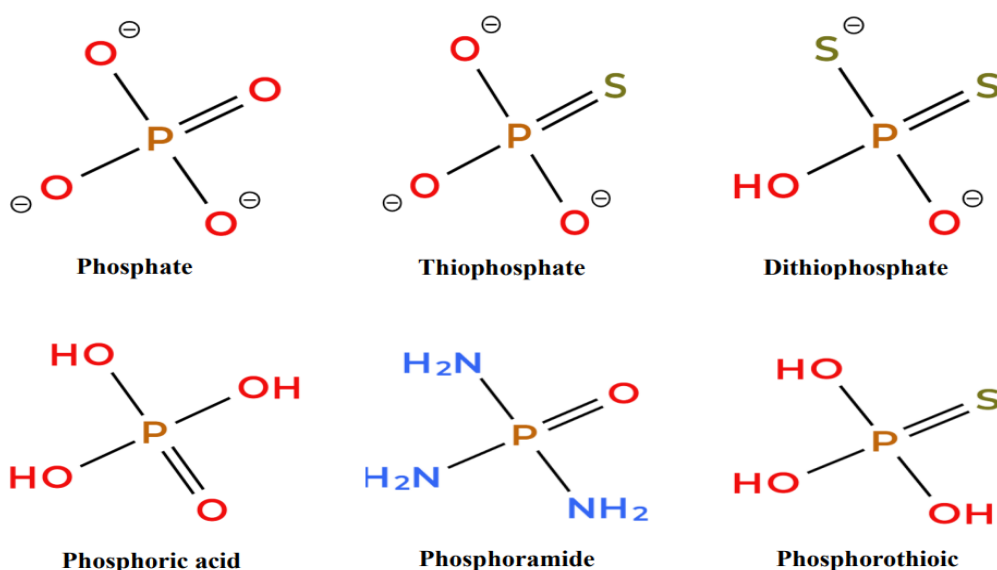


Figure 1.3: Classification of some organophosphate pesticide based on their structure.

1.2.3.2 Organochlorine Pesticides

Organochlorines pesticides (also known as chlorinated hydrocarbons) are organic compounds with five or more chlorine atoms. They were among the first insecticides to be produced and employed in agriculture and public health.¹⁸ The majority of them were widely employed as insecticides to control a wide variety of insects, and they have a long-term residual effect on the environment. These pesticides disturb the neurological systems of insects, resulting in convulsions and paralysis, followed by death. Organochlorines are a large class of compounds that include (1) DDT and its analogs, such as dichlorodiphenyldichloroethylene (DDE) and dichlorodiphenyldichloroethane (DDD). (2) hexachlorocyclohexane (HCH) such as lindane. (3) cyclodienes, such as aldrin,

dieldrin, endrin (sometimes referred to as "drins" in the literature), heptachlor, and chlordane. Many nations have now banned organochlorine pesticides from their markets due to their negative effects on human health and the environment, and they are regulated internationally under the Stockholm Convention on Persistent Organic Pollutants. (POP's) aldrin, chlordane, DDT, and dieldrin are examples.¹⁰ Though the manufacturing and application of DDT was outlawed in most industrialized nations, including the United States, many years ago, it is still utilized for vector control in most tropical countries with low GDP (particularly where malaria occurs).⁹ By and large this group of chemicals exhibits low selectivity and long-term biological stability. The impact of OCs on the environment can be seen as pollination reduction and the reduction in the numbers of bees and other insects that pollinate plants, as perhaps in the phenomenon called colony collapse disorder.¹⁹

Organochlorine pesticides share a common chemical modification; incorporation of chlorine substituted on aliphatic or aromatic carbons. Because of their structural similarities, these chemicals have similar physicochemical properties such as strong persistence, low polarity, poor aqueous solubility, and high lipid solubility. Organochlorine pesticides can infiltrate the environment through pesticide applications, contaminated trash dumped into landfills, and industrial units that synthesise these compounds.

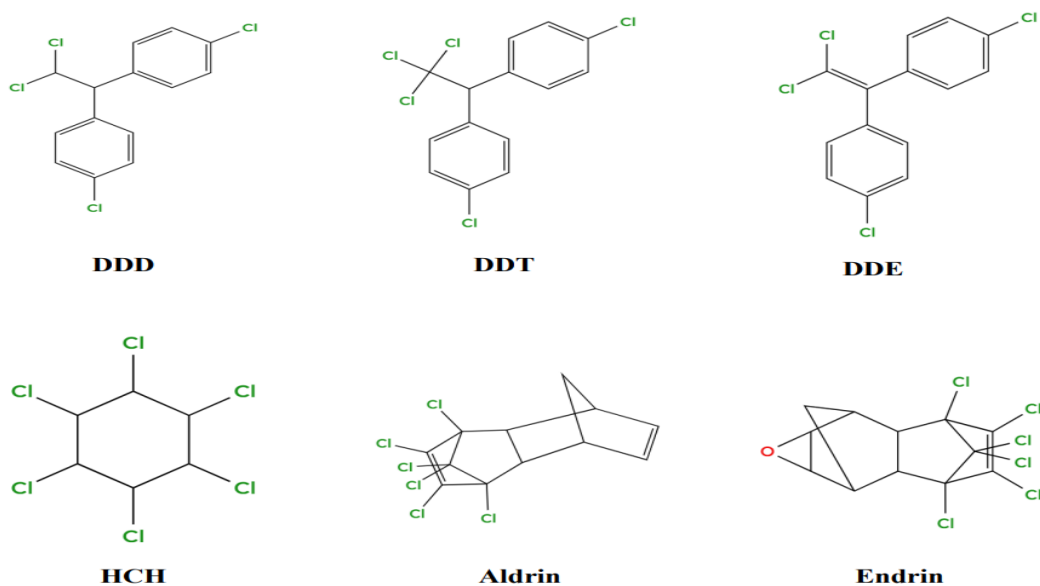


Figure 1.4: Structure of some organochlorines

They are volatile and stable; some may attach to soil and air, increasing the likelihood of high prevalence in the environment; and they have been recognized as chronic exposure agents in animals and humans. Figure 1.4 shows some compounds of organochlorine pesticides.

An examination of the impacts of various pesticide classes led to the conclusion that many of them are linked to hypertension, cardiovascular illnesses, and other health issues in Humans. Organochlorines operate as endocrine disrupting chemicals (EDCs) by interfering with the endocrine system's molecular circuitry and function.²⁰ Farm workers, their families, and individuals who walk through pesticide-treated areas can absorb detectable amounts of pesticides. Pesticide residues have been found in the blood plasma of agricultural field workers.²¹ Pesticide exposure, whether direct or indirect, causes neuromuscular problems and stimulates drug and steroid metabolism.²² More concerning, exposure to pesticides can occur through consumption of contaminated food. Fatty foods such as meat, fish, poultry, and dairy products are major contributors to this exposure pathway, it is worth noting that due to their chemical structure, these compounds are lipophilic, which gives them a longer half-life in biological systems and allows them to accumulate. Hence the reason why fatty foods are the main contributors to pesticide exposure.²³ A study conducted in Korea on 100 samples of baby food showed the presence of specific types of polychlorinated biphenyls (PCBs) and organochlorine pesticides (OCPs) such as PCBs, DDTs, HCHs, and chlordanes: dichlorodiphenyltrichloroethanes, hexachlorocyclohexanes, and chlordanes may vary with the country and the agency. Some of these MRLs are even still found in the regulations made by bodies like the European Food Safety Authority and the US Environmental Protection Agency. PCBs: MRLs for total PCBs in foodstuffs in most countries may range from nondetectable quantities to around 0.1-0.2 $\mu\text{g}/\text{kg}$ (100-200 pg/g). DDTs: MRLs may be in the range of 0.05-0.1 $\mu\text{g}/\text{kg}$ (50-100 pg/g) according to individual DDT isomers and local regulations. HCHs (β -HCH in particular): MRLs are generally of the order 0.1 $\mu\text{g}/\text{kg}$ (100 pg/g) per isomer. Chlordanes: MRLs for chlordane will be of the order 0.05 $\mu\text{g}/\text{kg}$ (50 pg/g). The mean concentration of the chemicals in Korean baby food study is as follows: PCBs: 37.5 pg/g , DDTs: 96.6 pg/g , HCHs: 26.0 pg/g , chlordanes: 13.2 pg/g . By applying general MRLs, concentrations documented here seem to be under limits of numerous jurisdictions' regulation, suggesting that baby food

homemade sample concentrations of these compounds fall into regulatory standards' safe margin.

Yet, concurrent examination of more than a single source of exposure, i.e., breast milk, is necessary for global risk assessment, especially for potentially more susceptible infants to the effect of these chemicals,..²⁴ Many organochlorine compounds have also been found to be neurotoxic and carcinogenic.²⁵ Of particular current concern is endosulfan which has been found to persist in the environment for extended periods of time and bioaccumulates in plants and animals, contaminating the human food chain.²⁶ Endosulfan primarily affects the central nervous system and has higher acute inhalation toxicity than cutaneous toxicity. Endosulfan is readily absorbed from the gastrointestinal tract.²⁷

1.2.3.3 Organonitrogen Pesticides

Organonitrogen pesticides (ONPs) are a type of insecticide and herbicide for annual control of grass and broad-leaved weeds. They are a group of structurally diverse compounds collectively names for the incorporation of one or more nitrogen atoms throughout their structure as shown in figure 1.5. These pesticides are divided into a number of subclasses, each having unique chemical characteristics and modes of operation. Organonitrogen pesticides work by interfering in the neurological or metabolic functions of insects. Neonicotinoids, that inhibit insects' nitric oxide receptors; the amidines impair insects' movement through interfering with the way their muscle's function. These illustrate the diverse structure/function modes of operation of organonitrogen pesticides.²⁸

ONPs and their degradation products are abundant in the global environment as a result of the widespread use of organonitrogen compounds as a pre- and post-emergent herbicide, primarily on maize, sorghum, and to a lesser extent on other crops, or as a non-selective herbicide for general weed control.²⁹ ONPs have been found, at approximately 3.96 to 75.88 ng/L in Egyptian aquatic environment.³⁰ They are, nevertheless, on official lists of chemical pollutants that need to be carefully monitored in the environment because of their low toxicity to mammals, as well as their persistence and accumulation in the environment.³¹ ONPs, found in a concentration range of 3.96 to 75.88 ng/L in the Egyptian water system, are important for a variety of reasons: Persistence and Accumulation: ONPs are chemical pollutants that require close monitoring as they are

persistent and bioaccumulate in the environment. Toxicity: Even though low in their mammalian toxicity, ONPs are toxic to the environment and human health. Evidence of their toxicity, persistence, and bioaccumulation made them banned in Egypt and other nations. Seasonal variation: amount of ONPs in water when runoff from agriculture lands has entered is a seasonally varying incident and is chiefly available two months after application. Surface Water Contamination: ONPs emerge with greater frequencies and quantities in surface water than in groundwater. They emerged in surface water samples as a result of runoff from cultivated land as per the study. Comparison with guidelines: ONP concentrations in surface water and groundwater of the study area in the two seasons are below safety levels when compared to Canadian guidelines on water quality for irrigation and fresh water.

Organonitrogen herbicides have been found to remain in the aquatic environment for many days after application.³¹ However, their persistence varies depending on several factors, including the chemical composition of pesticide, environmental conditions, and soil-water interactions, such that they remain in the soil from 1 to 15 months and in water from days to months because they may decompose quickly in water due to dilution. Organonitrogen dilution in water may accelerate their degradation by different mechanisms. These include increased chemical and microbial degradation, reduced inhibition with regard to concentration, increased light exposure (photolysis), and dilution as a hydrolysis catalyst. Dilution isolates herbicide molecules and increases their accessibility to microbial action and hydrolysis. High water concentrations provide other microbial communities to break down herbicides. Dilution reduces concentration, reducing inhibition and allowing higher rates of degradation. During dilution conditions, herbicide molecules become more uniformly distributed in the water column and therefore are exposed to light in larger quantities. Dilution is also a hydrolysis initiator, and this enables some herbicides to break down via hydrolysis. Dilution retards degradation under some conditions, for example, when the concentration of the herbicide is too low or under cold or stagnant water conditions. Generally, dilution accelerates decay through enhanced microbial access, photolysis, and reduction of inhibitory effect.³¹ As a result of their permanence in the environment, there is a considerable interest in studying the effects of pollution that results from this class chemicals. Their use is now restricted in some region, such as the European Union (EU) and United States (US) due to emerging evidence of their toxicity, persistence, and bioaccumulation in the

environment.³² The best-known members of ONPs are molinate, propazine and simetryn, which are registered and used in huge quantities in agriculture to kill weeds in corn and soybean fields in Egypt.³¹ In a study reported by El Bouraie, El Barbary, and Yehia in 2011, the authors examined the concentration of organonitrogen pesticides (ONPs) in waterways receiving runoff from agricultural fields vary seasonally, with the maximum amounts being observed six weeks to two months after application and lower to undetectable quantities the remainder of the year. In agricultural drains, the concentrations are highest sorghum during runoff after storms in the post-application period. ONPs do not adsorb as strongly to soil particles as other commercial herbicides. In most soils, the pesticide binds only weakly to soil particles depending on soil temperature, moisture and pH. Pesticide movement with soil moisture is restricted due to the partial expansion of soil particles and their low water solubility.³¹ Figure 1.5 shows some compounds of organonitrogen pesticides.

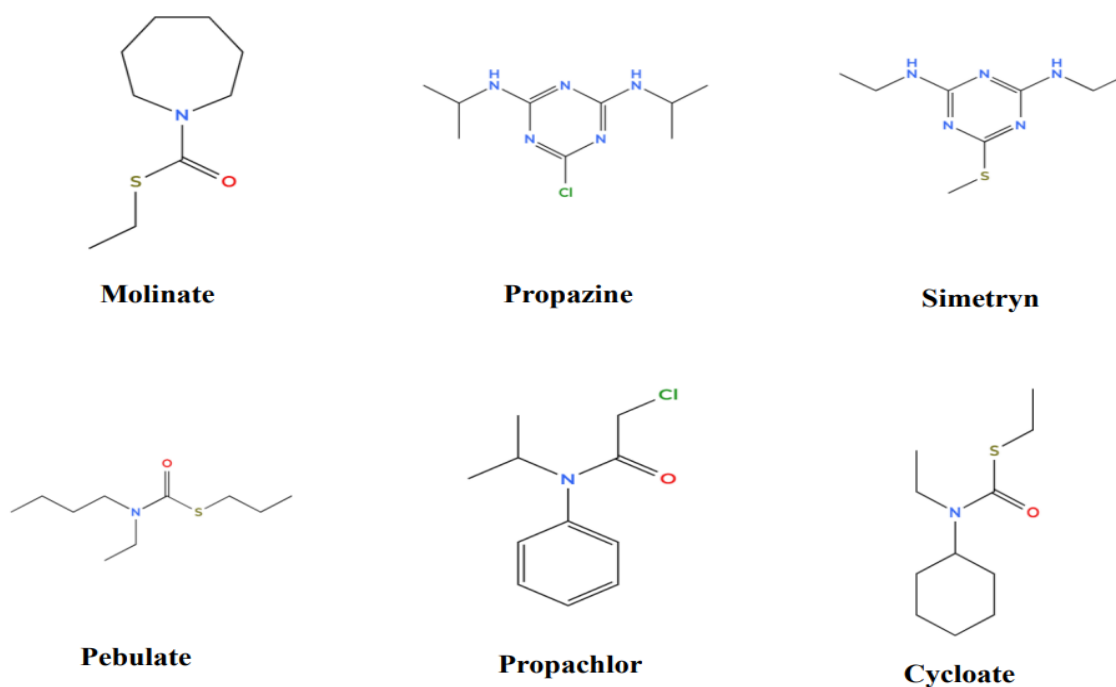


Figure 1.5: Structure of some organonitrogen.

1.2.3.4 Pyrethroids

Pyrethroids and pyrethrins are similar organic compounds isolated from the flowers of pyrethrums (*Chrysanthemum coccineum* and *C. cinerariaefolium*). Functional insecticidal pyrethroids are mainly esters of chrysanthemic and pyrethroic acids.³³ Of the two main types, pyrethroid pesticides are more effective at lower doses, they are also considered one of the most important groups of pesticides used to reduce the number of pests that cause great economic loss to farmers. However, they lack photostability and persistence, therefore they have mostly replaced pesticides from the carbamate and organophosphate families.³⁴ First-generation photo-labile pyrethroid insecticides (such as allethrin) were developed during WWII and are still used as active ingredients in insect repellents today.³⁵ Pyrethroids have a low degree of mammalian toxicity and undergo rapid biodegradation. Excessive exposure to these chemicals via the air, food, or water may result in giddiness, headaches, vomiting, muscular twitching, fatigue, convulsions, and loss of consciousness.³⁶ Synthetic pyrethroid pesticides are an organic pesticide class that may be created by mimicking the structure of natural pyrethrins. They are more stable and have longer lasting effects than natural pyrethrins.¹²

Pyrethroids are classified according to their chemical structure and mode of action into two types: Type I and Type II.

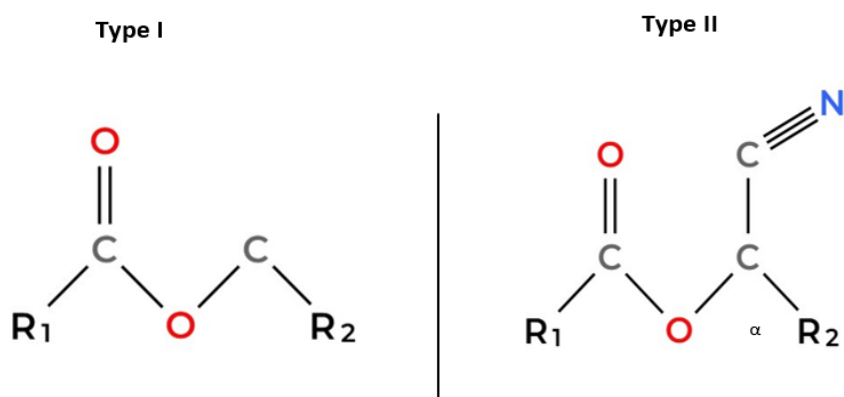


Figure 1.6: Typical structure of pyrethroids classified by types I and II.

Type I is pyrethroids that do not contain a cyano group at the alpha position, as in figure 1.6 for example: allethrin ($C_{19}H_{26}O_3$), tetramethrin ($C_{19}H_{25}NO_4$), resmethrin ($C_{22}H_{26}O_3$), permethrin ($C_{21}H_{20}Cl_2O_3$), bioresmethrin ($C_{22}H_{26}O$) and d-phenothrin ($C_{23}H_{26}O_3$). While Type II pyrethroids contain a cyano group at the alpha position (figure 1.6), examples include cypermethrin ($C_{22}H_{19}Cl_2NO_3$), cyfluthrin ($C_{22}H_{18}ClCFNO_3$), deltamethrin ($C_{22}H_{19}Br_2NO_3$), cyphenothrin ($C_{24}H_{25}NO_3$), fenvalerate ($C_{25}H_{22}ClNO_3$), and fluvalinate ($C_{26}H_{22}ClF_3N_2O_3$). Figures 1.7 and 1. 8 show examples of type I and II compounds, respectively.

Type I and II compounds affect the nervous system of insects by delaying the closure of sodium ion channels in nerve cells. In addition, type II also interfere with the function of the neurotransmitter gamma-aminobutyric acid.³⁷

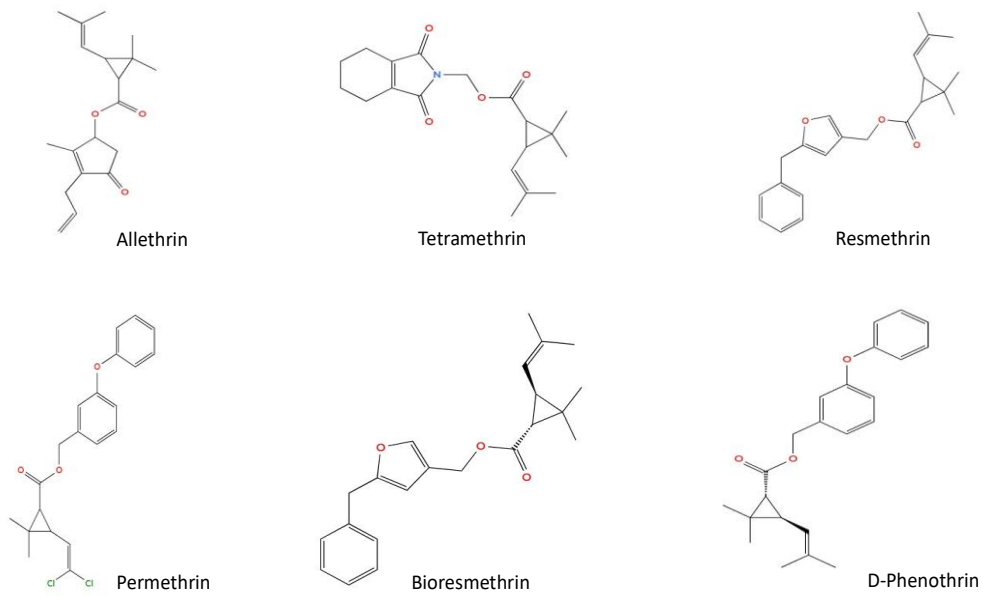


Figure 1.7: Chemical structure of type I of pyrethroid

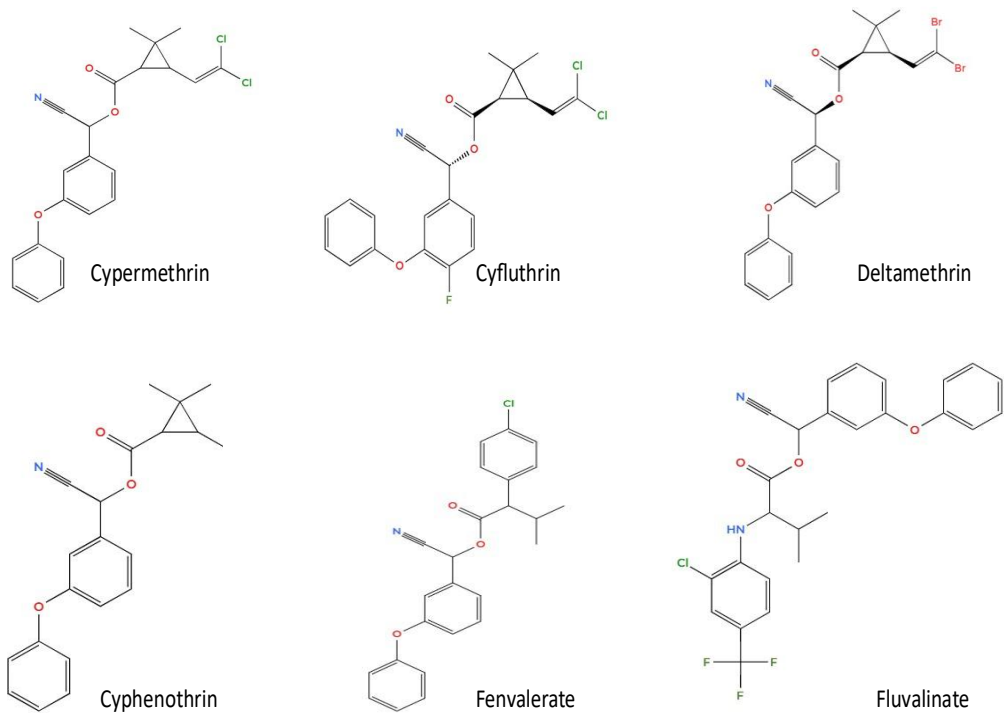


Figure 1.8: Chemical structure of type II of pyrethroid.

1.2.4 Negative Effects of Pesticides

Pesticides are used to control insect populations with a view to obtaining better harvests of foodstuffs. With that use comes a risk to the safety of both humans and other biological species as the active chemical ingredient that is released may be toxic to species other than that for which it was designed to control. The risk arises through a number of potential routes of introduction into foodchains: direct contact with skin, inhalation of small droplets from a spray application or by other methods that arise at point of consumption.³⁸ Pesticides do not degrade quickly upon application, with the duration of persistence varying significantly depending on the type of pesticide. Some may remain in the environment for only a few days, while others can persist for months or even years before they are fully metabolised, environmentally destroyed or sequestered.

One of the main concerns arises as an increased risk of pregnancy miscarriages that result from prolonged preconception exposure to pesticides such as phenoxy acid herbicides, carbamate insecticides such as carbaryl, and glyphosate.³⁹ Studies suggest that higher rates of miscarriages result when women handle certain pesticides three months prior to conception.⁴⁰ Additionally, further studies suggest that prolonged exposure to pesticides during early stages of pregnancy can bring high risks of birth defects.⁴¹

There is also mounting evidence proposing a moderate increase in the risk of developing a neurodegenerative disorder, such as Parkinson's disease (PD).⁴² This disease mostly affects those who are occupationally exposed to pesticides, especially gardeners and farmers. Long term exposure to pesticides may increase the risk of developing cancers and psychological impairment, hence increasing mortality rate among farmers and other workers.⁴³

Spraying pesticides onto food crops such as fruits may result in contamination of this produce. The majority of food substances that we purchase in supermarkets contain detectable pesticide residues. For instance, an analysis of several thousand stored food samples showed that 67% of fruits and vegetables, or eight out of every twelve, have pesticide residues. Thorough monitoring studies by EFSA, USDA PDP, or FDA indicate that approximately 67% of fruits and vegetables have detectable pesticide residues. The majority of the residues are below MRLs, and incidence is approximately 2-5% in the EU (EFSA data), 1-13% in the US (USDA PDP), and less than 5% in regulated markets. Averages globally are generally less than 5% in regulated markets but higher in imported

fruits and vegetables. Exceedances of MRLs are uncommon in regulated systems due to the fact that MRLs are established well below safety levels based on toxicology and most overruns are due to unapproved pesticides.⁴⁴

Some pesticides are extremely toxic; they destroy fungi, weeds, rodents and unwanted insects. At the same time, these same modes of toxicity may lead to similar long term harm to humans. Long term health effects attributed to pesticides include the development of cancer and reproductive disorder.

More common are short term effects, such as skin and eye inflammation as well as respiratory tract inflammation.⁴⁵

Although pesticides kill pests, they can harm plants that are beneficial to humans and animals. The bio-transformation products of pesticides in the environment are occasionally more toxic than the parent compound. Pesticide use that is excessive has a detrimental effect on the environment and animal species well beyond the intended use.⁴⁶

1.2.5 Legislation related to baby food quality

As discussed in the previous section the detriment to health from pesticide use that arises as a possibility from their presence in food, especially baby food, has seen the introduction of strict controls on residual levels of pesticides in many areas including foodstuff. Control of residual pesticides in baby food is especially important as nutrition plays a vital role in child development in the early years. Most countries recognize that baby foods must comply with highest safety standards and ensure that they are completely free of pesticides and other contaminants. A number of countries have developed legislation regulating the quality of baby food, including the United States, the European Union, amongst others. To provide infant food safety, nations employ a combination of regulatory mechanisms, surveillance, and inter-stakeholder collaboration. The practices are pivotal and involve strict regulation of the process of establishing limitary residues (MRLs) of pesticide and other food pollutants in foods, frequent inspections and monitoring for verification of compliance, and adherence to Good Agricultural Practices (GAP) to limit the pesticide residues. Food safety programs regulate food manufacturing, processing, and distribution of foods, and ensure compliance through inspection and action. Public education and awareness regarding food safety and safe infant foods are also required. Governments can collaborate with food manufacturers to encourage good

practices in food safety and quality assurance, e.g., safe production, transparency in ingredient sourcing, etc. Research and development continue to support policy-making decisions and, over time, improve the standards of safety. These are designed to render foods for infants safe, healthy, and free from lethal contaminants, keeping infants and preschool children healthy.⁴⁷

Legislation in the United States:

1. Federal Food, Drug, and Cosmetic Act (FFDCA):

The FFDCA states that all food, including baby food, must be safe, and sets limits for pesticides in baby food, with the FDA responsible for enforcing these standards.⁴⁸

2. Food Safety Modernization Act (FSMA):

Implementing controls and conducting risk analyses for food manufacturers is the requirement of the FSMA.⁴⁹

3. Infant Formula Act:

This act focuses on infant formula and ensuring that it is free of pesticides, in addition to ensuring that it meets the needs of infants at this age.⁵⁰

Legislation in the European Union:

1. Regulation (EU) No 609/2013:

This Regulation (EU) No 609/2013 of the European Parliament and of the Council was established to set specific rules for foods for infants and young children as well as foods intended for special medical purposes.⁵¹

2. Commission Regulation (EU) 2016/127:

Regarding the European Parliament and Council's Regulation (EU) No 609/2013 concerning the particular compositional and informational standards for infant formula and follow-on formula, as well as the requirements for information pertaining to the feeding of infants and young children.⁵²

Legislation in Other Countries:

Canada:

Under the Safe Food for Canadians Act (SFCA) and the Food and Drugs Act (FDA), The Canadian Food Inspection Agency (CFIA) regulates the testing of children's food safety.^{53,54}

1.3 Analytical methodology

With the increasing population, the need for food production increasing, and at the same time, pesticides residues in agriculture pose a major threat to food safety. Therefore, the safety of agricultural and food products has become an increasingly challenging due to pesticides use, which are essential for pests and diseases control. This has led to the development of pesticides analysis approach, which employs various analytical techniques and experimental processes to find, classify and quantify pesticide residues in diverse matrices like water, food, soil, or air. Many scientific researchers have contributed to the improvement of analytical techniques in the field of pesticide detection such as chromatography. This is to ensure food security, sustainability, and legal compliance.^{55,56}

A typical analytical workflow used for analyzing pesticides may consist of: sample preparation, separation, detection and data analysis as shown in figure 1.9.

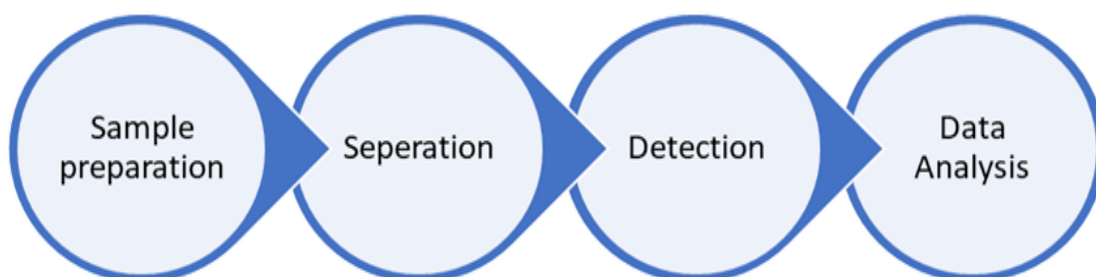


Figure 1.9: A typical analytical workflow used for analyzing pesticides.

1.3.1 Sample preparation

Aside from robustness and repeatability, the major goals of sample preparation are matrix component removal, analyte recovery, and notably analyte preconcentration, the latter two of which are sometimes combined under the phrase ‘enrichment factor’. Most micropollutants in environmental samples are present at trace levels (ng/L to µg/L), separation techniques alone are inadequate on their own at these concentration levels, and they can be achieved only if sample enrichment is applied.⁵⁷ Moreover, improvement in extraction selectivity for targeted analysis, and also coverage in non-target analysis is essential. The coupling to analytical separation techniques is critical.⁵⁸ There are many protocols for the recovery of pesticides from numerous substrates. These techniques or methods include liquid-liquid extraction (LLE), solid phase extraction (SPE), solid phase micro-extraction (SPME), dispersive liquid-liquid micro-extraction (DLLME), single drop micro-extraction (SDME), hollow fiber-liquid phase micro-extraction (HF-LPME), continuous flow micro-extraction (CFME), and the Quick, Easy, Cheap, Effective, Rugged and Safe (QuEChERS) method. The QuEChERS method is a common choice as it is a simple and straightforward extraction technique involving an initial partitioning followed by an extract clean-up using dispersive solid-phase extraction (d-SPE). The QuEChERS method was originally developed to recover pesticide residues from fruits and vegetables, but it quickly acquired favor in the complete separation of analytes from other matrices.⁵⁹⁻⁶¹ QuEChERS is a rapid and simple substitute for LLE that produces high-quality results in a limited number of stages and with little solvent and glassware usage. QuEChERS lives up to its name as an established protocol for trace level analysis applicable to pesticide residues in food matrices⁶², has acceptable recovery yields, is easy-going for high-throughput laboratories because it has standardized procedures, and is compatible with GC-MS and LC-MS analysis. It has also flexible in application as it can be easily modified to be compatible with different types of samples, which they contain water or dry. The QuEChERS procedure in the nominal form consists of primary extraction, salting-out partitioning, and cleanup (Figure 1.10). The simplified method makes QuEChERS a laboratory convenience technique, but method validation is required to ensure reproducible outcomes. However, this technique has limitation such as matrix effects that effect the accuracy of the analysis, such as fats as in milk which requires the use of additional materials such as PSA and C18 to get rid of fat. In addition to its inefficiency in extracting some compounds with very high and very low polarity, which

requires adjustments in the solvents. For some complex samples, such as animal products, additional steps may be required to ensure effective extraction.

In short, QuEChERS methodology excels over traditional methodologies regarding simplicity, rapidity, cost-savings, good recovery, scalability, and utility in GC-MS and LC-MS determination. However, it is desirable to verify its performance for the target analytes and matrix in order to provide credible results.

Table 1.1: Comparison between different Techniques

Method	Advantages	Disadvantages
LLE	High recovery, broad applicability	Large solvent use, labor-intensive
SPE	Good cleanup, customizable phases	Column clogging, higher cost
SPME	Solvent-free, portable	Limited fiber lifespan, low sensitivity
DLLME	High enrichment, fast	Requires optimization, emulsion risks
QuEChERS	Fast, cost-effective, high throughput	Matrix interference, variable recovery

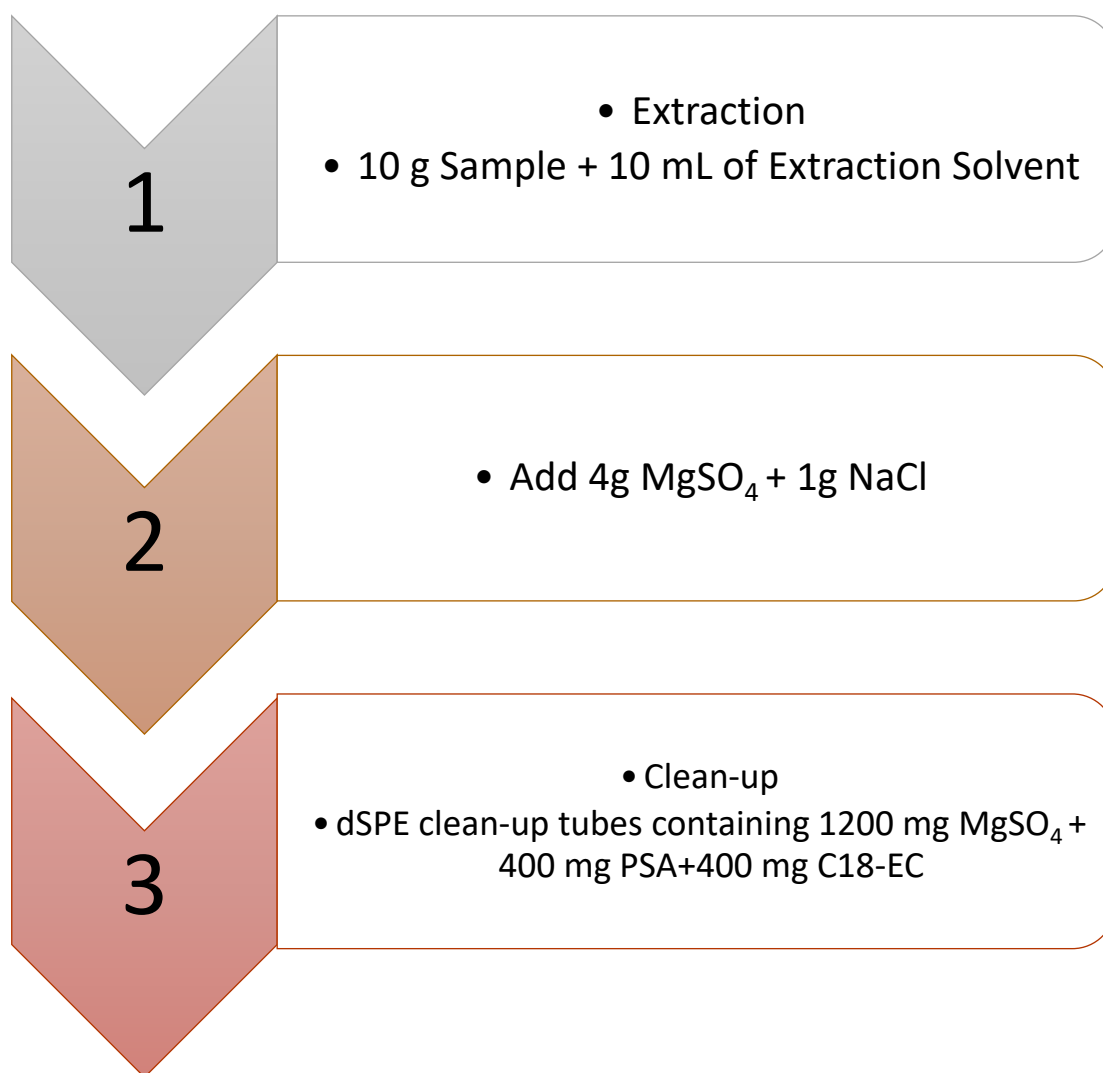


Figure 1.10: Schematic representation of QuEChERS-dSPE steps.

1.3.2 Separation and determination

Chromatography is a complex technique that is used for separating (and analysing, with a suitable detector) mixtures of multiple compounds. There are two major chromatography techniques that have been widely used in this respect, which are gas chromatography (GC) and liquid chromatography (LC). These are normally coupled with a detector e.g. GC-MS or LC-MS.

1.3.2.1 Gas Chromatography (GC)

A popular method of chromatography used in analytical chemistry for separating and studying substances that can be vaporized without decomposing is gas chromatography (GC). GC is frequently used to determine a substance's integrity or to separate the various components in a complex sample.⁶³ GC can be used in preparative chromatography to separate purified substances from a mixture at scale.⁶⁴ Vapor-phase chromatography (VPC) or gas-liquid partition chromatography are other names for gas chromatography (GLPC). In scholarly writing, these alternate titles and their corresponding abbreviations are commonly used. Gas Chromatography works by injecting a gaseous or liquid sample into a mobile phase, which is frequently referred to as the carrier gas, and moving the mixture through a column containing a stationary phase. Differential interactions between the various components of the mixture and the stationary phase give rise to a separation in time and thus a resolution of the mixture into its components at the detector. A neutral gas or unreactive gas, such as helium or hydrogen is most common, but other gases such as argon or nitrogen, have been reported as the mobile phase.⁶⁵ The stationary phase, also colloquially known as the column, is a microscopic coating of viscous liquid on a surface of a solid inactive solid base (fused silica). In some columns, the fixed phase may also be the particulate surface.⁶⁶ The fused silica or metal column that the mobile phase travels through are housed in an oven where the temperature of the gas can be adjusted with time to aid the equilibrium between the stationary and mobile phases. Upon exit from the column, automated detection (e.g. FID or MS etc.) records the elution time and other information such as area under the elution peak.⁶⁴ It is a separation technique that relies on the differential interaction of volatile or semi-volatile analytes with a stationary phase under controlled temperature and gas flow conditions. The fundamental physical chemistry behind GC separations involves thermodynamic partitioning and kinetic

processes, which together determine the efficiency, selectivity, and resolution of the analysis. Below is a detailed breakdown of the key factors governing GC separations.

1. Thermodynamic Basis: Partitioning and Retention.

The core principle of GC is the distribution of analytes between the mobile phase (carrier gas, e.g., He, H₂, N₂) and the stationary phase (a liquid or solid coating inside the column). This distribution is described by the partition coefficient (K):

$$K = \frac{C_s}{C_m} \quad \text{Eq.1.1}$$

where:

- C_s = Concentration of analyte in the stationary phase
- C_m = Concentration of analyte in the mobile phase

A high K means the analyte strongly interacts with the stationary phase, leading to longer retention time (t_a). The retention time is influenced by:

- Boiling Point (Volatility): Lower-boiling compounds elute faster because they spend more time in the gas phase.
- Polarity Interactions: Analytes with similar polarity to the stationary phase are retained longer (e.g., polar compounds on a PEG column).

The retention factor (k') quantifies this:

$$K' = \frac{t_R - t_0}{t_0} \quad \text{Eq.1.2}$$

Where t₀ is the dead time (time for an unretained compound to pass through).

2. Kinetic Effects: Band Broadening and Efficiency.

Even if two compounds have different K values, poor separation can occur due to peak broadening, governed by the van Deemter equation:

$$H = A + \frac{B}{U} + Cu \quad \text{Eq.1.3}$$

where:

- H = height equivalent to a theoretical plate (HETP, lower = better efficiency)
- A = Eddy diffusion (affected by column packing)
- B = Longitudinal diffusion (reduced at higher flow rates)
- C = Resistance to mass transfer (stationary/mobile phase kinetics)
- u = linear gas velocity

Optimal flow rate minimizes H, balancing diffusion and mass transfer.

3. Temperature and Phase Behavior

- Isothermal vs. Gradient Elution:

- Isothermal: Constant temperature; good for simple mixtures but may cause late-eluting peaks to broaden.

- Temperature Programming: Gradually increasing temperature improves resolution for complex samples.

- Van't Hoff Equation: Relates K to temperature (T):

$$\ln K = -\frac{\Delta H}{RT} + \frac{\Delta S}{R} \quad \text{Eq.1.4}$$

Where:

- ΔH (enthalpy)
- ΔS (entropy) describe phase-transfer energetics.

4. Selectivity (α) and Resolution (R_s).

- Selectivity (α): Measures how well two peaks are separated:

$$\alpha = \frac{t_{R2} - t_0}{t_{R1} - t_0} \quad \text{Eq.1.5}$$

- Resolution (R_s): Determines if two peaks are baseline-separated:

$$R_s = \frac{2(t_{R2} - t_{R1})}{w_{b1} + w_{b2}} \quad \text{Eq.1.6}$$

For $R_s > 1.5$, peaks are fully resolved.

5. Practical Considerations.

- Column Selection:

- Non-polar (e.g., DB-5): Separates by boiling point.

- Polar (e.g., Wax): Separates by polarity.

- Derivatization: Converts non-volatile analytes (e.g., acids, alcohols) into volatile derivatives (e.g., TMS ethers).

- Carrier Gas Choice:

- Hydrogen (H_2): Best efficiency but flammable.

- Helium (He): Safe and widely used.

GC separation is governed by thermodynamics (volatility, polarity, temperature) and kinetics (flow rate, diffusion). Understanding these principles allows optimization of column chemistry, temperature programs, and carrier gas flow for high-resolution analyses. Advanced techniques like GC \times GC or heart-cutting (MDGC) further enhance separations for complex samples.

1.3.2.2 Detectors

To attain accurate and precise identification of residues of pesticides, various kinds of detectors are employed to record the elution of compounds from the column.⁶⁷

Popular detectors include:

Flame Ionization Detection (FID) is among the more widely utilized detectors for pesticide analysis. FID is a detector that has a good response across many molecular types whilst providing a good linear response across an extensive dynamic range. An FID is useful for identifying pesticides across multiple classes, including organochlorine as well as organic phosphorus insecticides.

Mass Spectrometry (MS): A High sensitivity detector that can provide data on the molecular structure of analytes. Various types of MS instruments are used, such as single quadrupole, triple quadrupole instruments, Quadrupole time-of-flight (QToF) and Orbitrap mass spectrometers.

Mass analysers offer precise mass/charge determination for both the intact molecular ion as well as any molecular fragments. The precision in the m/z provided by the spectrometer is 'low' for SQ and TQ instruments but 'high' for QToF and Orbitrap instruments; thus, the latter instruments are able to provide molecular formula confirmation with increased confidence. An MS shows significant variations in detector response to different chemical structures.

Factors Dictating Precision of m/z Measurement:

1. Type of Mass Analyzer

- Low Resolution (e.g., Single/Triple Quadrupole, Linear Ion Trap):

Mass spectrometry devices achieve 0.5–1.0 Da units as their measurement precision when used traditionally.

This device provides specific substance identification while having an inability to differentiate between mass similar compounds such as CO and N₂ since they share the same weight (28 Da).

- High Resolution (e.g., QToF, Orbitrap, FT-ICR):

Exact mass measurements result from devices that resolve power between 10,000–500,000+ to allow detection of differences less than 0.001 Da.

To establish exact molecular formulas, it becomes necessary to have resolving power since both $C_8H_{12}N_4$ and $C_{10}H_{12}O_2$ parallel mass values at ~164 Da.

2. Resolving Power ($R = m/\Delta m$)

An instrument with R value at 50,000 separates peaks that vary by 100.0000 and 100.0020 Da from each other.

The Orbitrap together with FT-ICR surpass $R > 100,000$ yet QToF instruments deliver $R = 20,000$ – $60,000$ as their resolving power capability.

3. Calibration & Stability

All precision instruments need built-in calibration standards to achieve high measurement precision while Orbitrap mass spectrometers utilize lock mass correction systems for this purpose.

The combination of temperature fluctuations with electronic interferences produces adverse effects on measurement accuracy.

4. Ion Detection System

The Time-of-flight detection system which uses precise timing measurements lacks the precision of Orbitrap/FT-ICR frequency-domain detection approach.

How Precise Do You Need to Be?

- Unit Mass (~1 Da):
- Sufficient for targeted quantitation (e.g., triple quad for pesticide screening).
- High Resolution (< 0.01 Da):

An instrument is necessary to evaluate untargeted metabolites in proteomics projects and structures of these compounds and all chemical compositions.

Example:

The differentiation between glucose ($C_6H_{12}O_6$) with 180.0634 Da and aspirin ($C_9H_8O_4$) weighing 180.0423 Da requires an R value greater than 20,000.

- Ultra-High Resolution (< 0.001 Da):

The examination techniques in proteomics and petroleum require the implementation of this technology.

Practical Implications:

- Single/Triple Quad (Low Res): Good for known compounds in regulated workflows (e.g., LC-MS/MS quantitation).
- QToF/Orbitrap (High Res): Essential for unknown identification, isobar separation, and elemental composition assignment.

1.3.3 Mass spectrometry (MS)

Mass Spectrometry is an extremely common technique to find as the detector on a GC instrument. The MS detector works through ionization of compounds eluting through the GC column and then separating those ions based on their mass to charge ratio; this method of detection has proven to be excellent for measuring residual pesticides. MS detectors offer high levels of sensitivity, specificity and are available in many combinations of ion source and detection e.g. EIMS and MS/MS, EI-ToF and EI-Orbitrap. In pesticide evaluation, MS functions like a sophisticated fingerprinting scanner as the result is often diagnostic for a particular compound due to the reproducibility of the MS output. In outline an MS detector works with vaporized compounds from the GC column. These compounds enter the MS ion source and are ionized using e.g. electron beam to remove an electron and produce charged particles (M^+ ions). The MS uses the particles mass to charge ratio (m/z) to separate the ions generated into their individual masses by way of a quadrupole or other means (see section 1.3.3.2) to produce a distinct fingerprint for every pesticide. Similar to a QR code, this kind of fingerprint enables researchers to validate the existence of particular pesticides in an object as well as precisely identify them with unparalleled precision and sensitivity. Additionally, it is possible to quantify the amount of a molecule in the original extract through use of the detector's response via a

calibration procedure.⁶⁸ This makes it possible for MS to provide the identity of each pesticide present and the amounts of each substance within the sample analysed. As MS is an extremely sensitive technique, it can be used to identify even minute levels of pesticides which matches with the need of Regulatory authorities to provide guarantees for the integrity of foods at market.

Mass spectrometry (MS) creates a distinct mass spectral pattern which reveals itself by means of m/z separation after performing ionization and fragmentation on a molecule such as a pesticide. Mass spectrometry creates unique profiles for different compounds similar to fingerprint patterns which identify individual human beings.

Key Reasons for the Fingerprint:

1. Molecular Mass & Isotopic Pattern

A pesticide type produces distinctive fingerprints during mass spectrometry due to its unique molecular weight combined with the initial isotope distribution between ^{13}C and ^{12}C and ^{35}Cl and ^{37}Cl .

The chlorine compound pesticide DDT produces distinctive doublet peaks when it contains both chlorines with atomic masses 35 and 37 atoms.

2. Fragmentation Pattern

The pesticide substance creates predetermined fragment compositions through electron impact (EI) along with collision-induced dissociation (CID) ionization methods.

Process fragmentation of organophosphates releases the phosphate group (PO_3^-) but neonicotinoids break specific C-N chemical bonds during this process.

3. Retention Time (in LC/GC-MS)

The specification of pesticide detection through chromatography methods (LC-MS and GC-MS) relies on understanding the pesticide elution times.

How Is This Fingerprint Generated?

The following describes how MS fingerprints pesticides through a systematic process:

1. Ionization (Creating Charged Molecules)

High-energy electrons hit the pesticide while performing EI (GC-MS) ionization to create the primary molecular ion ($\text{M}^+\bullet$) and produce fragments from it.

During Electrospray Ionization (ESI and LC-MS) the technique produces mainly two ion types $[\text{M}+\text{H}]^+$ or $[\text{M}-\text{H}]^-$ while showing minimal fragment formation.

2. Mass Separation (Analyzer Filters Ions by m/z)

Specific m/z ions can pass through the device through the use of electric fields within the SQ/TQ system.

The Time-of-Flight (ToF) system detects how long ions require for flight tube transmission thereby indicating arrival order based on ion molecular weight.

- Orbitrap/FT-ICR: Uses high-resolution frequency measurements for ultra-precise m/z determination.

3. Detection & Fingerprint Generation

The detector creates mass spectra through its recording of m/z peak intensities which results in a visual representation of m/z values against signal strength.

Example:

- Malathion ($C_{10}H_{19}O_6PS_2$) shows:

Parent ion at m/z 330 ($[M+H]^+$)

The main fragments detected are PS_2^+ at m/z 127 alongside $C_4H_{11}O_3^+$ at m/z 99.

4. Database Matching (Like a QR Code Scanner)

Reference libraries such as NIST and Wiley are used to verify the identity of the pesticide through spectrum comparison.

The advanced QToF/Orbitrap MS technology enables precise molecular formula comparisons between $C_8H_{15}NO_3$ and $C_9H_{11}O_4$.

The information contained in this fingerprint proves so effective for multiple reasons.

The fingerprint technique demonstrates exceptional specificity by creating different identifying patterns from pesticide substances that resemble each other structurally such as imidacloprid compared to thiamethoxam.

The instrument achieves detection at levels extending to parts-per-billion (ppb) while surpassing even parts-per-trillion (ppt).

MS fingerprint analysis delivers structural proofs that function as a powerful alternative to immunoassays which might yield inaccurate positive results.

Example: Glyphosate Detection

- Parent ion: m/z 168 ($[M+H]^+$)

The major product fragment measures at m/z 150 after losing H_2O .

- Isotopic pattern: Confirms phosphorus (^{31}P) presence.

MS is also used to provide continual monitoring of environmental samples (It's like a security camera constantly recording what's happening, providing valuable insights into pesticide use) as a way to track pesticide concentrations in upstream food precursors,

watercourses, soils and the atmosphere. Mass spectrometry (MS) operates in an automated system that assesses environmental testing elements (water, soil, air, food) by allowing immediate sample analysis and recurrent analysis for time-based pesticide assessment to determine pollution levels instantaneously and categorize regulatory standards and research patterns. The MS systems linked to automated LC-MS/MS or GC-MS equipment provides detailed residue detection at low labor requirements to facilitate quick environmental response and enhance security and sustainability. Multiple MS instruments with triple quadrupoles and QTOF systems produce stable data feeds allowing software analytics systems to detect irregularities so MS analysis remains a vital tool for food safety and ecological sustainability and public defense. Further detail on MS analysers and detectors is presented below. In summary, the key components: the Ion Source, the Mass Analyser: and the Detector. A block diagram of a typical mass spectrometer can be found in figure 1.11.

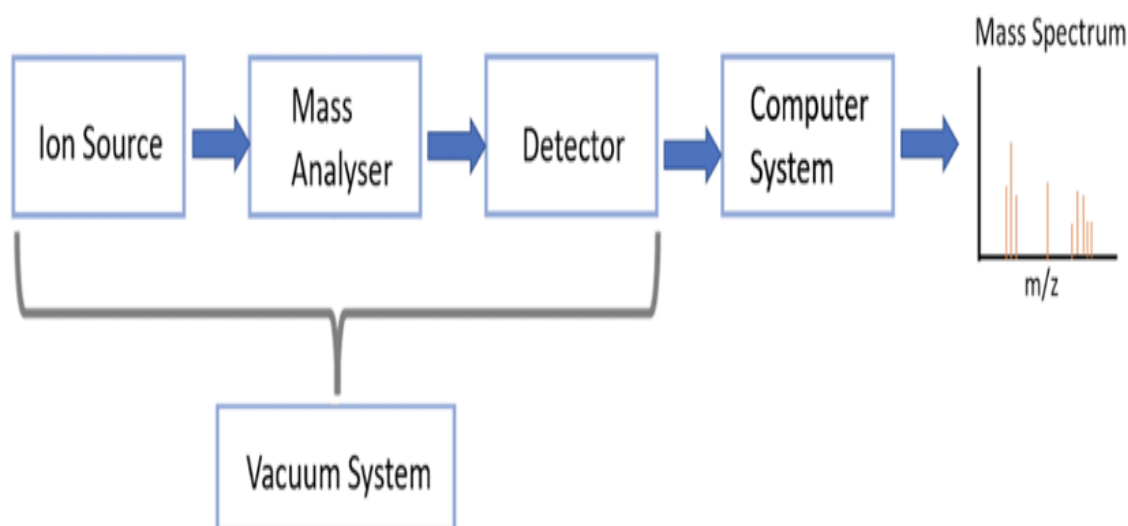


Figure 1.11: Schematic illustration of the basic components of a mass spectrometer.

1.3.3.1 Ion sources

There are many different types of ionization sources that can be used for GC-MS, Vacuum ionization techniques such as electron ionization (EI) or chemical ionization (CI) have been typically used to interface gas chromatography with mass spectrometry (GC-MS). Nonetheless, the generally low ionization efficiency achieved in CI as well as the high fragmentation seen in EI mean that, for some substances, may lead to reduced selectivity and the sensitivity in the determination of organic compounds.

EI technique in GC-MS instruments exposes molecules to strong electron impact to support spectral library analysis at the expense of fragmenting the molecular ion thereby reducing sensitivity for unstable compounds. The weight determination through protonation in Chemical Ionization depends on a reagent gas but its ionization efficiency remains low and structural information remains limited due to marginal molecular fragmentation. EI accomplishes exceptional performance through library matches and its robust way of ionizing compounds but its gentleness towards sensitive molecules coincides with reduced sensitivity and selectivity thus EI remains preferable for most analyses yet CI effectively confirms molecular weights when needed.

In the 1970s, researchers Horning et al. were the first to use a special type of source called atmospheric pressure ionization (API) source to connect a gas chromatography (GC) system to a mass spectrometer.⁶⁹ This setup was later modified by Mitchum et al. in the 1980s, and they used it to analyze different types of compounds such as tetrachlorinated dibenzo-p-dioxins, 2,3,7,8-tetrachloro dibenzofuran, nitro-polycyclic aromatic hydrocarbons (nitro-PAHs), and amino-PAHs.⁷⁰ In 1998, Lee et al. reported a different type of source called multichannel electrospray ionization (GC-ESI) to analyze more polar volatile organic compounds.⁷⁰ All of these API sources feature a soft ionization which helps to preserve the molecular or quasi-molecular ion. An API source is a device that produces ions (charged particles) which can be used to analyze substances. Over time, the number of API sources for GC-MS has increased, leading to the development of many new API sources.

These new sources can be classified into five different groups based on the way they produce ions: electrospray, plasma ionization, chemical ionization, laser ionization, and photoionization.⁷¹ A significant number of API sources have been reported, covering set-ups based on APCI mechanisms, APPI,⁷² atmospheric pressure laser ionization (APLI)⁷³, electrospray ionization (ESI), or atmospheric pressure plasma ionization.⁷³ The spectrum of uses for GC-API-MS has expanded thanks to all of these new sources. This, along with the first API sources for GC-MS being commercially available, has caused a noticeable increase in the number of publications utilizing these techniques. Some of the most significant flaws in vacuum ionization methods are clarified by API sources, such as the trade-off between sensitivity and selectivity when utilizing electron ionization (EI) or the typically low ionization efficiency attained with chemical ionization (CI).⁷⁴ connected to mass spectrometers that were originally made for liquid chromatography-mass

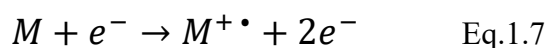
spectrometry applications (LC-MS). This fact has made it possible for analytical laboratories to quickly transition between GC and LC while still using the same low- or high-resolution mass spectrometer, lowering costs and increasing throughput.⁷⁵

1.3.3.1.1 Electron ionization (EI)

Electron ionization (EI), formerly known as electron effect ionization is an ionization method in which energetic electrons interact with solid or gaseous atoms or molecules to produce ions (Figure 1.12).⁷⁶ EI was one of the earliest ionization methods created for mass spectrometry.⁷⁷ However, this approach is still the most common ionization method when using a GC. EI generates ions using highly energetic electrons, produced in the source, to facilitate ionization; given the use of high energy electrons, this process is known as a hard (high fragmentation) ionization method. A hard ionization process often leads to significant fragmentation, which can be useful for figuring out the structures of unidentified chemicals. It is the preferred method for analyzing small, nonpolar, volatile compounds with a mass less than 1000 Da.^{78,79}

When an EI source operates it uses energetic electrons (typically at 70 eV) from a heated filament to bombard test molecules (M) in the gas state. The interaction proceeds as follows:

1. When an analyte molecule (M) absorbs a high-energy electron, it forms a radical cation ($M^{+\bullet}$) molecular ion while releasing an electron.



2. Excess Energy & Fragmentation: The molecular ion often retains excess internal energy, leading to bond cleavage and generation of fragment ions (e.g., A^{+} , B^{+}) and neutral species:



(or other fragment combinations)}

3. The output from EI ionization consists of both complete ions and their fragmented pieces which the mass analyzer accelerates as it separates them by their m/z ratio before detecting them to produce a distinctive mass spectrum

containing peaks representing original molecule structures and fragment structures.

Key Features of EI Ionization:

- The high-energy electrons from the ionization process generate substantial chemical fragmentation of the molecules during analysis.
- The first reaction product takes the form of a molecule with a positive charge called $M^{+\bullet}$ (radical cation).
- The library databases work with this method because fragmentation patterns show predictable results for matching against lists such as NIST.
- Mass Limit: Effective for molecules < 1000 Da (small, volatile, thermally stable compounds).

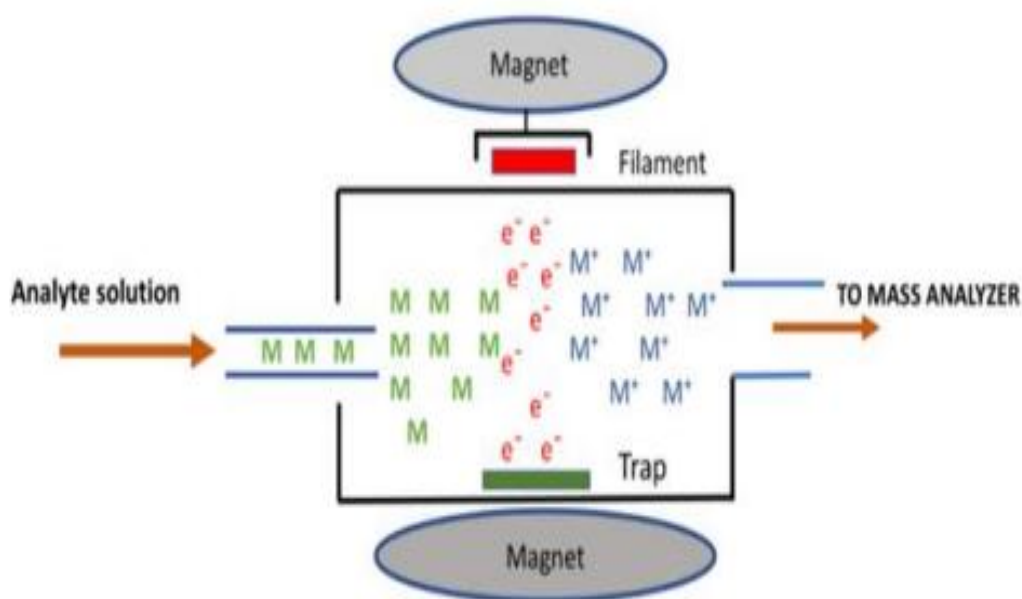


Figure 1.12: Schematic diagrams showing the ionization process in electron ionization.

In this process, an electron is expelled from the analyte (M) molecule during the collision process to convert the molecule into a positive ion with an odd number of electrons.⁷⁹ Electrons are created in an EI ion source using thermionic emission, which involves heating a wire filament with an electric current flowing through it. The ionization energy of the sample molecule should be less than the kinetic energy of the bombarding electrons. In the space between the filament and the ion source block's entrance, the electrons are accelerated to 70 eV. EI Electron Ionization typically operates at 70 electron volts standard because this setting maintains a balance between ionization precision and consistent fragmentation results while giving compatibility to historic spectral collections and providing enough power to ionize general organic molecules that need between 7 and 15 electron volts for fragmentation. These intermediate energy settings strike an effective balance which allows both the molecular ion to survive while the obtained fragments provide enough detail for identification purposes. The standard operating range of thermionic filaments and the requirement for reproducible comparisons between instruments makes 70 eV the accepted standard for GC-MS database matching procedures.

The test sample, which comprises the neutral molecules, is fed into the ion source with its direction perpendicular to the electron beam. The ionization and fragmentation of neutral molecules are brought on by the close passage of extremely energetic electrons at low pressure (between 10^5 and 10^6 torr).⁸⁰ A Schematic diagram illustrating the ionization process in electron ionization is shown in figure 1.12.

1.3.3.1.2 Dielectric barrier discharge ionization (DBDI)

Ambient ionization techniques have really changed modern mass spectrometric applications: they allow the ionization of samples without extensive sample preparation. Among them, Dielectric-Barrier-Discharge Ionization (DBDI), and Soft Ionization by Chemical Reaction in Transfer (SICRIT) stand as powerful techniques in analytical chemistry and microbial metabolomics. DBDI is used worldwide due to low energy consumption, ease of miniaturization, and compatibility for ionizing compounds from explosives to biochemicals. In contrast, SICRIT taps into ambient plasma ionization principles but espouses soft ionization through in-transfer chemical reactions, thus enabling complementary metabolite detection and enhanced ionization of lipids in positive mode. The elementary principles that DBDI rests on: ionization of nitrogen molecules via plasma interaction and reaction pathways leading to protonation. As for the operational principles demarcating SICRIT from other more classical forms of ionization sources and their developing role within microbial metabolomics. A comprehensive discussion comparing will highlight advantages and disadvantages of methods, backed by figures and data comparisons. This is all meant to be informative in the direction of source selection for specific applications, especially in highly complex bioanalytical situations⁸².

1.3.3.1.2.1 DBDI Ion Source: Mechanism and Instrumentational

Dielectric-Barrier-Discharge Ionization (DBDI) ambient ionization techniques dominate most areas in modern mass spectrometric analysis. It consists of using the dielectric barrier between electrodes at atmospheric pressure, within which low-temperature plasma is formed suitable for ionizing heat-sensitive analytes. They usually are made up of two electrodes that are adjacent and separated by a dielectric material and a controlled gas flow usually helium or argon acting as a discharge medium⁸³.

A. Ion Formation in DBDI

The application of a high voltage across a dielectric barrier during the alternating current operation is the initiation of the DBD plasma. The energy imparted to electrons causes the generation of highly energetic species known as metastables (such as He), which play an important role in the later ionization process. The Penning ionization process is very popular as one of the most common pathways for producing ions in DBDI. In this process, energetic metastables of helium heat energy nitrogens (N₂) present in the ambience to

form N_2^+ ions. These nitrogen ions are then reacting to water vapor in the external environment and are in turn forming protonated water clusters such as $H_3O^+(H_2O)_n$. Indeed, it works excellently as proton donors, forming protonated ions of analytes, which eventually go for detection by a mass spectrometer.

B. Instrumentation Setup and Scheme Representation

The actual operation of a DBDI setup typically entails connecting the nanoESI-DBDI ionization source to a mass spectrometer. An ion source is constructed so that a small needle electrode is inserted into a dielectric tube and serves as a high-voltage electrode. A counter electrode, in turn, closes the plasma circuit. There are different configurations illustrated by schematic representations cited in the literature. One such paper contains a schematic for single-cell analysis via LAESI-MS showing the configuration of the nanoESI-DBDI source and position of electrodes.

Figure 1.15 below provides a schematic representation of the DBDI instrumentation for single-cell analysis, which highlights the sample inlet, electrode assembly, and the nanoESI-DBDI ionization region where plasma is formed.

In summary, the overall reaction scheme can be:

1. Plasma Generation: AC (alternating current) high voltage produces a dielectric barrier that develops an electron avalanche and initiates plasma.
2. Metastable Formation: Energetic electrons excite helium atoms forming metastable helium species (He^*).
3. Penning Ionization: Metastable helium transfers its energies into atmospheric nitrogen and produces the formation of N_2^+ .
4. Proton Transfer: Water vapor reacts with N_2^+ to generate protonated water clusters that in turn protonate target analytes.

C. Mechanistic Details and Reaction Pathways

The mechanistic details of ionization involve quite a number of steps, which have received attention over the years. Following plasma ignition with AC voltage, the ionization region shows several zones characterized by electron energies and ion density distributions that differ. These zones are essential in considering the spatial distribution of ions generated within the plasma plume. Thus, the clearly defined reaction zone is

caused by the interaction of helium metastables with nitrogen molecules that lead into Penning ionization.

Again, different operating gas flows and voltage amplitudes will characterize the plasma differently. Under these conditions of reduced flow, emission maxima would again arise close to the cathode and towards the forward direction of the anode, indicating pretty complex plasma behavior. Further increases in the flows appear to suppress the cathodic maximum and push the active ionization region farther downstream. These observations are important for optimization efforts related to the DBDI applications.

D. Advantages and Limitations

DBDI offers many advantages:

1. **Low Energy Consumption:** Is chiefly operational under low voltage conditions; thus, energy wastage is minimized and low-power instrument design is facilitated.
2. **Solventless Operation:** No solvents needed for ionizing the sample; thus chemical waste is reduced, and sample preparation is made easier.
3. **Versatility:** DBDI may technically be coupled with other separation techniques like LC-MS, GC-MS, and IMS, thereby furthering its application to biological assays, forensic identifications, and food safety.

But the limitations regarding DBDI are still in place. Environmental conditions such as ambient humidity or interfering gases can affect the sensitivity and effectiveness of ionization processes. Furthermore, plasma conditions can cause signal variations that imprint a requirement for fine-tuning the discharge parameters for sustained analytical performance.

1.3.3.1.2.2 Principles and Advances in SICRIT Ion Source.

SICRIT stands for soft ionization by chemical reaction in-transfer and is a new emergent technique of ionization that promises to advance the challenge of ionization for complex biological samples, especially in the context of microbial metabolomics. In contrast to electrospray ionization, SICRIT uses dielectric barrier discharge, which creates chemical reactions during the transfer of the analytes into the mass spectrometer, achieving softer ionization and better preservation of molecular ions.⁸⁴

A. Fundamental Principles of Operation of SICRIT

Above what has been set for DBDI, SICRIT involves additional controls of the chemical reaction environment above which the ionized species are traversing the transfer zone. The ion source SICRIT maintains plasma discharge by applying a high voltage across a dielectric barrier, just as DBDI does. The term "chemical reaction-in-transfer" implies that there is considerable ionization resulting from chemical reactions occurring while the analyte molecules are being transferred from the ionization source into the mass spectrometer inlet.

The main steps in the SICRIT process are summarized as follows:

- **Plasma Generation:** Alternating high voltage initiates the formation of the plasma containing essentially metastable entities, such as He*.
- **Pre-Ionization Reaction Zone Formation:** The generated plasma in the end forms reactive species like N₂ and protonated water clusters.
- **In-Transfer Reactions:** During the very short duration of transfer into mass spectrometer, these reactive species interact with analyte molecules ionizing them through protonation, showed least amount of fragmentation - soft ionization.
- **Selective Ionization:** SICRIT has a tendency to ionize a different set of metabolites compared to its ESI counterparts. It has proven superiority over the former in its ionization efficiency towards lipids in a positive mode, which is eminent in the field of metabolomics.

B. Instrumentation and Source Design

While most overall designs for instruments in SICRIT were similar to those of DBDI, modifications were made that would accommodate dynamic chemical reactions occurring during the transfer phase. Specifically, the SICRIT system incorporates a special design that stabilizes the plasma environment and affords controlled ion-molecule interactions in an assigned reaction chamber.

A very important new innovation in the whole design of SICRIT is the careful control of the internal atmosphere within the ion source housing during the reaction. Gas flow, different voltage parameters, and types of discharge gases will be important contributors to the softening of the whole ionization process. Initial studies in which the performance of SICRIT has been compared with that of ESI show that SICRIT is capable of ionizing

metabolites, including some lipids, in considerably higher efficiency and specificity, indicating its possible expansion for future coverage in considering metabolic analyses of microbes.

C. Insights into SICRIT Ionization Mechanism

As far as detailed mechanistic studies into SICRIT are concerned, these are by no means exhaustive at this point, but what has been shown so far suggests that this ion source indeed produces a different profile of reactive species when compared to traditional DBDI setups. The import of in-transfer reactions in SICRIT signifies that its ionization process comprises a transient reaction region through which analytes come into close contact with reactive constituents of plasma.

This mechanism results in the following typical soft ionization process:

- Low Fragmentation: Analytes will receive soft protonation, which tends to ruin the structural integrity of the molecular ions and allows precision mass measurement.
- Selective Ionization: The chemical reactions transpiring within the transfer region lend themselves towards more selective ionization towards particular types of molecules such as lipids and provide a complementary profile of ions to what is seen with ESI.
- Fast Reaction Kinetics: The time in which the analytes are making the entrance into the mass spectrometer is very much short, so ionization occurs quickly, which favors high-throughput applications for metabolomics.

Thus, this mechanism will be found as one that avoids the disadvantages associated with conventional ionization techniques that are most of the time devoid of supplementary identification of known compounds, which holds much value in microbial metabolomics because so many different and complex metabolites are represented.

D. Advantages and Emerging Applications

There are various different advantages that SICRIT provides:

- Complementarity to ESI: Because ESI is frequently and widely used, resulting in the re-identification of known compounds, the complementarity of SICRIT is probably best configured for identifying new metabolites, primarily lipids, that may be neglected by ESI.
- Soft Ionization: The technique has been designed to ensure a minimal degree of fragmentation or, optimally, to keep the molecular ion intact. This leads to better identification accuracy.
- Efficiency in Microbial Metabolomics: Initial uses of SICRIT in the microbial environment are evidence that it generates a different and, at times, wider metabolite spectrum, aiding the discovery of new chemistries in microbial systems.

These advantages make SICRIT extremely attractive for those laboratories directed toward diversifying in analytical capabilities in the face of increased demand for the detection of subtle and complex metabolomic variation.

1.3.3.1.2.3 Comparative Analysis of DBDI and SICRIT

The advancement of ambient ionization technologies over the years has witnessed the transition from DBDI to SICRIT. While both methods operate on the same principle of arc discharge properties, slight modifications in design and reaction environment produce fundamentally different analytical outcomes.⁸⁵

A. Mechanistic Comparisons

Table 1.2: Comparative features of DBDI and SICRIT ion sources and their underlying ionization mechanisms

Feature	DBDI Ion Source	SICRIT Ion Source
Plasma Generation	AC high voltage across dielectric barrier produces plasma with helium metastables	Similar plasma generation mechanism using AC voltage; however, the emphasis is on maintaining a controlled reaction atmosphere during the in-transfer phase
Ionization Process	Predominantly involves Penning ionization where He* transfers energy to N ₂ , producing N ₂ ⁺ which subsequently forms protonated water clusters that ionize analytes	In-transfer chemical reactions facilitate the soft protonation of analytes without heavy fragmentation, leading to enhanced retention of the molecular ion
Fragmentation	Generally low fragmentation due to soft ionization, though conditions such as ambient humidity can influence the degree of fragmentation	Even lower fragmentation, with a focus on preserving intact molecular ions, especially lipids
Selectivity	Provides broad coverage suitable for various analytes including trace organics, explosives, and biological compounds	Offers enhanced selectivity for metabolites that are less efficiently ionized by ESI, with superior performance in lipid ionization
Key Reaction Pathway	Energy transfer via metastable helium leading to Penning ionization of N ₂ and subsequent proton transfer from water clusters	Controlled in-transfer protonation reactions that occur during the analyte's passage into the mass spectrometer, emphasizing chemical reaction dynamics in a confined environment

B. Instrumentation and Source Design

While the basic design principles have great similarities such as applying AC voltage and having a dielectric barrier, unlike other ion sources, an additional measure was taken by the SICRIT system to stabilize the in-transfer reaction kinetics. While a very basic electrode assembly with exposed plasma region potential between electrodes is used to realize the design of DBDI, the typical application of regular SICRIT illustrates the installation of a special chamber to control the ambient gas composition during ion transfer. This will cause an enhance softness and specificity ionization.

C. Application and Performance Issues

In terms of application-wise integration of both ion sources with separation techniques such as LC-MS, GC-MS, and IMS, new findings show that SICRIT distinguishes itself by targeting a set of metabolites distinct from ESI and even ordinary DBDI. Particularly with microbial metabolomics, where it is essential to detect new compounds, SICRIT exhibited great potential by cutting down the instances of "known unknowns" through better ionization for lipids and other bioactive molecules.

Thereby, certain conditions of operation play a key role:

- Environmental Sensitivity- Changes in humidity and ambient gas composition would cause DBDI performance to alter; meanwhile, the controlled in-transfer reaction chamber of SICRIT ensures increased reproducibility under diverse conditions.
- Ease of Miniaturization and Low Energy Consumption: DBDI is prized for its low energy requirements.

D. Comparative Insights Summary

In an elaborate comparison between the two ion sources, DBDI has always been a stalwart in ambient ionization techniques, whereas SICRIT has been a refined evolution for softer or more selective ionization. The main distinction between these methods largely relates to the nature of the reaction environment and the timing of the ionization: -DBDI utilizes external plasma processes and would work well on varying types of analytes, but it is subject to effects due to varying operating conditions. -SICRIT optimizes the ionization step during transfer, allowing for soft protonation and

greater profiling of metabolites, which is crucial for applications such as microbial metabolomics.

These differences are vital for practitioners choosing an ionization method that meets their own specific analytical objectives.

1.3.3.1.2.3 Visual Representations of Ion Formation Mechanisms

Visualizations are majorly helpful in explaining some of the more intricate aspects of chemistry strategy and overall plasma dynamics involved in ionization methods. Regarding this area, some schematic and flow diagrams characterizing the ion formation mechanisms for both DBDI and SICRIT are drawn.⁸⁶

A. Flowchart of DBDI Ion Formation Process

Below is a Mermaid flowchart that outlines the steps involved in DBDI ion formation (figure 1.13):

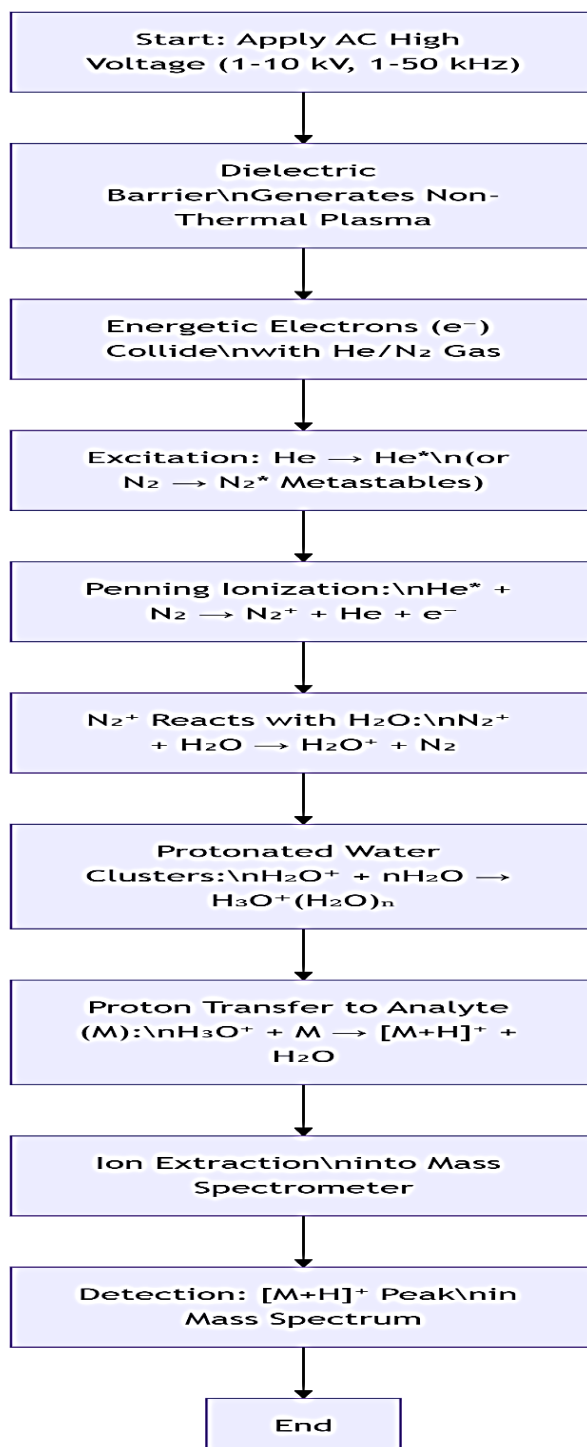


Figure 1.13: Flowchart detailing the step-by-step DBDI ion formation mechanism from plasma generation to analyte ionization.

B. Flowchart of DBDI Ion Formation Process

The unique in-transfer ionisation method used by SICRIT is depicted in the following Mermaid flowchart (figure 1.14):

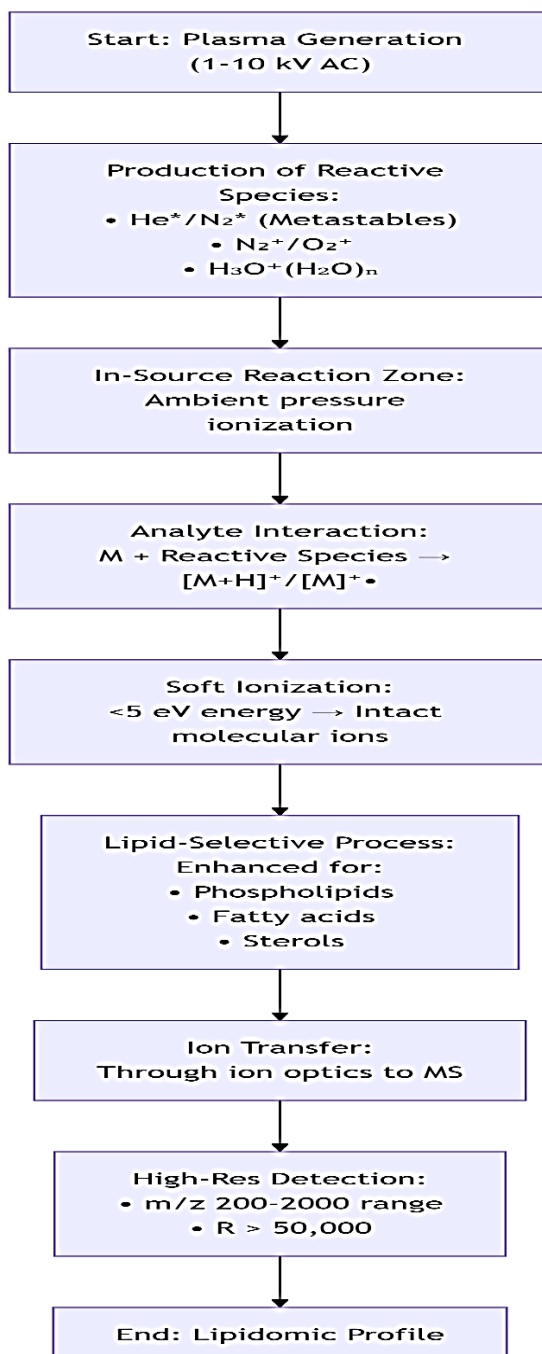


Figure 1.14: Flowchart illustrating the SICRIT ion formation mechanism, emphasizing the controlled in transfer chemical reactions that achieve soft ionization.

C. Comparative Diagram of Instrumentation Architecture

The following table visually summarizes differences in the instrument configurations of DBDI and SICRIT:

Table 1.3: summarizing the key instrument architecture differences between DBDI and SICRIT ion sources

Instrument Component	DBDI Ion Source	SICRIT Ion Source
Electrode Configuration	Needle electrode inside a dielectric tube with a counter electrode. Visualized in single-cell analysis schematics	Similar electrode design but with additional control elements for reaction environment stabilization.
Plasma Reaction Zone	Exposed plasma region where Penning ionization occurs.	Dedicated in-transfer reaction chamber regulating ambient gas composition.
Gas Flow Management	Reliant on ambient gases (helium/argon) with variable flow rates affecting plasma dynamics	Precisely controlled gas flows to optimize in-transfer reactions and minimize fragmentation.
Target Analyte Interaction	Ionization via proton transfer from water clusters generated in plasma	Ionization via direct in-transfer reactions promoting soft protonation

1.3.3.1.2.4 Applications, Advantages, and Limitations

A. Applications in Different Fields

DBDI and SICRIT set the way to ambient ionization in different arenas of analytical science⁸⁷:

- **Biological Analysis:** DBDI had already been used in the laser ablation electrospray ionization (LAESI-MS) technique for single-cell analysis, enabling proper biochemical characterization of cellular constituents.
- **Food Safety and Forensic Identification:** Quite suitable for analyzing pesticides, organochlorines, and forensic residues, DBDI applies low energy and does not require solvent extraction.
- **Microbial Metabolomics:** These lipid and metabolite ionization properties enable SICRIT to work in microbial metabolomics in a less redundant fashion, allowing the identification of terms from more novel backgrounds, whereas conventional ESI would produce well-characterized metabolite profiles.
- **Mass Spectrometry Imaging:** These ion sources find their application in imaging mass spectrometry techniques, but DBDI has mostly been demonstrated in coupling with TOF-SIMS and LA-ICP-MSI, thus revealing abundant spatial chemical information.

B. Advantages of DBDI

The chief advantages of DBDI are:

- **The Energy Efficient Way:** The low voltages at which DBDI operates and its minimum consumption of solvent render it cheap as well as eco-friendly.
- **Anytime Versatile:** The capacity/ability to ionize a wide range of analytes-small organic molecules to larger biomolecules-makes DBDI a universal tool in analytical.

C. Merits of SICRIT

SICRIT has a lot of novelties, which can make it more beneficial than other ionization techniques in respect to some of their limitations:

- **Soft Ionization:** The concentration of in-transfer chemical reactions maximizes the preservation of the molecular ion, especially on fragmentation, which is important for proper identification of the compound.
- **Increased Selectivity:** The ionization profile obtained by SICRIT shows exceedingly efficient performance in metabolite classes with lipids, which are among the least detected in ESI spectra.
- **Diverse Analytical Coverage:** In combination with ESI, SICRIT can detect further metabolites thus reducing the chances of duplicate detections and attaining a more thorough metabolic profile.

D. Limitations and Challenges

Both ion sources suffer from some disadvantages:

- **Environmental Dependence:** The entire performance of DBDI is highly subjected to the environmental humidity and gas compositions. Variations of those parameters will create inconsistency concerning the ion production and signal intensity.
- **Signal Variable:** Since DBDI has a different distribution of the plasma and an ionization efficiency declining across the ionization region, effects may be witnessed in the variability of signal reproducibility and hence accurate calibration and optimization must be employed.
- **Technical complexity for Reaction control:** Though SIGRIT offers an acceptable increase in selectivity, setting and maintaining appropriate conditions inside the in-transfer reaction chamber need a fine control parameter with respect to the above-mentioned amplifications.

This work provides a comparative overview of DBDI and SICRIT ion sources for application in modern mass spectrometry. DBDI generates a low-temperature plasma via AC high voltage, creating metastable helium species that instigate Penning ionization of atmospheric nitrogen. This technology enjoys a high degree of versatility and compatibility with different coupling techniques, although it is very sensitive to ambient conditions. SICRIT expands upon the concept of DBDI, incorporating an in-transfer reaction mechanism that stresses soft ionization, especially germane for lipid analytes in the field of microbial metabolomics. It provides complementary ionization profiles to that offered by conventional ESI with the potential to minimize the rediscovery of known compounds in metabolomic studies. A controlled reaction chamber is integrated to facilitate a rapid and gentle protonation process with minimized fragmentation, thereby securing molecular ion fidelity.

In both processes, ionization takes place in the presence of plasma; however, they differ with respect to timing and environmental control. DBDI stands as a solid and versatile technique, while SICRIT holds realize value for applications demanding high selectivity and soft ionization. The choice of either technique should take into account sample type, requisite analytical sensitivity, environmental conditions, and the needs for complementary data from more classical ionization methods.

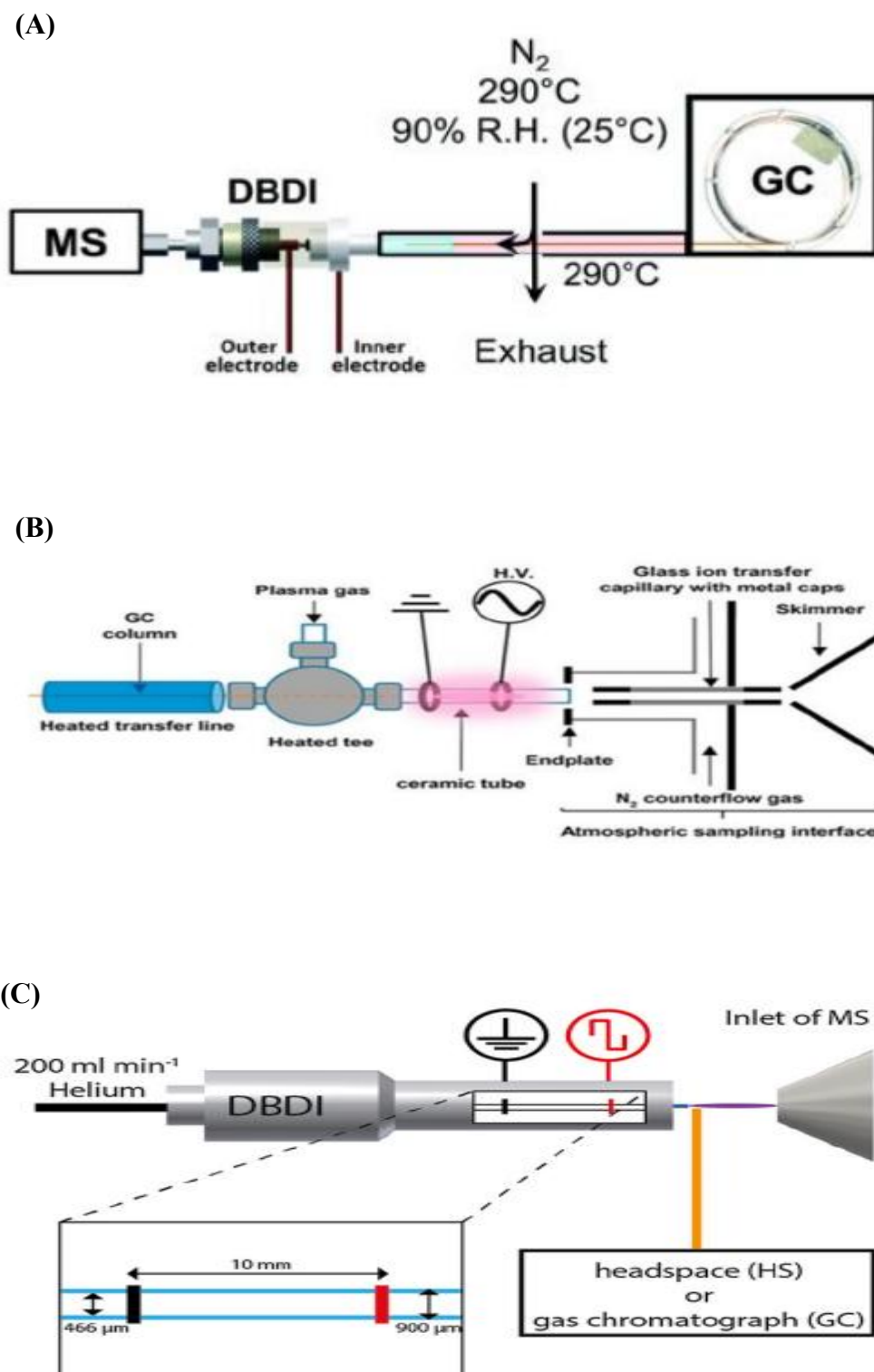


Figure.1.15: (A) active capillary ionization DBDI, (B) AP-DBD, (C) DBDI.⁸²

1.3.3.2 Mass Analyzers

Mass detectors are used in GC to detect and provide a m/z for the different analytes that elute from the chromatographic column. For the reason of identifying and quantifying compounds, GC is commonly combined with EI MS; however, other masses analyzer types may be employed in GC-MS devices.

A number of different mass analysers were used in this study: a quadrupole mass spectrometer (SQ), an ion trap mass spectrometer (ITQ), both of which are low resolution analyzers, SQ mass analyzers along with ion traps serve distinctive purposes which separate them functionally since quadrupoles operate continuously with electric field oscillation (5-20 Hz) for rapid scanning for quantification applications yet ITQ works sequentially across three dimensions applying dynamic fields (0.1-2 Hz) for superior sensitivity and MS^n fragmentation analysis. This combine obtaining structural information about unknown samples because ITQ devices analyze compounds within one instrument with multi-stage fragmentation capabilities and obtaining high speed measurements of narrow peaks because quadrupoles deliver better precision and broader range and faster response times. In addition to a linear ion trap mass spectrometer (LTQ), and an orbitrap mass spectrometer, these are detailed in turn below.

1.3.3.2.1 The Ion Trap Quadrupole (ITQ) MS

A quadrupole ion trap, is a type of ion trap known as a Paul trap, where charged particles are trapped using dynamic electric fields. An ITQ consists of two end-cap electrodes and another electrode in the form of a ring, so that the two end-cap electrodes are opposite each other and the ring electrode is placed between them, as shown in the figure 1.16. A direct current (DC) voltage is applied to the end-cap electrodes and an oscillating RF voltage is applied to the ring electrode, which creates a dynamic electric field.

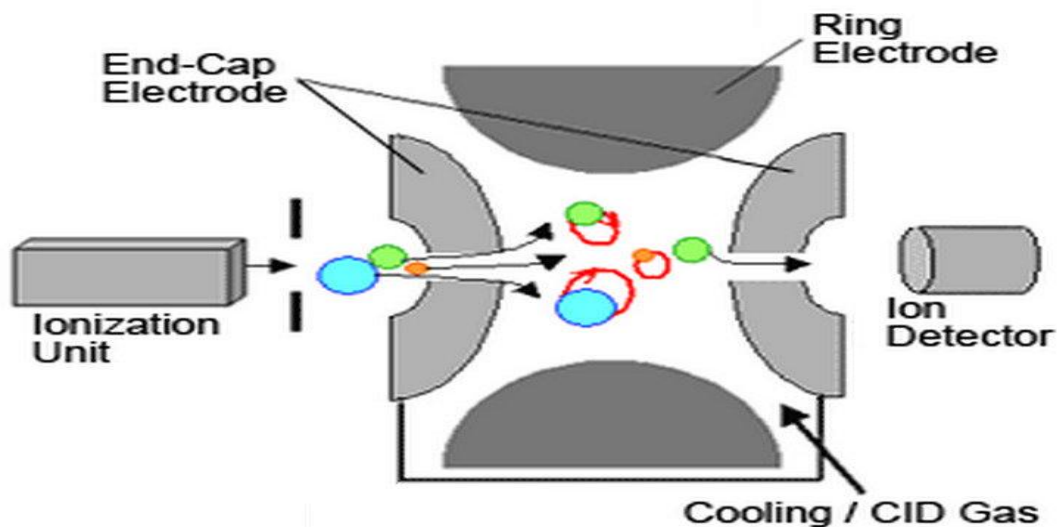


Figure 1.16: Schematic of a trap quadrupole¹⁶¹

The mass analyzer can store ions (individual ions and selectable ranges) and manipulate ions for mass spectrometric analysis. Ion traps are able to perform MS² experiments (MS/MS). An ITQ is able to detect low abundance ions due to its high sensitivity but are generally slower than quadrupoles because their sequential operation of trapping, stabilization and mass-selective ejection steps consume time during each scan in addition to the period needed for field reset. ITQ systems have a lowered peak acquisition speed because of their ion-focusing requirements which means they work better with broad peaks rather than rapid GC separations with narrow peaks. However, they achieve high sensitivity through ion accumulation and a MSⁿ structural analysis capability which quadrupoles lack.

ITQMS has many applications including pharmaceutical analysis and environmental analysis such as pesticides.⁸⁸

1.3.3.2.2 Quadrupole Mass Analyzer (QMS)

A Quadrupole MS is a mass analyzer that uses a single quadrupole as the mass analyzer consisting of four horizontal metallic rods placed in a rectangle arrangement, where each pair of rods is connected together electrically and given either +ve or -ve DC voltage. A radio frequency voltage is applied between the pairs of rods. The applied radio frequency

voltage is varied to allow all ions to pass or to select transmission of ions of a desired m/z ratio. where it is desirable to select a particular m/z , the radio frequency voltage is used to make the trajectory of all other ions passing through the quadrupole unstable. These ions non-selected ions simply collide with the rods and are not detected (Figure 1.17). By selecting identifying ions of interest, the quadruple functions as a mass filter, shifting across a range of m/z values

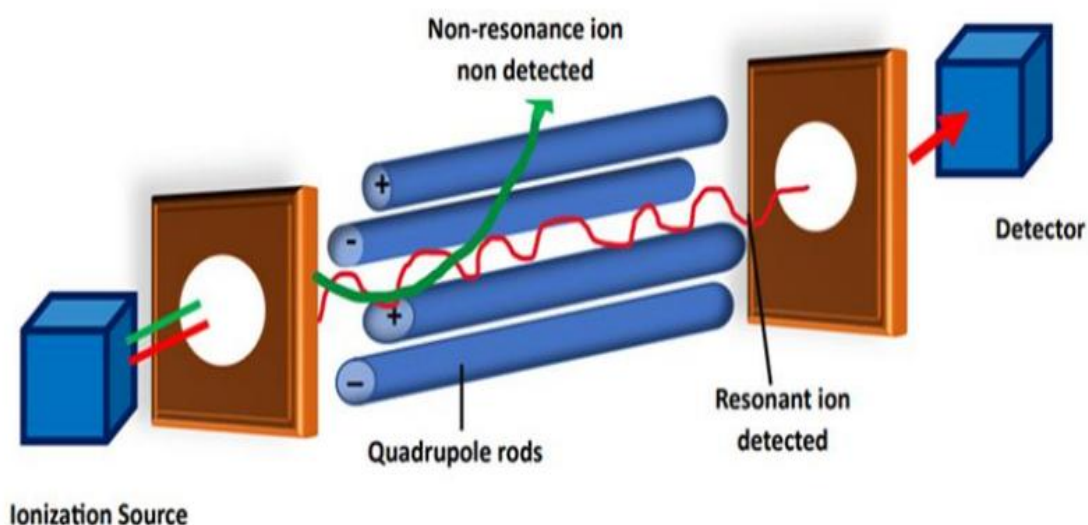


Figure 1.17: Quadrupole mass analyzer schematic.⁹⁸

A quadrupole mass analyzer is selective, as it is able to isolate specific ions in complex mixtures based on the m/z ratio. It is sensitive, as it has a high efficiency for ion transmission, and are regarded as robust enough for punishing routine operation thus. maintenance is infrequent giving a high ratio of uptime vs cleaning/repair.

It has several applications, including: Pharmaceutical Analysis, Environmental Monitoring, Food Safety, and Forensic Science. There are currently a number of GCMS available in the market that feature a single quadrupole analyzer, Agilent GC/MSD is one such device that is widely used in environmental and food analysis⁸⁹.

Comparative Analysis of Low-Resolution Analyzers (ITQ vs. SQ):

The ITQ and SQ analyzers belong to the category of low-resolution tools ($R < 4,000$) although they possess distinct features as shown in table 1.4.

Table 1.4: summarizing the differences between ITQ and SQ

Performance Characteristic	Ion Trap (ITQ)	Quadrupole (SQ)
Mass Analysis Principle	Sequential ejection/storage	Continuous filtering
Resolution	0.2-0.8 Da (unit mass)	0.5-1.0 Da
Mass Range	50-2000 m/z	10-3000 m/z
Scan Speed	Moderate (0.5-2 Hz)	Fast (up to 20 Hz)
Tandem MS Capability	MS ⁿ in same device	Requires multiple quadrupoles
Sensitivity	Higher (ion storage)	Lower
Dynamic Range	Limited by space charge	Wider linear range
Quantitation Precision	±15-20% RSD	±5-10% RSD
Fragmentation Control	Excellent (CID in trap)	Limited
Cost	Moderate	Lower

Key Advantages of ITQ:

- Superior MS/MS capabilities without additional analyzers
- Higher sensitivity due to ion accumulation

The instrument allows operators to perform consecutive fragmentation steps known as MSⁿ.

Key Advantages of SQ:

The instrument can analyze at speeds fitting GC peak durations.

- Better quantitative precision
- More robust for routine analysis
- Lower susceptibility to space charge effects

1.3.3.2.3 Orbitrap Mass Analyzer

The Orbitrap mass analyzer is a type of ion trap mass spectrometer known for its high resolution, high mass stability and excellent mass accuracy.

An outside electrode that resembles a barrel surrounds a central axis inside the Orbitrap analyzer. Charged ions are injected into the orbitrap, they process around and across the center spindle to create an image potential in the outermost electrode. Measurement and Fourier transformation of this image current creates a time-based spectrum to which m/z values can be ascribed. A simple diagram of an orbitrap mass analyser is shown in figure 1.18.

The orbitrap analyzer is perfect for precise mass measurements, this can help with the identification of unknown substances.

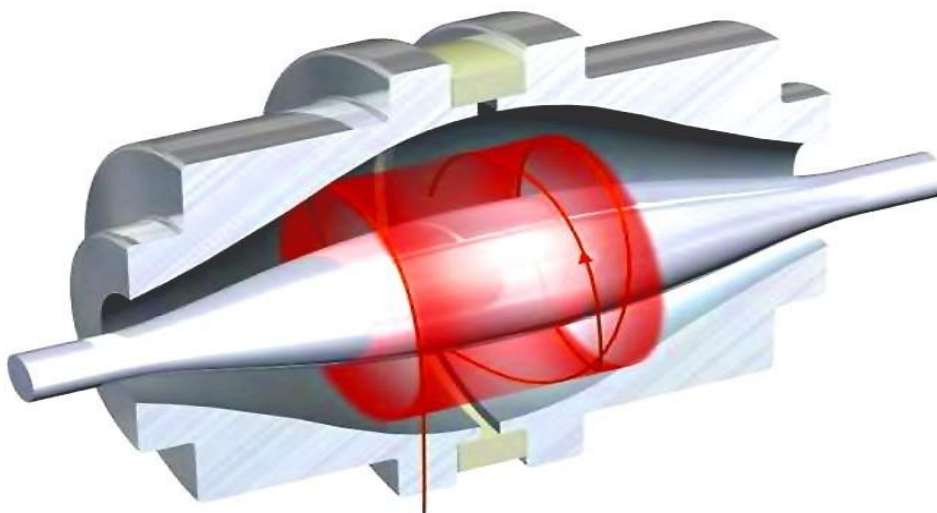


Figure 1.18: Orbitrap mass analyzer schematic. ¹⁶⁰

To provide a powerful tool for high-resolution and high-accuracy mass spectrometry, a Linear Trap Quadrupole (LTQ) and an Orbitrap mass analyzer are combined to give a hybrid instrument.

The benefits of the two-mass analyzers, the Orbitrap and the linear ion trap arise a result of the combined setup leveraging the capabilities two complimentary mass analysers. Both mass analyzers work in tandem, but the LTQ can be used independently of the orbitrap to perform addition experiments whilst the orbitrap is occupied. This synergistic

working mode enables the generation of a wealth of data consisting of complimentary highly accurate mass measurements with similarly detailed ion fragmentation spectra.

The Orbitrap equation refers to the fundamental relationship used in Orbitrap mass spectrometry to determine the mass-to-charge ratio (m/z) of ions based on their oscillatory motion in the electrostatic field of the Orbitrap analyzer. The equation links the angular frequency (ω) of an ion's axial oscillations to its m/z value.

Key Equation:

The frequency of an ion's harmonic oscillation in the Orbitrap is given by:

$$\omega = \sqrt{\frac{k \cdot (z \cdot e)}{m}} \quad \text{Eq.1.7}$$

Where:

- ω = Angular frequency of the ion's axial motion (rad/s)
- k = Field curvature constant (depends on Orbitrap geometry and voltage)
- z = Charge number of the ion
- e = Elementary charge ($\sim 1.602 \times 10^{-19}$ C)
- m = Mass of the ion (kg)

Rearranging to solve for m/z (where z is the charge state and m is the mass):

$$\frac{m}{z} = \frac{k \cdot e}{\omega^2} \quad \text{Eq.1.8}$$

Since $\omega = 2\pi f$ (where f is the measured frequency in Hz), the equation becomes:

$$\frac{m}{z} = \frac{k \cdot e}{(2\pi f)^2} \quad \text{Eq.1.9}$$

The Orbitrap detects these oscillations via **image current** and uses **Fourier Transform (FT)** to convert the time-domain signal into a frequency spectrum, from which m/z values are calculated with high precision.

Fourier Transform (FT) is a mathematical operation that decomposes a time-domain signal (e.g., the oscillating image current from ions in the Orbitrap) into its constituent **frequencies** and their **amplitudes**. In mass spectrometry:

- **Input:** A time-dependent signal of ion oscillations.
- **Output:** A frequency spectrum (peaks at specific f_{z}), which is converted to m/z using the Orbitrap equation.

FT enables ultra-high-resolution mass analysis by precisely resolving closely spaced frequencies (and thus m/z values).

Key Role in Orbitrap:

- Converts transient ion oscillation data into a mass spectrum.
- Allows resolution $>100,000$ (FWHM) by measuring frequency differences as small as microhertz.

LTQ Orbitrap analyzer

The system used in this study was a ThermoScientific Orbitrap XL.

The ions produced by the ion source normally first pass through the LTQ mass analyzer, where ions are trapped and held in a linear quadrupole trap by electric fields, and then based on mass-to-charge ratio m/z , the trapped ions are extracted (Figure 1.18). The analyzer can act in transmission mode where all ions are passed to the orbitrap or in a mass selection mode, where user/instrument defined mass ranges are captured before orbitrap mass analysis. The Orbitrap detector receives the selected ions or ion fragments, that are of interest after they have been selected/created in the LTQ, for accurate mass measurement (Figure 1.19).

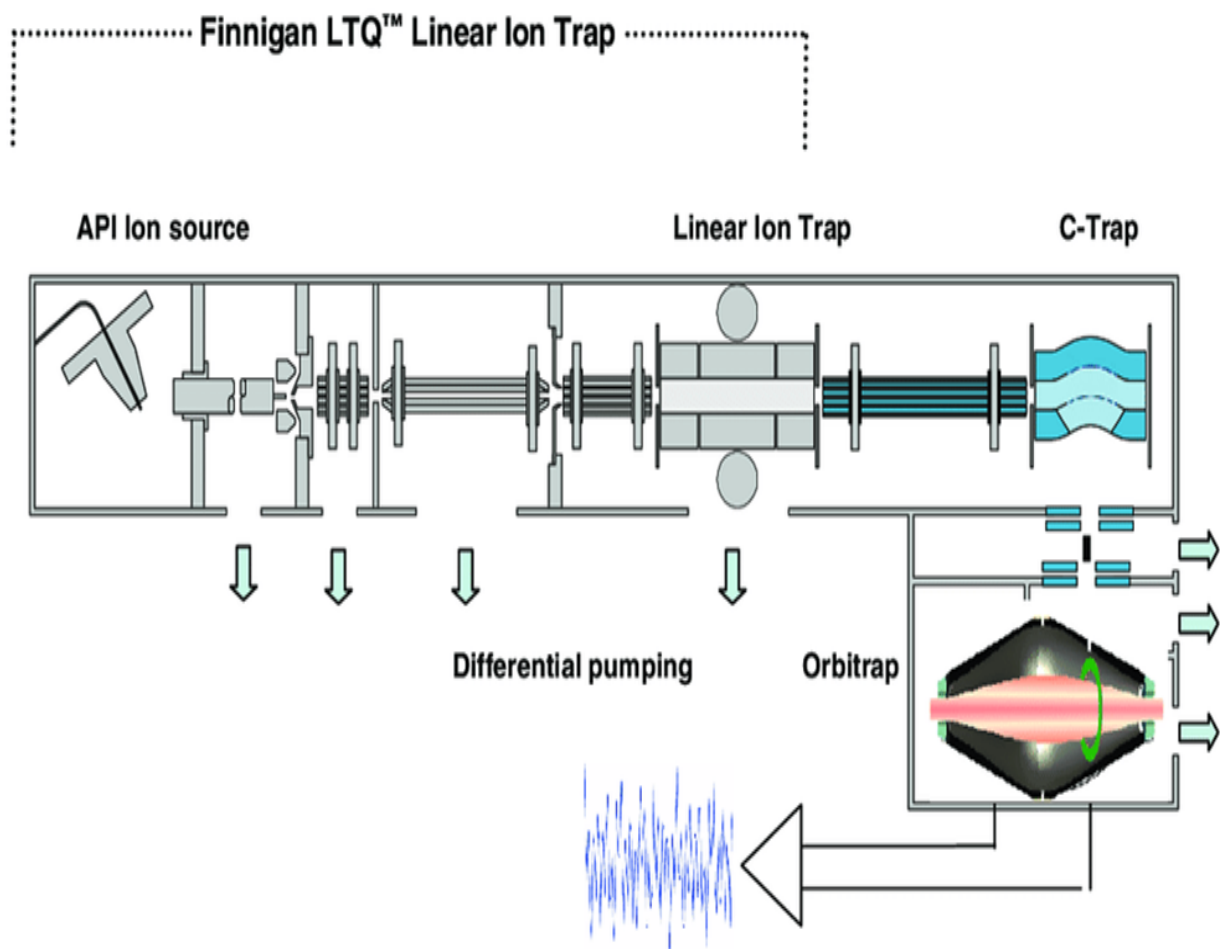


Figure 1.19: Schematic of LIT-Orbitrap.¹⁶⁰

1.3.3.3 Detector

A detector is an essential part of a mass spectrometer, playing an important role in identifying and measuring ions. There are several types of detectors, some of the commonly used types include electron multipliers (EM), Faraday cups (FC), photomultiplier conversion dynodes and array detectors each with specific characteristics and functions, each with its own strengths and weakness, and are selected based on the instrument requirements by the instruments manufacturer. The detector is characterized by Sensitivity, Accuracy, Speed, and Versatility, making it an important part of a mass spectrometer⁹⁰.

In this study, several types of MS were used, each with a specific type of detector that depends on the mechanism of analysing the ions and recording the signal.

1. LTQ Orbitrap MS: Employs an image current detector.
2. MSD (Mass Selective Detector): Typically incorporates either an electron multiplier detector or a photomultiplier tube.
3. ITQMS (Ion Trap Quadrupole MS): Utilizes an electron multiplier detector.

1.3.3.4 Computer system

The computer system is an integral part of mass spectrometry operations where data is acquired and analysis performed. Through the computer system, instrument parameters can be adjusted, signals processed, real-time monitoring and peak identification can be carried out.

After completing the workflow, from sample introduction to data analysis, the entire analytical workflow must be validated through a method validation process.

1.3.4 Method validation

Validation of methods is an important process in analytical chemistry, ensuring that a particular analytical method being developed is suitable for the intended application. It involves a critical examination of the performance characteristics of the method being validated so that the reliability, accuracy and robustness of the results to be obtained are confirmed which should be meaningful and reproducible. It covers all aspects of the method, including range and linearity, limit of detection (LOD), limit of quantification (LOQ), precision, accuracy, selectivity, and matrix effects, in detail.

1.3.4.1 Range and linearity

Range: The volumetric range wherein a technique is shown to yield accurate and repeatable responses is referred to as its range of values. It defines a range of concentrations of a pesticide that the method/instrumentation can accurately identify and quantify; it should be noted that these parameters are compound specific. A larger range shows that the technique can precisely identify levels of pesticide both high and low.⁹¹

Linearity: The capacity of an analysis to yield findings that are exactly proportionate with the concentrations of the component within the specimen is known as linearity. This implies that the statistical technique's responsiveness ought to vary linearly with changes in analyte concentration. In practice, this guarantees precise quantification over a broad intensity range. The linearity is assessed by the correlation coefficient (R^2) values from a calibration curve close to 1 show good linearity.⁹²

1.3.4.2 Limit of detection (LOD)

LOD is one of the most important parameters in analytical chemistry, which defines the lowest concentration of an analyte that can be differentiated with certainty from background noise using a developed analytical method.⁹³ This is the threshold below which the presence of the analyte cannot be detected with statistical confidence, and above which it can be identified and quantified with a certain reliability.

The LOD is typically estimated from considerations of statistics based on Signal/Noise measurements. Conventionally, an S/N of 3:1 or, in some instances, 2:1 defines the LOD. This means that the analyte signal differs from instrumental or sample matrix noise by a 2 or threefold multiplier. To determine the LOD, it is necessary to prepare and analyze blank samples (samples containing no analyte) and samples spiked with a low concentration of the analyte. These results are then used in calculating the LOD, which depends on the variability of the detected compound observed in the blank and the low concentration sample's signal response. Statistical methods such as the slope of a calibration curve can also be applied by preparing a series of low concentration standards and measuring their response by constructing a calibration curve. The slope of the calibration curve is calculated and the standard deviation of the response is found. The LOD is then calculated by applying the following formula:⁹⁴

$$\text{LOD} = 3.3 \sigma / S \qquad \text{Eq.1.10}$$

Where:

- σ = the standard deviation of the response
- S = the slope of the calibration curve

The calibration curve method is more general and can be applied to different analytical methods. In addition, it is more accurate because in the measurements, it considers the full range of data and also the variability inherent to the data.

A lower LOD indicates that the analytical method is more sensitive, hence it can detect trace quantities of the analyte with greater confidence. This is important, especially in environmental monitoring, food safety, and pharmaceutical applications where the detection of residues or active substances at low levels can be very critical to compliance and safety assessment requirements.

It is within the LOD that method validation is harnessed to affect overall effectiveness in real-world applications of analytical techniques. The accurate determination of the LOD would mean that methods are being developed able to detect analytes at concentrations relevant to regulatory standards and practical requirements, ensuring reliable and precise measurements in complex sample matrices.

1.3.4.3 Limit of quantification (LOQ)

Quantification is that important parameter in analytical chemistry which gives the lowest level of concentration of an analyte in a sample that may be reliably quantified with acceptable precision and accuracy. In contrast to the Limit of Detection, the LOQ is about the reliable and reproducible quantification of an analyte at low concentration levels rather than the capability to detect the presence of an analyte.⁹⁵

The LOQ is based mainly on statistical analysis of calibration graphs relative to signal-to-noise ratios and is usually set at an S/N ratio of 10:1. This ensures that measurements are not only above the noise level but also provide reliable quantification with minimum variations. The LOQ is determined through use of a series of samples spiked with known concentrations of the analyte, and by assessing the consistency in the measurements, as well as precision and accuracy of results obtained.

By applying statistical analysis, the LOQ can be calculated by applying the following equation:⁹⁶

$$\text{LOQ} = 10 \sigma / S \qquad \text{Eq.1.11}$$

Where:

- σ = the standard deviation of the response
- S = the slope of the calibration curve

The lower the LOQ, the higher the sensitivity of the analytical method. High sensitivity is very important to detect and quantify trace levels of any substances, especially for

pharmaceuticals, environmental analysis, and food safety. Consequently, the LOQ in any regulation may be such that it can offer measurements of residual pesticides, contaminants, or active ingredients at concentrations relevant to regulations associated with health and safety with required accuracy.

The LOQ is an inseparable part of method validation and establishes the reliability of the analytical method in relation to practical applications. It confirms that the method will be able to quantify analytes present at low concentrations with enough accuracy and precision, hence proving its effectiveness in real-world scenarios by collecting accurate data to meet regulatory standards.⁹⁷

The standard deviation (σ) is used instead of the standard error (SE) when calculating the Limit of Detection (LOD) because the LOD is concerned with distinguishing an analyte's signal from background noise in individual measurements, not with the precision of the mean estimate. In order to determine the minimum detectable signal with statistical confidence (usually 3.3σ for 99.7% certainty), the standard deviation is essential because it captures the inherent variability (noise) in replicate measurements (such as blanks or low-concentration samples). The standard error (σ/\sqrt{n}), on the other hand, represents the mean's uncertainty and is unimportant for identifying noise in individual observations. While σ guarantees that the detection threshold allows for real-world measurement scatter, in accordance with regulatory guidelines (e.g., IUPAC, ISO) and practical analytical requirements, using SE would artificially lower the LOD, increasing the risk of false positives.

1.3.4.4 Precision

Regarding the evaluation of pesticides, precision pertains to the reproducibility or uniformity of outcomes resulting from successive measurements with the same material within identical conditions. Assuring that the approach to analysis can yield dependable and repeatable findings constitutes a crucial component of the validation process as well as assessment. The level of concordance between each measurement and test findings achieved within specific circumstances is known as precision. It provides a measure of how multiple measurements of a single material provide comparable outcomes in the larger setting of pesticide testing.

Precision Categories

- Consistency, also known as intra-day precision, measures the methods ability to generate the same level of precision throughout a brief period of time—usually on the comparable day—while maintaining identical operational circumstances. It evaluates the consistency with which results may be replicated by an identical researcher utilizing the exact same methods and instruments.
- The expression "intermediary precision" refers to the level of accuracy that varies among different days, experts, or equipment in a single lab. It evaluates the technique's resilience across time and across the different system in a single lab.
- Reliability goes beyond low precision to encompass accuracy attained in different environments, like other labs or with different equipment. It evaluates the resilience of the procedure in multiple settings.⁹⁸

Precision can be expressed as the standard deviation, relative standard deviation (RSD), or coefficient of variation (CV).

1.3.4.5 Accuracy

The degree to which a value that is determined for a concentration of pesticide approaches its actual or suitable level is referred to as accuracy during pesticide testing. Establishing all analytical findings are reliable and can be trusted for making judgments about food security, ecological impact, as well as adherence to regulations is a crucial part of validation of methods and quality control. The degree of precision among the measured value produced by a technique of analysis and the actual amount of the pesticide level in the specimen, or a recognized standard, is referred to as accuracy. It shows that the technique may yield findings that accurately represent the concentration of pesticides actually present. Accuracy is determined by recovery, which is assessed through a recovery study. This study involves adding a known quantity of a compound(s) to the sample and measuring the amount recovered using the following equation:⁹⁹

$$\text{Recovery (R)\%} = \frac{C_{\text{experimental}}}{C_{\text{theoretical}}} \times 10 \quad \text{Eq.1.12}$$

Where:

- (C theoretical) = known concentration
- (C experimental) = experimental concentration

1.3.4.6 Selectivity

The capacity of an analyzer to distinguish and precisely quantify the specific compound(s) that are important regardless of additional chemicals that could be found within the matrix of samples is referred to have selectivity during its analysis. This is a crucial feature that guarantees the technique can precisely identify and measure compounds with no influence from additional co-eluting substances or matrix elements. The ability of a method of analysis to identify and quantify the desired pesticide(s) in an intricate sample matrix, like food and ecological samples, avoiding influence by potential additional elements is known as selectivity.

1.3.4.7 Matrix effects

The impact of elements encountered in a sample matrix upon the precision and reproducibility of quantitative measures of the residual pesticide are commonly referred to by the term matrix effects in the investigation of pesticides. If the sample matrix is found to interfere with the analytical outcome this may affect the identification and measurement of the targeted analytes. these consequences may impede the evaluation and introduce bias or errors into the results.

Matrix Effect Categories:

Suppression: In a chromatographic evaluation, matrix elements may decrease the signal strength by suppressing ionization or identification of target substances. Due to this, the levels determined of analytes may be less than those found in the specimen.

Enhancement: On the other hand, matrix elements may improve targeted pesticide adsorption or identification, resulting in an elevated response. As a consequence, the amounts of analytes reported may be greater than those found in the specimen.

The Matrix effect, on a per analyte basis, can be calculated using the following formula:⁹⁵

$$M.E. = \left(\frac{\textit{Spike in matrix}}{\textit{Spike in pure solvent}} - 1 \right) \cdot 100\% \quad \text{Eq.1.13}$$

in case of more than 20% signal suppression or enhancement, A value of 100% is considered as no effect, $\pm 20\%$ values are considered as soft ME, $\pm 50\%$ values are considered moderate ME, and the values outside $\pm 50\%$ are considered as strong ME.⁹⁵

Below are different ways to deal with matrix effects (ME) in chromatographs: sample cleanup (e. g., SPE, QuEChERS), which removes the interference from matrix components; use of matrix-matched calibration to compensate for level of signal suppression/enhancement; addition of isotope-labeled internal standards to compensate for variability; dilution of the sample to control matrix interference; optimization of chromatographic methods (e. g., choice of column, mobile phases, etc.) to increase the analyte resolution; quasiperiodic application of post-column infusion for prediction of the ME regions; and the other ionization modes (e. g., ESI+, ESI-) for suppression mitigation. Providing reliable quantitation data solutions with strong ME ($> \pm 50\%$) is a challenge, needing matrix-matched calibration standards and internal standards combined with specific cleanup procedures.

2. Material and methods

2.1 Chemicals & Samples

2.1.1 Standard solution preparation

Restek (Restek Ltd, Buckinghamshire, England) provided 103 compounds in pesticide solution kits that were purchased (see Table 8-1 of Appendix Tables). Interim concentrations of 10 mg/L for each insecticide were made in Acetonitrile (MeCN), LC/MS purity grade and kept at -4°C in the dark in amber screw-capped vials made of glass. Dilution in MeCN was used to generate an effective solution at a proportion of 1 mg/L, which was then kept at -4°C . In MeCN, the calibration lines were produced using mixed standards at 1, 5, 10, 25, 50, 100 and 500 $\mu\text{g/L}$. As a reference standard (IS) for GC-MS analysis, α -BHC-D6 and parathion-D10 at 40 $\mu\text{g/mL}$ in MeCN from Restek Ltd., Buckinghamshire, England, were utilized. The last stage of the extraction process was completed using the operational IS solution (10 $\mu\text{g/L}$ in MeCN) before the resultant specimen was injected into the GC-MS device.

2.1.2 Baby food samples

The baby food samples viz., milk, cereal flour, and baby rice were randomly collected from local markets. The samples were packed in plastic bags with their respective infant formula and stored at ambient temperature until investigation.

2.1.3 General Equipment

- Vortex, Whirlimixer, UK
- Centrifuge, Thermo ScientificTM Sorvall ST 8 centrifuge, UK
- Analytical balance, Sartorius ENTRIS 64-1S, UK

2.2 Preparation of samples

2.2.1 QuEChERS Extraction

Two types of extraction kits were used: original unbuffered procedure: contains 4 g of anhydrous MgSO₄ and 1 g of NaCl, and AOAC 2007.01 method: contains 6 g anhydrous of MgSO₄ and 1.5 g anhydrous of NaOAc were acquired from Restek Ltd. in Buckinghamshire, England. The AOAC Certified QuEChERS Method was applied to extract the pesticide residues with minimal modifications. A 50 mL polypropylene centrifuge tube was filled with 15 grams of homogenized baby food samples, and the mixture was manually stirred for 10 seconds. After adding 15 milliliters of MeCN, that had been acidulated with 1% acetic acid (v/v), the resulting solution was swirled for one minute using vortex. Following vortexing, the tube was filled with 6.0 g of anhydrous MgSO₄ and 1.5 g of NaOAc. It was then vortexed once more for one minute. The resulting mixture was placed in the centrifuge then it was spun up at 4500 rpm for five minutes at ambient temperature. Results showed significant similarity between both kits (see Appendix, figure 8.10). However, the AOAC method was ultimately adopted in the experiment because its formulation includes NaOAc. This compound adjusts the pH of the extraction environment, enhancing the stability of target components particularly critical given diverse chemical structures of the tested pesticides.

2.2.2 Clean-up Procedures

A clean-up procedure is required after the first extraction from an aliquot of supernatant (organic solvent layer) to get rid of co-extracted matrix elements that can affect the analysis. A dispersive solid-phase extraction (d-SPE) approach was utilized, a crucial component of the QuEChERS methodology, that were acquired from Restek Ltd. in Buckinghamshire, England.

The d-SPE procedure was as follows:

1. Aliquot Transfer:

- An aliquot of the supernatant from the centrifuged extract was transferred to a 15 mL polypropylene centrifuge tube.

2. Sorbent Addition:

- 400 mg of C18-EC (end-capped)
- 400 mg of PSA (primary secondary amine)
- 1200 mg of MgSO₄
- These sorbents were added to the tube containing the extract aliquot.

3. Mixing:

- The tube was vortexed for 1 minute to ensure thorough mixing of the extract with the sorbents.

4. Centrifugation:

- The mixture was centrifuged at 4500 rpm for 5 minutes at room temperature.

5. Extract Collection:

- The supernatant was carefully collected for subsequent analysis. A graphical overview of the process is presented in figure 2.1.

Acetonitrile (MeCN) is not suited as a GC injection straight solvent because it has a very low boiling point (82°C), which translates as bad analyte focusing at the column head and therefore either very broad peaks or split peaks as well as liner/column degradation in GC. QuEChERS elute is in MeCN so a ****solvent exchange**** (e.g., evaporation and reconstitution to GC-usable solvents such as ethyl acetate or hexane) is typically necessary to achieve peak shapes, system stability and sensitivity in GC-MS measurements. This is essential to prevent the MeCN from fouling chromatography and introducing matrix effects, as solvent exchange is very important for reliable results, although large-volume injection (LVI) with liners optimized for this purpose offers alternatives.

The role of each sorbent in the d-SPE clean-up:

- C18-EC (octadecylsilane, end-capped): Removes non-polar interfering substances such as lipids and some pigments.
- PSA (primary secondary amine): Removes polar matrix components like organic acids, some pigments, and some sugars.

- MgSO_4 : Removes any residual water and helps to improve the separation of the liquid phases.

This clean-up step is crucial for:

- Reducing matrix effects that can affect the ionization efficiency in mass spectrometry.
- Improving the chromatographic separation by removing potential interfering compounds.
- Protecting the analytical instrument from contamination, thereby increasing its longevity.

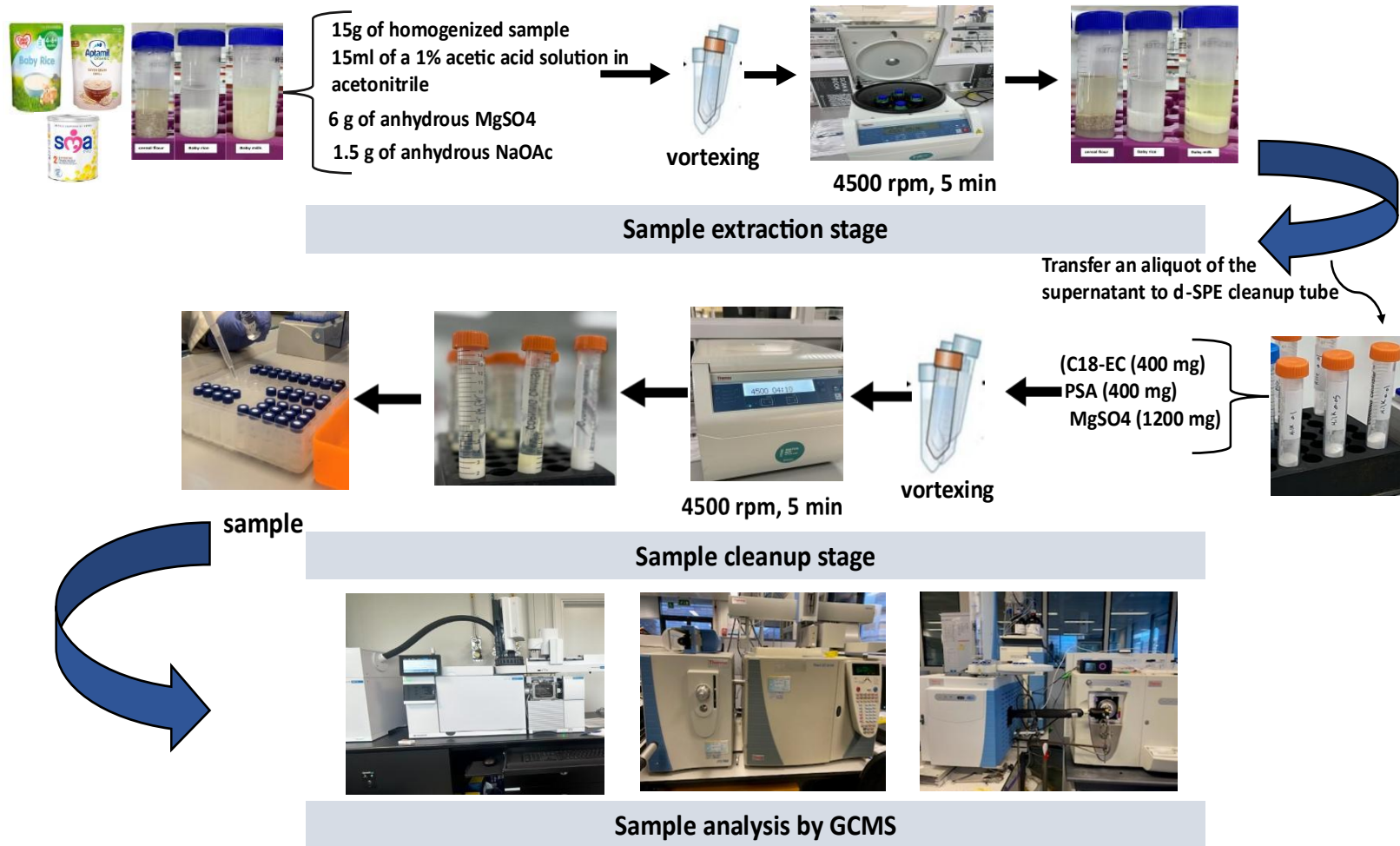


Figure 2.1: QuEChERS Sample Preparation Procedures.

2.3. Improving chromatographic analysis methodology: development of experimental conditions and evaluation of efficiency.

In this section, the focus is on developing a chromatographic analysis methodology with the aim of improving separation performance in each experiment. So multiple GC analytical parameters were optimized to obtain optimal separation and sensitivity and reproducibility for analyzing the pesticides. The approach involved optimizing multiple elements such as column selection and temperature program optimization as well as carrier gas flow rate efficiency and ion source and MS conditions and method validation. Two columns of different lengths were used, Rxi-5HT GC Capillary Column, 15 m, 0.25 mm ID, 0.25 μm and Rxi-5ms GC Capillary Column, 30 m, 0.53 mm ID, 1.5 μm . Although these two types have the same chemical composition and both are Low-polarity phase, 5% diphenyl / 95% dimethyl polysiloxane, the studied pesticides were not detected using Rxi-5HT but they were detected using Rxi-5ms as shown in figures 8.5, 8.6, 8.7, and 8.8 in the appendix section. The chosen phase for the column demonstrated remarkable ability to separate pesticides from four major categories including organophosphorus, organochlorine, organonitrogen, and pyrethroids. The chosen dimensions of the column strike a balance between peak resolution and method completion duration. Peaks that co-eluted showed optimal resolution when analyzed through the 30 m column compared to column length 15 m. After verifying the effectiveness of the selected column, Analyte separation and detection were performed by (GC–SICRIT-LTQ Orbitrap MS) table 1.5. The results indicate that both methods have the ability to separate, but the first method involved interference between compounds, as shown in figure 2.2, which may affect the accuracy of the analysis. In contrast, the second method achieved better and clearer separation, as shown in figure 2.3, increasing the reliability of the results. This was applied to all pesticides, as shown in figure 8.15, 8.16, 8.17, and 8.18 in the appendix.

Table 2.1: Gas Chromatography-Mass Spectrometry –(GCMS-TIC) Parameters for pesticides analysis methods.

Parameter	Method 1	Method 2
Carrier gas	Helium	Helium
Inlet temp	250°C	250°C
Mode	splitless	splitless
Injection volume	1 µL	1 µL
column	An Rxi-5MS low-polarity phase; Cross bond diphenyl dimethyl polysiloxane with 30 m × 0.25 mmID, 0.25 µm column	An Rxi-5MS low-polarity phase; Cross bond diphenyl dimethyl polysiloxane with 30 m × 0.25 mmID, 0.25 µm column
Flow rate	1.4 mL/min	1 L min ⁻¹
Oven program	It starts at 90 °C/min to 320 °C (hold five minutes), 8.5 °C/min	It starts at 70°C for one minute, then increase to 190 °C at a rate of 4.5 °C/min, and increase to 330°C at a rate of 4.5°C per minute with a hold at the maximum temperature for a total of one minute.

The optimal temperature ranges from 70°C to 90°C was selected to prevent peak broadening of volatile pesticides during their retention period. A temperature increase rate of 4.5°C/min delivered the most suitable chromatographic conditions for compounds that elute in the middle to late retention times. The experiment tested two final temperature settings to confirm thorough elution of high-boiling-point pesticides which occurred at 330°C. The research compared two carrier gas flow rates ranging from 1.0 mL/min through 1.4 mL/min was chosen because it combined adequate resolution with appropriate analysis time. EI was selected for fragmentation reproducibility yet SICRIT was chosen for gentle ionization to avoid moisture effects on signal intensity. The equipment maintains capillary temperature at 250°C as part of the design to reduce sputtering of late-eluting pesticides. In the ionization process using the GC-SICRIT-

LTQMS instrument, wet and dry nitrogen were used, but through the results obtained, it was shown that the presence of water affects the sensitivity and accuracy of the measurements. Comparison with the use of 'dry' nitrogen in our experiments showed that more reliable results are obtained, figure 8.11 in the appendix section.

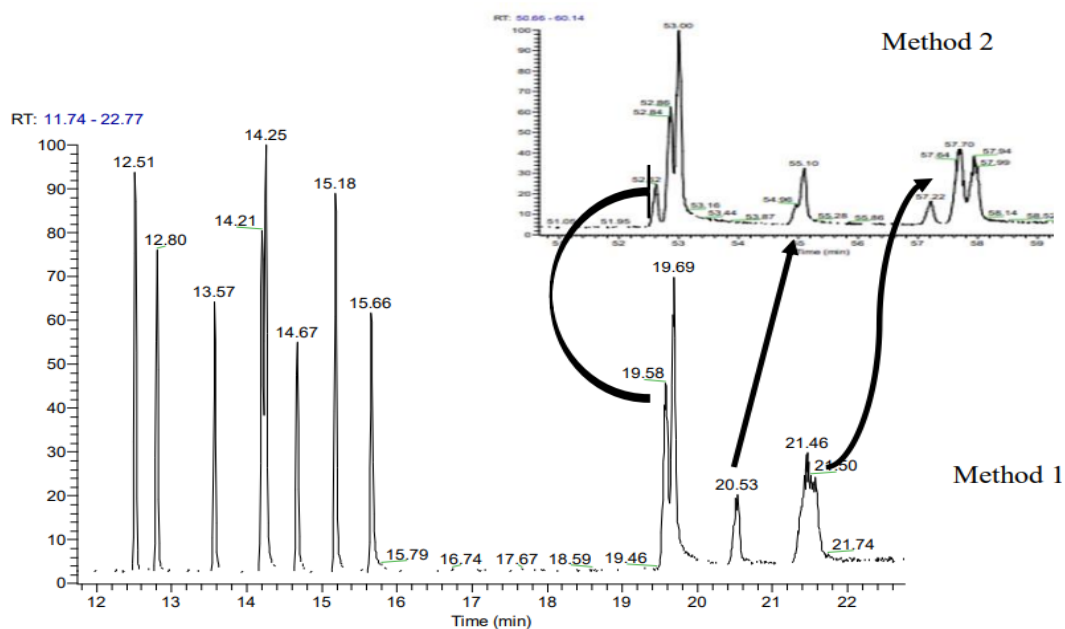


Figure 2.2. GC-MS-TIC separation chromatogram of organophosphorus pesticides (16 Compound), method 1.

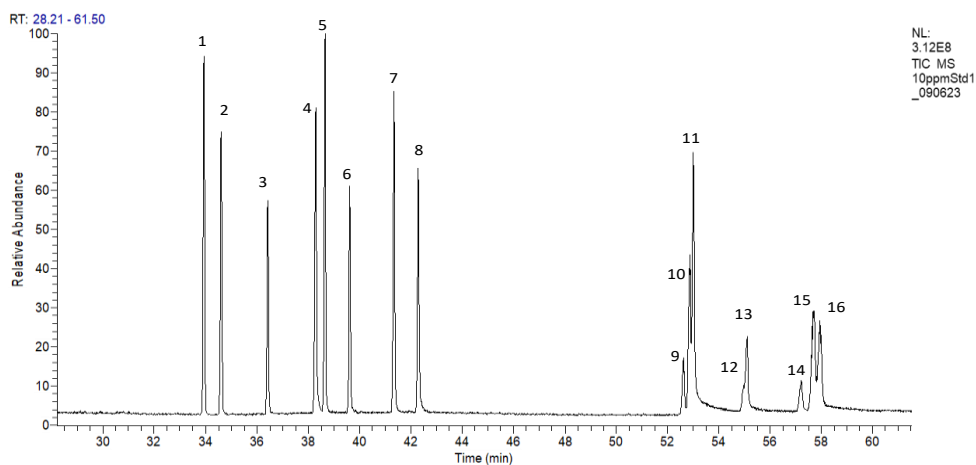


Figure 2.3. GC-MS-TIC separation chromatogram of organophosphorus pesticides (16 Compound), method 2.

2.4 Equipment

2.4.1 GC-SICRIT-MS Instrumentation & Setup

Gas Chromatography.

An Rxi-5MS low-polarity phase; Cross bond diphenyl dimethyl polysiloxane with 30 m × 0.25 mmID, 0.25 μm column and a Topaz Liner, Splitless Single Taper w/Wool 4mm x 6.5 x 78.5, (Restek, UK) were fitted to a Thermo Trace 1300 GC. A gas flow velocity of 1.4 mL/min of He (99.999%) was employed as the mobile phase. A Thermo Scientific UK AI 1310 autosampler was used to inject 1 μL aliquot samples with a splitless time of 1.1 minutes, while maintaining an injector temperature of 250°C. The heating of the oven was preset to start at 70°C for one minute, then increase to 190 °C at a rate of 4.5 °C/min, and increase to 330°C at a rate of 4.5°C per minute with a hold at the maximum temperature for a total of one minute. A heated transfer line and a readily available GC-/SPME-module (Plasmion GmbH, Augsburg, Germany) were used to connect the GC to the MS in a manner identical to that outlined by Mirabelli et al.⁶⁸The GC column was directly connected through the transfer line (290 °C) to a heated GC liner (250 °C, 4 mm x 6.3 x 78.5 mm I.D.) in the SPME module, with a final position of approximately 5 mm away from the ionization source. The gap between the GC column end and the ionization source reduces the possibility of the sample being adsorbed or condensed on the SPME liner. To achieve the approximate 1 L min⁻¹ flow rate for gas of the LTQ Orbitrap, the carrier gas was mixed with N₂ (5 L min⁻¹), which was pre-hydrated by passing the gaseous flow via an air bubbler submerged in LC-MS quality solution (Figure 2.4). The transfer line operated at 290°C and GC liner maintained 250°C which preserved the stability of the SICRIT plasma source throughout but also avoided condensation of analyte molecules since excessive heat damage the dielectric barrier and disrupts the low-temperature ionization protocol. The analysis system demonstrated its validity through symmetric peak patterns and detection rates of more than 95% for pyraclofos pesticide together with the implementation of short column separation and 5 L/min N₂ gas flow which avoided analysis disturbances at cold spots as confirmed by time retention stability (less than 2% RSD) and N₂ gas dryness verification in Appendix Figure 8.11. The method design delivered precise ionization performance using well-formed peaks which complied with SICRIT-MS requirements for gentle ionization.

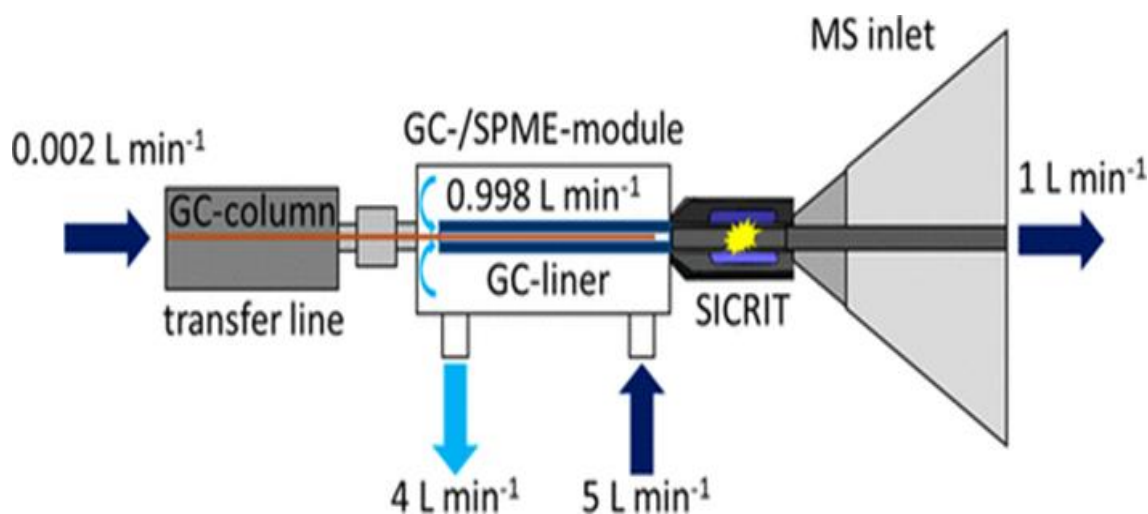


Figure 2.4: Diagram of the apparatus utilised in this investigation. Light blue arrows represent passive gas flow, and dark blue arrows represent actively created gas flows¹⁶²

Ionization Source.

For ionization, a SICRIT SC-30, sold commercially (Plasmion GmbH, Augsburg, Germany) was utilized. In summary, a quartz glass capillary with an outer diameter (OD) of 1.0 mm and an inner diameter (ID) of 0.7 mm is attached to the mass spectrometer's inlet. The perpetual tension of the device ensures that the capillary system flows at a constant rate of 1.7 L/min. The first electrode is a stainless-steel capillary that is put into the glass capillary. The capillary is surrounded by a 5 mm wide (1.0 mm ID) copper ring that serves as the counter electrode. A dielectric discharge ignites a plasma inside the capillary by supplying elevated voltage (peak to peak 1.5–4 kV) that is sine modulated (5750 Hz) to the electrodes. This ionizes the sample molecules and passing air, see figure 2.4 for a schematic diagram of source.

High-Resolution Mass Spectrometry.

An LTQ Orbitrap was used for quantification based on positive ionization full scan mode with centroid acquisition in high-resolution mode (30k FWHM), for measurement and identification. The capillary voltage was configured at 2.6 V, the tube glass lens was adjusted to 70 V, and capillary was maintained at 250 °C. A m/z 50–500 range was used.

2.4.2 GC-FID Instrumentation

Samples were analyzed by a Thermo Scientific™ TRACE™ 1310 GC equipped with a modular split/splitless (SSL) injector and a flame ionization detector (FID). The separation was accomplished using a capillary column, Rxi-5MS low-polarity phase; Cross bond diphenyl dimethyl polysiloxane with 30 m × 0.25 mmID, 0.25 μm. Injection was operated in the splitless mode, a Topaz Liner (Splitless Single Taper w/Wool 4mm x 6.5 x 78.5, (Restek, UK)) was used. The injection port and detector temperature were set at 220°C and 280°C, respectively. The initial temperature program for the GC column of 80°C and, post injection, was increased at a rate of 30°C min⁻¹ to 300°C and then held for 10 min at the final temperature. The total run time was 60 min. Helium (99.994% purity) at flow rate of 0.8 mL/min was used as the gas carrier. The GC-FID make-up gas for FID was Nitrogen at a flow rate at 30 mL/min. The GC-FID detects different signals than mass spectrometry (MS) while sharing many common chromatographic features whenever possible. The GC-MS methods used slower ramp rates of 4.5°C/min and higher final temperatures of 320°C to optimize mass spectral identification yet the GC-FID method operated at 30°C/min ramp rate and 300°C final temperature to minimize screening run times down to 60 minutes from the approximately 40-minute times of MS methods. The FID operated with lower detector-injector temperatures at 220°C/280°C while using less helium flow at 0.8 mL/min because it required makeup gas N₂ at 30 mL/min to protect itself from contamination. We synchronized chromatographic analyses through the combination of Rxi-5MS column phases with comparable initial settings at 80–90°C that were verified by pesticide standards analysis. The FID ramp rate at high speed introduced only moderate retention time changes for compounds with long retention times but critical pairs such as dimethachlor and propanil displayed baseline separation leading to equivalent qualification outcomes between systems.

2.4.3 GC-ITQMS Instrumentation & Setup

A Thermo Scientific ITQ 1100 ion trap mass spectrometer connected to a Thermo Scientific TRACE GC Ultra gas chromatograph outfitted with a Thermo Scientific Triplus^{RSH} liquid autosampler was utilized. The spectrometer was run in electron impact ionization mode (EI, 70 eV). A fused-silica capillary column, an Rxi-5ms GC Capillary Column, 30 m, 0.53 mm ID, 1.5 μm and with a Topaz Liner, Baffled PTV 2mm x 2.75 x 120 from RESTEK, UK was utilized for the pesticides analysis being conducted. A flow rate of 1.4 mL/min was fixed. Helium (99.999%) was used as the carrier gas. The acquisition was carried out using a full scan of m/z 50 to 550. The conditions of the instruments are listed in table 2.2.

Table 2.2: Conditions of GC-ITQMS instrument.

Parameter	Value
Injection volume	1 μl
Inlet	PTVsplitless mode at 250 °c
Column temperature program	90 °C/min to 320 °C (hold five minutes), 8.5 °C/min
Ion source temperature	300 C°
Transfer line temperature	290 C°
Flow rate and Carrier gas	Constant flow, Helium at 1.4 mL/min

2.4.4 GC/MSD Instrumentation

An Agilent 8890 GC (Agilent Technologies, UK) fitted with an Agilent 7693A autosampler (Agilent Technologies, UK) connected to Agilent 5977C mass-selective detector (Agilent Technologies, UK) comprised the GC–MS system used in this study. The electron impact (EI) ionisation method was used to operate the detector at an electron intensity of 70 eV. The GC was equipped with a J&W HP-5MS UI fused silica capillary column from Agilent, which had a 0.25 µm film thickness and a 30 m × 0.25 mm ID non-polar stationary phase (5% phenyl methylpolysiloxane). Helium (99.999%) was used as the carrier gas. Data acquisition made use of both Selected Ion Monitoring (SIM) and full scan operating modes. The conditions of the instruments are listed in table 2.3.

Table 2.3: Condition of GC-MSD instrument.

Parameter	Value
Injection volume	1 µl
Inlet	Pulsed splitless 50 psi until one minute Split/splitless 250 °C Purge 50 mL/min at one minute.
Column temperature program	40 °C (hold for one minute) 25 °C/min to 160 °C (hold three minutes), 6 °C/min to 312 °C
Ion source temperature	250 C°
Transfer line temperature	250 C°
Quadrupole temperature	200 C°
Flow rate and Carrier gas	Constant flow, Helium at 1.2 mL/min

The optimization of GC conditions resulted in different protocols for each instrument (GC-FID, GC-EI-MS, GC-SICRIT-MS) after systematic tests performed by me to meet specific analytical needs and detection approaches. The GC-FID system needed faster temperature ascent rates (30°C per minute) and a 300°C final temperature because rapid screening required them but the MS approaches used slower heating profiles (6-8.5°C per minute) and 312-320°C maximum temperatures to reach sufficient resolution and allow high-boiling compounds to reach detection. The different systems required separate values for splitless injection parameters because FID needed standard splitless but MS needed pulsed splitless. The instruments operated with comparable chromatographic profiles because they employed matching Rxi-5MS column phases together with common retention time verifications utilizing shared standards along with peak symmetry validation through %RSD checks that maintained method equivalence without sacrificing FID speed or MS confirmation capability.

2.5 Method Validation for baby food

The validation method is a multifaceted part of the analytical method that is not only used in the determination of suitability but also plays a significant role in the delivery of accurate results. In this analysis, the SANTE/12682/2019 step-by-step procedure that was specifically recommended by the European Commission (2019) was followed, this procedure effectively ensures the accuracy of the developed method for analysis of multi-residue pesticides, particularly in baby food samples. This procedure is based on the following key parameters, by utilizing this the process especially the validation process was done carefully which not only makes the methodological approach more accurate but also reliable.

Such methodologies are particularly based on the following factors: selectivity, linearity, accuracy, precision, matrix effects, limits of detection (LOD) and quantification (LOQ).¹⁰⁰ Such parameters were calculated by using Microsoft Excel, version 2408.

The validation process based on SANTE/12682/2019 evaluated every instrumental setup independently with details revealed for selectivity and linearity ($R^2 > 0.99$ across 1-500 $\mu\text{g/mL}$ range), accuracy (80-120% recoveries), precision (RSD < 15%), matrix effects and sensitivity (LODs 0.001-0.009 $\mu\text{g/mL}$). The validation tests proved method reliability in all instrumentation by optimizing GC-FID for quick screening at a 30°C/min ramp but MS methods used 6 to 8.5°C/min ramps for resolving and sensitive residue pesticide analysis in baby foods that complied with EU regulatory guidelines.

2.5.1 Linearity

The research showed outstanding linear calibration behavior ($R^2 > 0.999$) for majority of pesticides throughout all tested concentration points from 1 to 500 $\mu\text{g/L}$ in solvent solutions. The calibration points at 1, 5, 10, 25, 50, 100, and 500 $\mu\text{g/L}$ showed linear accuracy since every result remained within ± 0.20 units of prediction values. The 0.99 R^2 threshold functioned uniformly across all measurable analytes from 1 $\mu\text{g/L}$ trace to 500 $\mu\text{g/L}$ high concentration levels to show proportional detector response. The quantification accuracy of the method proved dependable for tracing pesticides near EU MRLs in baby food at the minimum standard concentration of 1 $\mu\text{g/L}$.

2.5.2. Limit of detection and quantification

The next parameter is the Limit of Detection (LOD), considered one of the most important parameters; this parameter represents the lowest quantity of an analyte that can be consistently distinguished from the background noise^{101,102}. The next parameter is the Limit of Quantitation (LOQ); this is the smallest quantity of an analyte that can be consistently determined accurately and precisely according to the selection conditions of the method.^{103,104}

LOD and LOQ were calculated based on two factors, firstly on a standard deviation of the calibration curve and secondly, on the slope of the regression curve, these two factors were calculated for each analyte. Two equations were used for the calculation of the LOD and LOQ as follows:

$$\text{LOD} = 3.3 \sigma / S \quad \text{Eq.2.1}$$

$$\text{LOQ} = 10 \sigma / S \quad \text{Eq.2.2}$$

Where:

- σ = the standard deviation of the response
- S = the slope of the calibration curve

2.5.3 Precision

The precision is also a part of an analytical method validation, it represents the closeness of agreement between quantitative values that are obtained through repeating quantitative measurements, according to the specified conditions, multiple times.¹⁰⁵ This method was specifically performed to determine repeatability precision or intra-run precision⁴. This involved measuring different concentration levels of individual analytes which included low, medium and high concentration samples. To calculate this parameter, a sample was measured multiple times during a single analytical run. This parameter was also evaluated not only for the same analytical instrumentation but also in the same environment over a short period. This parameter is expressed as % RSD, which is the percentage of the relative standard deviation.¹⁰⁶

2.5.4 Accuracy

The accuracy of a calculated sample concentration is determined by comparing the prepared concentration of a sample to the value determined by the analytical procedure.^{90,95,92} This accuracy is evaluated by calculating the percentage of recovery. Recovery is determined by comparing the known concentration (*C* theoretical) to the concentration measured after spiking the sample with the matrix (*C* experimental). In this study, samples were spiked with 0.05 µg/mL and 0.1 µg/mL of the analyte in the selected matrix. The recovery was calculated using the equation below.¹⁰⁷

$$\text{Recovery (R)\%} = (C_{\text{experimental}}|C_{\text{theoretical}}) \times 100 \quad \text{Eq.2.3}$$

2.4.5 Matrix Effect

The matrix of the sample is known to, in many cases, play an active role when analyte extraction is conducted, the term used to describe this is the ‘matrix effect’. This parameter is influenced by different factors which include sample preparation, sample composition and instrument parameters. This parameter’s effect may be positive or negative because this method depends on the nature of the interference. A positive matrix effect not only increases sensitivity but also enhances signal. On the other hand, a negative matrix effect not only suppresses the signal but also reduces sensitivity for an analyte.

These effects were evaluated for each analyte extracted from matrices that included milk, rice and cereal. The QuEChERS procedure was first used to extract the matrix. After extraction, the matrix was spiked with the analyte at a final concentration of approximately 50 ng/mL. The spiked sample is particularly injected into the analytical instrument GC-MS. The instrumental response from the spiked matrix sample is compared to the response from spiked solvent samples. This comparison helps in the determination of matrix effects.

Such effects are calculated specifically using the following formula:

$$M.E. = \left(\frac{\textit{Spike in matrix}}{\textit{Spike in pure solvent}} - 1 \right) \cdot 100\% \quad \text{Eq.2.4}$$

Where:

- $\textit{Spike in matrix}$ (Response in Matrix) = The signal obtained from the spiked matrix sample
- $\textit{Spike in solvent}$ (Response in Solvent) = The signal obtained from the spiked pure solvent sample.

3. Quantitative analysis of Organophosphorus pesticide residues in baby food by gas chromatography with dielectric barrier discharge ionization-mass spectrometry (GC-DBDI-MS)

3.1 Introduction

Pesticides are frequently applied to plants because they prevent colonisation or kill undesired organisms which include insects, fungi, and weeds. The pesticides of the organophosphorus pesticide (OPPs) class are considered the largest group of pesticides because they are structurally diverse and widely used. The main outcome from pesticide use is that they enhance the quality and yield of foodstuffs. These compounds were first introduced in 1937 after the discovery of Tabun by Gerhard Schrader.¹⁰⁸ These compounds have their origins in warfare as nerve agents. The OPP class of compounds were developed solely for agrochemical purposes to kill undesirable plants and organisms.¹⁰⁹ It is noted that contamination by OPPs not only produces long-term negative health impacts but also produces a negative impact on the general insect population.¹¹⁰ On the other hand, consumption of contaminated food is considered the main route for human OPP exposure.^{111,112} These Organophosphorus Pesticides (OPPs) have been found in baby foods including, applesauce, pears and green beans.¹¹³ According to the Environment Working Group (EWG), an independent nonprofit organization founded by Ken Cook and Richard Wiles, baby food, specifically non-organic products, were found to contain fewer pesticides when compared to fresh produce. However, the same group noted that non-organic pear-based baby foods were amongst the most contaminated foods tested in a comprehensive analysis carried out in 2023.¹¹⁴ Children, specifically infants, are more vulnerable to toxic substances due to their rapid growth and development.¹¹⁵ It has been shown that pesticides not only harm the nervous system development but also development of the immune and reproductive systems.¹¹⁶ Due to these highly toxic effects, OPPs are banned in several countries, but even with bans in place the application of OPPs is believed to be increasing.¹¹⁷ Such is the increase in OPP application that it has given rise to public concern and thus policymakers have taken action to ensure food and environmental safety.¹¹⁸ Different countries and organisations set limits for residual pesticide content on primary foodstuff, thus a variety of techniques are utilised for the detection and analysis necessary to enforce these imposed limits and ensure compliance. Amongst these analytical techniques, chromatographic-based

methods with absorbance, fluorescence, electrochemical and mass spectrometric detection are common.

In this study, our focus is on chromatography-based analysis with pesticide detection using two types of ionisation sources: EI and SICRIT. The analysis reported below was carried out using a mixture of 16 OPP compounds as examples of this class diversity. The work evaluates detection limits for these pesticides from baby food matrices (milk, rice and cereal).

3.2 Chromatographic separation in GC-FID, GC-EI-ITQMS, GC-EI-MSD and GC-SICRIT-LTQMS.

Initial experiments focused on the chromatographic separation of the OPPs. A mixture of 16 OPPs was purchased (see table 3.1) and an initial solution was prepared at 10 µg/mL concentration in acetonitrile. This mixture was then analyzed using four different GC based analytical systems: GC-FID, GC-EI-ITQMS, GC-SICRIT-LTQMS and GC-MSD. The GC methods were developed and optimized for each system. To enhance separation, several adjustments have been implemented, including modifications to temperature settings, flow rates, column type and liner type, as outlined in the methodology chapter. Figures 3.1, 3.3, 3.4, and 3.5 show the chromatograms obtained from these four systems. While detection of all 16 pesticides was observed, several peaks were co-eluted in the analysis. Specifically, peak 4 and 5 correspond to fenitrothion and pirimiphos-methyl, peaks 10 and 11 represent phosmet and EPN, peaks 12 and 13 indicate phosalone and azinphos-methyl, and peaks 15 and 16 are associated with azinphos-ethyl and pyraclofos. Therefore, the use of the MS detector was necessary to identify and distinguish between these overlapping peaks. Figure 3.1 displays the GC-FID chromatogram. The peaks are well-resolved, indicating good chromatographic separation of the pesticides. Each numbered peak corresponds to a specific pesticide as listed in table 3.1. Figure 3.3 presents the GC-EI-ITQMS total ion chromatogram (TIC). This method provides both separation and mass spectral information. The chromatogram shows distinct peaks for each pesticide, demonstrating the method's ability to separate and detect these compounds. Figure 3.4 shows the GC-MSD chromatogram. Similar to the previous methods, it successfully separates and detects all 16 pesticides. Figure 3.5 displays the GC-SICRIT-LTQMS chromatogram. This method, which uses soft ionization, also achieves good separation and detection of all pesticides. The peaks are well-defined, indicating the method's sensitivity and selectivity.

Table 3.1: Compounds obtained through chromatography separation

Peaks	Component Name	Formula
1	Diazinon	C ₁₂ H ₂₁ N ₂ O ₃ PS
2	Isazophos	C ₉ H ₁₇ ClN ₃ O ₃ PS
3	Chlorpyrifos-methyl	C ₇ H ₇ Cl ₃ NO ₃ PS
4	Fenitrothion	C ₉ H ₁₂ NO ₅ PS
5	Pirimiphos-methyl	C ₁₁ H ₂₀ N ₃ O ₃ PS
6	Chlorpyrifos	C ₉ H ₁₁ Cl ₃ NO ₃ PS
7	Pirimiphos-ethyl	C ₁₃ H ₂₄ N ₃ O ₃ PS
8	Quinalphos	C ₁₂ H ₁₅ N ₂ O ₃ PS
9	Pyridaphenthion	C ₁₄ H ₁₇ N ₂ O ₄ PS
10	Phosmet	C ₁₁ H ₁₂ NO ₄ PS ₂
11	EPN	C ₁₄ H ₁₄ NO ₄ PS
12	Phosalone	C ₁₂ H ₁₅ ClNO ₄ PS ₂
13	Azinphos-methyl	C ₁₀ H ₁₂ N ₃ O ₃ PS ₂
14	Pyrazophos	C ₁₄ H ₂₀ N ₃ O ₅ PS
15	Azinphos-ethyl	C ₁₂ H ₁₆ N ₃ O ₃ PS ₂
16	Pyraclofos	C ₁₄ H ₁₈ ClN ₂ O ₃ PS

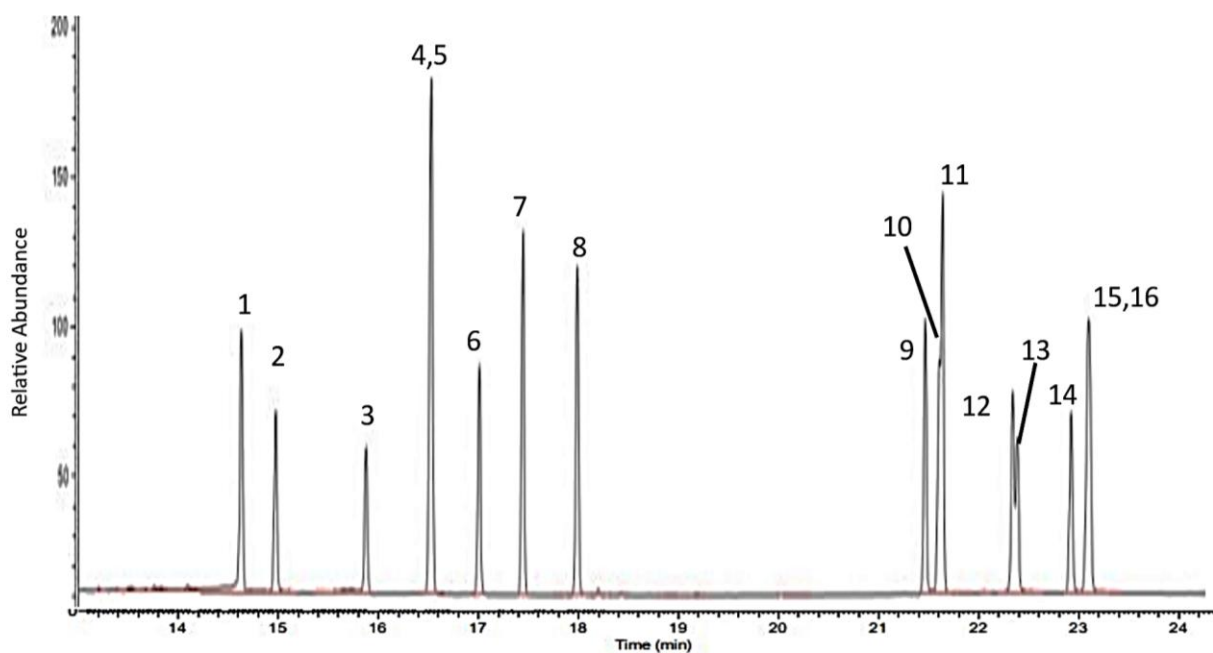


Figure 3.1: GC-FID Chromatogram of a mixture of 16 organophosphorus pesticides (compounds identity in table 3.1) at 10ppm.

The figure 3.1 represents the chromatographic conditions using a ThermoFisher Gas Chromatography-Flame Ionization Detector (GC-FID) system for the 16 targeted OPPs (see methods section for instrument details). The compounds present are plotted on the x-axis as retention time and the relative detector response is on the y-axis. The peaks represented by numbers point to the different pesticides as shown in table 3.1. The chromatogram reveals that the pesticides are well separated with almost all the compound's peaks baseline resolved. There are some overlapping peaks, for instance; peaks 4 and 5; 15 and 16, which is normally expected in the case of compound mixtures. For example, peaks 4 and 5 correspond to fenitrothion ($C_9H_{12}NO_5PS$) and pirimiphos-methyl ($C_{11}H_{20}N_3O_3PS$), respectively. Although they are structurally different as shown in figure 3.2, fenitrothion contains a nitro group, and pirimiphos-methyl having a pyrimidine ring and a different substitution pattern. their retention times are very close, causing the peaks to overlap in chromatogram. Similarly, peaks 15 and 16 correspond to azinphos-ethyl ($C_{12}H_{16}N_3O_3PS_2$) and pyraclofos ($C_{14}H_{18}ClN_2O_3PS$).

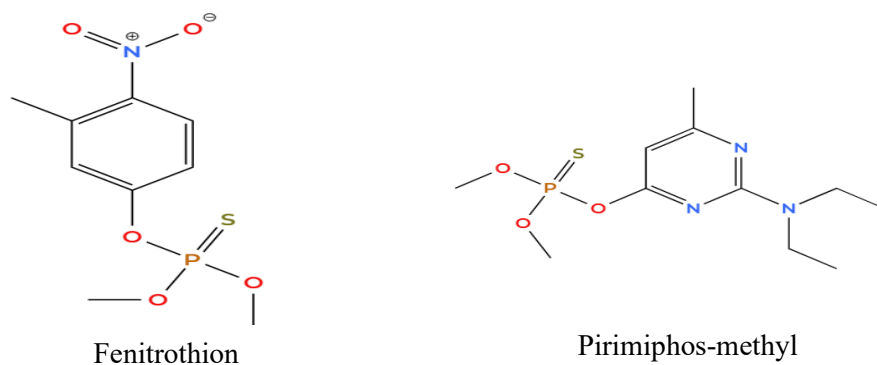


Figure 3.2: Structures of Pirimiphos-methyl and Fenitrothion.

Despite their structural differences azinphos-ethyl has two sulfur atoms while pyraclofos has chlorine atom and a different substitution pattern. their retention times are close enough to cause overlapping peaks. The FID response of the compounds thus shows variation and this is most probably due to carbon contents and structure of the compounds in the mixture. The study addressed polar organophosphorus pesticide signal reduction

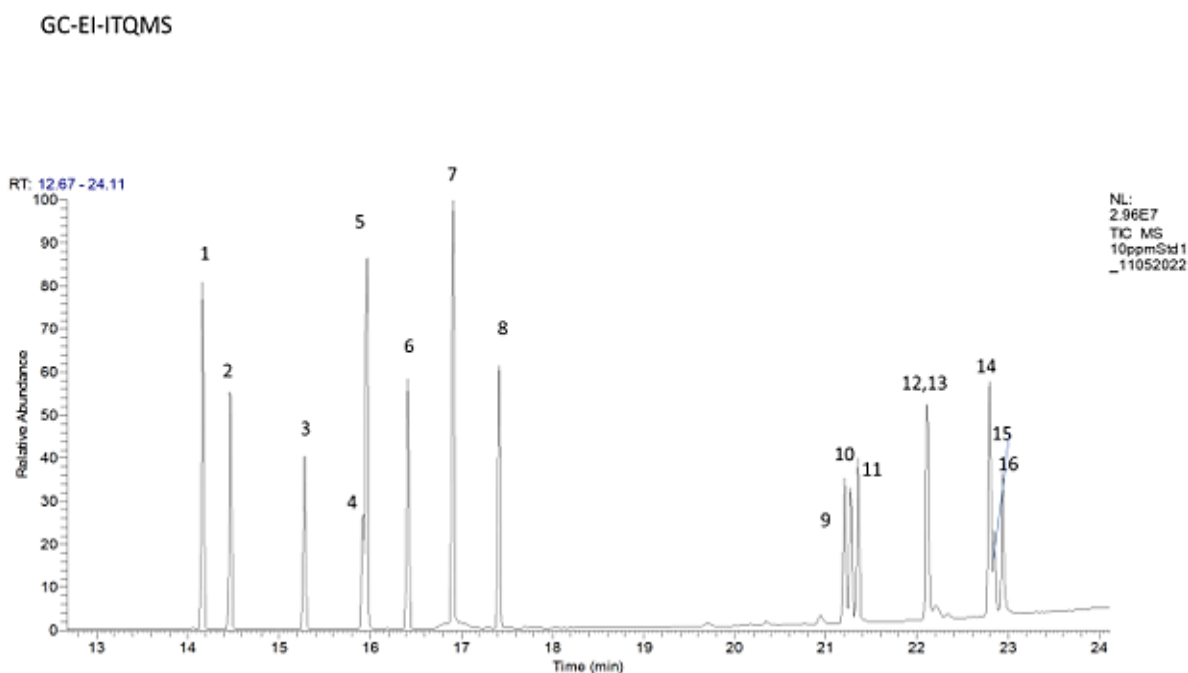


Figure 3.3: GC-EI-ITQ TIC-MS of a mixture of 16 Organophosphorus Pesticides (compounds identity in table 3.1) at 10ppm.

systematically through complete preparation and testing involving acephate recovery tests at >85% followed by cereal matrix effect evaluation at -50% suppression levels and through method-specific Rxi-5MS column optimization for polar compound retention without derivatization. Matrix-matched calibration enabled detection of polar OPPs successfully between 1-500 µg/L concentrations despite their EI ionization inefficiency which resulted in slightly elevated LODs of 0.005 to 0.01 µg/mL. GC-SICRIT-MS offered improved sensitivity to these compounds because of its softer ionization mechanism when compared to EI-MS. The technical measures provided detection reliability for a wide range of polarities and satisfied regulatory standards for performing multi-residue analysis.

Figure 3.3 & Table 3 display the Total Ion Current (TIC) output from a Thermo Scientific GC-EI-ITQMS (see methods section for instrument details). As above, the retention time is plotted on the x-axis ranging from 12 to 24 min, and the y-axis shows the relative detector response. All of the 16 pesticides are detected and, in most cases, chromatographically well resolved. There are some unresolved peaks towards the end of the GC run. The peaks are generally narrower and more symmetrical compared to the chromatogram obtained using GC-FID, indicating the better chromatographic performance of this technique. The differences in the peak heights are likely to be due to differences in ionization efficiency of the various pesticides under electron impact ionisation.

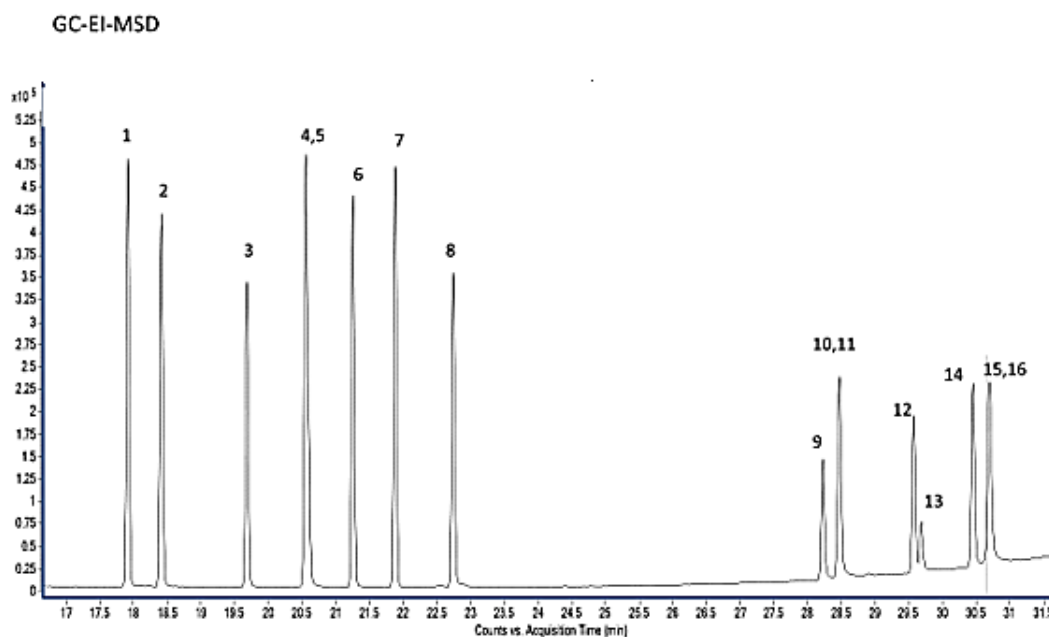


Figure 3.4: GC-EI-SQ TIC-MS of a mixture of 16 Organophosphorus Pesticides (compounds identity in table 3.1) at 10ppm.

Figure 3.4 shows the result obtained from an Agilent Gas Chromatography-Electron Impact-Mass Selective Detector (see methods section for instrument details). Similar to Figure 3.3, it shows excellent chromatographic separation for the majority of the 16 pesticides tested. There are some overlapping of the co-elutions, for instance, compounds 4 and 5, 10 and 11, and 15 and 16. In comparison to the previous spectra presented, the separation achieved on this instrument is considered enough to analyze and quantify the concentration of the pesticides adequately.

GC-SICRIT-LTQMS

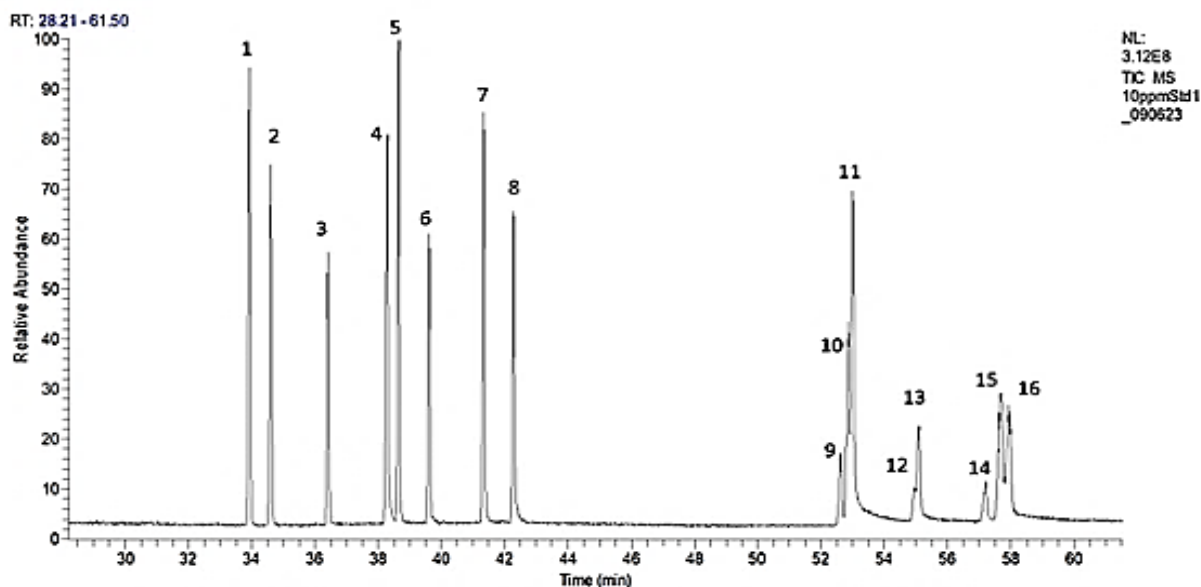


Figure 3.5: GC-SICRIT-LTQ TIC-MS of a mixture of 16 Organophosphorus Pesticides (compounds identity in table 3.1) at 10ppm.

The representation of pesticide analysis runs using GC-SICRIT-LTQMS system can be found in Figure 3.5. The ThermoScientific gas chromatograph instrument equipped with Plasmion SICRIT ionization source used a ThermoScientific Orbitrap XL mass spectrometer (GC-SICRIT-LTQMS) in positive mode to generate this chromatogram. This image shows the pesticide compound relative abundances depicted on the y-axis as the sample elutes from 30 to 60 minutes on the x-axis. The analytical method separated 16 pesticides successfully using specific and distinct peaks.

The analysis runs for 60 minutes at a much longer duration than standard GC-MS operations because of particular chromatographic rules. The clear distinct peaks between numbers 1 to 8 show effective separation of most analyzed compounds. The compounds of Peak group 9-16 show broad peaks with tails indicating the necessity for improving the chromatographic conditions. The SICRIT ionization technique works well but Peak symmetry and resolution require improvement to optimize performance. Peak heights and shapes vary because the system contains cold spots together with the lengthy run time which both result in band broadening. The problems manifest due to excessive duration of GC transfer line components. The observed challenges do not prevent a clear resolution of all pesticide compounds. The observed peak tailing along with broadened shapes can most likely be attributed to the operational temperature of the column but not to ionization

processes. A complete investigation would benefit from Extracted Ion Chromatograms (EICs) showing individual pesticide behavior at specified mass-to-charge (m/z) ratios.

3.3 Ionisation Mechanism and Mass Spectrometry Results

After confirming the separation capabilities, the focus shifted to understanding the ionization mechanisms, particularly comparing SICRIT (Soft Ionization by Chemical Reaction in Transfer) with conventional Electron Impact (EI) ionization.

Table 3.2 provides a comprehensive comparison of the ions observed in the GC-EI-MS and GC-SICRIT-MS spectra for each pesticide. It details the exact mass, molecular formula, and the primary ions observed in each method. A key finding is that most compounds analysed using SICRIT ionised predominantly as $[M+H]^+$ ions. The soft ionisation mechanism of SICRIT particularly produces molecular ions specifically with minimal fragmentation. In this ionization source, the sample is passed through a dielectric barrier discharge (DBD) generated nitrogen plasma, at approximately atmospheric pressure. After that, the analytes interact with the plasma which leads to ionisation. This method is regarded as 'soft' specifically keeping the ionized adduct structure of the compounds intact; this seems to hold for the less volatile species as well. After this, the ionized sample is transferred into the mass spectrometer through a heated transfer line. Inside the MS, the ions are separated based on the m/z ratio and either the orbitrap mass analyser (high mass resolution) or the LTQ mass analyser (low mass resolution) can be used to record the ions generated. In contrast, EI typically results in more extensive fragmentation.

The procedures for gas chromatography mass spectrometry ionization differ significantly between SICRIT (Soft Ionization by Chemical Reaction in Transfer) and traditional Electron Impact (EI) ionization because they produce divergent effects during compound quantification. During EI mass spectrometric ionization analytical molecules undergo powerful electron bombardment to generate main molecular ion fragments and numerous fragment ions and the intact parent ion. EI mass spectrometric analysis creates unreliable identification of the parent substance through its fragmentation patterns because the detected ions are disconnected from their original compound. The accurate measurement of stable ions remains the key basis yet molecular fragmentation can make this procedure exceedingly difficult to perform. When fragmentation occurs irregularly it produces difficulties for ionization efficiency during quantitative analysis. Quantification accuracy

varies through matrix effects since these variables possess a unique ability to produce new measurement variation. The quantification process that uses fragment ions faces heightened calibration complexities because the signal response generates non-linear concentrations when it performs targeted compound fragmentation. The quantitative benefits offered by SICRIT ionization surpass those of EI because of its advanced features. The method produces detectable molecular ions through its structural platform leading to lower parameter fluctuation with simplified calibration procedures that enhance the sensitivity rate. SICRIT offers superior ion conservation behavior than EI so it enables better detection of low-level quantitative measurements. The implementation of SICRIT ionization stands superior to EI by utilizing gentle ionization techniques for structure protection in quantitative mass spectrometry applications for complex mixtures particularly pesticide examinations.

If ion fragments were found, the fragmentation was based on the following common mass losses for all pesticides in this class:

- Loss of a methyl group (CH₃): $[M]^+ \rightarrow [M-CH_3]^+ + CH_3-$
- Loss of a hydroxy group (OH): $[M]^+ \rightarrow [M-OH]^+ + OH-$
- Loss of a phosphorus-containing group: $[M]^+ \rightarrow [M-P]^+ + P$
- Loss of a sulfur-containing group: $[M]^+ \rightarrow [M-S]^+ + S$

In GC-EI-MS, the majority of the OPP compounds analysed undergo fragmentation after ionisation, which is indicated as “frg” in table 3.2 and is a significant feature of electron impact ionisation. The fragmentation patterns follow from the structure of the analyte under study and thus can be used in confirming the structure of the compounds. On the contrary, GC-SICRIT-MS ionisation showed mainly the molecular ion, which is present as $[M+H]^+$, showing the intact pesticide plus a proton. This technique offered a highly accurate measurement of the m/z for each analyte which was used to generate candidate molecular formulae (within a 3 ppm window of the measure m/z); the closest matching molecular formula generated was found to match that of the OPP under study.

Structural Moieties and Their Stability in SICRIT Ionization

The SICRIT ionization method depends on structural moiety stability because it determines both the ionization process efficiency and the preservation of ionized species. These notes on structural moieties that are likely to show stability changes in SICRIT ionization sources emerge from regular mass loss patterns found in Table 3.2 pesticide compounds.

1. Phosphorus-Containing Groups: Some organophosphorus pesticides (OPPs) show as main decomposition pattern the dissociation of phosphorus-containing groups that produce $[M-P]^+$ ions. The SICRIT method demonstrates stronger resistance to alter the parent ion $[M+H]^+$ than conventional EI procedures do. Because phosphorus exists with high reactivity characteristics its chemical properties can cause instability. The stabilization of phosphorus-containing entities within the matrix matters because such compounds may produce fragments though to a lesser extent than EI methods would.

2. Hydroxyl Groups ($-OH$): Research shows that the removal of $-OH$ functional groups represent a usual fragmentation mechanism. Some pesticides contain reactant groups which help stabilize structures yet these same groups enable fragmentation to occur at times. The SICRIT ionization technology affects hydroxyl-containing compounds delicately but unstable structures will still break down during nitrogen plasma exposure.

3. Alkyl Chains (CH_3): Both SICRIT and EI methods cause the loss of methyl groups ($-CH_3$) but SICRIT shows more favorable results regarding their loss. Structural identification and quantitative assessment improve through SICRIT when molecular ions form intact because specific alkyl chains remain intact in the process.

4. Chlorine and Bromine Atoms:

The loss of halogen atoms occurs to Chlorpyrifos and Chlorpyrifos-methyl under specific circumstances. Molecular fragmentations are limited when using SICRIT since its soft ionization procedures protect chemical structures although partial molecule destruction may arise from weak bond forces.

5. Secondary Nitrogen Structures: Different pesticide structures containing secondary nitrogen atoms present various degrees of stability in SICRIT. Parts of the nitrogen ring exposed to volatile groups have the potential to generate molecular fragmentation when subjected to harsh environmental conditions. Scientific Ion Chromatography and Thermal

Ionization Reaction Implementation provides favorable conditions that facilitate preservation of molecular structures.

SICRIT ionization maintains molecular ions while reducing fragmentation but certain chemical groups such as phosphorus structures as well as hydroxyl groups and halogen atoms tend to break down under certain instrument operation conditions. The gentler operating conditions of SICRIT help maintain native structural elements in samples thereby making it the better option for pesticide detection in complex matrix solutions. Knowledge about these structural behaviors leads to better efficiency and more accurate quantitative results for the ionization technique.

Figures 3.6 - 3.8 provide detailed mass spectra for selected pesticides, comparing SICRIT and EI ionization: Figure 3.6 (Diazinon): The SICRIT spectrum shows a prominent $[M+H]^+$ peak at m/z 305.1102 while the EI spectrum displays significant fragmentation with major peaks at m/z 179, 137, and 199. Figure 3.7 (Isazophos): SICRIT produces a clear $[M+H]^+$ peak at m/z 314.0511, whereas EI results in multiple fragment ions (m/z 162, 119, 172). Figure 3.8 (Fenitrothion): The SICRIT spectrum shows the $[M+H]^+$ ion at m/z 278.0265, while EI produces a complex fragmentation pattern with major peaks at m/z 260, 125, and 109.

Figures 3.6, 3.7, and 3.8 showcase the mass spectra analysis of pesticides Diazinon, Isazophos, and Fenitrothion using both SICRIT and Electron Impact (EI) ionization techniques. The fundamental differences depicted concerning the mechanisms of ionization suggest the general pros and cons of each method in regard to fragmentation of the ions and the resulting intact molecules.

1. Diazoin (Figure 3.6)

- **SICRIT Ionization:** As previously mentioned, in the case of Diazinon, it is SICRIT technique which positively impacts the interpretation of mass spectra. Diazinon is topped with the molecular ion $[M + H]^+$, at 305.1102. As the correlation has to do with fragmentation in soft ionization methods, Diazinon achieves success with soft fragmentation techniques preserving almost totally intact molecular structures because fragmentation is performed in a mild fashion. The overwhelming retention of structural integrity permits, practically, unambiguous identification of the compound, which strengthens the value of SICRIT technique in accurate molecular ascertainment towards monetary targets.

- **EI Ionization:** On the other hand, the EI spectrum exhibits fragmentation at m/z 179, 137, and 199. These three peaks appear to be dominant. More often than not, spectra contain innumerable fragments and therefore the spectrum simplifies. This becomes troublesome to ascertain parent ion identity. Likewise, the numerous fragment ions do indeed allow structural information to be obtained but the presence of multiple fragment ions renders while structural information could potentially be gleaned, quantifying such information could be tricky due to the differing fragmentation.

2. Isazophos (Figure 3.7)

SICRIT Ionization: When you look at the SICRIT results, a crisp $[M+H]^+$ peak pops up around m/z 314.0511. This clear signal shows the molecule hangs together nicely – a detail that really counts for both figuring out what it is and measuring how much is there. It's a neat outcome that keeps the whole picture in view.

EI Ionization: Now, switch over to EI ionization and things get a bit messier. The spectrum breaks the molecule apart, giving peaks at roughly m/z 162, 119, and 172. Much like what you'd see with Diazinon, this breakup offers hints about its structure but, in most cases, ends up muddying the waters when it comes to consistent quantification. Variations in these fragment peaks can lead to inconsistencies that complicate comparing samples.

3. Fenitrothion (Figure 3.8)

SICRIT Ionization: Here, the SICRIT setup again shows its strength by producing a clear $[M+H]^+$ peak at m/z 278.0265. Generally speaking, this means the molecule stays intact during the process, which is great for nailing down an accurate mass and keeping most of the structural details intact—this little bit of stability really boosts confidence in the results.

EI Ionization: In contrast, the EI spectrum for Fenitrothion tells a more complicated story. You see a jumble of fragment peaks, with notable signals around m/z 260, 125, and 109, which makes the overall response less predictable. The reliance on these fragments for measurement can be tricky, since their levels can change a lot depending on what else is in the sample and the finer points of the experiment. Overall, this variability can make precise quantification a real challenge.

Take Aways from Ionization Processes

In comparative learning tasking, SICRIT ionization is clearly superior to the addition of the molecular ion labelled $(M+H)^+$ in all three pesticide samples, making identification and quantification easier. As with EI ionization, fragmentation ultimately hinders both the ability to visualize spectra directly and the ability to subjectively make quantification stable (and therefore reliable).

1. Stable, Definable, & Accurate Quantification: A defined SICRIT stable $(M+H)^+$ can very accurately quantify pesticide residues, which is an important aspect of learning to ensure safety and for regulation of studies.
2. Fragmentation Characteristics: While fragmentation with EI can produce structural information that can be useful, the fragmentation did less to help what is quantified, and rather contributed to what the detection level is when the response is equal to some mass the replication of the experiment is usually random because of the fragmentation;

Table 3.2: Ionisation mechanism and mass spectrometry results.

Peaks	Component Name	Formula	Exact Mass	GC-EI-MS	Ion form	GC-SICRIT-MS	Ion form
1	Diazinon	C ₁₂ H ₂₁ N ₂ O ₃ PS	304.101	179,137,199,84	frg	305.1102	M+H
2	Isazophos	C ₉ H ₁₇ ClN ₃ O ₃ PS	313.0416	119,97,162,172,130,146	frg	314.0511	M+H
3	Chlorpyrifos-methyl	C ₇ H ₇ Cl ₃ NO ₃ PS	320.8949	286,288,125,79,93	frg	321.9049	M+H
4	Fenitrothion	C ₉ H ₁₂ NO ₅ PS	277.0173	260,125,109,79,277	frg	278.0265	M+H
5	Pirimiphos-methyl	C ₁₁ H ₂₀ N ₃ O ₃ PS	305.0962	290,180,125,233,305	frg	306.1057	M+H
6	Chlorpyrifos	C ₉ H ₁₁ Cl ₃ NO ₃ PS	348.9262	197,258,169,314	frg	349.936	M+H
7	Pirimiphos-ethyl	C ₁₃ H ₂₄ N ₃ O ₃ PS	333.1275	168,166,182,318,333	frg	334.1383	M+H
8	Quinalphos	C ₁₂ H ₁₅ N ₂ O ₃ PS	298.0541	156,118,146	frg	299.0648	M+H
9	Pyridaphenthion	C ₁₄ H ₁₇ N ₂ O ₄ PS	340.0646	199,97,340,109	frg	341.0764	M+H
10	Phosmet	C ₁₁ H ₁₂ NO ₄ PS ₂	316.9945	160,133,77	frg	160.0414, 318.0059	frg
11	EPN	C ₁₄ H ₁₄ NO ₄ PS	323.0381	157,169,141,77,110	frg	324.0496	M+H
12	Phosalone	C ₁₂ H ₁₅ ClNO ₄ PS ₂	366.9868	182,111,138,367	frg	182.0018, 367.9968	frg
13	Azinphos-methyl	C ₁₀ H ₁₂ N ₃ O ₃ PS ₂	317.0057	77,132,160	frg	132,160,260.98	frg
14	Pyrazophos	C ₁₄ H ₂₀ N ₃ O ₅ PS	373.0861	221,265,193,232	frg	374.0956	M+H
15	Azinphos-ethyl	C ₁₂ H ₁₆ N ₃ O ₃ PS ₂	345.037	77,132,160	frg	132,160,289,346.47	frg
16	Pyraclufos	C ₁₄ H ₁₈ ClN ₂ O ₃ PS	360.0464	194,138,139,360	frg	361.0558	M+H

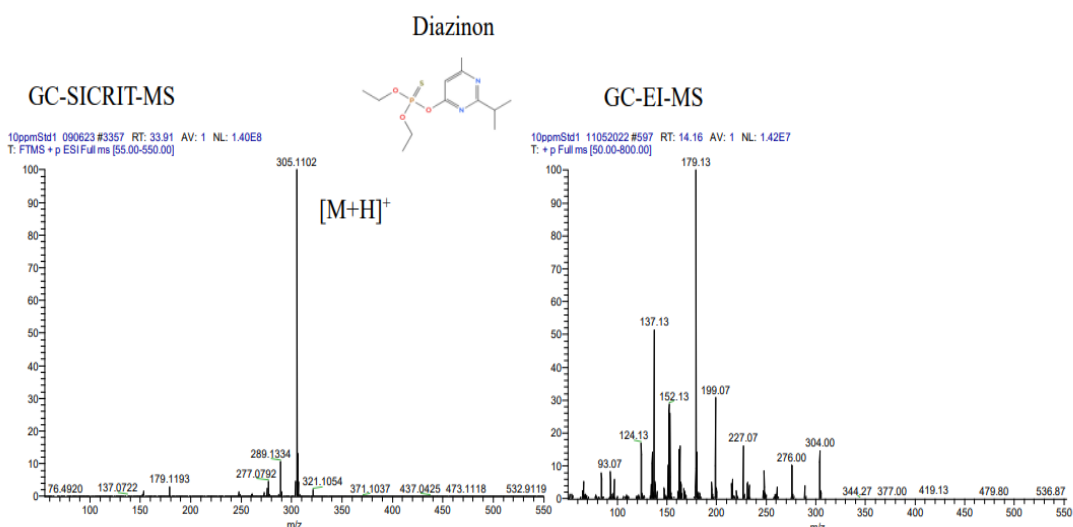


Figure 3.6: *EI-MS and of SICRIT-MS spectra (positive ionization mode) of Diazinon (m/z 304.101 (see table 3.2) at 10ppm, analyzed by GC-SICRIT- LTQ Orbitrap mass spectrometer and GC-EI-ITQMS.*

Figure 3.6 Comparative Mass Spectra of diazinon Using GC-SICRIT-MS and GC-EI-MS. This figure displays the mass spectra for diazinon, a pesticide, obtained through Soft Ionization by Chemical Reaction in Transfer (SICRIT) and Electron Impact (EI) ionization methods. The SICRIT spectrum shows a prominent molecular ion labeled as $[M+H]^+$ at m/z 305.1102, indicating effective soft ionization that preserves the molecular structure with minimal fragmentation. In contrast, the EI spectrum reveals significant fragmentation with major peaks at m/z 179.13, 137.13, and 199.07, complicating compound identification and quantification. The table summarizes the component name, exact mass, molecular formula ($C_{12}H_{21}N_2O_3PS$), and key ion forms for both methods. The molecular structure of diazinon is illustrated in the inset, highlighting its functional groups.

GC-SICRIT-MS spectrum:

In the GC-SICRIT-MS spectrum of diazinon, notable features include a peak at m/z 305.1102 which contains the molecular ion $[M+H]^+$. This corresponds to a protonated version of Diazinon, (containing a proton), the value 304.1010 being the exact mass of unprotonated diazinon molecule would equate to 304.1010 in mass. Other valuable peaks contain m/z 289.1360 and 277.0816, released due to exchange or fragmentation, of the ethyl group (C_2H_4) from the molecular structure. Acquired value of $[M+H]^+= 305.1102$ could not be calculated hence using reflect SICRIT's method of ionization which does not fragment the ion. As known, the least mument of precision determines the range but,

in this case, exact mass determined with two places would need to restate 'highlight'. For understanding purpose spectral figure accompanying would be useful, with noting that ion bound version remains is required exact form diazinon will yield 304.1010.

So, ionization methods show soft features of SICRIT but can further be added details of work describing reasoning calrifying this would enhance understanding of spectral data.

GC-EI-MS spectrum:

On the other hand, the EI spectrum shows extensive fragmentation. The highest mass notes, is m/z 304.0 which corresponds to the molecular ion of diazinon. The most intensive peak in the spectrum has at m/z 179.13 This is the base peak of this compound. which is clearly a major fragment ion but does not represent a simple single bond cleavage. Other major peaks are observed at m/z 137.13 and 199.07. The fragmentation pattern obtained for diazinon fragmentation pattern is characteristic and diagnostic for this analyte and while helpful for structural analysis might pose some problems for quantification. Fragmentation in EI-MS creates major barriers to quantification. Since typically each compound would have diverse fragmentation patterns and responses to changes in experimental conditions, ie sensitivity will vary as well, the technician cannot develop a calibration curve as that curve would depend on three variables (the analyte, the type of response, and the experiment conditions). In some cases, the recordable fragment ions response could be very different than the intact molecular ions response. This loss of detail makes subsequent correlation of detected ions and a concentration of the analyte essentially impossible. Any contribution from the matrix will alter the levels of fragment ions including through dilution or concentration in the matrix or a combination of both, the quantifying can become mere speculation. There is sometimes more than one analyte consisting of different fragmentation products which creates greater effort as the professionals must use representative ions which can add to uncertainty and delay the validation of methods.

To clarify, it is suggested that the figure with both the GC-SICRIT-MS and GC-EI-MS spectra should be calibrated to the same scale and be the same area (or size) and that every peak should have enough room to be labelled; specifically the molecular ions ($[M+H]^+$) and prominent fragment ions (especially where the molecular ion and majority of the combined fragment ion area were especially high). Finally, a table summarizing essential characteristics of the compound name, exact mass, molecular formula and most

significant ions should be included too, and that a redraw of the diazinon molecular structure indicating the functional group structure so that that even the ion labelling on the SICRIT spectrum refers to the protonated version.

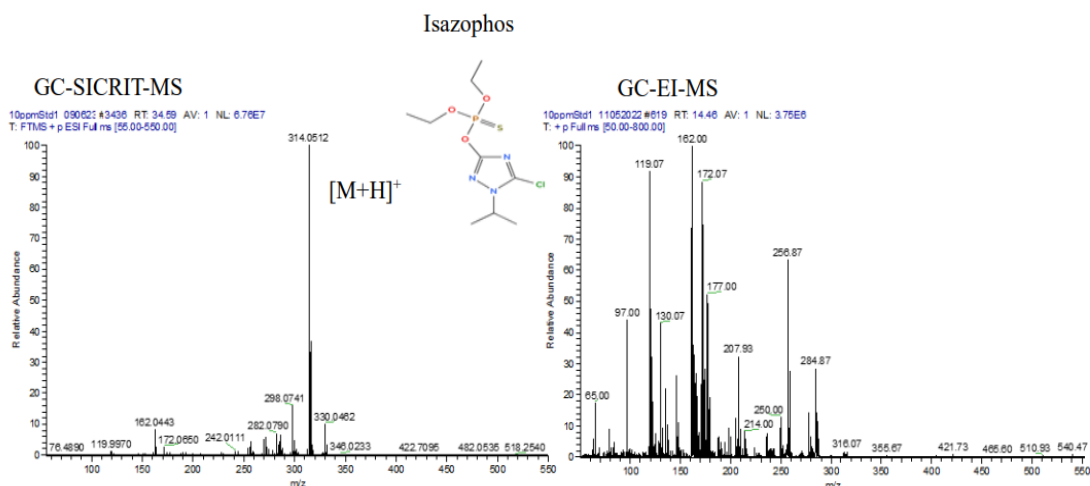


Figure 3.7: EI-MS and of SICRIT-MS spectra (positive ionization mode) of isazophos (m/z 313.0416) (see table 3.2) at 10ppm, analyzed by GC-SICRIT- LTQ Orbitrap mass spectrometer and GC-EI-ITQMS.

GC-SICRIT-MS spectrum:

In the spectrum in Figure 3.7, the main ion reported for the SICRIT ionization of Isazophos is m/z 314. 0511, matching to the molecular weight of the protonated analyte of 314.0495 Da and assigned to the $[M+H]^+$ ion of Isazophos. This again illustrates how SICRIT the preference for soft protonation as a mode of ionization prevalent when using SICRIT as earlier noted. The other minor peaks of note are m/z 298. 0767 (O for S exchange) and m/z 316.0507(Chlorine 37 isotope). There are numerous other ions that are represent major structural fragments. The most noticeable peak in the Isazophos spectrum at m/z 314.0511 is the $[M+H]^+$ of the molecule and, with the monoisotopic mass for Isazophos calculated to be 314.04950 Da, this further displays the intended capability of our soft protonation format realized through SICRIT to account for the intended protonation. The calculated difference in parts per million (ppm) at approximately 5.04 ppm provides evidence of the level of precision we achieve in mass measurement with SICRIT. Other peaks in the spectrum at m/z 298.0767, which may be due to an exchange

of sulfur for an oxygen, and m/z 316.0507, due to chlorine-37, may provide insight into other aspects of structural change in the molecule.

GC-EI-MS spectrum:

It is clear from the EI spectrum that it has multiple intense peaks suggesting that the compound is greatly fragmented. There are conspicuously large peaks at m/z 162.00, 119.07, and 172.07. The molecular ion peak is absent, or very weak, which is typical for EI spectra. Presence of Cl in the analyte is clear from the fragments at m/z 284.87 and 256.87 as they show a second peak at 2 mass units higher.

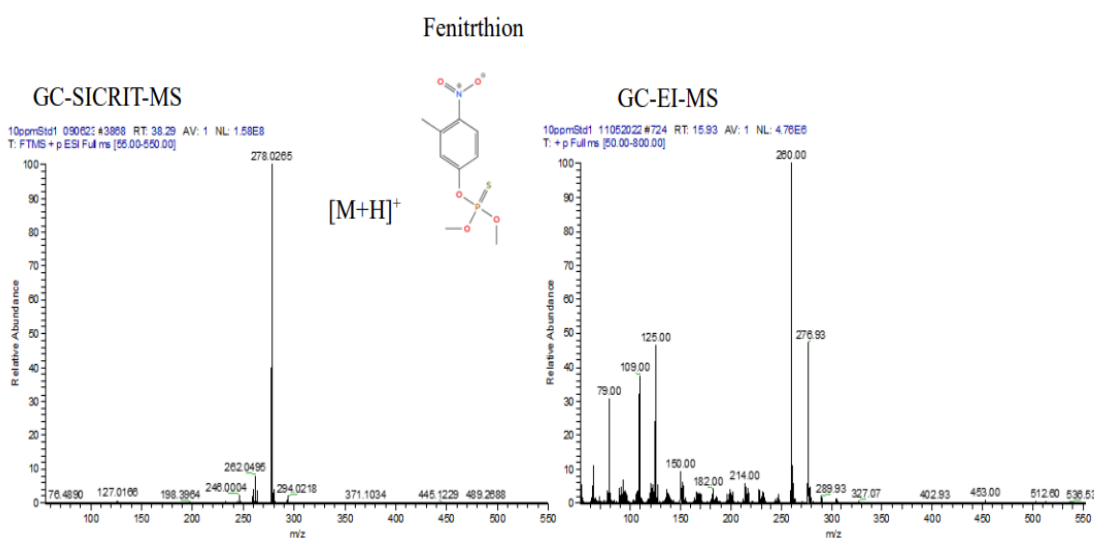


Figure 3.8: EI-MS and of SICRIT-MS spectra (positive ionization mode) of fenitrothion (m/z 277.0173) (see table 3.2) at 10ppm, analyzed by GC-SICRIT- LTQ Orbitrap mass spectrometer and GC-EI-ITQMS.

Fenitrothion, which has an exact mass of 277.0173 Da, was easily identified from the SICRIT-Orbitrap MS as there is a clear ion at 278.0290 which gives a most likely molecular weight of the protonated analyte and assigned to the [M+H]⁺ ion of Fenitrothion, and at m/z 277.0215 is the molecular ion peak, very close to the exact mass. The other major fragment is: loss of a CH₃ group at m/z 262.0518. The GC-EI-MS shows a strong molecular ion at m/z 276.93 and either loss of O or exchange of S for O at m/z 260.00. This suggested that this molecular structure is remarkably robust as an intact molecular ion or pseudo molecular ion were seen under both ionization conditions. (see figure 3.8 above).

3.4 Fragmented pesticides

Although Phosmet ($C_{11}H_{12}NO_4PS_2$), Phosalone ($C_{12}H_{15}ClNO_4PS_2$), Azinphos-methyl ($C_{10}H_{12}N_3O_3PS_2$) and Azinphos-ethyl ($C_{12}H_{16}N_3O_3PS_2$). (Figure 3.8) were analyzed by GC-LTQMS with SICRIT ionization no molecular ions was seen, the spectra recorded were complex showing significant fragmentation. Figure 3.9 illustrate these cases:

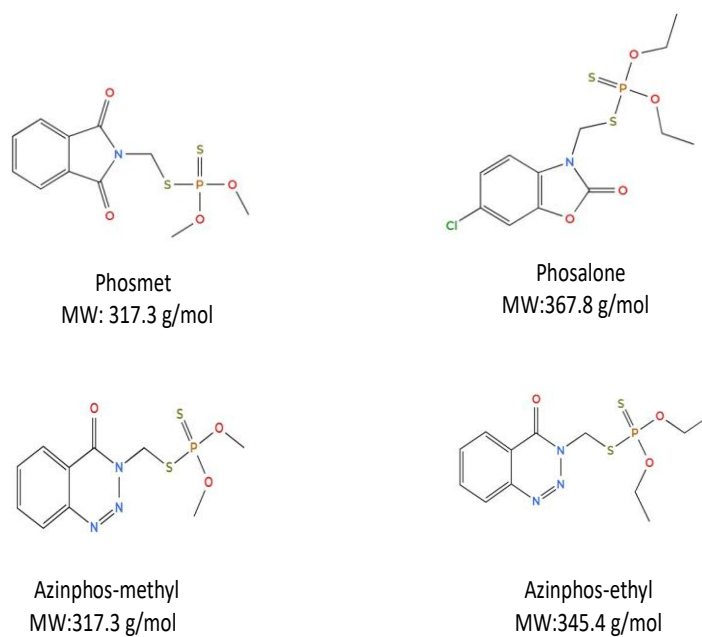


Figure 3.9 Structure of the fragmented pesticides in GC-SICRIT-LTQMS.

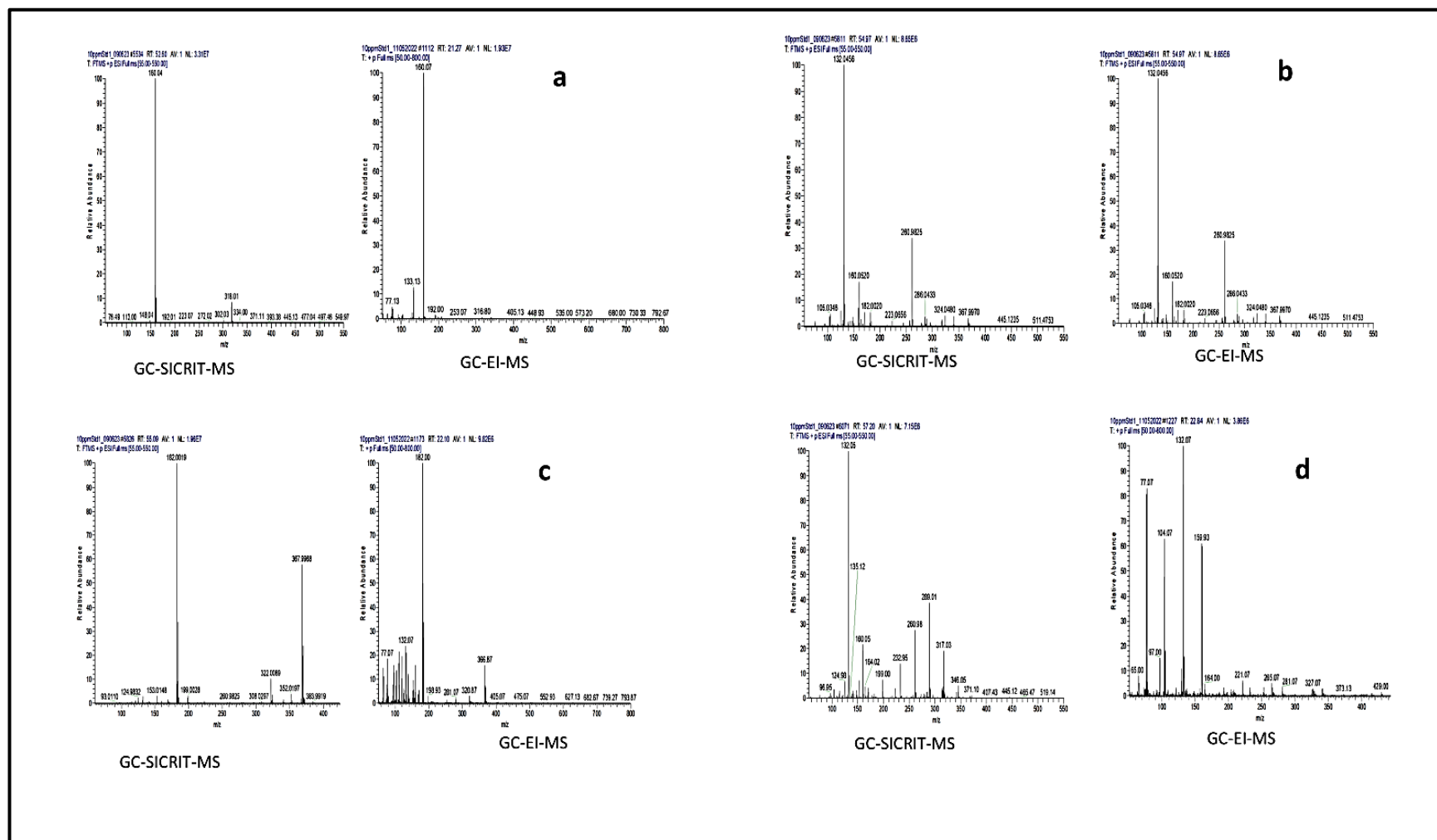


Figure 3.10: EI-MS and of SICRIT-MS spectra (positive ionization mode) of (a)phoamet (b)phosalone (c)azinphos-methyl (d)azinphos-ethyl (see table 3.2) at 10ppm, analyzed by GC-SICRIT- LTQ Orbitrap mass spectrometer and GC-EI-ITQMS.

Figure 3.9 a (Phosmet): Both SICRIT and EI produce a major fragment at m/z 160, but SICRIT also shows the $[M+H]^+$ ion at m/z 318.01 albeit with low intensity. Figure 3.9 b (Phosalone): SICRIT produces both a fragment at m/z 182.00 and the $[M+H]^+$ ion at m/z 367.99, while EI shows more extensive fragmentation. Figure 3.9 c (Azinphos-methyl): both ionization methods show significant fragmentation, with SICRIT producing ions at m/z 132, 160, and 260.98. Figure 3.9 d (Azinphos-ethyl) shows similar fragmentation to its methyl analog. Both ionization methods cause fragmentation, but SICRIT still shows the $[M+H]^+$ ion at m/z 346.05. These results demonstrate that while SICRIT generally produces less fragmentation than EI, some compounds are prone to fragmentation regardless of the ionization technique. This information is crucial for developing targeted analytical methods for these pesticides.

3.5 Method validation

Once the investigation of the ionization of the OPP pesticides was complete, validation of the analytical method was carried out following the procedure established in the relevant EU SANTE guidelines.¹¹⁹ This method is used not only in assessing the linearity of calibration curves but also for the determination of instrument limits of detection and method limits of quantification. Method linearity is determined by injecting standard solutions multiple times at 5 concentration levels which were chosen as 0.001, 0.005, 0.010, 0.050, 0.100 and 0.500 $\mu\text{g/mL}$. This method is also used for the determination of the coefficient (R^2) and to assess deviation of back-calculated concentrations from their expected values. The instrument detection limits particularly the (LOD) are determined according to the lowest detectable concentration level and calibration curves were constructed from calibration standards in both solvent and matrix extracts.

3.5.1 Linearity

Linearity is determined by repeated injections of calibration standard solutions at different levels. It includes 0.001, 0.005, 0.010, 0.050, 0.100 and 0.500 µg/mL. Replicates were run at each level. Standards were prepared in a solvent suitable for GC-ITQMS, GC-SICRIT-LTQMS and GC-MSD. All of the evaluated analytes produced calibration curves with an R^2 value higher than approximately 0.999. The high linearity showed a good agreement between the concentration of the pesticides in the multiplexed standard preparations and the detector response. This shows that good and accurate quantitative measurements are achievable over a wide calibration range.

3.5.2 LOD and LOQ

The LOD measurement is useful as it sets a base level of a specific analyte present in the sample that can be reliably seen by the detector above the background noise. Even though the specific analyte can be seen, its presence does not provide reliable precision or accuracy of quantification information at this concentration level. The LOD and LOQ are values unique to an individual analyte and must be determined for every analyte the method is designed to give quantification data for. These values are important in the data analysis process as they provide insights into sensitivity but also accuracy on a per analyte basis.¹¹¹ Reported below are the LOD and LOQ values for all pesticides studied across the three analytical systems used in this thesis (Table 3.3).

Table 3.3: LOD, LOQ, and linearity of organophosphorus pesticides in GC-ITQMS, GC-MSD, and GC-SICRIT-LTQMS.

Component Name	GC-ITQMS			GC-MSD			GC-SICRIT-LTQMS		
	LOD µg/mL	LOQ µg/mL	R ²	LOD µg/mL	LOQ µg/mL	R ²	LOD µg/mL	LOQ µg/mL	R ²
Diazinon	0.003	0.008	0.9999	0.003	0.0076	0.999	0.002	0.007	0.9996
Isazophos	0.004	0.013	0.9996	0.003	0.0093	0.9993	0.002	0.005	0.9998
Chlorpyrifos-methyl	0.004	0.013	0.9996	0.003	0.0104	0.9992	0.003	0.009	0.9994
Fenitrothion	0.005	0.015	0.9995	0.003	0.0097	0.9987	0.004	0.012	0.9989
Pirimiphos-methyl	0.003	0.01	0.9998	0.001	0.003	0.999	0.001	0.004	0.9999
Chlorpyrifos	0.004	0.012	0.9996	0.003	0.0087	0.9994	0.002	0.005	0.9998
Pirimiphos-ethyl	0.004	0.012	0.9997	0.007	0.0217	0.9964	0.001	0.004	0.9999
Quinalphos	0.003	0.009	0.9998	0.001	0.0037	0.9999	0.002	0.005	0.9998
Pyridaphenthion	0.005	0.014	0.9985	0.005	0.0164	0.9994	0.005	0.014	0.9985
Phosmet	0.003	0.011	0.9997	0.002	0.0073	0.9996	0.001	0.004	0.9999
EPN	0.004	0.013	0.9995	0.003	0.0091	0.9994	0.003	0.008	0.9995
Phosalone	0.007	0.023	0.9988	0.002	0.0046	0.9998	0.002	0.007	0.9997
Azinphos-methyl	0.008	0.025	0.9985	0.003	0.0103	0.9992	0.003	0.009	0.9999
Pyrazophos	0.004	0.011	0.9991	0.003	0.0092	0.9994	0.004	0.011	0.9991
Azinphos-ethyl	0.009	0.027	0.9982	0.002	0.0052	0.9998	0.003	0.009	0.9993
Pyraclofos	0.009	0.026	0.9983	0.003	0.0104	0.9993	0.002	0.007	0.9996

In this section, we review and analyze data collected from different systems to ensure their equivalence and provide a comprehensive assessment of their consistency. Analysis of variance (ANOVA) is employed to determine statistical differences between groups, while Levene’s test is used to evaluate the homogeneity of variances. Additionally, Tukey HSD analysis allows for a detailed comparison of results from different systems and helps identify analytical methods that give significantly different results. These statistical evaluations provide a solid foundation for validating the accuracy and reliability of the data for subsequent stages of the study.

Descriptive statistics is a branch of statistics that focuses on summarizing and presenting data in an understandable way. This part aims to summarize the information contained in table 3.3 of the LOD.

Table 3.4: Descriptive statistics for LOD of ITQMS,SQMS,and LTQMS

	N	Mean	Std. Deviation	Std. Error	95% Confidence Interval for Mean		Minimum	Maximum
					Lower Bound	Upper Bound		
GC-ITQMS	16	.0049	.00211	.00053	.0038	.0061	.00	.01
GC-MSD	16	.0029	.00144	.00036	.0022	.0037	.00	.01
GC-SICRIT-LTQMS	16	.0025	.00115	.00029	.0019	.0031	.00	.01
Total	48	.0035	.00191	.00028	.0029	.0040	.00	.01

A summary of descriptive statistics appears in the table for three groups (GC-ITQMS, GC-MSD, and GC-SICRIT-LTQMS) containing 16 observations each to show their measurement characteristics. Within each group the data shows average values at 0.0049, 0.0029 and 0.0025 together with standard deviations that demonstrate minimal variability between 0.00115 and 0.00211 indicating repeatable measurement results. Standard errors are low which signifies accurate mean estimation and the 95% confidence range for GC-ITQMS runs from 0.0038 to 0.0061. Analysis of all groups shows their data points extend from 0.00 to 0.01 which indicates uniform measurement ranges.

Levene statistic is a statistical test designed to test the equality of variances between different groups. This test is important because it allows to determine whether the assumptions regarding equality of variance are correct, which is essential in many statistical analyses such as analysis of variance (ANOVA).

The test of homogeneity of variances, as shown in table 3.5, aims to determine whether the variances of LOD are equal among the three different systems.

Table 3.5: test of homogeneity of variances for LOD.

Levene Statistic	df1	df2	Sig.
3.127	2	45	.054

The Test of Homogeneity of Variances conducts statistical testing on different groups to check variance similarities in advance of ANOVA testing. In this output from SPSS: The computed Levene statistic equals 3.127. A calculated Levene Statistic value shows the extent of difference between separate variances. Both separate groups show larger quantitative differences according to the statistic value. A df1 of 2 and a df2 of 45 appear in this test. df1 corresponds to the total number of groups minus one because the study features three distinct groups (2 because 3 groups minus one equal 2). The significance value (Sig.) obtained in this research equates to .054. This p-value reveals how likely the results would become based on a hypothesis that states different groups possess equal variance levels. The result with .054 above the conventional 0.05 cutoff leads to non-rejection of the null hypothesis which indicates that the sample data insufficiently proves distinct statistical variances between groups. ANOVA can proceed with the assumption of equal variances being supported by Levene's test evaluation though the result shows marginal acceptance.

ANOVA (Analysis of Variance) is a multi-group statistical technique. ANOVA determines whether there are statistically significant differences between the means of three groups. The average of the three devices used was compared based on LOD variable as shown in table 3.6.

Table 3.6: ANOVA results for LOD across three devices.

	Sum of Squares	df	Mean Square	F	Sig.
Between Groups	.000	2	.000	10.315	.000
Within Groups	.000	45	.000		
Total	.000	47			

All values in the ANOVA table demonstrate zero variations between group means and within-group observations because both the between-group and within-group sum of squares register 0.000. The analysis includes two between-groups degrees of freedom since there are three groups and 45 degrees of freedom for within-groups due to the total number of observations minus the groups present. An F statistic value of 10.315 indicates possible significance yet both mean squares values equal 0.000 thereby making the division by zero invalid. Characterization by the p-value at .000 suggests an extremely significant outcome, yet this result becomes meaningless because there is no data variability.

The HSD (Tukey's Honestly Significant Difference) is a statistical test used after analysis of variance (ANOVA) to determine which groups (or means) differ from each other. Tukey HSD test used when there are three or more groups and need to analyze the differences between these groups after conducting an ANOVA.

The table 3.7 display the results of the Tukey HSD test for multiple comparisons between different groups based on the dependent variable LOD.

Table 3.7: results of Tukey HSD multiple comparisons for LOD.

(I) Method	(J) Method	Mean Difference (I-J)	Std. Error	Sig.	95% Confidence Interval	
					Lower Bound	Upper Bound
GC-ITQMS	GC-MSD	.00200*	.00057	.003	.0006	.0034
	GC-SICRIT-LTQMS	.00244*	.00057	.000	.0011	.0038
GC-MSD	GC-ITQMS	-.00200*	.00057	.003	-.0034-	-.0006-
	GC-SICRIT-LTQMS	.00044	.00057	.726	-.0009-	.0018
GC-SICRIT-LTQMS	GC-ITQMS	-.00244*	.00057	.000	-.0038-	-.0011-
	GC-MSD	-.00044-	.00057	.726	-.0018-	.0009

*. The mean difference is significant at the 0.05 level.

The data in the table reveals the results obtained from analyzing the dependent variable "LOD" through three methods (GC-ITQMS, GC-MSD, and GC-SICRIT-LTQMS) using the Tukey HSD post-hoc test. The mean values obtained from GC-ITQMS exceed GC-MSD and GC-SICRIT-LTQMS by 0.00200 and 0.00244 respectively thus producing significant differences ($p = 0.003$ and $p < 0.001$). The analysis demonstrates that GC-SICRIT-LTQMS produces no considerably different results than GC-MSD ($p = 0.726$). Significant method differences persist based on the non-inclusion of zero in the confidence intervals of the compared values. The research indicates that GC-ITQMS produces superior measurement results than the other two methods though GC-MSD and GC-SICRIT-LTQMS show no meaningful variations between their readings.

Using the same statistical methods mentioned above, the LOQ is analysis to ensure the accuracy and reliability if the results.

The statistical description of LOD provides a comprehensive overview of the data and enhances its understanding, as shown in table 3.8.

Table 3.8: Descriptive statistics for LOQ of ITQMS, SQMS, and LTQMS

	N	Mean	Std. Deviation	Std. Error	95% Confidence Interval for Mean		Minimum	Maximum
					Lower Bound	Upper Bound		
GC-ITQMS	16	.0151	.00633	.00158	.0117	.0185	.01	.03
GC-MSD	16	.0092	.00465	.00116	.0067	.0116	.00	.02
GC-SICRIT-LTQMS	16	.0075	.00303	.00076	.0059	.0091	.00	.01
Total	48	.0106	.00580	.00084	.0089	.0123	.00	.03

The SPSS Descriptive Statistics table 3.8 presents the distances of LOQ values between GC-ITQMS, GC-MSD, and GC-SICRIT-LTQMS detection methods through sample data summaries including N values, mean measurements and standard deviations and errors as well as confidence intervals and range minimums and maximums. Analysis using GC-ITQMS produced a maximum mean LOQ of 0.0151 at the same time that GC-SICRIT-LTQMS provided the minimum mean LOQ of 0.0075. The data shows that GC-ITQMS also presents the greatest measurement variability at 0.00633. The confidence intervals of 95% for the means indicate that the actual means will exist within specified ranges for each method but demonstrate different levels of uncertainty regarding the mean analysis. The GS-ITQMS method displayed the greatest maximum value of 0.03 together with a minimum measurement of 0.01 and GS-SICRIT-LTQMS exhibited minimum and maximum results of 0.00 and 0.01, respectively.

Next, the Levene's test of variance is performed to examine the variance between groups. This test is essential and indicates whether the different groups have equal variance, an important requirement for analysis of variance (ANOVA). Table 3.9 show the results of Test of Homogeneity of Variances.

Table 3.9: test of homogeneity of variances for LOQ.

Levene Statistic	df1	df2	Sig.
3.310	2	45	.046

The output from SPSS reveals essential data about the equality of variances between the Limit of Quantification (LOQ) measurements obtained from GC-ITQMS, GC-MSD, and GC-SICRIT-LTQMS detection methods. The Levene Statistic reaches a value of 3.310 between groups and error terms (2 and 45 respectively). An analysis of the p-value (0.046) demonstrates statistical significance for variance group differences because it falls below the standard alpha threshold (0.05). The test results lead us to reject homogeneity of variance as an assumption because the detection methods possess non-equal variances.

Then, the ANOVA is performed to determine whether there are statistically significant differences between the different groups. Table 3.10 displays the results of an ANOVA analysis of LOQ for different methods.

Table 3.10: ANOVA results for LOQ across three devices.

	Sum of Squares	df	Mean Square	F	Sig.
Between Groups	.001	2	.000	10.874	.000
Within Groups	.001	45	.000		
Total	.002	47			

The SPSS ANOVA results demonstrate that there exists a statistically significant difference between the LOQ value means of GC-ITQMS, GC-MSD, and GC-SICRIT-LTQMS detection methods. The Sum of Squares Between Groups stands at 0.001 because different group means display minimal variability but Sum of Squares Within Groups also equals 0.001 due to minimal point-to-point variation among group members. Between-group degrees of freedom equal two while within-group degrees of freedom amount to forty-five. Statistics reveal that the F statistic equals 10.874 while the p-value

demonstrates a 0.000 result which indicates that there exists a statistically meaningful difference between the means of the groups. The significant F-value confirms the existence of unique effectiveness among detection methods for LOQ measurement although the variation between data points remains small.

Finally, the Tukey HSD test is used to make pairwise comparisons between groups, which helps determine which groups differ significantly from each other. Table 3.11 displays the results of the Tukey HSD test to compare of LOQ between different methods.

Table 3.11: results of Tukey HSD multiple comparisons for LOD.

(I) Method	(J) Method	Mean Difference (I-J)	Std. Error	Sig.	95% Confidence Interval	
					Lower Bound	Upper Bound
GC-ITQMS	GC-MSD	.00596*	.00172	.003	.0018	.0101
	GC-SICRIT-LTQMS	.00762*	.00172	.000	.0035	.0118
GC-MSD	GC-ITQMS	-.00596*	.00172	.003	-.0101-	-.0018-
	GC-SICRIT-LTQMS	.00166	.00172	.601	-.0025-	.0058
GC-SICRIT-LTQMS	GC-ITQMS	-.00762*	.00172	.000	-.0118-	-.0035-
	GC-MSD	-.00166-	.00172	.601	-.0058-	.0025

*. The mean difference is significant at the 0.05 level.

The Tukey HSD multiple comparisons table 3.11 demonstrates that detection methods GC-ITQMS and GC-SICRIT-LTQMS along with GC-MSD showed different LOQ measurement values. Data obtained from GC-ITQMS analysis shows a significantly higher mean LOQ than both GC-MSD and GC-SICRIT-LTQMS with mean differences of 0.00596 ($p = 0.003$) and 0.00762 ($p = 0.000$) respectively. Statistical significance was confirmed by both results since their confidence intervals excluded zero. The data analysis between GC-MSD and GC-SICRIT-LTQMS shows no significant variation based on their p-values (0.601) because the confidence intervals span zero. The study results show that GC-ITQMS achieves better substance detection sensitivity than each of the alternative methods.

Figure 3.10 provides a graphical view of the LOD and LOQ values highlighting the slight differences in LODs and LOQs that are observed for each individual pesticide when they were analysed using the different instrumentation setups for this thesis. Some of these values may indicate potential method-dependent variations in sensitivity and detection capabilities.

In general, the LOD for all compounds analyzed using GC-SICRIT-LTQMS demonstrated lower values, ranging from 0.001 to 0.004 $\mu\text{g/mL}$, in comparison to those obtained with GC-ITQMS and GC-MSD.

Phosalone, azinphos-methyl, pyrazophos, azinphosethyl, and pirimiphos-ethyl display noticeable differences in LODs and LOQs across the three instrumentation setups, suggesting that the choice of instrumentation influences these parameters. The same sample was used for each instrument to ensure consistency, and measurements were repeated to assess inter-run variations. factors on their analysis. For diazinon, the LOD values are 0.003 $\mu\text{g/ml}$ for GC-ITQMS, 0.003 $\mu\text{g/ml}$ for GC-MSD, and 0.002 $\mu\text{g/ml}$ for GC-SICRIT-ITQMS. The corresponding LOQ values are 0.0080 $\mu\text{g/ml}$, 0.0076 $\mu\text{g/ml}$, and 0.0070 $\mu\text{g/ml}$, respectively. The R^2 values for all methods are exceptionally high, indicating strong linearity in the calibration curves, with values close to 1 (0.9999 for GC-ITQMS, 0.999 for GC-MSD, and 0.9996 for GC-SICRIT-ITQMS). Similar trends can be observed for Pyridaphenthion which exhibits LOD value is 0.005 $\mu\text{g/ml}$ across the three GC methods.

Isazophos, chlorpyrifos-methyl, fenitrothion, chlorpyrifos, pirimiphos-ethyl quinalphos, phosmet, EPN and pyrazophos all demonstrate similar trends in LOD, LOQ, and linearity across the three GC methods. The LOD values range from 0.001 $\mu\text{g/ml}$ to 0.004 $\mu\text{g/ml}$, the LOQ values range from 0.003 $\mu\text{g/ml}$ to 0.015 $\mu\text{g/ml}$, and the R^2 values are consistently high, indicating strong linearity in the calibration curves for each pesticide.

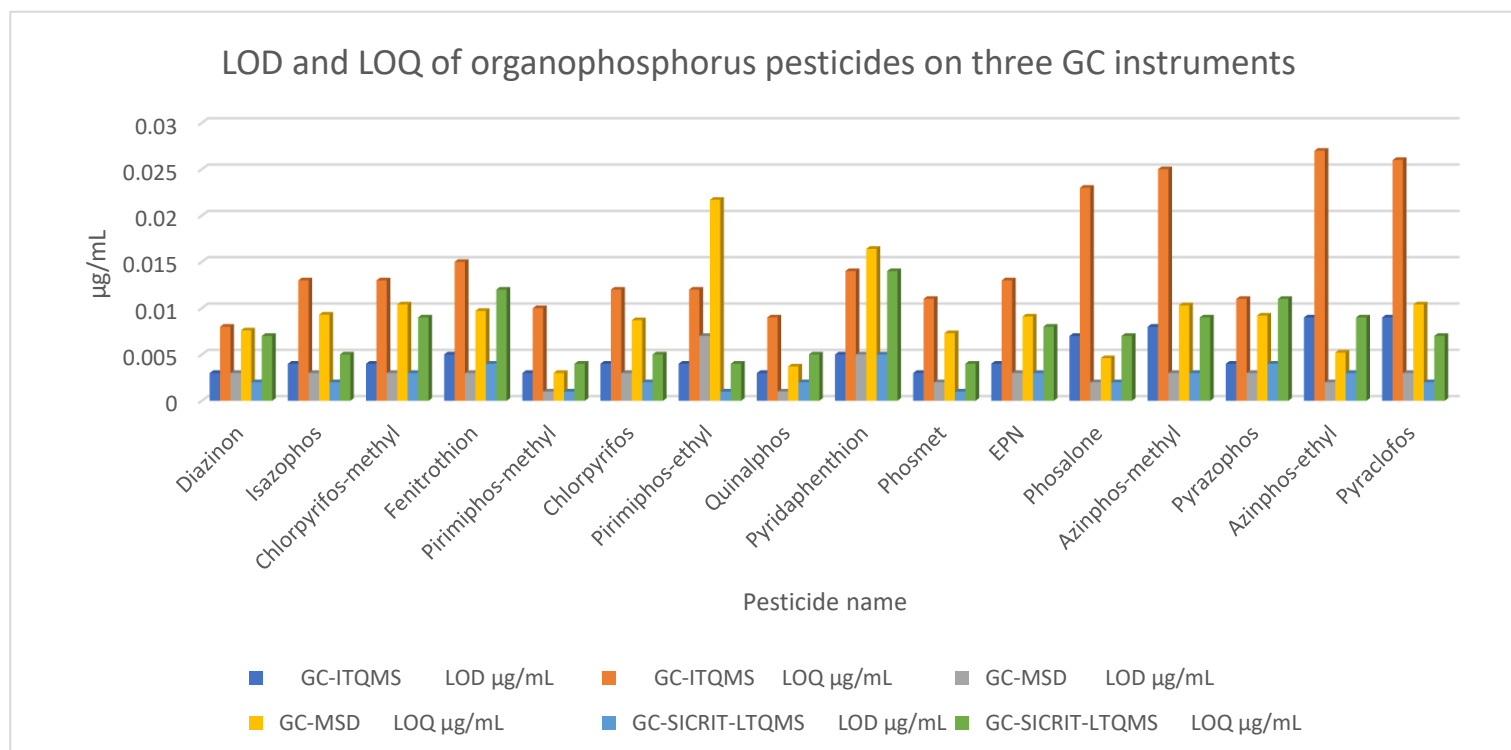


Figure 3.11: LOD and LOQ of organophosphorus pesticides in GC-ITQMS, GC-MSD and GC-SICRIT-LTQMS

3.5.3 Matrix Effect evaluation of multiple organophosphorus pesticide residues in selected baby food matrices (milk, rice and cereal)

Baby foods generally contain complex compounds as in studied matrices that have distinct compositions that can affect pesticide detection, such as, milk, which is a complex matrix rich in fats, proteins, and sugars. The high-fat content can potentially lead to the retention of lipophilic pesticides, as well as rice, which is primarily composed of carbohydrates (starch) with some protein content and phenolic compounds that affect the distribution of pesticides during extraction process. It has a relatively simpler matrix compared to milk. In addition to cereal, which is also rich in carbohydrates, but may contain a mix of grains, fibers, and potentially added vitamins or minerals and secondary plant compounds that contribute to matrix interaction, creating a more complex matrix than rice but less so than milk. Some analyte types are more affected than others and thus the matrix effect must be evaluated for each matrix/analyte combination.^{120,121}

The assessment of multiple organophosphorus pesticide residues in analyzed baby food matrices such as milk and rice and cereal depend on how extraction and clean-up methods impact the interferences that occur during measurement procedures. The analytical measurement response of an analyte suffers changes because of matrix components that lead either to signal detection enhancement or suppression effects. The measurement of matrix effect (ME %) depends on extracting peak area measurements of pesticides from matrix samples compared to peak area measurements of pesticides in solvent-based standards.

In this research, QuEChERS (Quick Easy Cheap Effective Rugged and Safe) techniques for pesticide residue extraction were used as the main extraction method due to their capability to reduce matrix effects in terms of reducing interference from non-target components. This is followed by a dispersive solid-phase extraction (d-SPE) step which includes, C18-EC (end-capped), PSA (primary secondary amine), and MgSO₄ to contributes to the removal of contaminants according to the sample type and improve separation efficiency.

The effect of the matrix on analysis of pesticides in studied matrices (infant formula, rice, and cereal) is evaluated using GC-EI-ITQMS, AND GC-SICRIT-LTQMS. The QuEChERS method is used as the extraction method, followed by a clen-up step to ensure

the removal of interfering compounds and accurate measurement of pesticide concentrations.

To ensure that matrix effects are minimized, the spiked samples are prepared as described in the methodology section. Then the matrix effect (ME %) is calculated by comparing the peak area of a pesticide in the stock standard prepared in the matrix to the peak area of the same pesticide in the standard prepared in the solvent diluent.¹²³

$$\text{ME}\% = ((\text{Area (Standard in matrix)}) / (\text{Area (Standard in solvent)}) - 1) * 100$$

Through this monitoring and calculation, the impact of matrix is evaluated, and its positive and negative effect on the detector response is compared.

A value of 100% is considered no effect, a value of $\pm 20\%$ is considered a soft ME, $\pm 50\%$ values are considered a moderate ME, while values more than $\pm 50\%$ are considered a strong ME. The matrix effect results for organophosphorus pesticides are summarized in table 3.4.

In addition, the matrix effect was studied for three different samples using three different instrumental setups, so it is expected that the matrix effect values will be affected by type of pesticides, the type of matrix, and the type of the ion source.

In this study the task was to estimate the matrix effect for 16 organophosphorus pesticides in three different samples (milk, rice and cereal) by three different instruments GC-MSD, GC-SICRIT-LTQMS, and GC-EI-ITQMS. This is done by spiking blank baby food samples with known concentration of pesticides; QuEChERS was used as the extraction method for the pesticides and dSPE was used as clean-up protocol.

This research aimed to assess 16 organophosphorus pesticide matrix effects on milk and rice cereal and baby food mixture using GC-MSD and an advanced device combo comprising GC-SICRIT-LTQMS with GC-EI-ITQMS. Analysis of the matrix effect required blank baby food samples to receive planned pesticide spike concentrations. This research applied QuEChERS extraction as its extraction method because it displays great ability for gathering pesticides from complex materials while still being suitable for milk rice and cereal testing. The analytical process utilized dSPE (dispersive Solid-Phase Extraction) to achieve co-extractant removal because inadequate removal would lead to measurement distortion of pesticide levels. The systematic method exposes matrix effects of instruments and food matrices in a detailed manner to validate pesticide detection accuracy for baby foods. The analytical responses for organophosphorus pesticides need accurate determination through the implementation of established methods in this study.

3.5.3.1 Matrix effect of organophosphorus pesticides on baby food samples based on GC-MSD

Table 3.4 presents matrix effects (ME%) observed for various pesticides analyzed using Gas Chromatography-Mass Spectrometry (GC-MSD) in three different food matrices: milk, rice, and cereal. There is variability in the matrix effect across different pesticides and matrices. For instance, diazinon ($C_{12}H_{21}N_2O_3PS$) exhibits a higher ME% in milk (403%) compared to rice (182%) and cereal (232%), indicating that the matrix components in milk have a greater influence on the ionization efficiency of diazinon.

EI mass spectrometry ion source efficiency undergoes significant modification because of complex sample matrices found in baby foods present in milk rice and cereal samples. The EI source encounters both organic and inorganic compounds present in each matrix that attempt to secure ionization against the analyte diazinon. The high-fat content of milk causes competition with electron impact which results in strong changes to both analyte signal suppression and enhancement. The intricate nature of the matrix causes diverse

interactions between its elements and pesticides that produces varying ionization efficiency patterns. Diazinon recorded an exceptionally high matrix effect (ME%) value of 403% when analyzed in milk which demonstrates that the matrix constituents have a significant impact on its ionization capabilities. To obtain precise pesticide analysis of food substances accurate method development must overcome matrix effects because these effects lead to measurement modifications.

Similarly, isazophos, chlorpyrifos-methyl, Fenitrothion, Chlorpyrifos, Pirimiphos-ethyl, Azinphos-methyl, and Pyrazophos also display higher ME% in milk compared to rice and cereal, suggesting that these pesticides may interact more strongly with the matrix components present in milk. A positive matrix effect (+Ve) indicates that the presence of milk enhances the detection signal of pesticides. The matrix effect ME% is the amount of change in the instrument's response compared to the standard solution, when ME% is 100%, it means that the instrument exhibits a response similar to the sample, meaning that there is no noticeable matrix effect on the analytical signal. In contrast, values greater than 100 % indicate signal enhancement due to the impact of matrix components, such as milk for diazinon, which has ME% 403.

This is particularly evident in gas chromatography, due to several key factors, the most important of which are the effects on injection and evaporation. Some matrices, such as milk, enhance the evaporation of some pesticides, increasing the amount of compound entering the column and thus enhancing the signal. Also, some sample components may enhance ionization, especially with GC-EI. This increases the efficiency of ion production, affects signal intensity, and thus improves it.

Furthermore, there are variations in matrix effects among pesticides within the same matrix. For example, in milk, chlorpyrifos-methyl shows a higher ME% (549%) compared to other pesticides like chlorpyrifos (459%) and quinalphos (126%). This discrepancy may be attributed to differences in the chemical properties of these pesticides and their interactions with the milk matrix components. Similarly, in rice, fenitrothion exhibits a higher ME% (203%) compared to azinphos-methyl (174%) and pyridaphenthion (94%), indicating differential matrix effects among these pesticides within the rice matrix. Moreover, some pesticides demonstrate consistent matrix effects across different matrices. For instance, pirimiphos-methyl displays relatively consistent ME% values across milk (421%), rice (406%), and cereal (468%), suggesting that the

matrix components present in these matrices have similar effects on the ionization efficiency of pyrazophos. Conversely, other pesticides such as azinphos-ethyl exhibit

varying matrix effects across different matrices, indicating that the composition of the matrix may influence the extent of matrix effects for these pesticides (Figure 3.11).

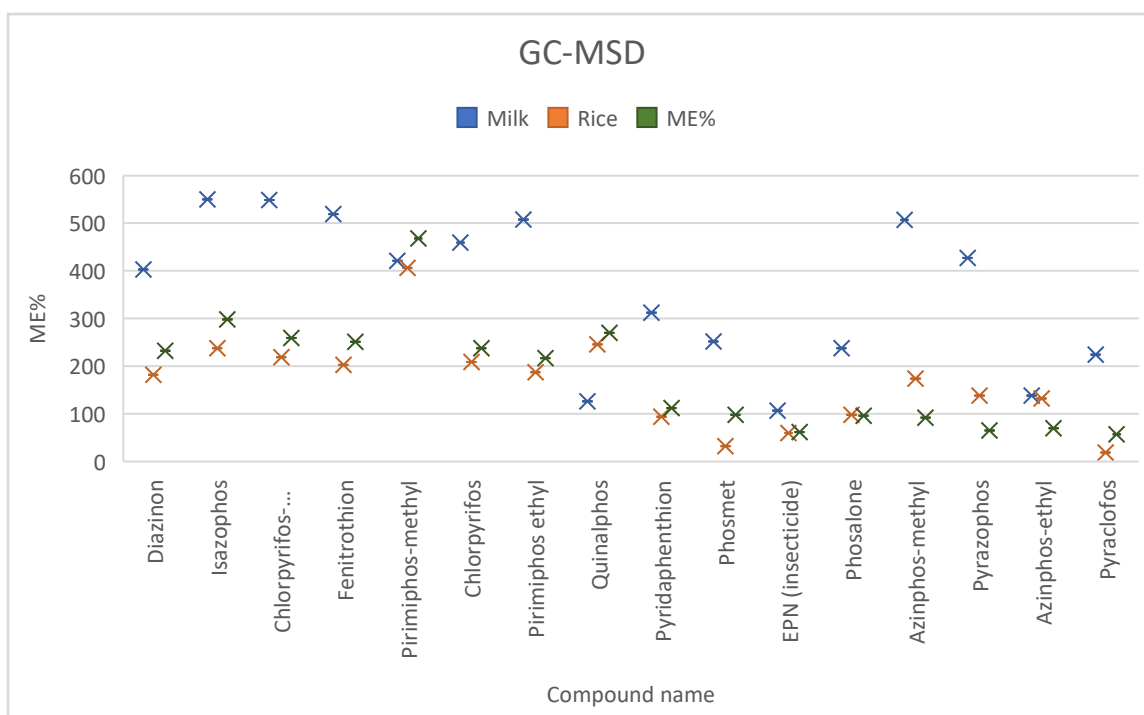


Figure 3.12: ME% of organophosphorus pesticides in GC-MSD.

3.5.3.2 Matrix effect of organophosphorus pesticides on baby food samples based on GC-SICRIT-LTQMS

Table 3.4 provides data on matrix effects (ME%) observed for various pesticides analyzed using Gas Chromatography coupled with SICRIT ionization/Linear Ion Trap Quadrupole Mass Spectrometry (GC-LTQMS) in three different food matrices: milk, rice, and cereal. This table predominantly displays negative matrix effects across the board for all compounds and matrices. This suggests that the matrix components present in milk, rice, and cereal suppress the ionization efficiency of the analyzed pesticides when using GC-SICRIT. This consistent negative trend in matrix effects could indicate that the matrix components interfere with the ionization process, resulting in decreased sensitivity or response for the pesticides analyzed. While the magnitude of the matrix effect varies

among different pesticides, there is a general similarity in the pattern of matrix effects across the various compounds within each matrix. For instance, in milk, all pesticides exhibit negative matrix effects ranging from -66 to -100, indicating a consistent suppression of ionization efficiency regardless of the specific pesticide. Similarly, in rice and cereal matrices, the majority of pesticides also display negative matrix effects within a relatively narrow range, suggesting a uniform impact of matrix components on ionization efficiency across different compounds within these matrices. There are some variations in the magnitude of matrix effects among different matrices for individual pesticides. For example, pirimiphos-methyl displays a slightly higher negative matrix effect in rice (-82) compared to milk (-100) and cereal (-79), indicating that the rice matrix may have a slightly greater suppressive effect on the ionization efficiency of pirimiphos-methyl compared to the other matrices. Similarly, phosalone exhibits a relatively lower negative matrix effect in rice (-66) compared to milk (-98) and cereal (-78), suggesting that the rice matrix may interfere less with the ionization efficiency of phosalone compared to the other matrices (Figure 3.12).

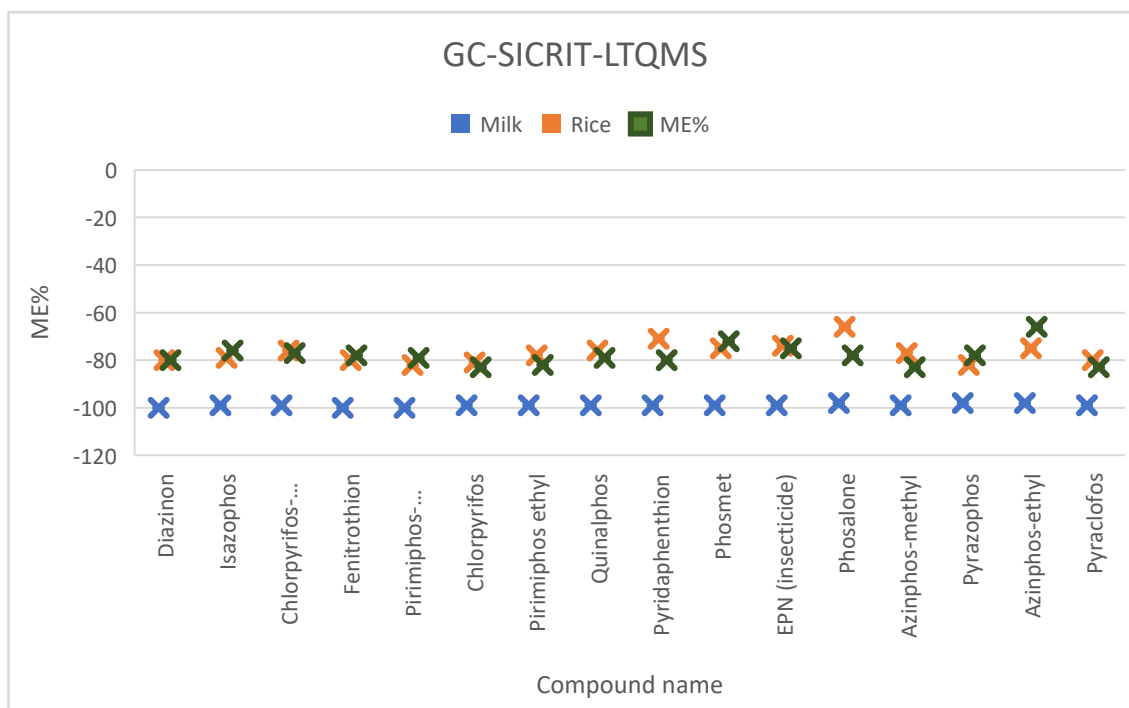


Figure 3.13: ME% of organophosphorus pesticides in GC-SICRIT-LTQMS.

3.5.3.3 Matrix effect of organophosphorus pesticides on baby food samples based on GC-ITQMS

Table 3.4 presents matrix effects (ME%) observed for various pesticides analyzed using Gas Chromatography coupled with Ion Trap Mass Spectrometry (GC-ITQMS) in three different food matrices: milk, rice, and cereal. Eleven out of 16 compounds exhibit relatively high ME% values in milk compared to rice and cereal, with matrix effect values ranging from 16% to 529% for milk, while in rice and cereal ME% values ranging from 13% to 179% and 11% to 202%, respectively. indicating a strong influence of the matrix components present in these matrices on the ionization efficiency of these pesticides. Conversely, pyrazophos and azinphos-methyl and phosmet display low ME% values across all matrices, suggesting minimal interference from matrix components on the ionization efficiency of these pesticides. Moreover, within each matrix, there are variations in matrix effects among different pesticides. For example, in milk, pyridaphenthion shows a higher ME% (529%) compared to phosmet (94%), indicating that the matrix components in milk may have a greater impact on the ionization efficiency of pyridaphenthion compared to phosmet. Similarly, in rice, chlorpyrifos exhibits a higher ME% (177%) compared to azinphos-methyl (41%), suggesting differential matrix effects among these pesticides within the rice matrix (Figure 3.13).

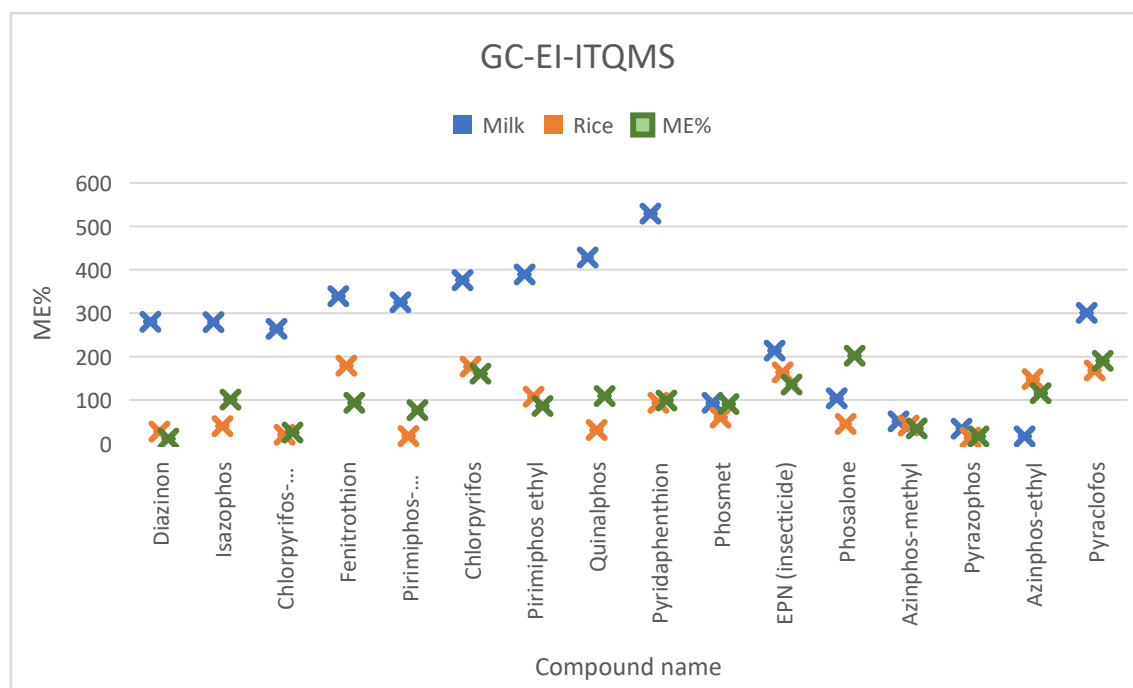


Figure 3.14: ME% of organophosphorus pesticides in GC-EI-ITQMS.

3.5.4 Comparison of matrix effect of organophosphorus pesticides on baby food samples

Across all matrices, GC-SICRIT-LTQMS consistently demonstrates negative matrix effects for all compounds, indicating a suppression of ionization efficiency in the presence of matrix components. In contrast, both GC-MSD and GC-ITQMS display positive matrix effects, indicating an enhancement of ionization efficiency for all compounds as shown in figure 3.15. The matrix effect (ME%) significantly impacts the analysis of pesticides in GC-MS, and the type of ion source used can influence this effect. The matrix effect refers to the alteration of the analytical signal due to co-eluting matrix components, which can either enhance or suppress the signal. Different ion sources, the Soft Ionization by Chemical Reaction in Transfer (SICRIT) ion source is known for its “soft” ionization, which minimizes fragmentation and can lead to differences in matrix effects compared to more traditional ion sources like Electron Ionization (EI). SICRIT operates at atmospheric pressure and uses a dielectric barrier discharge to ionize analytes, which can help in reducing matrix effects by providing a more stable and controlled ionization environment.¹¹⁵ This can be particularly beneficial in the analysis of pesticides, where matrix effects can significantly impact the accuracy and sensitivity of the measurements. Although the matrix effect is positive for all pesticides in three different samples when using both instruments (GC-MSD and GC-ITQMS), the ME% values differed according to the matrix, with the matrix effect value being higher in milk samples than in rice and cereal.

A TIC overlay to determine if any pesticides exist within the baby milk samples. Yet for the accurate results, this TIC must be overlaid with the TIC of a blank sample to determine which peaks exist merely due to background interference. One example of an actual detection of a pesticide as opposed to interference is called co-elution, in which two or more compounds are detected at the same retention time. The figure 3.14 shows the TIC of three matrices in addition to the organophosphorus pesticides studied, which ensures that no levels of these pesticides in particular can be detected in the three matrices (milk, rice, and cereal). This enhances the reliability of the analysis.

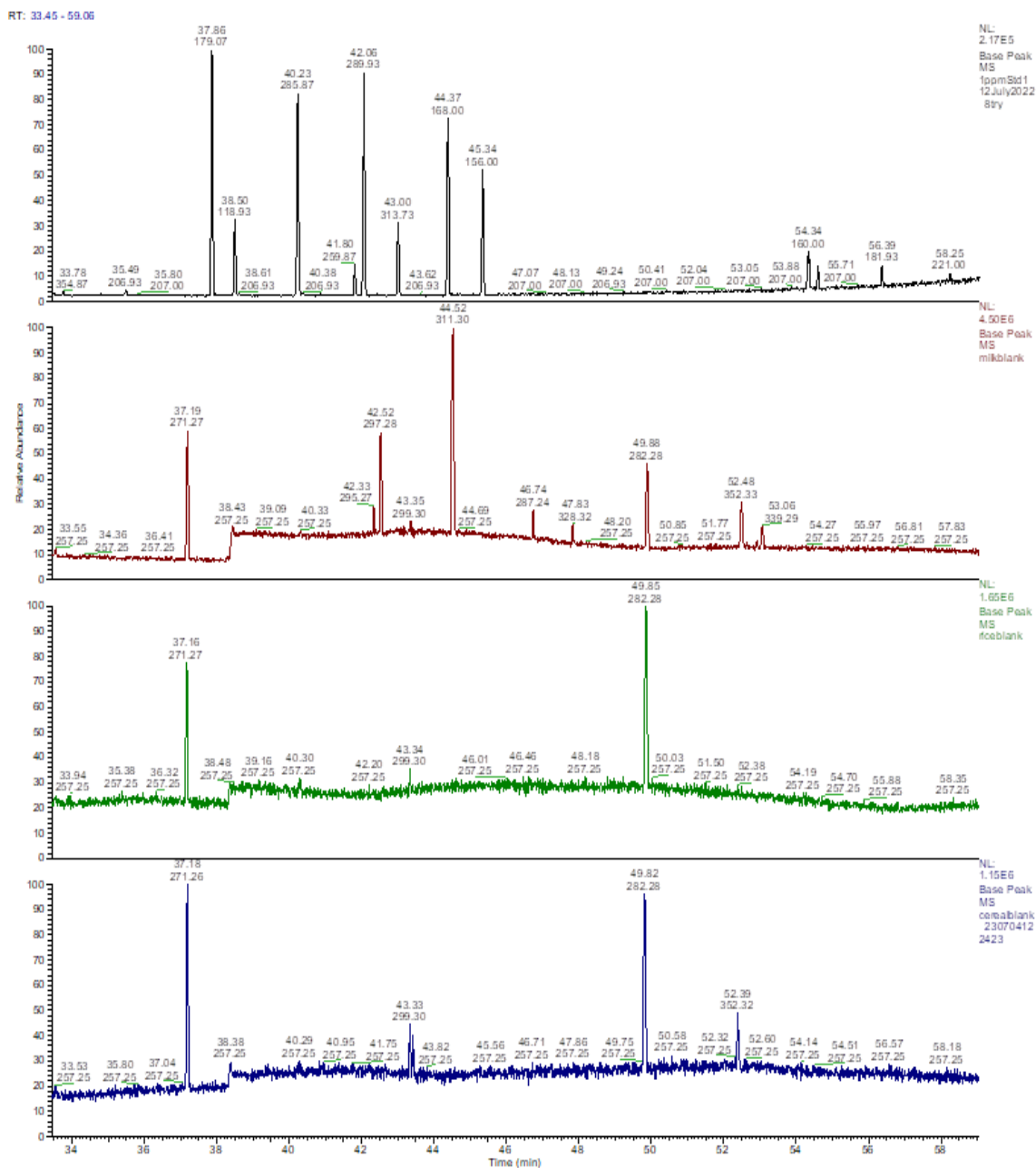


Figure 3.15: Chromatogram (a) milk blank, (b) cereal blank, (c) rice blank, and (d) standard organophosphorus pesticides, which are described in table 4.2 by using GC-LTQMS

Table 3.12: Matrix effect on baby food samples based on GC-MSD, GC-SICRIT-LTQMS, and GC-ITQMS.

Pesticide	Method	Matrix (Milk) ME%	Matrix (Rice) ME%	Matrix (Cereal) ME%
Diazinon	GC-MSD	403%	182%	232%
	GC-SICRIT	-100%	-80%	-80%
	GC-ITQMS	280%	27%	11%
Isazophos	GC-MSD	550%	238%	298%
	GC-SICRIT	-99%	-79%	-76%
	GC-ITQMS	279%	40%	101%
Chlorpyrifos-methyl	GC-MSD	549%	219%	259%
	GC-SICRIT	-99%	-76%	-77%
	GC-ITQMS	264%	20%	25%
Fenitrothion	GC-MSD	519%	203%	251%
	GC-SICRIT	-100%	-80%	-78%
	GC-ITQMS	339%	179%	94%
Pirimiphos-methyl	GC-MSD	421%	406%	468%
	GC-SICRIT	-100%	-82%	-79%
	GC-ITQMS	325%	17%	77%
Chlorpyrifos	GC-MSD	459%	209%	238%
	GC-SICRIT	-99%	-81%	-83%
	GC-ITQMS	376%	177%	161%
Pirimiphos ethyl	GC-MSD	508%	187%	217%
	GC-SICRIT	-99%	-78%	-82%
	GC-ITQMS	389%	108%	86%
Quinalphos	GC-MSD	126%	246%	270%
	GC-SICRIT	-99%	-76%	-79%
	GC-ITQMS	428%	31%	109%
Pyridaphenthion	GC-MSD	312%	94%	112%
	GC-SICRIT	-99%	-71%	-80%
	GC-ITQMS	529%	94%	99%
Phosmet	GC-MSD	252%	32%	98%
	GC-SICRIT	-99%	-75%	-72%
	GC-ITQMS	94%	60%	91%
EPN (insecticide)	GC-MSD	107%	60%	62%
	GC-SICRIT	-99%	-74%	-75%
	GC-ITQMS	214%	164%	136%
Phosalone	GC-MSD	238%	98%	96%
	GC-SICRIT	-98%	-66%	-78%
	GC-ITQMS	104%	45%	202%
Azinphos-methyl	GC-MSD	507%	174%	92%
	GC-SICRIT	-99%	-77%	-83%
	GC-ITQMS	51%	41%	35%
Pyrazophos	GC-MSD	427%	138%	65%
	GC-SICRIT	-98%	-82%	-78%
	GC-ITQMS	34%	13%	16%
Azinphos-ethyl	GC-MSD	138%	132%	70%
	GC-SICRIT	-98%	-75%	-66%
	GC-ITQMS	16%	148%	116%
Pyraclofos	GC-MSD	224%	19%	57%
	GC-SICRIT	-99%	-80%	-83%
	GC-ITQMS	301%	168%	190%

During analytical measurements the sample matrix elements from milk rice and cereal produce Matrix effects (ME%) that affect the detection and quantitative analysis of analytes. Multiple conclusions about pesticide measurement using GC-MSD, GC-SICRIT and GC-ITQMS become evident regarding matrix effects in various analytical samples.

Comparison of Methods:

The sample matrix exhibits a positive impact on GC-MSD signal detection because the system displays consistent high ME% readings throughout different matrices. This effect results in better pesticide detection results.

GC-SICRIT demonstrates generally negative ME% patterns which indicates that the interfering substance in the matrix likely degrades the measured signal of pesticides. The presence of the sample matrix leads to decreased pesticide concentration measurements in actual field examples.

The matrix effects of GC-ITQMS vary based on pesticide and sample type because this method displays both positive and negative ME% results. Matrix elements have different effects on pesticide analysis with some pesticides maintaining minimal interferences but others experiencing major disruptive effects.

Effect of Sample Type:

All detection techniques depend significantly on the selected matrix type for their ME% values. When analyzed through GC-MSD and GC-ITQMS milk shows greater positive ME% outcomes than rice and cereal which suggests the matrix characteristics of milk support pesticide ionization and detection. The ME% evaluation of rice and cereal samples with GC-SICRIT reveals extensive negative values which indicates major possible interference in their matrix components.

Pesticide-Specific Observations:

The results indicate diazinon experiences profound matrix enhancement in milk with a 403% ME% although GC-SICRIT reveals its complete disappearance as -100%. The GC-ITQMS analysis shows moderate enhancement that leads to get varying results based on the methods they selected for sample analysis. GC-MSD generates significant matrix effects of 550% in milk while GC-SICRIT produces different negative effect percentage values demonstrating the vulnerability of

this pesticide to interferences within matrixes. The GC-MSD analysis detected substantial enhancement of 549% in milk whereas GC-SICRIT produced significant suppression of -99% thus demonstrating the sensitivity difficulties of the latter method for interference. Green colorimetric (GC-MSD) screens high matrix effect percentages for Fenitrothion tests yet its black and red colorimetric (GC-SICRIT) findings remain negative because of comparable interfering factors across both techniques.as shown in table 3.12.

Impact of Matrix Effects on Quantification:

The use of GC-SICRIT to estimate pesticide concentrations produces false results in safety and compliance analysis because of its high negative ME% values. Proper pesticide quantification of complex matrices requires extensive method validation in combination with appropriate calibration because the methods generate inconsistent measurement results. The effectiveness of pesticide detection depends on different analytical procedures because each approach creates varied intensity of matrix effects during measurement. The GC-MSD generates stronger signals in presence of high positive matrix effects that contrasts with GC-SICRIT which produces reduced signals because of negative matrix effects. Scientific analysis of pesticides requires the correct combination of methods with suitable sample preparation procedures based on the observed differences found during testing. Valid confirmation methods must be established for implementing food safety regulations and standards that measure the detection accuracy.

The positive matrix effect detected by GC-MSD systems leads to improved pesticide signal detection performance primarily when analyzing rich matrices such as milk. The milk matrix components elevated the ionization of isazophos to 550% ME% because they interacted favorably with lipid components found within milk.

The GC-SICRIT revealed substantial negative ME% values which reached -100% specifically in diazinon milk measurements. The evaluation of complex matrices comprising milk or rice or cereal leads to extreme reduction of ionization efficiency. Detecting pesticide levels inappropriately becomes inaccurate due to the suppression effects that may occur. Method selection must consider matrix samples because different analytical instruments produce uneven ME% results between GC-MSD and GC-SICRIT and GC-ITQMS. Pesticide detection depends heavily on different ionization methods

because GC-MSD exhibits increased response yet GC-SICRIT maintains steady suppression across various matrices. The analysis with NIST SRM reveals that complex matrix samples such as milk need method validation procedures after SRM testing to achieve accurate results. The NIST standards serve as a reference for determining proper ionization efficiency because this reference is essential for proper ME% data interpretation for certain pesticides, like pyridaphenth.

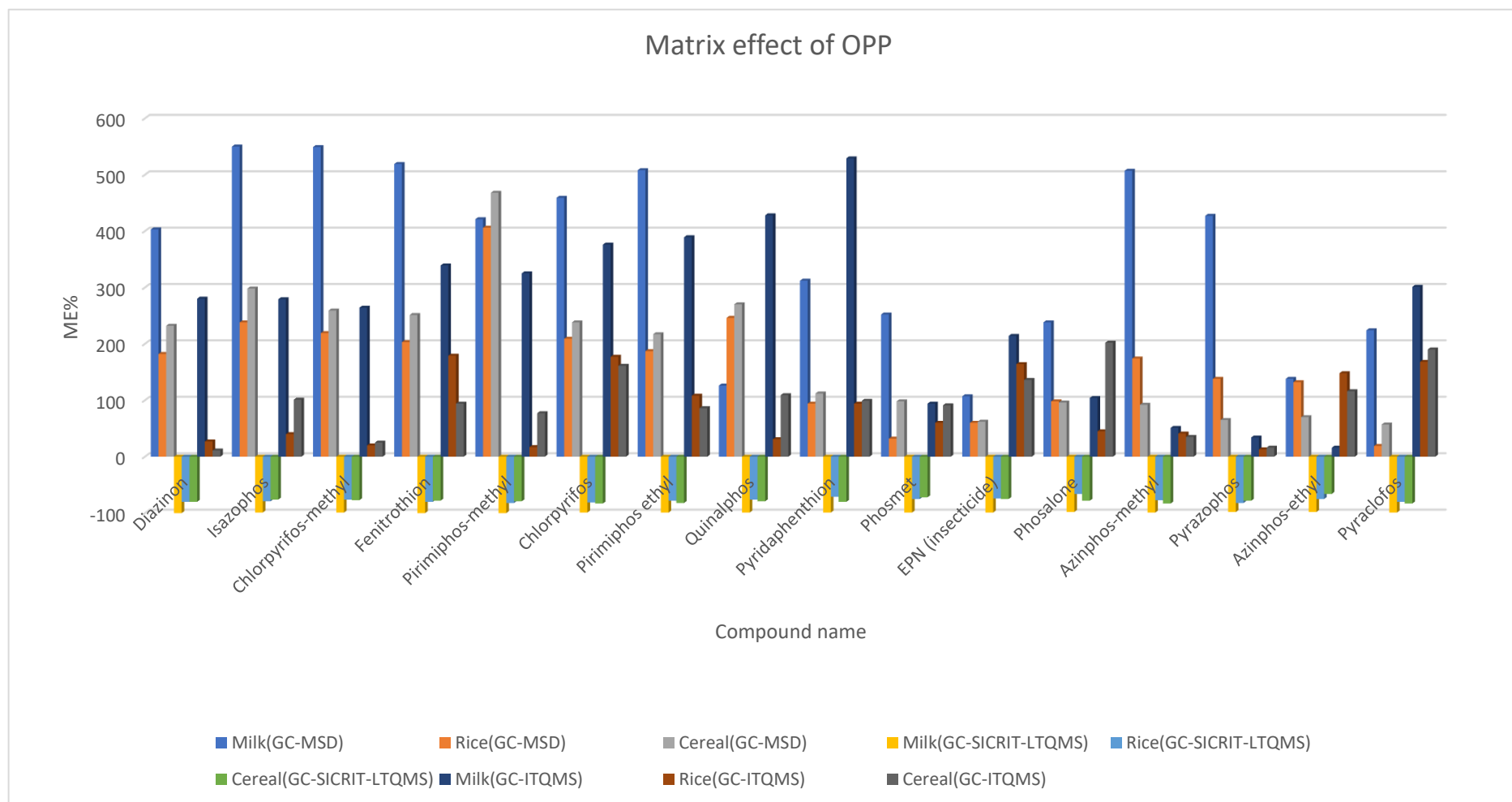


Figure 3.16: ME% of organophosphorus pesticides in GC-SICRIT-LTQMS, and GC-EI-ITQMS.

4. Quantitative analysis of Organonitrogen pesticide residues in baby food by gas chromatography with dielectric barrier discharge ionization-mass spectrometry (GC-DBDI-MS).

4.1 Introduction

Organonitrogen pesticides are a group of structurally diverse compounds collectively. They are extensively used in agriculture and pest control due to their nitrogen-based molecular structure, which works to enhance their effectiveness against pests such as insects, weeds, and fungi. These compounds play an effective role in maintaining crop health and increasing productivity by targeting pests by inhibiting the enzyme or disrupting the nervous system. Organonitrogen pesticides include various chemical classes, each of them has its own specific applications.^{124,125}

Examples:

Carbamates: they organic compounds with the general formula $R_2NC(O)OR$. They are derived from a carbamic acid. They include carbaryl and aldicarb. They work to eliminate insects by inhibiting the enzyme acetylcholinesterase.

Ureas: they organic compounds with the general formula $CO(NH_2)_2$. They have two amino groups. They include diuron and linuron. They target weeds and prevent their photosynthesis.

Triazines: they organic compounds with the molecular formula is $C_3H_3N_3$. They exist in three isomeric forms. They target weeds and they inhibit photosynthesis in plants.

These pesticides are effective but these types of pesticides not only increase the risk of the environment but also produce negative effects specifically on health. Due to their high solubility in water. Pesticides are detected consistently and repeatedly in various water samples, such as drinking water, rivers and surface runoff water.^{126,127} Hence, they certainly pose a great danger to humans and animals. The U.S. Environmental Protection Agency (USEPA) has evaluated some pesticides, such as metribuzin, for its potential to cause cancer, in addition to its potential to cause endocrine disruption.^{128,129}

In this study, our main focus is on chromatography-based analysis. In this analysis, two types of ionisation sources are used, the first is EI and the second is SICRIT. This analysis performs used a standard mix of 29 ONPs particularly. The study will examine baby food samples which include matrices such as milk, rice and cereal). Sample preparation and extraction are an important part of the analysis. Sample preparation and extraction procedures have been previously detailed; extraction and cleanup were performed as described elsewhere using the QuEChERS technique.

4.2 Chromatographic separation in GC-FID, GC-EI-ITQMS, GC-EI-MSD and GC-SICRIT-LTQMS.

In this study, we investigated the separation and detection of organonitrogen pesticides (ONPs) using four different analytical techniques: the detection techniques were: GC-FID, GC-EI-ITQMS, GC-SICRIT-LTQMS, and GC-EI-MSD. The pesticide mixture stock, containing 29 compounds, was prepared at 100 µg/ml concentration in toluene; starting analytical samples were prepared by diluting this stock 10 fold using acetonitrile.

Table 4.1 lists 29 pesticides studied and detected in this research, numbered to correspond to peaks as shown in individual GCMS traces shown subsequently.

Table 4.1: Compounds obtained through chromatography separation.

Peaks	Compound	Molecular Formula
1	Allidochlor	C ₈ H ₁₂ ClNO
2	Pebulate	C ₁₀ H ₂₁ NOS
3	N-(2,4-Dimethylphenyl) formamide	C ₉ H ₁₁ NO
4	Propachlor	C ₁₁ H ₁₄ ClNO
5	Cycloate	C ₁₁ H ₂₁ NOS
6	Diallate 1	C ₁₀ H ₁₇ Cl ₂ NOS
7	Diallate 2	C ₁₀ H ₁₇ Cl ₂ NOS
8	Clomazone (Command)	C ₁₂ H ₁₄ ClNO ₂
9	Propyzamide	C ₁₂ H ₁₁ Cl ₂ NO
10	Triallate	C ₁₀ H ₁₆ Cl ₃ NOS
11	Dimethachlor	C ₁₃ H ₁₈ ClNO ₂
12	Propanil	C ₉ H ₉ Cl ₂ NO
13	Acetochlor	C ₁₄ H ₂₀ ClNO ₂
14	Alachlor	C ₁₄ H ₂₀ ClNO ₂
15	Propisochlor	C ₁₅ H ₂₂ ClNO ₂
16	Linuron	C ₉ H ₁₀ Cl ₂ N ₂ O ₂
17	Metolachlor	C ₁₅ H ₂₂ ClNO ₂
18	Diphenamid	C ₁₆ H ₁₇ NO
19	Metazachlor	C ₁₄ H ₁₆ ClN ₃ O
20	Flutolanil	C ₁₇ H ₁₆ F ₃ NO ₂
21	Pretilachlor	C ₁₇ H ₂₆ ClNO ₂
22	Oxadiazon	C ₁₅ H ₁₈ Cl ₂ N ₂ O ₃
23	Norflurazon	C ₁₂ H ₉ ClF ₃ N ₃ O
24	Methoxychlor	C ₁₆ H ₁₅ Cl ₃ O ₂
25	Fenpropathrin	C ₂₂ H ₂₃ NO ₃
26	Tebufenpyrad	C ₁₈ H ₂₄ ClN ₃ O
27	Pyridaben	C ₁₉ H ₂₅ ClN ₂ OS
28	Fluquinconazole	C ₁₆ H ₈ Cl ₂ FN ₅ O
29	Prochloraz	C ₁₅ H ₁₆ Cl ₃ N ₃ O ₂

4.2.1 Gas Chromatography-Flame Ionisation Detection (GC-FID)

GC-FID is a common technique for analysing volatile organic compounds.¹³⁰ In this technique, the sample is vaporised and moved through the chromatographic system by an inert gas. Figure 4.1 shows the optimized GCFID trace for the separation of the 29 ONP compounds in this study. Detection is via flame ionisation, each compound, when it exits the column, is burned with hydrogen flame-producing ions, which generate an electrical signal. The intensity of the signal is directly proportional to the concentration of compounds.¹³¹ Flame ionization detection is a technique that has high sensitivity and excellent linearity of response for a wide range of organic compounds.

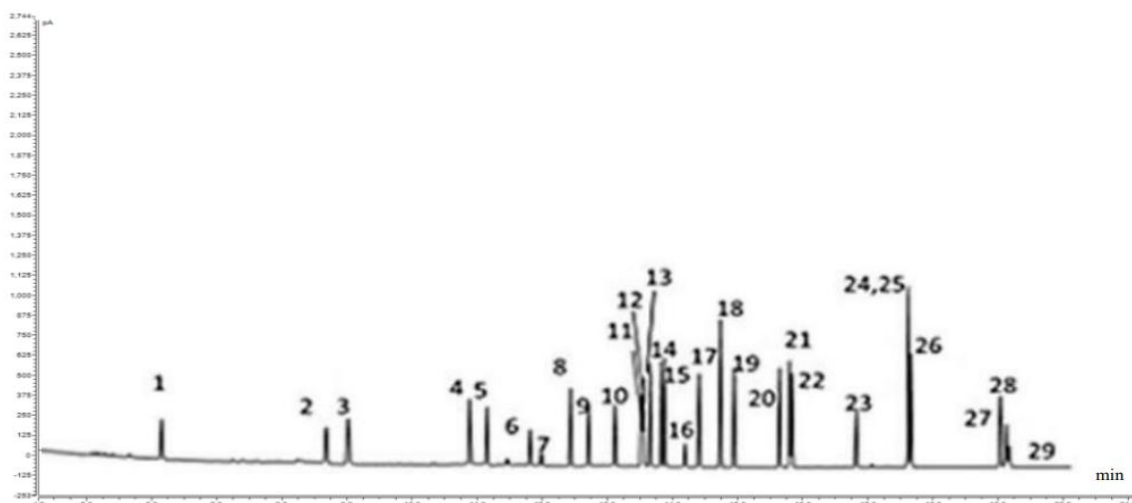


Figure 4.1: GC-FID Chromatogram of a mixture of 29 organonitrogen pesticides (compounds identity in table 4.1) at 10ppm.

Figure 4.1 shows the optimized GC-FID chromatogram recorded for the separation and detection of the 29 different organo-nitrogen compounds in this test sample. The horizontal axis gives the retention times in minutes, and the vertical axis shows the detector response, which also correlates with the concentration of each compound. In figure 4.1, there are 29 peaks with overlapping peaks, and each peak corresponds to a different organonitrogen compound. The height of each peak detected is a measure of the relative abundance of the compound within the sample, where the intensity of the peaks represents how the detector responds to these compounds.

Although the separation is very effective; it is necessary to use GCMS to confirm it by mass spectrometry as a FID detector does not give any mass or structural information.

4.2.2 Gas Chromatography-Electron Ionisation Ion Trap Quadrupole Mass Spectrometry (GC-EI-ITQMS)

The combination of GC-EI-ITQMS with separation provided by the GC and detection of eluted analytes by mass spectrometry provides benefits of simple detection of an analyte eluted from the GC column.¹³² However, after the separation in the GC column, the compounds are then ionised through electron impact, which causes them to initially lose an electron to give a molecular ion, and in many cases subsequently break down into fragment ions.¹³³ These ions are then analysed via an “ion trap quadrupole mass spectrometer”, which offers a richer information set compared to an FID, including ion masses and insights into the molecular structure of compounds. It also enables the precise determination and quantification where the higher sensitivity and specificity of GC-EI-ITQMS makes it ideal for identifying lower levels of ONPs in complicated matrices.

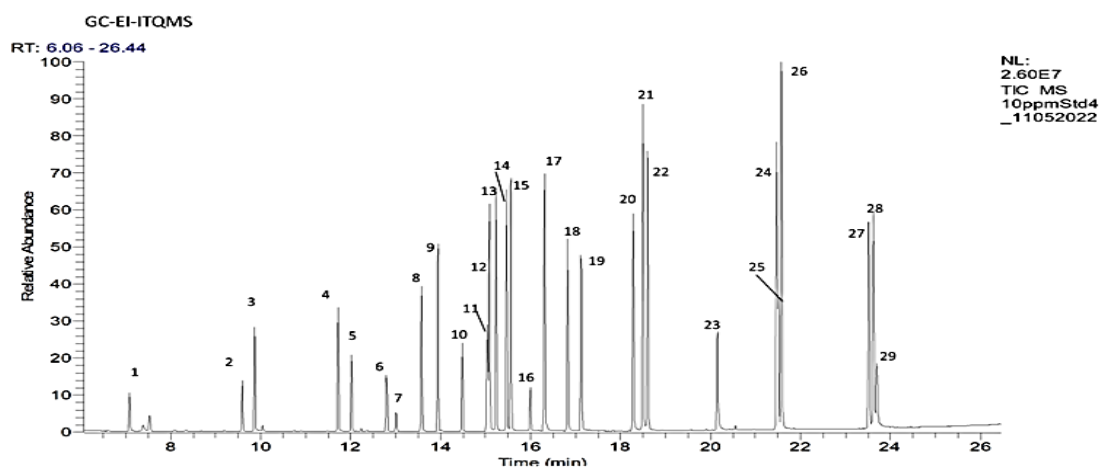


Figure 4.2: GC-EI-ITQ TIC-MS of a mixture of 29 organonitrogen pesticides (compounds identity in table 4.1) at 10ppm.

Figure 4.2 highlights the chromatogram attained from GC-EI-ITQMS analysis of a mixture of 29 ONPs showing separation and detection of all of the different pesticides over the time range of 6 to 26 minutes. The tallest peak labelled 26, eluting just before 22 minutes, was identified as Tebufenpyrad ($C_{18}H_{24}ClN_3O$) has the highest detector response. Other peaks also have varying heights, showing the presence of additional compounds where each elute at different times. Although the chromatogram shows good separation of some compounds such as Metolachlor ($C_{15}H_{22}ClNO_2$), which represents peak number 17, indicating effective separation from other compounds, there are instance of co-elution observed between peaks, where the instance co-overlap was observed between Dimethachlor ($C_{13}H_{18}ClNO_2$) and Propanil ($C_9H_9Cl_2NO$).

4.2.3. Gas Chromatography-Soft Ionisation by Chemical Reaction in Transfer and Linear Trap Quadrupole Mass Spectrometry (GC-SICRIT-LTQMS)

GC-SICRIT-LTQMS differs only from the other techniques used in that the detection is via an ion source that is known as a soft ionisation source. The switch to a soft source reduces analyte fragmentation for many analytes thus preserving molecular ions.¹³⁴ This technique, as noted before, uses a cold nitrogen plasma for ionisation which for many analytes sees the dominant ionisation method of proton addition. This approach assists in maintaining the integrity of molecular ions by providing better determination of ONPs.

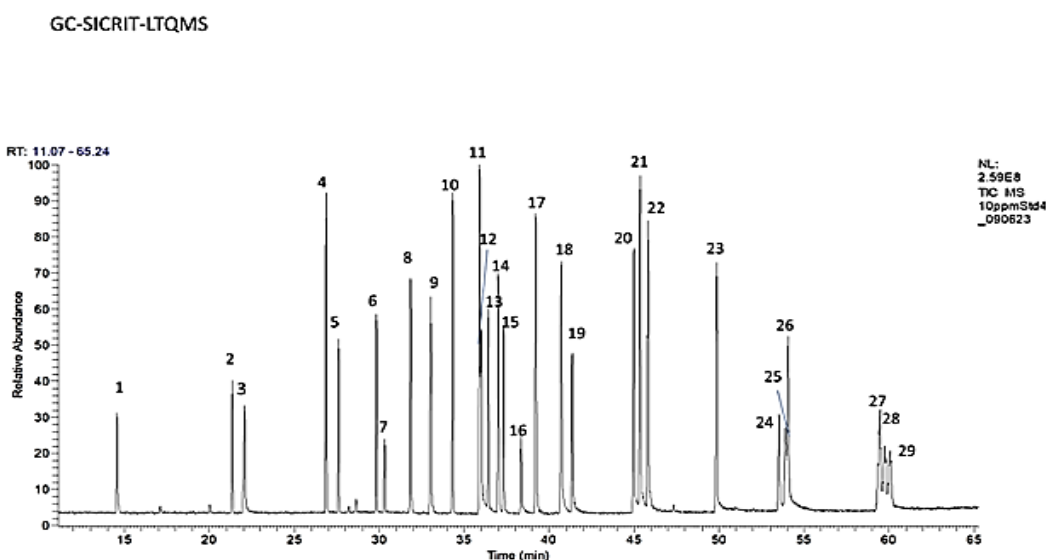


Figure 4.3: GC-SICRIT-LTQ TIC-MS of a mixture of 29 organonitrogen pesticides (compounds identity in table 4.1) at 10ppm.

Figure 4.3 demonstrates the GC-SICRIT-LTQMS which illustrated the detection of different compounds ranging from 0 to 65 minutes. The horizontal axis represents the retention time, and the vertical axis shows the relative abundance of ions detected of each compound. In general, the chromatogram shows a separation similar to that produced by GC-EI-ITQMS, with good separation for some compounds and overlap between peaks for some compounds. The response of the pesticides to detector varies compared to when using GC-EI-ITQMS, with poorer resolution and broader peaks observed at the tail end of the chromatogram. For example, In the GC-SICRIT-LTQMS method, the highest peak is propachlor ($C_{11}H_{14}ClNO$), while in the GC-EI-ITQMS method, the highest peak is tebufenpyrad ($C_{18}H_{24}ClN_3O$).

4.2.4 Gas Chromatography-Electron Ionisation Mass Selective Detection (GC-EI-MSD)

GC-EI-MSD is an effective technique which combines gas chromatography along with electron ionisation and mass selective detection¹³⁵. However, after the separation in the GC column, the compounds are then ionised through electron impact, leading to, in many cases, fragmentation. The selective mass detector then analyses these fragments and offers detailed mass spectra for each compound. Using the same pesticides at the same concentration using a different analytical technique, all pesticides in this study were detected and exited from the analyzer in specific order, as indicated in the table 4.1. All chromatograms demonstrate good separation of some peaks and overlap between peaks as well. This is all that was observed in the four instruments. The difference in retention time, peak lengths, and resolution, were observed in all the instruments used.

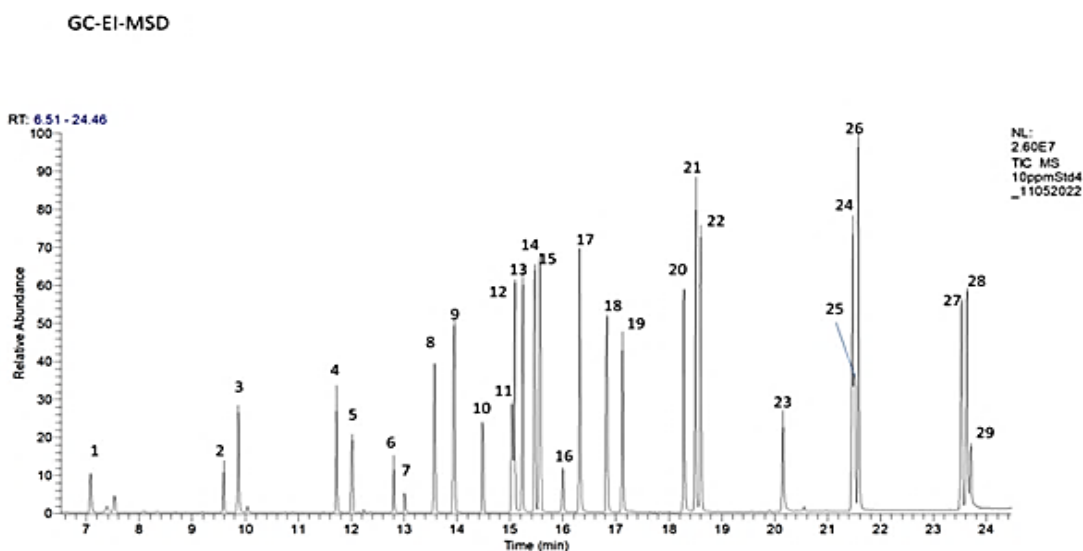


Figure 4.4: GC-EI-SQ TIC-MS of a mixture of 29 organonitrogen pesticides (compounds identity in table 4.1) at 10ppm.

It was observed that peaks 11 and 12 corresponding to dimethachlor and propanil respectively in all chromatograms still overlapped despite using four different instruments and different GC method. They have different molecular weights and different chemical structure as shown in figure 4.5, but they have the same retention time, so confirmation using mass spectrometry is important to identify these compounds. Similarly, peaks 24 and 25, which indicate the presence of methoxychlor and fenpropathrin respectively, are

overlapping peaks. Despite the chemical difference between them, they have the same retention time.

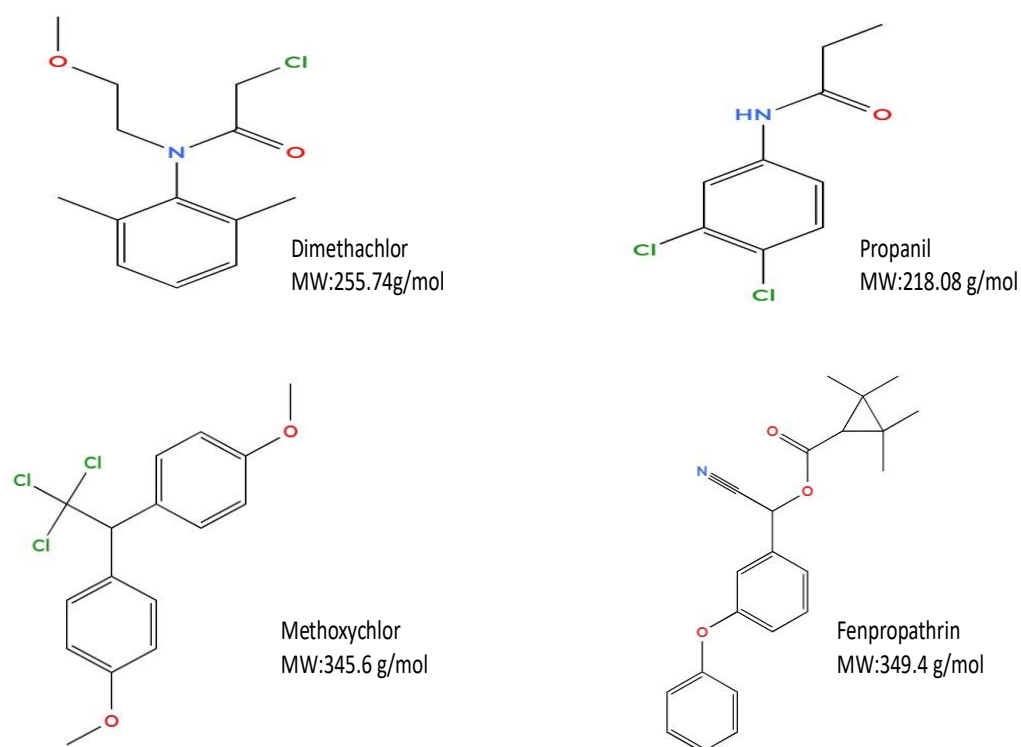


Figure 4.5: Chemical structure of dimethachlor, propanil, methoxychlor, and fenpropathrin.

4.3 Ionisation Mechanism and Mass Spectrometry Results

In GC-EI-MS, the ionisation process comprises higher-energy electrons (typically 70 eV), which were effectively generated by thermionic emission from a heated filament. These electrons are accelerated and collide with the neutral analyte molecules in the gas phase. Typically, the impact of the high energy electrons initially produces radical cations (M^+); the energy involved is high and thus the loss of energy from the initial radical cation most often results in fragmentation, which structure dependent fragment ions denoted as “frg” in table 4.2. Contradictorily, GC-SICRIT-MS incorporate the soft ionisation approach, which reduces the fragmentation and preserves molecular ions denoted as “M + H”. However, the soft ionisation process consists of protonation, where a (H^+) is combined with the analyte molecule, forming a protonated molecular ion. The ionization results for 29 organonitrogen compound studied are summarize in table 4.2.

Table 4.2: Ionisation mechanism and mass spectrometry results.

Peaks	Compound	Molecular Formula	Exact Mass	GC-EI-MS	Ion form	GC-SICRIT-MS	Ion form
1	Allidochlor	C ₈ H ₁₂ ClNO	173.06	56,96,138,132	frg	174.0698	M+H
2	Pebulate	C ₁₀ H ₂₁ NOS	203.13	128,161,57,72,90	frg	204.1436	M+H
3	N-(2,4 Dimethylphenyl) formamide	C ₉ H ₁₁ NO	149.08	120,106,77,121,149	frg	150.0927	M+H
4	Propachlor	C ₁₁ H ₁₄ ClNO	211.07	120,77,93,176,57	frg	212.0855	M+H
5	Cycloate	C ₁₁ H ₂₁ NOS	215.13	154,83,55	frg	216.1432	M+H
6	Diallate 1	C ₁₀ H ₁₇ Cl ₂ NOS	269.04	234,236,192	frg	270.0504	M+H
7	Diallate 2	C ₁₀ H ₁₇ Cl ₂ NOS	269.04	234,236,150,192	frg	270.0498	M+H
8	Clomazone (Command)	C ₁₂ H ₁₄ ClNO ₂	239.07	125,204,89,107,99	frg	240.0802	M+H
9	Propyzamide	C ₁₂ H ₁₁ Cl ₂ NO	255.02	173,175,145,74,254,256	frg	256.0315	M+H
10	Triallate	C ₁₀ H ₁₆ Cl ₃ NOS	303.001	268,270,226,186,143	frg	304.0131	M+H
11	Dimethachlor	C ₁₃ H ₁₈ ClNO ₂	217.006	161,163,217,99,125,74	frg	218.0158	M+H
12	Propanil	C ₉ H ₉ Cl ₂ NO	255.1026	134,148,197,117,77,190,105	frg	256.1128	M+H
13	Acetochlor	C ₁₄ H ₂₀ ClNO ₂	269.1182	146,132,174,223	frg	148.11,224.09,270.1277	frag
14	Alachlor	C ₁₄ H ₂₀ ClNO ₂	269.1182	160,146,188,118,132	frg	162.13,238.10,270.1282	frag

Peaks	Compound	Molecular Formula	Exact Mass	GC-EI-MS	Ion form	GC-SICRIT-MS	Ion form
15	Propisochlor	C ₁₅ H ₂₂ ClNO ₂	283.1339	162,132,146,223,163,000	frg	148.11,224.09,284.14	frag
16	Linuron	C ₉ H ₁₀ Cl ₂ N ₂ O ₂	248.01	61,124,187,161,133,200	frg	249.0218	M+H
17	Metolachlor	C ₁₅ H ₂₂ ClNO ₂	283.13	162,238,133	frg	284.1433	M+H
18	Diphenamid	C ₁₆ H ₁₇ NO	239.13	167,72,165,115,239	frg	240.14	M+H
19	Metazachlor	C ₁₄ H ₁₆ ClN ₃ O	277.0981	132,133,117,160,209	frg	210.07,134.1,278.1079	frag
20	Flutolanil	C ₁₇ H ₁₆ F ₃ NO ₂	323.1	173,145,281,95	frg	324.1226	M+H
21	Pretilachlor	C ₁₇ H ₂₆ ClNO ₂	311.16	162,132,202,262,117	frg	312.1743	M+H
22	Oxadiazon	C ₁₅ H ₁₈ Cl ₂ N ₂ O ₃	344.06	175,112,258,147	frg	345.0789	M+H
23	Norflurazon	C ₁₂ H ₉ ClF ₃ N ₃ O	303.03	145,303,95,75	frg	304.0491	M+H
24	Methoxychlor	C ₁₆ H ₁₅ Cl ₃ O ₂	344.0137	227,238	frg	236.9,238.9,227.1,345.0234	frag
25	Fenpropathrin	C ₂₂ H ₂₃ NO ₃	349.16	181,265,152,210,127	frg	350.1775	M+H
26	Tebufenpyrad	C ₁₈ H ₂₄ ClN ₃ O	333.16	276,333,318,171,131	frg	334.17	M+H
27	Pyridaben	C ₁₉ H ₂₅ ClN ₂ OS	364.13	147,119,117,132	frg	365.1489	M+H
28	Fluquinconazole	C ₁₆ H ₈ Cl ₂ FN ₅ O	375.0089	340,298,108,313	frg	376.0205	M+H
29	Prochloraz	C ₁₅ H ₁₆ Cl ₃ N ₃ O ₂	375.0308	180,308,138,70	frg	376.0426	M+H

Table 4.2 offered an overview comparison of the ionisation mechanism and fragmentation of the different organonitrogen compounds in this study, which have also been analysed with the help of different mass spectrometry techniques such as GC-EI-ITQMS and GC-SICRIT-LTQMS. For example, Propachlor (Exact Mass 211.07 Da) produces ion fragments with m/z values of 120, 77, 93, 176, and 57. Conversely, GC-SICRIT-LTQMS shows mainly at m/z 212.0855, which corresponds to the $[M+H]^+$.

Figures 4.6 and 4.7 present mass spectra for selected pesticides, comparing the results from GC-SICRIT-MS (left spectrum) and GC-EI-MS (right spectrum) for each compound. These figures provide a visual representation of the ionization differences between the two techniques. Figure 4.5 shows the spectra obtained for the pesticide allidochlor. The SICRIT MS spectrum shows a prominent $[M+H]^+$ ion at m/z 174.0698, indicating the presence of Cl, while the EI spectrum displays significant fragmentation with major ion at m/z 138, which lack of Cl, in addition to another fragments at m/z 56, and 96. Figure 4.6 shows the spectra obtained for the pesticide cycloate. The SICRIT spectrum shows a strong $[M+H]^+$ ion at m/z 216.1432, contrasting with the EI spectrum that shows a base peak at m/z 154 and several other fragments.

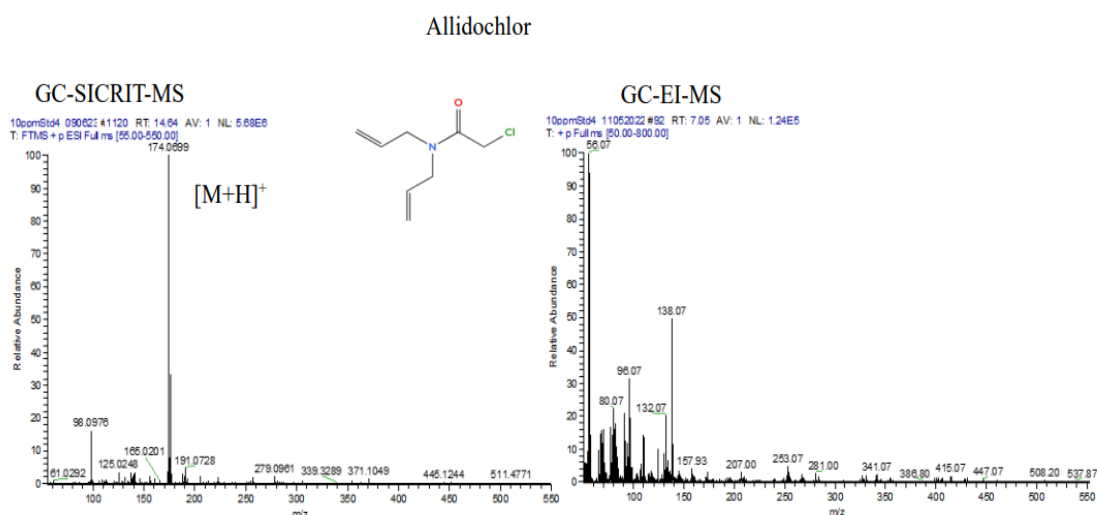


Figure 4.6: EI-MS and SICRIT-MS spectra (positive ionization mode) of allidochlor (m/z 2173.06) (see table 4.2) at 10ppm, analyzed by GC-SICRIT- LTQ Orbitrap mass spectrometer and GC-EI-ITQMS.

Figure 4.6 shows the mass spectra of allidochlor obtained using GC-SICRIT-MS in the right figure and GC-EI-MS in the left figure. The SICRIT mass spectrum shows mainly a m/z of 174. 0698, which corresponds to the $[M+H]^+$ ion for this pesticide. This shows that SICRIT has the capacity for soft ionization without extensive fragmentation. However, the EI spectrum shows a much more complex spectrum that features significant fragmentation with representative peaks at m/z 138 that indicates the loss of a chlorine atom (Cl), at m/z 132, that suggests the loss of a hydrogen atom (H) from the ion at 138 or loss of an allyl group, at m/z 56 this peak indicate a smaller ion and could represent an alkyl or amine group. This fragmentation pattern is typical for the ionization with high-energy electrons in impact ionization. The comparison clearly shows the level of difference between the two types of ionization techniques and shows that SICRIT gives a clearer picture that is more targeted to the molecular ion.

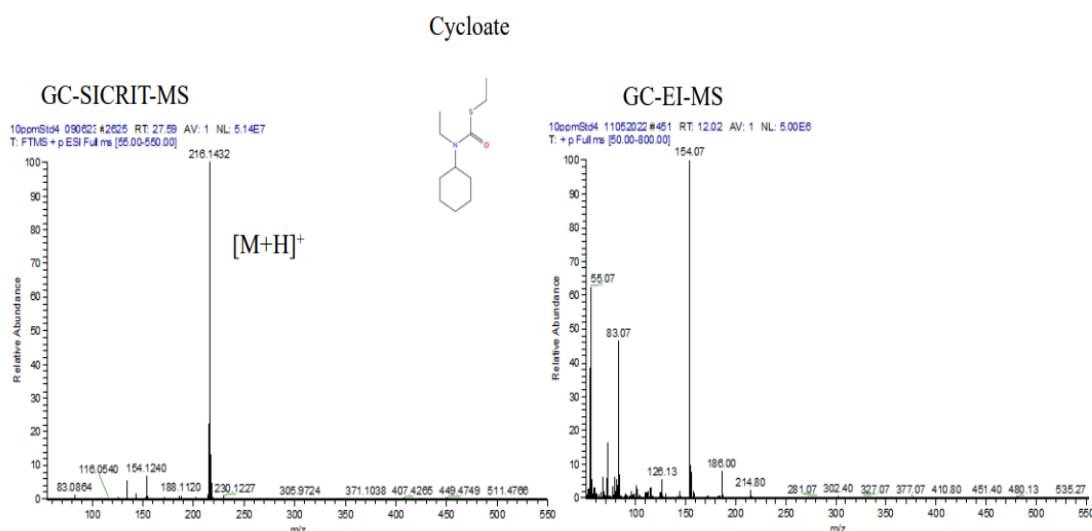


Figure 4.7: EI-MS and SICRIT-MS spectra (positive ionization mode) of cycloate (m/z 215.13) (see table 4.2) at 10ppm, analyzed by GC-SICRIT- LTQ Orbitrap mass spectrometer and GC-EI-ITQMS.

Figure 4.7 shows the spectra of cycloate in both GC-SICRIT-MS and GC-EI-MS. In the GC-EI-MS spectrum for cycloate, the base peak at m/z 154.1 is the most intense, signifying a highly stable fragment, this may indicate the loss of a small group such as C_2H_7 . Additionally, the presence of peaks at m/z 83.1, resulting from further fragmentation. It could represent cyclohexane. The molecular ion at m/z 214.80 corresponds to cycloate but tends to fragment extensively making it a non-typical base peak in GC-EI-MS analysis. A significant stable fragment occurs at m/z 154.1 because of

the pathway starting with C₂H₇ group elimination from the initial molecule. Further fragmentation leads to formation at *m/z* 186.0 which potentially matches an ethyl group structure together with *m/z* 83.1 which might signal cyclohexane or another cyclic fragment. The particular fragmentation pattern serves as an essential indicator for cycloate recognition because it shows important structural features and fragmentation behavior of the compound.

4.4 Fragmented pesticides

Although acetochlor (C₁₄H₂₀ClNO₂), alachlor (C₁₄H₂₀ClNO₂), propisochlor (C₁₅H₂₂ClNO₂), metazachlor (C₁₄H₁₆ClN₃O), and methoxychlor (C₁₆H₁₅Cl₃O₂) were analyzed by GC-LTQMS with SICRIT, these compounds underwent significant fragmentation.

Figures 4.8 and 4.9 illustrate the mass spectra for two of the compounds that underwent some fragmentation even with SICRIT ionization: acetochlor, alachlor, propisochlor, metazachlor, and methoxychlor. These spectra demonstrate that while SICRIT generally produces less fragmentation than EI, some compounds may still exhibit characteristic fragment ions alongside the protonated molecular ion.

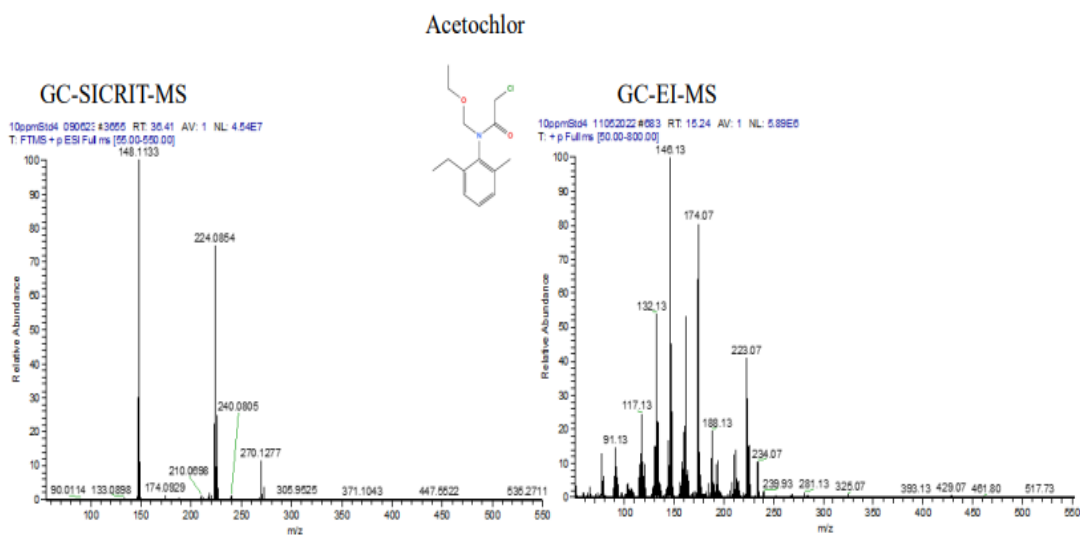


Figure 4.8: EI-MS and SICRIT-MS spectra (positive ionization mode) of acetochlor (*m/z* 269.1182) (see table 4.2) at 10ppm, analyzed by GC-SICRIT- LTQ Orbitrap mass spectrometer and GC-EI-ITQMS.

Figure 4.8 shows the mass spectra of Acetochlor using GC-SICRIT-MS side by side with the corresponding GC-EI-MS spectrum. In the SICRIT spectrum, we observe three main fragments, these are the ions: *m/z* 148.11, 224.09, and 270.12. The highest mass detected,

at m/z 270.12, represents the protonated molecular ion of acetochlor, which has a molecular weight of 269.11 Da. Hence, results such as fragment ions (148.11 and 224.09) show that despite using soft ionization, acetochlor is more prone to fragmentation. Where the peak at m/z 148 likely represents a fragment that has lost specific group from compound, indicating that Cl is still present. At m/z 224 and 226, these two peaks differ by 2 units, indicating the presence of isotopes. At m/z 224 may represent the presence of Cl in the fragment, while m/z 226 may represent a similar fragment but with Cl isotope.

Fragmentation Group:

For acetochlor ($C_{14}H_{20}ClNO_2$), the fragments observed suggest the fragmentation is by loss of functional groups that include chlorine and the remaining components. These peaks are the ones that can be considered:

- m/z 148.11 would likely be a group that has lost a specific entity, maybe one chlorine atom since Cl is present.
- m/z 224.09 might be a fragment that has kept the chlorine atom, while m/z 226.09 is a chlorine isotope fragment (^{37}Cl).

Reasoning behind Fragmentation

1. Soft Ionization: SICRIT being a softer ionization process tends to hold on to the protonated molecular ion more compared to previous techniques like EI. However, with softer processes too, some of the groups within the molecular structure tend to cause fragmentation, especially the ones that are capable of stabilizing as free radicals after losing part of their structure.
2. Structural Instability: Chlorine atoms within the acetochlor molecular structure would generate fragmentation mechanisms by which loss of Cl becomes more facile through creation of detectable fragment ions.
3. Isotope Patterns: 2-unit discrepancy from m/z 224 and m/z 226 points toward isotopic peaks. Isotope Ratio of Chlorine

The abundance of the following isotopic is used to determine the ratio of ^{35}Cl and ^{37}Cl to discuss:

Natural abundances:

- ^{35}Cl : ~75.76%
- ^{37}Cl : ~24.24%

Using this ratio, the peaks observed (given 1:2 ratio since 226 due to isotopic spread of 224), the ratio of ^{35}Cl to ^{37}Cl in natural samples can be estimated approximately as 3:1 from their relative abundance.

Fragmentation is mostly due to the loss of chlorine or conjugate groups.

The occurrence of fragmentation patterns and isotopes in the mass spectra can provide structural information.

The approximate ^{35}Cl to ^{37}Cl natural abundance ratio would be approximately 3:1.

Significantly more fragmentation is observed in the EI spectrum with high intense peaks at m/z 146.13, 174.07, and 223.07. It is very difficult to identify the molecular ion peak for the compound here; the peak at m/z 269 appears very weak and its intensity is almost negligible in the EI spectrum. This comparison shows that even though SICRIT generates less fragmentation, it can, for some structures, provide structural insights from fragmentation.

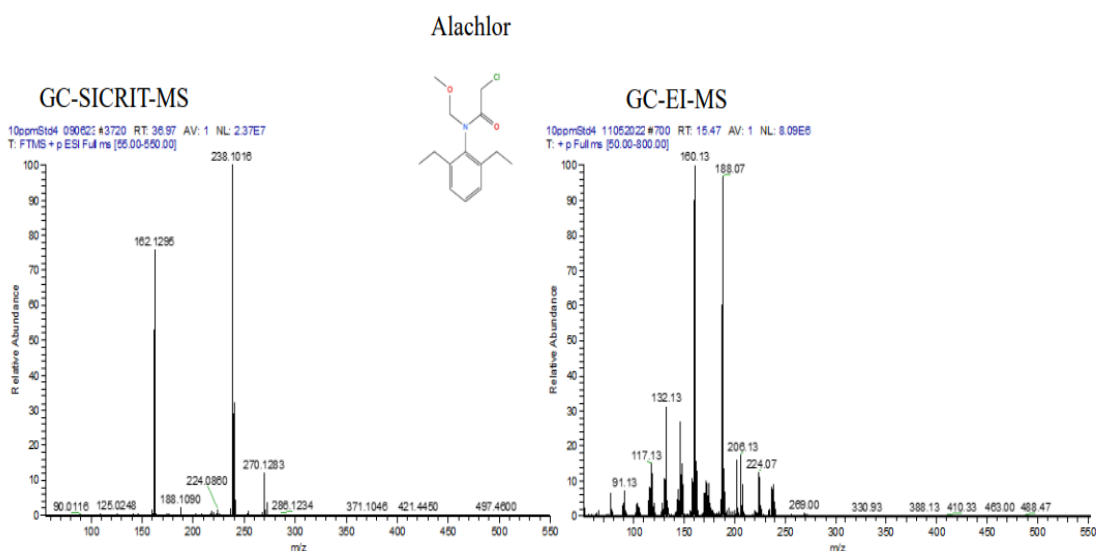


Figure 4.9: EI-MS and SICRIT-MS spectra (positive ionization mode) of alachlor (m/z 269.1182) (see table 4.2) at 10ppm, analyzed by GC-SICRIT- LTQ Orbitrap mass spectrometer and GC-EI-ITQMS.

Figure 4.9: The SICRIT spectrum of Alachlor shows masses for two major fragments at m/z 238.1, 162.13. The peak at m/z 270.123 is the protonated molecule $[M+H]^+$ where peak at m/z 238.1 indicates an ion resulting from the loss of the OMe while retaining chlorine (Cl), and at m/z 162.13, this might represent an ion formed by losing multiple fragments along with Cl, although not as extensive as EI, offers the structural data of Alachlor. The EI spectrum on the other hand shows strong peaks at m/z 160.13, 188.07, and 146.13 with the molecular ion at m/z 269 (of low intensity). Where peak at m/z 160.1 indicates to represent an ion formed by losing a large group along with Cl, and at m/z 188, this may indicate the loss of specific group like H₂O or Cl.

SICRIT produced ions with a softer ionization as opposed to EI while still delivering some diagnostic fragments.

This comparison has highlighted the fact that for a compound that typically undergoes fragmentation, SICRIT generally still shows the molecular ion information and reduces the amount of fragmentation, this is in contrast to the EI spectra where more extensive fragmentation is the norm.

These figures altogether are indicative of the fact that while SICRIT, in essence, generates a gentler kind of ionization and as such, compounds analyzed by it are destined to yield less fragmentation than those analyzed by EI, it is nonetheless evident that fragmentation is possible for some compounds with when ionised via SICRIT. Nevertheless, SICRIT gives constant molecular ion information, unlike the EI spectra which may give molecular ion information that may be of a low intensity or completely absent. This characteristic of SICRIT can be useful for easier analysis of pesticides extracted from challenging matrices or when the molecular ion becomes essential for the identification of a compound.

4.5 Method validation

Validation experiments were performed using two mass spectrometers. The first was GC-EI-ITQMS, the second is GC-MSD both giving low resolution mass data; high resolution mass data was available when using an orbitrap detector (GC-SICRIT-LTQMS). Validation was carried out following the procedure established in the EU SANTE guidelines.¹³⁶ The developed method was assessed for linearity of calibration curves, instrument limits of detection and method limits of quantification and matrix effects.

Linearity was checked by injecting standard solutions at 5 concentration levels (0.001, 0.005, 0.010, 0.050, 0.100 and 0.500 $\mu\text{g/mL}$), three times each, to evaluate the determination coefficient (R^2) and deviation of back-calculated concentrations. The instrument detection limit (LOD) was determined based on the lowest detectable concentration level measured with repeatability, ensuring that the relative standard deviation $\text{RSD} < 20\%$. Calibration curves have been constructed from calibration standards in solvent and from matrix extracts

4.5.1 Linearity

The linearity of the method was assessed by repeated injections of the same sample at all prepared concentration levels (0.001, 0.005, 0.01, 0.05, 0.1 and 0.5 $\mu\text{g/mL}$). The solution is prepared in the method diluent for all instruments/detectors evaluated - GC-ITQMS, GC-SICRIT-LTQMS and GC-MSD. All of the pesticides analysed showed R^2 values that were greater than 0.999, for all instruments evaluated, as summarised in Table 4.3. In this scenario, the high linearity meant good agreement between the concentration of the pesticides analysed and the detector response. It is evaluated that good and accurate quantitative measurements are specifically made over a wide calibration range.

4.5.2 LOD and LOQ

While the LOD is useful for identifying the minimal detectable concentration of an analyte, it does not provide information about the precision and accuracy of quantification at low concentrations. The LOQ, however, is more valuable for technique validation and data analysis as it provides insights into both sensitivity and accuracy.¹³⁷ Using data from the linearity study for each pesticide analyzed on each instrument, the estimated LOD and LOQ were calculated. The results are summarized in table 4.3.

Table 4.3: LOD, LOQ, and Linearity of organonitrogen pesticides in GC-ITQMS, GC-MSD, and GC-SICRIT-LTQMS.

Component Name	GC-ITQMS			GC-MSD			GC-SICRIT-LTQMS		
	LOD µg/mL	LOQ µg/mL	R ²	LOD µg/mL	LOQ µg/mL	R ²	LOD µg/mL	LOQ µg/mL	R ²
Allidochlor	0.009	0.028	0.997	0.003	0.009	0.999	0.004	0.010	0.999
Pebulate	0.006	0.019	0.999	0.001	0.005	0.999	0.004	0.010	0.998
N-(2;4-Dimethylphenyl) formamide	0.006	0.018	0.999	0.004	0.012	0.999	0.004	0.010	0.999
Propachlor	0.003	0.0103	0.999	0.004	0.011	0.999	0.003	0.010	0.999
Cycloate	0.004	0.0128	0.999	0.003	0.010	0.999	0.004	0.010	0.999
Diallate 1	0.006	0.020	0.998	0.003	0.008	0.999	0.003	0.010	0.999
Diallate 2	0.007	0.022	0.998	0.003	0.010	0.999	0.003	0.010	0.999
Clomazone	0.003	0.011	0.999	0.003	0.009	0.999	0.005	0.010	0.999
Propyzamide	0.002	0.006	0.999	0.003	0.009	0.999	0.002	0.007	0.999
Triallate	0.003	0.010	0.999	0.003	0.009	0.999	0.003	0.010	0.999
Propanil	0.004	0.013	0.999	0.002	0.006	0.999	0.006	0.018	0.999
Dimethachlor	0.002	0.005	0.999	0.003	0.010	0.999	0.010	0.030	0.998
Acetochlor	0.003	0.010	0.999	0.003	0.008	0.999	0.010	0.030	0.997
Alachlor	0.003	0.008	0.999	0.001	0.004	0.999	0.003	0.010	0.999

Propisochlor	0.0016	0.005	0.999	0.003	0.009	0.999	0.008	0.02	0.998
Metolachlor	0.0015	0.005	0.999	0.003	0.009	0.999	0.005	0.01	0.999
Diphenamid	0.003	0.009	0.999	0.002	0.006	0.999	0.003	0.010	0.999
Metazachlor	0.004	0.012	0.999	0.004	0.013	0.999	0.004	0.010	0.999
Flutolanil	0.003	0.010	0.999	0.001	0.003	0.999	0.005	0.016	0.999
Pretilachlor	0.003	0.010	0.998	0.004	0.012	0.999	0.004	0.010	0.997
Oxadiazon	0.002	0.007	0.999	0.003	0.009	0.999	0.002	0.006	0.999
Norflurazon	0.004	0.013	0.999	0.004	0.013	0.999	0.002	0.007	0.999
Methoxychlor	0.002	0.005	0.999	0.001	0.003	0.999	0.003	0.009	0.999
Fenpropathrin	0.006	0.018	0.999	0.009	0.029	0.997	0.003	0.008	0.999
Tebufenpyrad	0.001	0.003	0.999	0.001	0.003	0.999	0.002	0.007	0.999
Pyridaben	0.003	0.010	0.999	0.003	0.010	0.999	0.003	0.010	0.999
Fluquinconazole	0.004	0.013	0.999	0.003	0.010	0.999	0.003	0.009	0.999
Prochloraz	0.008	0.020	0.998	0.004	0.013	0.999	0.003	0.010	0.999

In this part, the process of analyzing LOD and LOQ will be presented using a set of statistical methods. Both LOD and LOQ are essential indicators for assessing the accuracy and reliability of analytical methods, as they define the lowest concentration levels that can be accurately detected and measured in samples.

First, the statistical description begins to provide an overview of the data, focusing on means and standard deviation as shown in table 4.4

Table 4.4: Descriptive statistics for LOD of ITQMS, SQMS, and LTQMS

	N	Mean	Std. Deviation	Std. Error	95% Confidence Interval for Mean		Minimum	Maximum
					Lower Bound	Upper Bound		
GC-ITQMS	28	.0038	.00203	.00038	.0030	.0046	.00	.01
GC-MSD	28	.0030	.00154	.00029	.0024	.0036	.00	.01
GC-SICRIT-LTQMS	28	.0041	.00212	.00040	.0032	.0049	.00	.01
Total	84	.0036	.00195	.00021	.0032	.0041	.00	.01

The data shows that measurement techniques GC-ITQMS, GC-MSD and GC-SICRIT-LTQMS detect similar levels of sensitivity which yields detection limits in between 0.003 to 0.004. Each measurement technique shows consistent results because standard deviations are low together with measurement ranges between 0.00 and 0.01. The experimental results demonstrate these methods maintain equivalent effectiveness in detecting trace concentrations because they deliver exact results with minimal detection threshold allowing sensitive work.

Next, the Levene test is applied to verify the homogeneity equal variance as shown in table 4.5.

Table 4.5: test of homogeneity of variances for LOD.

Levene Statistic	df1	df2	Sig.
2.326	2	81	.104

The Levene's test for homogeneity of variances produced this table to determine any equality of variations in LOD measurement based on these three methods. A Levene statistic value of 2.326 exists alongside two degrees of freedom (2) separating group information from 81 degrees of freedom (df2) being the total sample count minus individual group samples. The results indicate that the significance value (Sig.) exceeds 0.05 indicating statistical insignificance. The Levene's test results demonstrate that the measurement methods have equal variances since no significant statistical difference exists among them. ANOVA analysis requires this condition to be met during its execution.

The LOD is then analyzed using ANOVA analysis of variance to determine if there are statistically significant differences between the means.

Table 4.6: ANOVA results for LOD across three devices.

	Sum of Squares	df	Mean Square	F	Sig.
Between Groups	.000	2	.000	2.404	.097
Within Groups	.000	81	.000		
Total	.000	83			

The ANOVA table 4.6 demonstrates if there exist statistical differences among the mean LOD values obtained from three measurement methods. Groups cannot perceive major mean differences because both the Between Groups sum of squares value shows emptiness and Within Groups sum of squares value demonstrates a value of zero. Analysis of the F-value yielded 2.404 while the p-value (Sig.) exceeded 0.05 to reach 0.097 and thus passed the default 0.05 standard. Statistical calculations confirm that the measurement methods detect equally at the average level. The testing methods produce equal detection limit performances in analysis conditions due to their minimal mean measurement variations.

Tukey HSD test helps determine which methods most effectively achieve LOD and LOQ levels. Table 4.7 displays the results of the Tukey HSD test to compare LOD between different methods.

Table 4.7: results of Tukey HSD multiple comparisons for LOD.

(I) group	(J) group	Mean Difference (I-J)	Std. Error	Sig.	95% Confidence Interval	
					Lower Bound	Upper Bound
GC-ITQMS	GC-MSD	.00083	.00051	.246	-.0004-	.0020
	GC-SICRIT-LTQMS	-.00025-	.00051	.880	-.0015-	.0010
GC-MSD	GC-ITQMS	-.00083-	.00051	.246	-.0020-	.0004
	GC-SICRIT-LTQMS	-.00107-	.00051	.098	-.0023-	.0002
GC-SICRIT-LTQMS	GC-ITQMS	.00025	.00051	.880	-.0010-	.0015
	GC-MSD	.00107	.00051	.098	-.0002-	.0023

This table demonstrates the Tukey HSD post-hoc test results that differentiate the average Limit of Detection (LOD) between every method pair to find out if any differences exist. The mean difference between GC-ITQMS and GC-MSD equals 0.00083 while the calculated confidence range spans from -0.0004 to 0.0020 and the p-value reaches 0.246 thus establishing no significant difference. The mean differences between the LODs of GC-ITQMS and GC-SICRIT-LTQMS equals -0.00025 (p=0.880) while GC-MSD and GC-SICRIT-LTQMS have a difference of -0.00107 (p=0.098). The p-values in this experiment exceed the accepted threshold of 0.05 so these methods demonstrate no statistically important differences in their average detection limits. The post-hoc analysis reveals the detection limits of all three techniques have equivalent statistical values.

Table 4.8: Tukey HSDa results for LOD.

group	N	Subset for alpha = 0.05
		1
GC-MSD	28	.0030
GC-ITQMS	28	.0038
GC-SICRIT-LTQMS	28	.0041
Sig.		.098

Means for groups in homogeneous subsets are displayed.

a. Uses Harmonic Mean Sample Size = 28.000.

A table contains the Tukey HSD test results that evaluate LOD mean differences between GC-MSD, GC-ITQMS and GC-SICRIT-LTQMS analytical methods. The mean LODs of all the groups belong to a single subset as their data points show no statistically relevant differences between them. The mean detection limit of GC-MSD approaches 0.0030 mg/L while GC-ITQMS measures at 0.0038 mg/L and GC-SICRIT-LTQMS detects up to 0.0041 mg/L. The overall significance level (Sig.) measures 0.098 and exceeds 0.05 which proves the differences in means are statistically insignificant. The detection limits of all three methods remain similar since they show no meaningful difference in this analysis.

Before conducting ANOVA analysis for LOQ, descriptive statistics are used to understand the nature of data as shown in table 4.9.

Table 4.9: Descriptive statistics for LOQ of ITQMS, SQMS, and LTQMS.

	N	Mean	Std. Deviation	Std. Error	95% Confidence Interval for Mean		Minimum	Maximum
					Lower Bound	Upper Bound		
GC-ITQMS	28	.0119	.00607	.00115	.0095	.0143	.00	.03
GC-MSD	28	.0094	.00487	.00092	.0075	.0112	.00	.03
GC-SICRIT-LTQMS	28	.0117	.00599	.00113	.0094	.0140	.01	.03
Total	84	.0110	.00572	.00062	.0097	.0122	.00	.03

A compilation of descriptive statistics exists regarding LOQ measurements for GC-ITQMS, GC-MSD and GC-SICRIT-LTQMS analysis methods. This table displays statistical data for each technique: GC-ITQMS, GC-MSD, and GC-SICRIT-LTQMS based on (N=28) samples and contains mean LOQ measurements (~0.0094 to 0.0117) with standard deviation and standard error calculation. The average quantification limits between these analytical techniques match up based on 95% confidence intervals for their mean LOQ measurements. A review of assay data reveals that all measurement techniques achieve LOQ detection between 0.00 to 0.03 within their respective sample sets effectively. All methods demonstrate equivalent sensitivity achievement for quantification tasks according to these provided descriptors.

Levene's test is important because it helps determine whether the basic assumption of analysis of variance (ANOVA) is met, as this analysis requires that the variance between groups be equal. Table 4.10 shows the test of homogeneity of variances for LOQ

Table 4.10: test of homogeneity of variances for LOQ.

Levene Statistic	df1	df2	Sig.
1.438	2	81	.243

The data from LOQ analysis tested across three procedures indicated no significant differences of variances through Levene's test presented in this table. The Levene statistic equals 1.438 while the degrees of freedom amount to 81 and the group factor degrees of freedom amount to 2. The obtained significance value (Sig.) amounts to 0.243 exceeding the threshold of 0.05. The results of Levene's test demonstrate that LOQ variances remain statistically comparable among the methods thus satisfying the condition of equal variances. ANOVA analysis can proceed because the equality condition holds true for conducting subsequent tests.

Table 4.11: ANOVA results for LOQ across three devices.

	Sum of Squares	df	Mean Square	F	Sig.
Between Groups	.000	2	.000	1.724	.185
Within Groups	.003	81	.000		
Total	.003	83			

The ANOVA table confirms whether the average LOQ shows significant variations across the three measurement methods. The Between Groups sum of squares is near zero because group means remain quite similar but the Within Groups sum of squares reveals measurement differences within each method. The F-value of 1.724 along with the p-value (Sig.) of 0.185 shows no statistical significance in LOQ mean differences between the methods. The result indicates that the three measurement techniques produce equivalent quantification limits since this evaluation shows no distinction between them.

Tukey HSD is suitable for multiple comparison after ANOVA analysis, as it allows to determine which system differ significantly.

Table 4.12: results of Tukey HSD multiple comparisons for LOD.

(I) group	(J) group	Mean Difference (I-J)	Std. Error	Sig.	95% Confidence Interval	
					Lower Bound	Upper Bound
GC-ITQMS	GC-MSD	.00254	.00152	.221	-.0011-	.0062
	GC-SICRIT-LTQMS	.00022	.00152	.989	-.0034-	.0038
GC-MSD	GC-ITQMS	-.00254-	.00152	.221	-.0062-	.0011
	GC-SICRIT-LTQMS	-.00232-	.00152	.282	-.0059-	.0013
GC-SICRIT-LTQMS	GC-ITQMS	-.00022-	.00152	.989	-.0038-	.0034
	GC-MSD	.00232	.00152	.282	-.0013-	.0059

Table 4.12 shows the results of pairwise comparisons of the mean LOQ among the three methods using Tukey's HSD test. The mean differences between each pair are small, and the significance (Sig.) values are all above 0.05, indicating no statistically significant differences. For example, the difference between GC-ITQMS and GC-MSD is 0.00254, but with a p-value of 0.221, it's not statistically significant. The confidence intervals also include zero, confirming that there's no meaningful difference in LOQ values among these methods. Overall, this suggests all three techniques have comparable LOQs.

Table 4.13: Tukey HSD^a results for LOQ

group	N	Subset for alpha = 0.05
		1
GC-MSD	28	.0094
GC-SICRIT-LTQMS	28	.0117
GC-ITQMS	28	.0119
Sig.		.221

Means for groups in homogeneous subsets are displayed.

a. Uses Harmonic Mean Sample Size = 28.000.

The table 4.13 displays the results of a Tukey HSD test comparing the means of LOQ for three measurement techniques. All three methods—GC-MSD, GC-SICRIT-LTQMS, and GC-ITQMS—are grouped into a single subset, suggesting no significant differences among their average LOQ values. Specifically, GC-MSD has a mean LOQ of 0.0094, GC-SICRIT-LTQMS is at 0.0117, and GC-ITQMS is slightly higher at 0.0119. The overall significance (Sig.) is 0.221, which exceeds the typical threshold of 0.05, indicating no statistically meaningful difference in LOQ among these methods. Essentially, all three techniques perform similarly in terms of quantification detection limits.

Through this comprehensive methodology, LOD and LOQ will be able to accurately evaluate and analyze, contributing to understanding of the quantitative performance of analytical methods used.

Figure 4.10 shows slight differences in the measured LODs and LOQs are observed for these ONP pesticides when analyzed using different instruments, indicating potential method-dependent variations in sensitivity and detection capabilities.

In general, LOD values of GC-ITQMS, GC-MSD, and GC-SICRIT-LTQMS are somewhat close, with these values ranging from 0.001 to 0.01 $\mu\text{g}/\text{mL}$. The R^2 values for all selected pesticides are relatively high, indicating strong linearity in the calibration curves across all three GC methods, with values ranging from 0.9978 to 0.9995%.

Dimethachlor ($\text{C}_{13}\text{H}_{18}\text{ClNO}_2$) and acetochlor ($\text{C}_{14}\text{H}_{20}\text{ClNO}_2$) exhibit LOD values of 0.01 and 0.01 $\mu\text{g}/\text{ml}$ for GC-SICRIT-LTQMS, which are high compared to the values measured using GC-MSD and GC-ITQMS, with LODs of 0.0018 and 0.0032 $\mu\text{g}/\text{mL}$ respectively for GC-ITQMS, and LOD values of 0.0032 and 0.0026 $\mu\text{g}/\text{mL}$ respectively for GC-MSD.

Many of the compounds display noticeable differences in LODs and LOQs across the three GC techniques, suggesting the influence of instrumental and methodological factors on their analysis. For example, allidochlor exhibits LOD values of 0.0094 $\mu\text{g}/\text{ml}$ for GC-ITQMS, 0.0030 $\mu\text{g}/\text{ml}$ for GC-MSD, and 0.004 $\mu\text{g}/\text{ml}$ for GC-SICRIT-LTQMS. Correspondingly, the LOQ values are 0.0286 $\mu\text{g}/\text{ml}$, 0.0090 $\mu\text{g}/\text{ml}$, and 0.01 $\mu\text{g}/\text{ml}$, respectively. The R^2 values for allidochlor are relatively high, indicating strong linearity in the calibration curves across all three GC methods, with values ranging from 0.9978 to 0.9995. Clomazone, propyzamide, triallate, propanil, dimethachlor, acetochlor, alachlor, propisochlor, metolachlor, diphenamid, metazachlor, flutolanil, pretilachlor, and oxadiazon all exhibit comparable patterns in LOD, LOQ, and linearity across the three GC methods, with consistently high R^2 values indicating strong linearity in calibration.

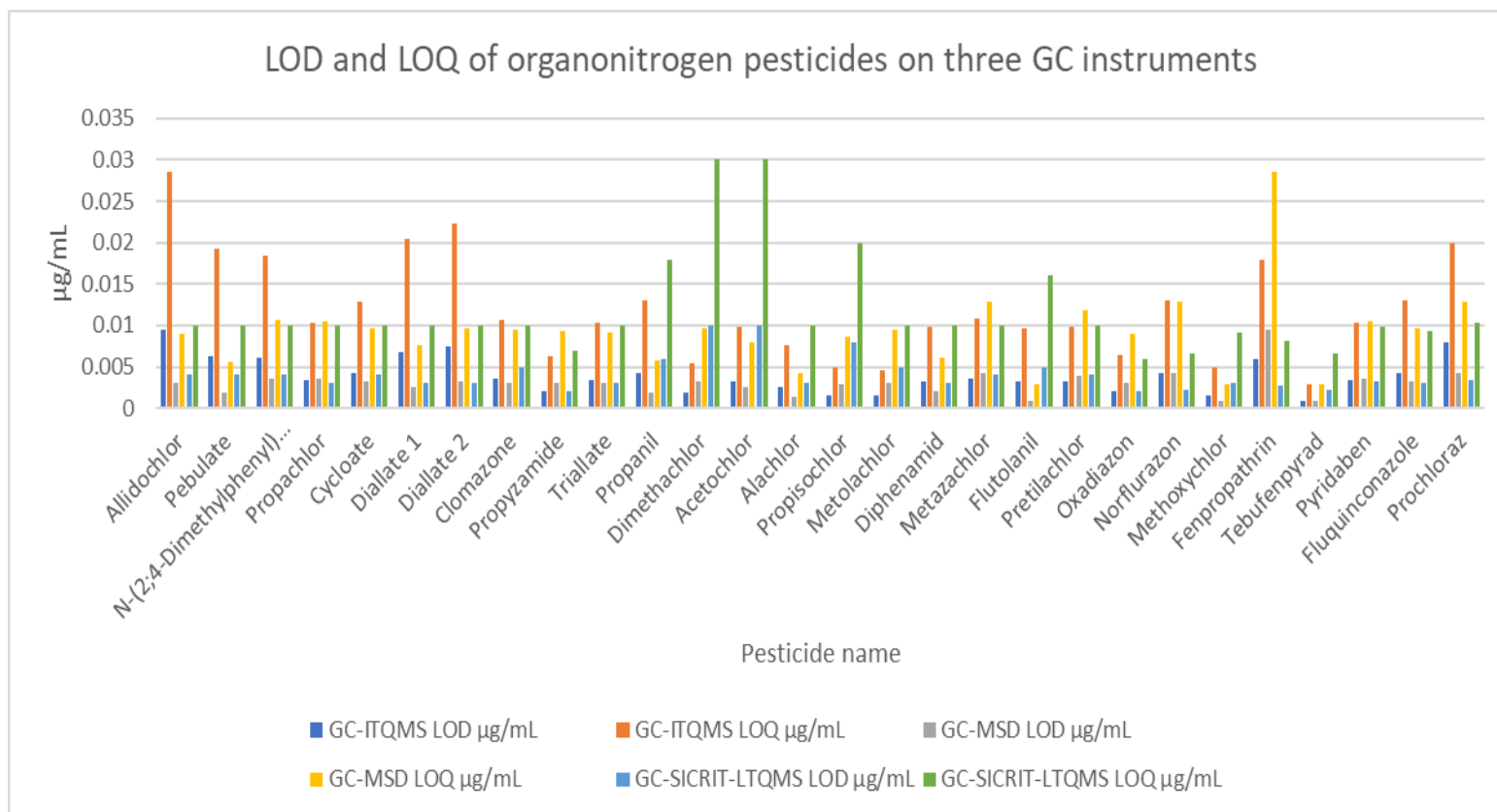


Figure 4.10: LOD and LOQ of organophosphorus pesticides in GC-ITQMS, GC-MSD, and GC-SICRIT-LTQMS.

4.5.3 Matrix Effect evaluation of multiple organonitrogen pesticide residues in selected baby food matrices (milk, rice and cereal)

In this study the task is to estimate the matrix effect for 29 organonitrogen pesticides in three different samples (milk, rice and cereal). This is done by spiking blank baby food samples with known concentration of pesticides, after using QuEChERS as an extraction method and followed with dSPE as clean-up method. The matrix effect can be calculated using the following equation1

$$ME = \left(\frac{\text{Response in matrix}}{\text{Response in Solvent}} - 1 \right) \times 100 \quad \text{Eq.4.1}$$

Ion suppression and enhancement are the two main consequences of the matrix effect. a value of 100% is considered no effect, a value of $\pm 20\%$ is considered a soft ME, $\pm 50\%$ values are considered a moderate ME, while values outside of $\pm 50\%$ are considered a strong ME. The matrix effects results for organonitrogen pesticides are summarized in table 4.14.

Table 4.4 presents the matrix effects observed for various organonitrogen pesticides when analyzed in the different baby food matrices evaluated using three different gas chromatography techniques. GC-MSD, GC-SICRIT-LTQMS, and GC-ITQMS represent the three different types of GC-MS systems available in our lab. Matrix interferences on the other hand are interferences to the ionisation of analytes extracted from a particular matrix due to components that have been co-extracted. These interferences can bring about a change in the quantitative results.

Table 4.14: Matrix effect on baby food samples based on GC-MSD, GC-SICRIT-LTQMS and GC-ITQMS.

Component Name	GC-MSD			GC-SICRIT-LTQMS			GC-ITQMS		
	Milk	Rice	Cereal	Milk	Rice	Cereal	Milk	Rice	Cereal
Allidochlor	257	105	94	83	-84	-21	123	92	73
Pebulate	496	249	31	4	-88	-27	225	49	69
N-(2;4-Dimethylphenyl) formamide	484	266	87	7	-90	30	139	98	97
Propachlor	344	166	171	1	-89	16	304	124	212
Cycloate	256	163	40	1	-91	-9	222	163	90
Diallate 1	125	62	42	1	-90	-74	199	74	87
Diallate 2	225	62	88	5	-87	-28	85	68	89
Clomazone	469	256	272	3	-91	-29	231	105	77
Propyzamide	644	88	11	6	-89	-53	255	46	84
Triallate	283	129	119	2	-88	-19	283	92	83
Propanil	166	105	99	20	-89	15	127	67	86
Dimethachlor	467	128	152	4	-91	-53	233	112	101
Acetochlor	207	45	152	19	-89	-70	100	95	154

Alachlor	687	430	498	5	-90	-38	123	34	88
Propisochlor	269	42	62	16	-94	-45	89	57	70
Metolachlor	101	59	39	8	-93	-30	134	93	130
Diphenamid	287	132	122	3	-88	-21	223	37	46
Metazachlor	414	172	88	1	-91	-47	120	79	89
Flutolanil	402	187	256	11	-93	-6	402	122	186
Pretilachlor	62	39	198	2	-88	3	90	25	88
Oxadiazon	398	354	288	1	-88	2	125	54	160
Norflurazon	187	92	76	2	-83	-63	177	82	99
Methoxychlor	344	166	171	1	-89	-80	304	124	212
Fenpropathrin	256	163	40	1	-91	-9	222	163	90
Tebufenpyrad	283	129	119	2	-88	-19	283	92	83
Pyridaben	166	105	99	20	-89	15	127	67	86
Fluquinconazole	101	59	39	8	-93	-30	134	93	130
Prochloraz	283	129	119	2	-88	-19	283	92	83

4.5.3.1 Matrix effect of organonitrogen pesticides on baby food samples based on GC-MSD

Table 4.4 presents matrix effects (ME%) observed for various pesticides analyzed using Gas Chromatography-Mass Spectrometry (GC-MSD) in three different food matrices: milk, rice, and cereal. There is variability in matrix effects across different pesticides and matrices, 26 out of 29 compounds showed a higher matrix effect in milk compared to rice and cereal, probably due to the fatty components of milk, which indicates that the matrix components have a high positive effect. For instance, pebulate exhibits a higher ME% in milk (496%) compared to rice (249%) and cereal (31%), indicating that the matrix components in milk have a greater influence on the ionization efficiency of pebulate. Furthermore, there are variations in matrix effects among pesticides within the same matrix. For example, in milk, propyzamide shows a higher ME% (644%) compared to other pesticides like propachlor (344%) and fluquinconazole (101%). This discrepancy may be attributed to differences in the chemical properties of these pesticides and their interactions with the milk matrix components. Similarly, in rice,alachlor exhibits a higher ME% (43%) compared to clomazone (256%) and pretilachlor (39%), indicating differential matrix effects among these pesticides within the rice matrix. Many pesticides exhibit varying matrix effects across different matrices, indicating that the composition of the matrix may influence the extent of matrix effects for these pesticides (Figure 4.11).

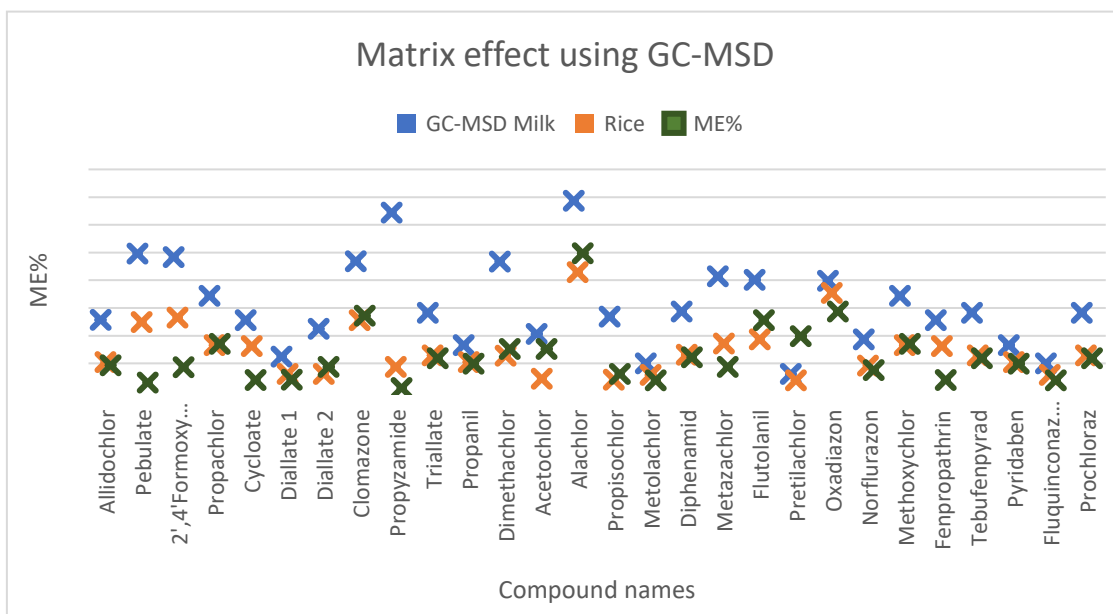


Figure 4.11: ME% of organonitrogen pesticides in GCMSD.

4.5.3.2 Matrix effect of organonitrogen pesticides on baby food samples based on GC-SICRIT-LTQMS

Table 4.4 provides data on matrix effects (ME%) observed for various pesticides analyzed using Gas Chromatography coupled with Linear Ion Trap Quadrupole Mass Spectrometry (GC-LTQMS) in three different food matrices: milk, rice, and cereal. This table predominantly displays negative matrix effects across the board for all compounds in rice and cereal matrices. This suggests that the matrix components present in rice, and cereal suppress the ionization efficiency of the analyzed pesticides when using GC-LTQMS. This consistent negative trend in matrix effects could indicate that the matrix components interfere with the ionization process, resulting in decreased sensitivity or response for the pesticides analyzed. While the magnitude of the matrix effects varies among different pesticides, there is a general similarity in the pattern of rice and cereal matrix effects across the various compounds within each matrix. For instance, in rice, all pesticides exhibit negative matrix effects ranging from -83 to -93, indicating a consistent suppression of ionization efficiency regardless of the specific pesticide. Similarly, in the cereal matrix, the majority of pesticides also display negative matrix effects within a relatively narrow range, suggesting a uniform impact of matrix components on ionization efficiency across different compounds within these matrices. There are some variations in the cereal matrix, N-(2,4-Dimethylphenyl) formamide, propachlor, propanil, pretilachlor, oxadiazon, and pyridaben all see a exhibit positive matrix effect, unlike other pesticides in the same matrix. (Figure 4.12).

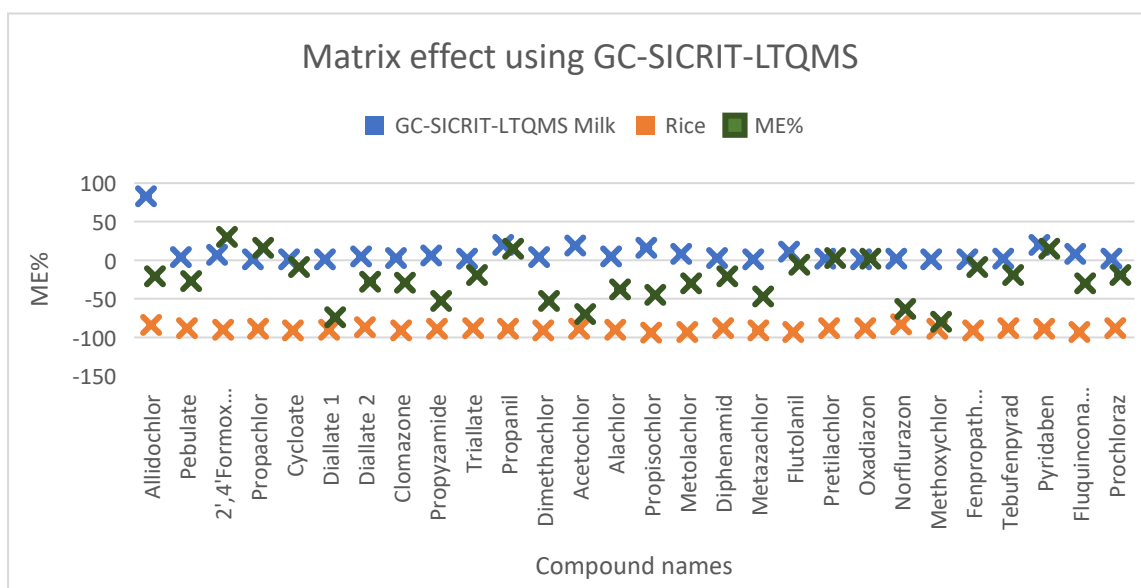


Figure 4.12: ME% of organonitrogen pesticides in GC-SICRIT-LTQMS.

4.5.3.3 Matrix effect of organonitrogen pesticides on baby food samples based on GC-ITQMS

Table 4.4 presents matrix effects (ME%) observed for various pesticides analyzed using Gas Chromatography coupled with Ion Trap Mass Spectrometry (GC-ITQMS) in three different food matrices: milk, rice, and cereal. 86% of the studied compounds exhibit relatively high ME% values in milk compared to rice and cereal, with matrix effect values ranging from 85% to 402% for milk, while in rice and cereal ME% values ranging from 37% to 163% and 46% to 212%, respectively. indicating a strong influence of the matrix components present in these matrices on the ionization efficiency of these pesticides.

Moreover, within each matrix, there are variations in matrix effects among different pesticides. For example, in milk, flutolanil shows a higher ME% (402%) compared to diallate 2 (85%), indicating that the matrix components in milk may have a greater impact on the ionization efficiency of flutolanil compared to diallate 2. Similarly, in rice, fenprothrin exhibits a higher ME% (163%) compared to pretilachlor (25%), suggesting differential matrix effects among these pesticides within the rice matrix (Figure 4.13).

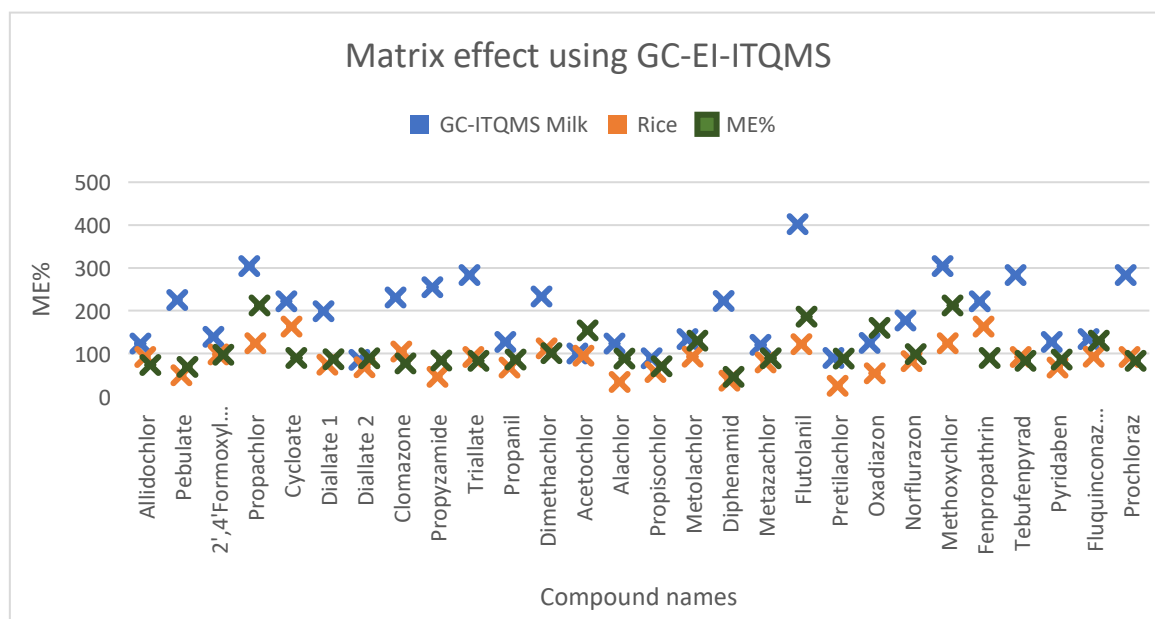


Figure 4.13: ME% of organonitrogen pesticides in GC-EI-ITQMS.

4.5.4 Comparison of matrix effect of organonitrogen pesticides on baby food samples

Infant foods, such as milk, rice, and cereals, have complex compositions and contain a wide range of natural compounds, including proteins, lipids, and sugars, similar to infant formula. These components affect the efficiency of chemical pesticides analysis. Rice and cereals contain carbohydrates as a major component. Rice also contains phenolic compounds, which may affect pesticides recovery and distribution during extraction. In contrast, cereals contain lipids and plant compounds, which can lead to matrix effects on the analysis process.

This section aims to study the effect of matrix components on the analysis of organonitrogen pesticides. Where the possibility of any effects of these matrices on the accuracy of the results is evaluated. By displaying the chromatograms of these three matrices, the absence of detectable levels of target pesticides is verified and compared to the chromatograms of standard pesticides, as shown in figure 4.14, enhancing the reliability of the analysis.

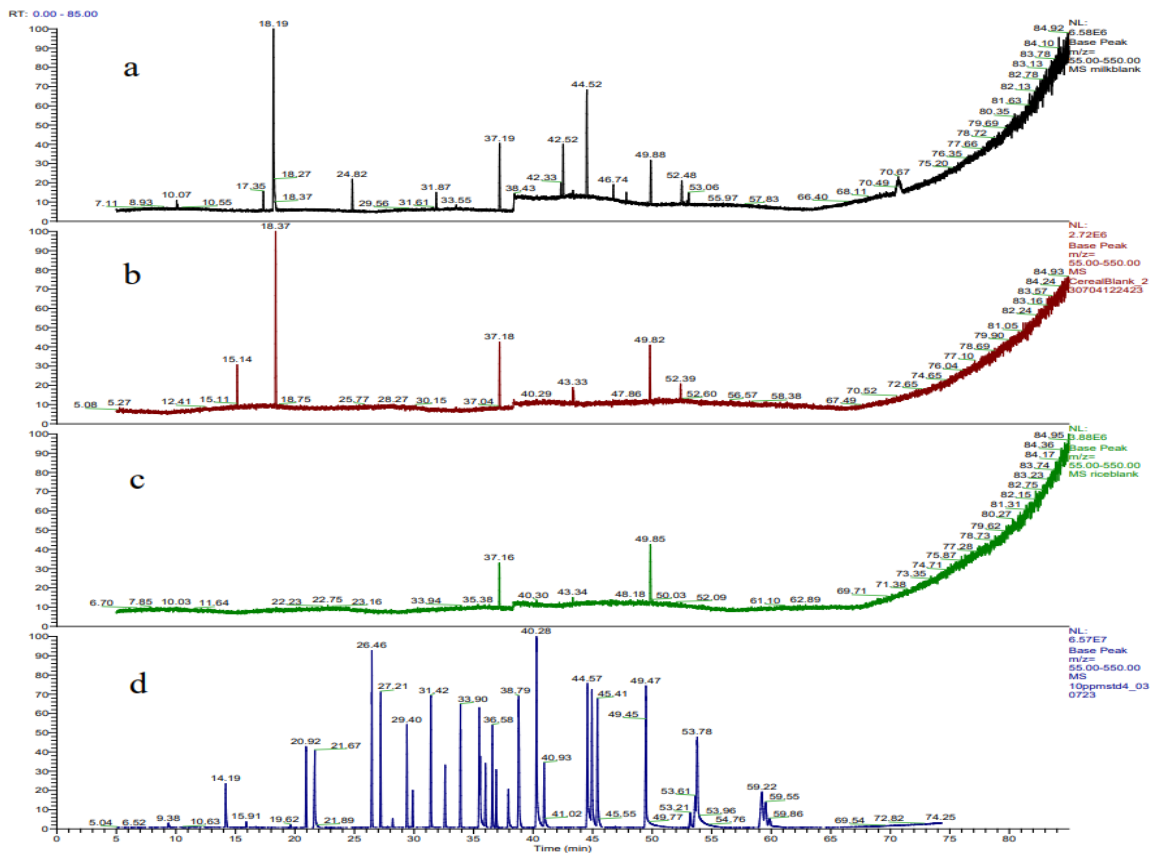


Figure 4.14: Chromatogram (a) milk blank, (b) cereal blank, (c) rice blank, and (d) standard organonitrogen pesticides, which are described in table 4.2 by using GC-LTQMS.

Technical Basis of Matrix Effects Across Platforms

Instrument design differences together with ionization mechanism differences lead to observed matrix effects variations. Milk matrices containing lipids harm the ionization efficiency of GC-MSD because its standard electron ionization method causes wide range fragmentation that reacts strongly to co-eluting background compounds. Signal enhancement amounts to 687% according to measurements taken for specific pesticide compounds. The GC-SICRIT-LTQMS operates with gentle chemical ionization yet shows strong sensitivity to competitive ionization effects which causes matrix components to take available charge from target compounds. The analysis of rice samples containing high levels of carbohydrates leads to an extreme reduction of -94% because sugars and starches compete during ionization. GC-ITQMS achieves matrix interference control through target ion selection that happens after initial ionization because its ion trap mechanism provides selective ion filtering while maintaining strong sensitivity.

Practical Implications for Analytical Workflows

The high detection ability of GC-MSD requires strict calibration with matrix-matched standards because single-solvent standards would produce inaccurate measurement results. GC-SICRIT-LTQMS requires complex sample purification or expensive isotope-labeled internal standards which match the retention times of targets. GC-ITQMS provides the best solution for routine analysis because calibration errors can be corrected through standard addition or dilution methods when facing its predictable moderate enhancement. Laboratories analyzing different sample types should operate GC-ITQMS systems daily but also maintain GC-MSD instruments because these instruments supply different analytical abilities which produce independent verification outcomes during combined examination. Food safety monitoring shows decreased performance from GC-SICRIT-LTQMS instruments relative to GC-ITQMS and GC-MSD because incorrect negative results trigger major regulatory issues.

Table 4.15 Comparison of organonitrogen pesticides in GC-MSD, GC-ITQMS, and GC-SICRIT-LTQMS.

Parameter	GC-MSD	GC-SICRIT-LTQMS	GC-ITQMS
Dominant Effect	Strong enhancement	Extreme suppression	Moderate enhancement
Milk Performance	Excellent (50-687)	Poor (1-20)	Good (100-402)
Rice Performance	Variable (45-430)	Worst (-94 to -83)	Best (25-163)
Cereal Performance	Good (11-498)	Variable (-80 to 30)	Excellent (46-212)
Precision	Moderate	Low	High
Recommended Use	Targeted analysis	Research	Routine screening
Calibration Needs	Matrix-matched	Isotope standards	Standard may suffice

The analysis of multiple baby food matrices should use GC-ITQMS since it produces precise results without significant matrix distortion but GC-MSD requires specialized calibration and interpretation due to its enhanced sensitivity. GC-SICRIT-LTQMS does not have proper suppression control during rice analysis so it remains unfit for regular use at present. The instrument needs optimized methods for successful performance as well as internal standard adjustments. Laboratories must adopt GC-ITQMS as their primary analytical device while retaining GC-MSD for sensitive confirmatory assessments yet continue developing methods to remove suppression barriers of GC-SICRIT-LTQMS for potential applications. Finally, Table 4.15 shows a Comparison of performance of GC-MSD, GC-ITQMS, and GC-SICRIT-LTQMS when analysing organonitrogen pesticides.

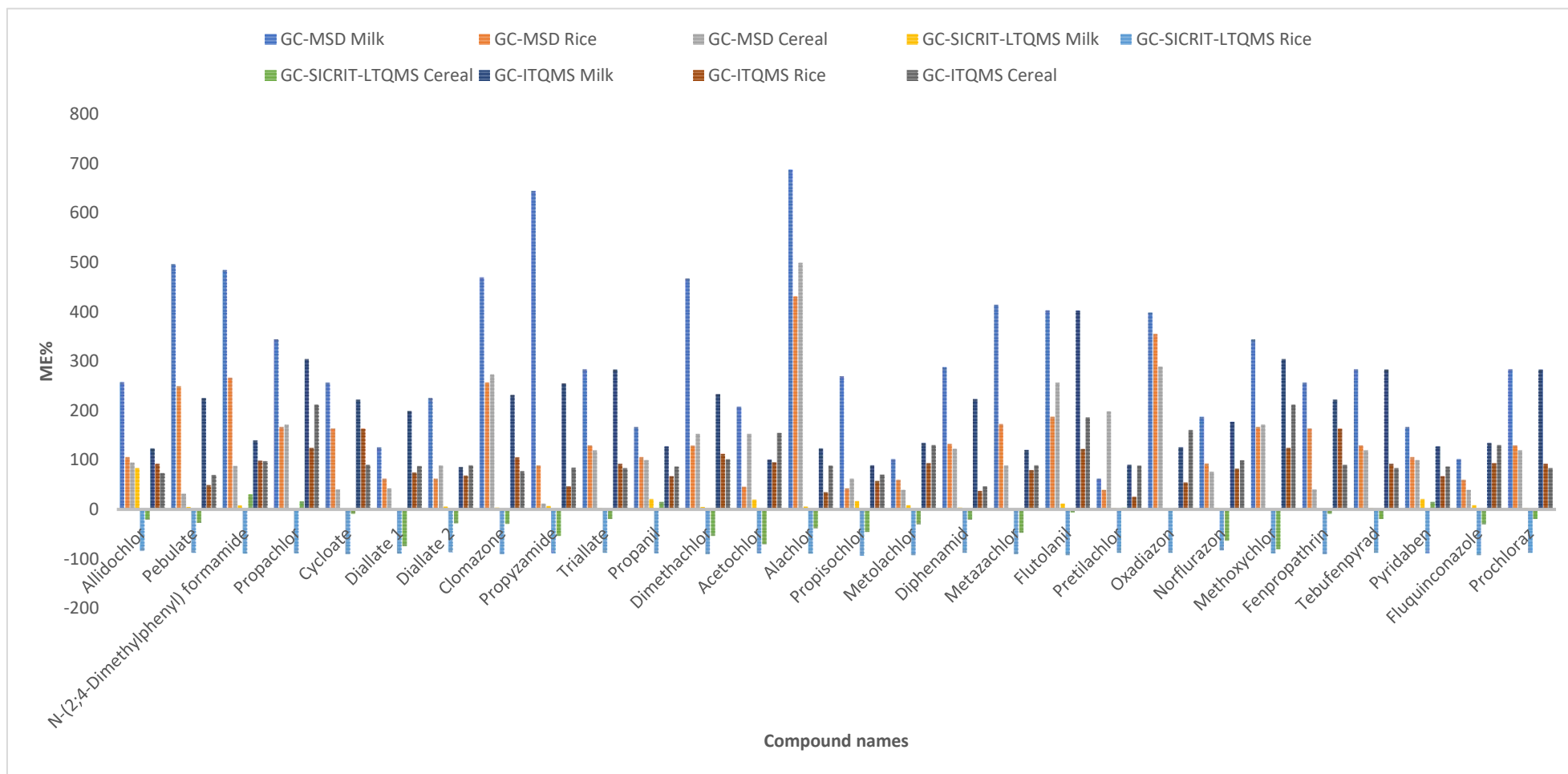


Figure 4.15: ME% of organonitrogen pesticides in GC-MSD, GC-ITQMS, and GC-SICRIT-LTQMS.

5. Development of GC method for separation and determination of selected pyrethroid Pesticides

5.1 Introduction

Pyrethroids are synthetic compounds that are similar to natural pyrethroids produced by *Chrysanthemum cineraria folium*. They were developed to increase the effectiveness of insecticides, increase their stability to light, and their residence period in the environment.¹³⁸ In recent years, pyrethroids have been considered as alternative to organochlorine pesticides because they are less toxic and less stable in the environment than organochlorine compounds.¹³⁹ Pyrethroids are the most widely used pesticides worldwide because they are an essential tool in agriculture used for protecting crops from pests. They are also used as household insecticides in addition to their importance in the field of public health.¹⁴⁰ However, they are more toxic to humans and animals than natural pyrethroids.¹⁴¹ Pyrethroids are compounds that have high resistance to water and therefore have low solubility in water, so they are rapidly adsorbed by solid particles.¹⁴² Pyrethroids can be degraded by several pathways, including microorganisms and sunlight. However, some recent compounds have been found to remain in the environment for several months before degrading.¹⁴³ Some symptoms and effects that pyrethroid pesticides may cause on the human immune system have been reported.¹⁴⁴ Exposure of children to pyrethroids is a concern and has increased in recent years.^{145,146}

5.2 Structural Classification and Separation of Pyrethroids

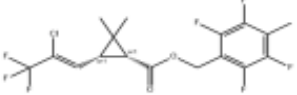
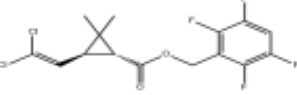
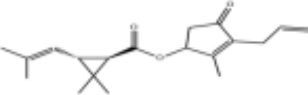
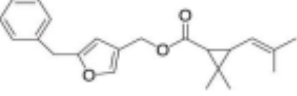
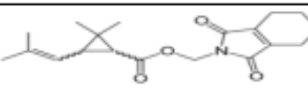
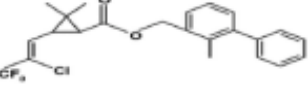
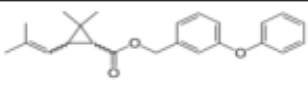
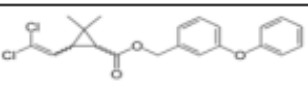
Pyrethroids are chiral compounds consisting of 2 or 3 chiral centres. Type I typically has two chiral centers, resulting four diastereoisomers or two enantiomeric pairs. While Type II has three chiral centers, resulting in the possibility of six diastereoisomers.¹⁴⁷

Isomers are molecules that have the same molecular formula as the original compound but differ in structure or arrangements of atoms.

- Diastereomers are type of isomers that do not have mirror images of each other and their physical and chemical properties are different.
- Enantiomeric are type of isomer that that are non-superimposable mirror images of each other and their physical properties are the same but they can have different chemical reactions.

Multiple isomers have different properties and are therefore useful for different applications, but this leads to different levels of toxicity of the isomers depending on their properties. Therefore, recent studies have focused largely on separating these isomers to understand and manage their toxicity.¹⁴⁸ In this study, a mixture of 18 synthetic pyrethroid compounds including type I and II pyrethroids was analyzed using three different GC instruments: GC-FID, GC-EI-ITQMS, and GC-SICRIT-LTQMS. Table 5.1 summarize the results obtained from the separation of 18 compounds, indicating in the number of isomers produced for each pesticide by each instrument used.

Table 5.1: Description of the pyrethroids studied and summary of chromatography achievement

Pyrethroid	Structure	Pyrethroid Type	Chiral centres	GC-FID Peaks	GC-EI-MS Peaks	GC-DBDI-MS Peaks
Tefluthrin		I	2	1	1	1
Transfluthrin		I	2	1	1	1
Anthraquinone		I	2	1	1	1
Bioallethrin		I	2	1	1	1
Resmethrin		I	2	2	2	2
Tetramethrin		I	2	2	2	2
Bifenthrin		I	2	1	1	1
Phenothrin		I	2	2	2	2
Permethrin, cis		I	2	1	1	1

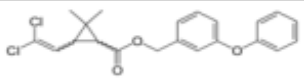
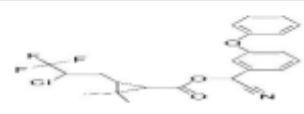
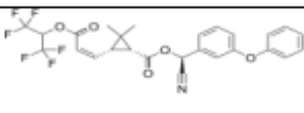
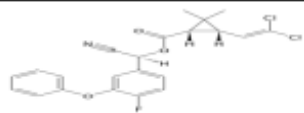
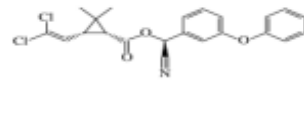
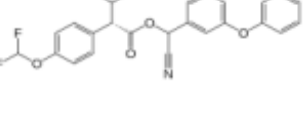
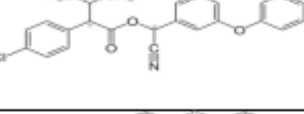
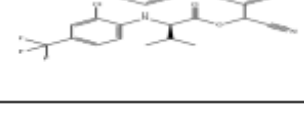
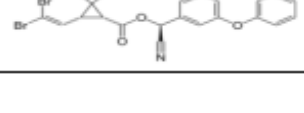
Permethrin, trans		1	2	1	1	1
lambda-Cyhalothrin		I	2	1	1	1
Acrinathrin		II	3	1	1	1
Cyfluthrin		II	3	4	4	-
Cypermethrin		II	3	4	4	-
Flucythrinate		II	3	2	2	-
Fenvalerate		II	3	2	2	-
tau-Fluvalinate		II	3	2	2	-
Deltamethrin		II	3	1	1	-

Table 5.2 lists all 30 peaks detected using GC-EI-MS and GC-FID, including the 18 parent compounds and their isomers. This table provides essential information such as compound names, molecular weights, and chemical formulas. The presence of isomers for several compounds (e.g., resmethrin, tetramethrin, cyfluthrin, cypermethrin) is indicated. Table 5.2 also lists the compounds and isomers detected by GC-SICRIT-MS and compares some compounds, particularly those with higher molecular weights that were not detected or poorly resolved using GC-SICRIT-LTQMS.

Resmethrin, tetramethrin, and phenothrin are Type I pyrethroid showed two isomers in all instruments. cyfluthrin, cypermethrin are Type II pyrethroid showed four isomers in GC-FID and GC-EI-ITQMS, while flucythrinate, fenvalerate, and tau-fluvalinate showed two peaks.

Table 5.2: Synthetic Pyrethroid Compounds and their isomers that appear in GC-EI-MS and GC-FID

No ^a	Component Name	Molecular weight	Formula	GC-FID	GC-EI-ITQMS	GC-SICRIT-LTQMS
1	Tefluthrin	418.7	C ₁₇ H ₁₄ ClF ₇ O ₂	√ ^b	√	√
2	Transfluthrin	371.1	C ₁₅ H ₁₂ Cl ₂ F ₄ O ₂	√	√	√
3	Anthraquinone	208.2	C ₁₄ H ₈ O ₂	√	√	√
4	Bioallethrin	302.4	C ₁₉ H ₂₆ O ₃	√	√	√
5	Resmethrin 1	338.4	C ₂₂ H ₂₆ O ₃	√	√	√
6	Resmethrin 2	338.4	C ₂₂ H ₂₆ O ₃	√	√	√
7	Tetramethrin 1	331.4	C ₁₉ H ₂₅ NO ₄	√	√	√
8	Tetramethrin 2	331.4	C ₁₉ H ₂₅ NO ₄	√	√	√
9	Bifenthrin	422.8	C ₂₃ H ₂₂ ClF ₃ O ₂	√	√	√
10	Phenothrin 1	350.4	C ₂₃ H ₂₆ O ₃	√	√	√
11	Phenothrin 2	350.4	C ₂₃ H ₂₆ O ₃	√	√	√
12	Cyhalothrin, lambda-	449.8	C ₂₃ H ₁₉ ClF ₃ NO ₃	√	√	√
13	Acrinathrin	541.4	C ₂₆ H ₂₁ F ₆ NO ₅	√	√	√
14	Permethrin, cis-	391.2	C ₂₁ H ₂₀ Cl ₂ O ₃	√	√	√
15	Permethrin, trans-	391.2	C ₂₁ H ₂₀ Cl ₂ O ₃	√	√	√
16	Cyfluthrin 1	434.2	C ₂₂ H ₁₈ Cl ₂ FNO ₃	√	√	X ^c
17	Cyfluthrin 2	434.2	C ₂₂ H ₁₈ Cl ₂ FNO ₃	√	√	X
18	Cyfluthrin 3	434.2	C ₂₂ H ₁₈ Cl ₂ FNO ₃	√	√	X
19	Cyfluthrin 4	434.2	C ₂₂ H ₁₈ Cl ₂ FNO ₃	√	√	X
20	Cypermethrin 1	416.2	C ₂₂ H ₁₉ Cl ₂ NO ₃	√	√	X
21	Cypermethrin 2	416.2	C ₂₂ H ₁₉ Cl ₂ NO ₃	√	√	X
22	Cypermethrin 3	416.2	C ₂₂ H ₁₉ Cl ₂ NO ₃	√	√	X
23	Cypermethrin 4	416.2	C ₂₂ H ₁₉ Cl ₂ NO ₃	√	√	X
24	Flucythrinate 1	451.4	C ₂₆ H ₂₃ F ₂ NO ₄	√	√	X
25	Flucythrinate 2	451.4	C ₂₆ H ₂₃ F ₂ NO ₄	√	√	X
26	Fenvalerate 1	419.9	C ₂₅ H ₂₂ ClNO ₃	√	√	X
27	tau-Fluvalinate 1	502.9	C ₂₆ H ₂₂ ClF ₃ N ₂ O ₃	√	√	X
28	Fenvalerate 2	419.9	C ₂₅ H ₂₂ ClNO ₃	√	√	X
29	tau-Fluvalinate 2	502.9	C ₂₆ H ₂₂ ClF ₃ N ₂ O ₃	√	√	X
30	Deltamethrin	505.1	C ₂₂ H ₁₉ Br ₂ NO ₃	√	√	X

^a the peaks numbers in the order, ^b the compound has been detected, ^c the compound not detected

5.3 Chromatographic separation

Method development began with analysis of the pesticide mixture using GC-FID; all pesticides and some of their isomers were detected using a stock concentration of 10ppm.

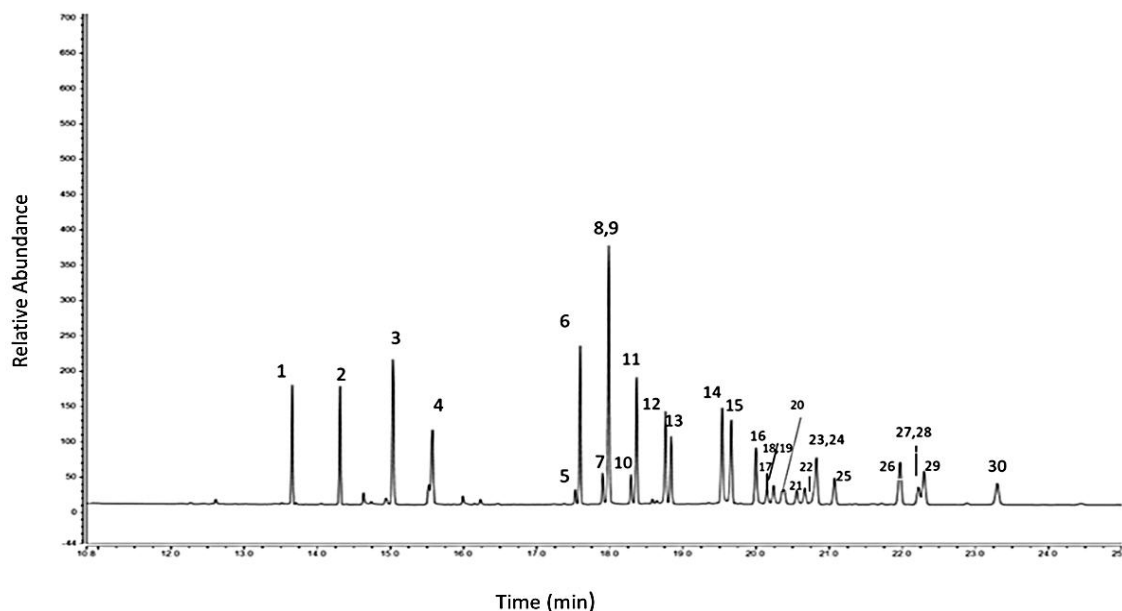


Figure 5.1: GC-FID Chromatogram of pyrethroid pesticides at 10µg/mL. GC-FID Chromatogram of a mixture of 18 parent pyrethroid pesticides with their isomers (compounds identity in table 5.2) at 10ppm

Figure 5.1 depicts the chromatogram of the stock pyrethroid sample mixture. The result shows a total of 30 peaks that correspond to the 18 synthetic pyrethroid pesticides and their isomers that were present in the stock mixture. Although the use of an FID allows for robust detection, it does not provide structural data and thus it is impossible, without access to the individual compound and their isomers to assign this chromatogram fully. An initial assignment was made based on the chromatogram supplied with the purchase pesticide standard. The x-axis shows the retention time and the y-axis the detector response.

In order to confirm the tentative assignments made using the FID data/manufacture chromatogram, analysis was repeated on a GC-EI-MS system (Figure 5.2).

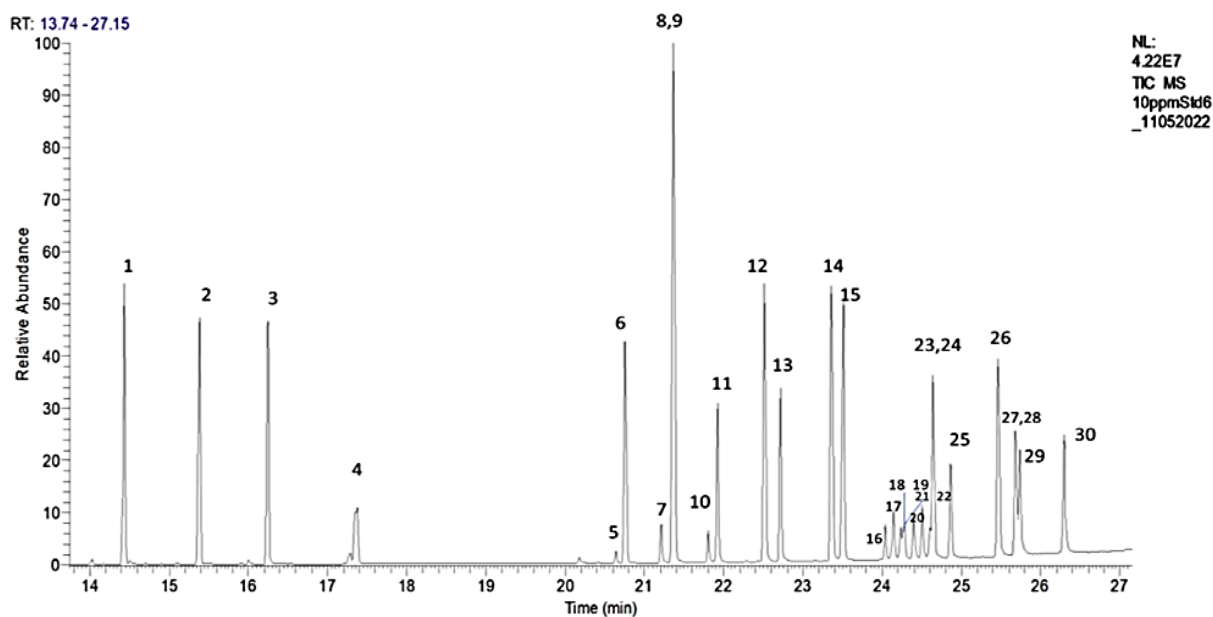


Figure 5.2: GC-EI-ITQ TIC-MS Chromatogram of a mixture of 18 parent pyrethroid pesticides with their isomers (compounds identity in table 5.2) at 10ppm.

Figure 5.2 shows the chromatogram obtained from the GC-EI-MS of the same 18 pesticide standard at 10ppm. The chromatogram obtained is remarkably similar to that obtained via GC-FID, showing peaks eluting in similar relative positions in each analysis (these peaks are numbered in table 5.3 according to the retention time). Some overlapping peaks were observed in both instruments, for example peak 8 overlapped with peak 9, peak 23 with 24, and peak 27 with peak 28. Where peak 8 represents tetramethrin 2 ($C_{19}H_{25}NO_4$) and peak 9 represents bifenthrin ($C_{23}H_{22}ClF_3O_2$). Peak 23 represents cypermethrin 4 ($C_{22}H_{19}Cl_2NO_3$) and peak 24 represents flucythrinate ($C_{26}H_{23}F_2NO_4$). Peak 27 represents tau-fluvalinate 1 ($C_{26}H_{22}ClF_3N_2O_3$) and peak 28 represents fenvalerate 2 ($C_{25}H_{22}ClNO_3$). Figure 5.3 shows the chemical structures of these compounds. Peaks 8 and 9 in both instruments represent the highest peaks in the chromatogram, indicating the sensitivity of the detector response in GC-FID and GC-ITQMS to tetramethrin 2 ($C_{19}H_{25}NO_4$) and bifenthrin ($C_{23}H_{22}ClF_3O_2$).

The total running time of GC-ITQMS appears to be almost the same as the running time of GC-FID. The chromatography obtained from SPPs analysis using GC-ITQMS is clearly different from GC-FID in terms of the intensity of the peaks, indicating the difference in the sensitivity of the GC-ITQMS detector to these pesticides.

Figure 5. shows that method transfer between systems was achieved. However, using GC-EI-MS gives extra mass spectral data of each peak, through which it becomes easier to confirm the identity of compounds.

A chemical structure was obtained for all compounds that were separable by gas chromatography as depicted in figure 5.4. Identical m/z values and similar retention times were used to assign the relevant stereoisomers present. Resmethrin, tetramethrin, and phenothrin, which are type I pyrethroids, exhibited two isomers. Cyfluthrin and cypermethrin, classified as type II pyrethroids, showed four isomers, while flucythrinate, fenvalerate, and tau-fluvalinate displayed two isomers.

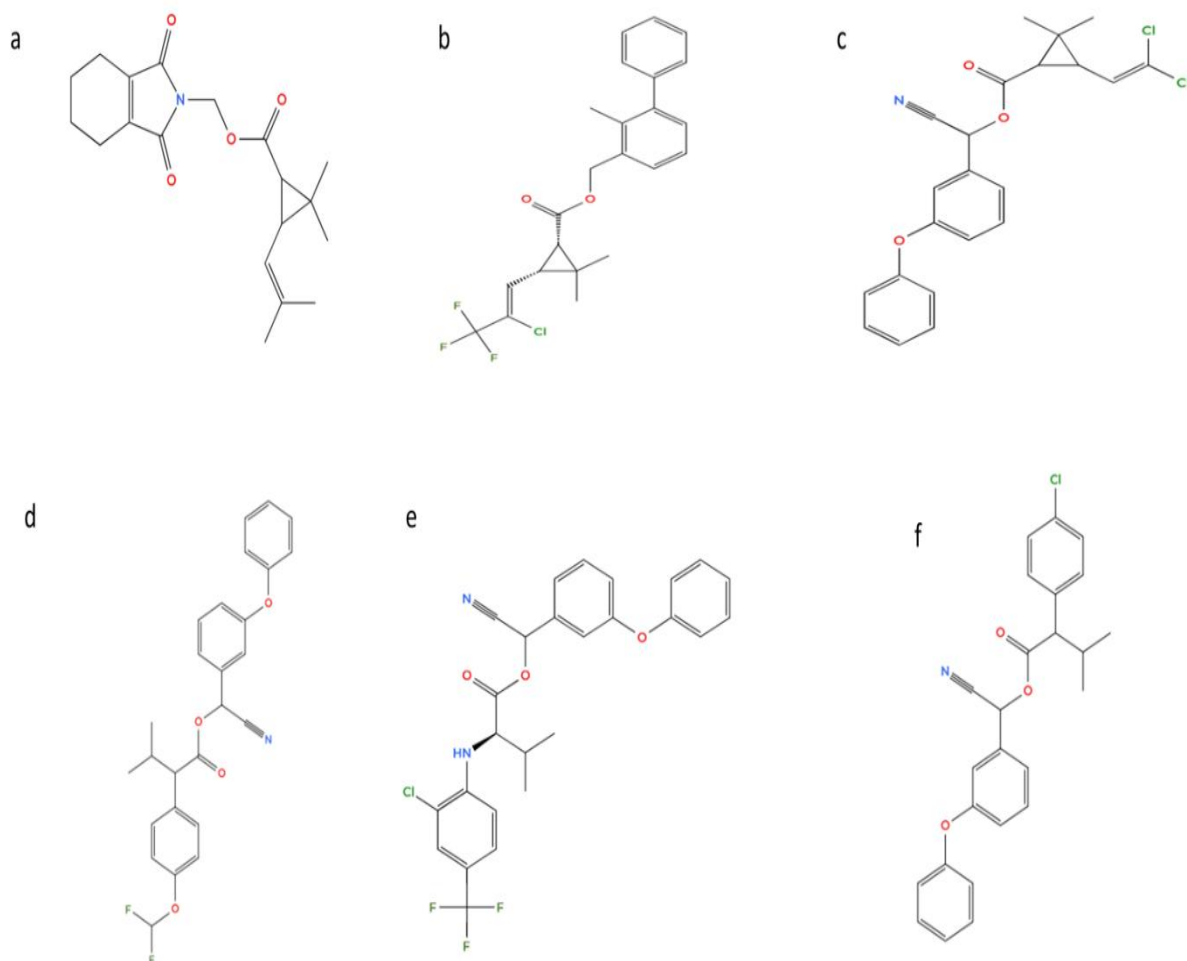


Figure 5.3: Chemical structure of different pyrethroid pesticides (a) tetramethrin (b) bifenthrin (c) cypermethrin (d) flucythrinate tau-fluvalinate (f) fenvalerate.

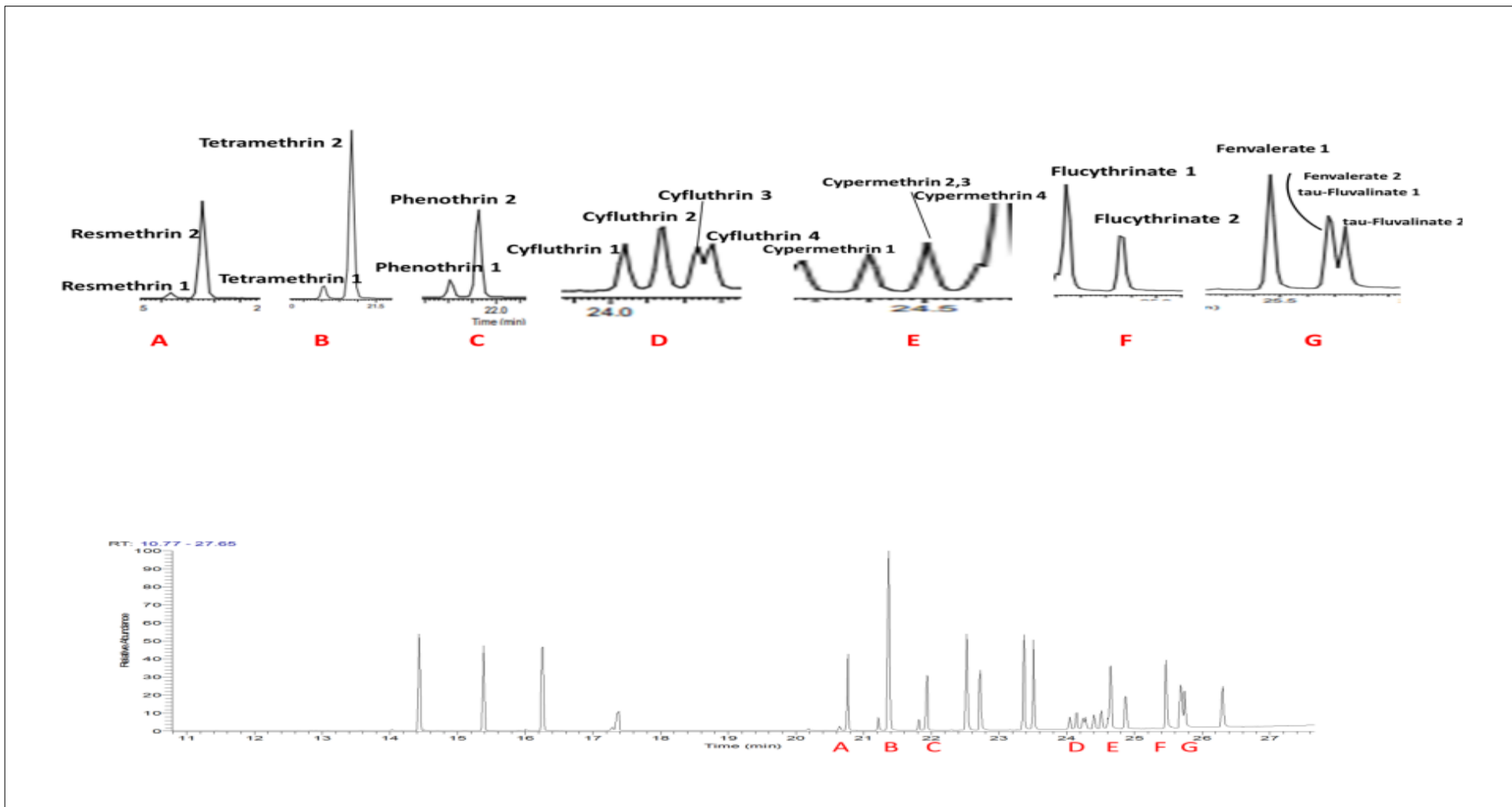


Figure 5.4: GC-ITQMS Chromatogram of pyrethroid compounds and their isomers

Thirdly, these same standards (10ppm) were analysed using GC using SICRIT as an ionization source. This technique resulted in detection of many but not all compounds. This can likely be ascribed to the longer chromatographic run.

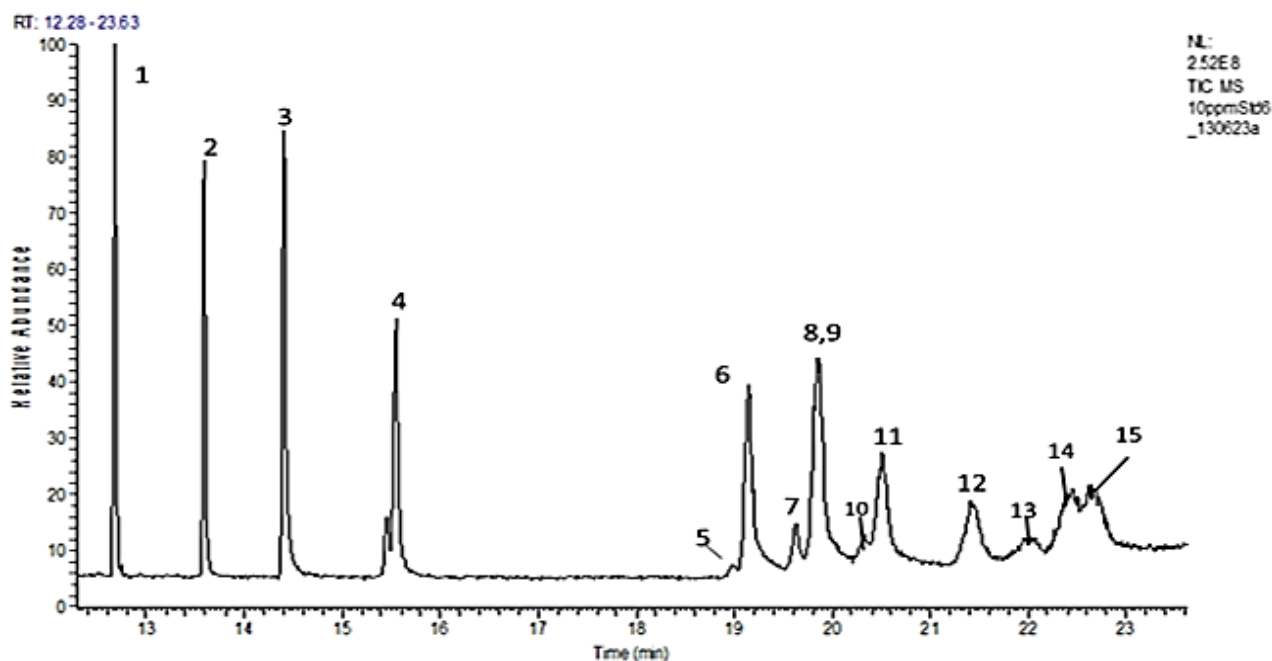


Figure 5.5: GC-SICRIT-MS Chromatogram of a mixture of parent pyrethroid pesticides with their isomers (compounds identity in table 5.2) at 10ppm.

Figure 5.5 is the chromatogram resulting from the GC-SICRIT-MS (Gas Chromatography with Soft Ionization by Chemical Reaction in Transfer Mass Spectrometry) of the pesticide standard at 10 ppm. Interestingly, this chromatogram has a significantly smaller number of peaks than the ones observed in Figures 5.1 and 5.2 suggesting that not all the compounds that were identified using GC-FID and GC-EI-MS were detectable using SICRIT ionization. In addition, some compounds were not fully resolved in contrast to the GC-EI experiments detailed previously. Figure 5.6 shows a comparison of two techniques' ability to separate and analyze pyrethroids.

There are various reasons for the appearance and absence of compounds. One of the primary reasons is the ionisation efficiency of SICRIT, as some compounds may not ionise due to the lower ionisation potential of this ionisation mode, resulting in weak or untraceable signals¹⁴⁹. However, compounds having low volatility or having interaction with the stationary phase in the GC column have not eluted adequately which is the more likely reason for the missing peaks. In addition, there is a possibility that the GC method

used may not be compatible with the detection of all pyrethroids compounds with isomers or higher molecular weights.

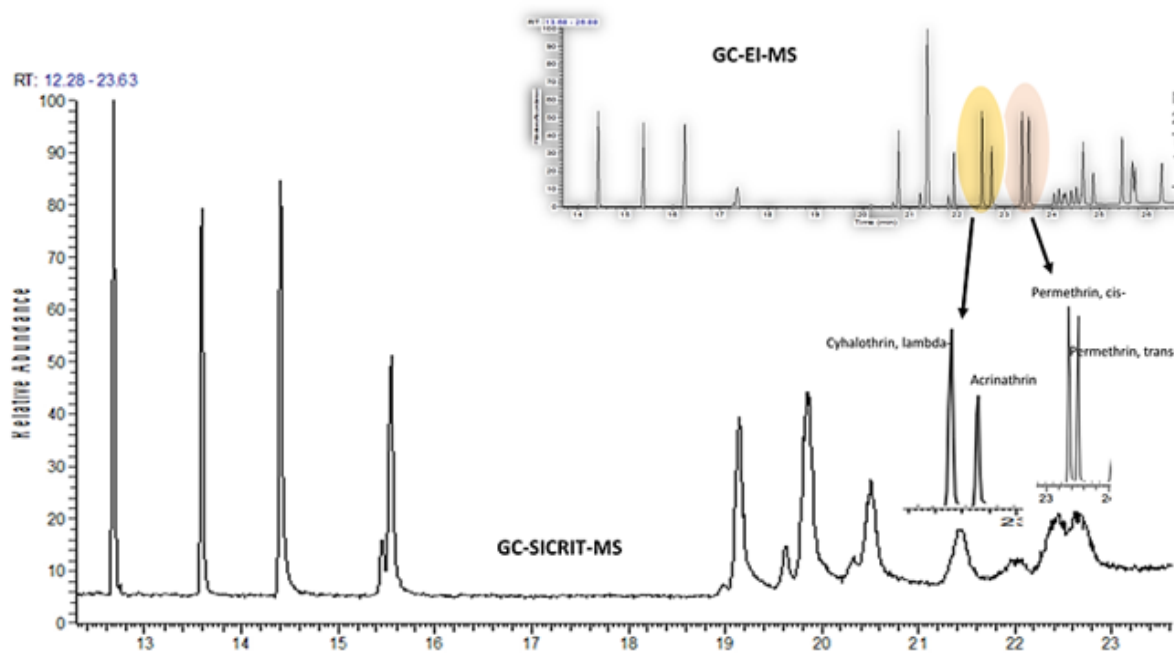


Figure 5.6: Difference in pyrethroid chromatography between GC-EI-MS and GC-SICRIT-MS

5.4 Linearity, LOD and LOQ for GC-EI-MS

The Linearity of Absolute Response of analytes was determined by analysing standardised solutions, in triplicate, in the range of 0.001 to 0.5 $\mu\text{g}/\text{mL}$ (ppm). The assessment of linearity was calculated with the help of the correlation coefficient (R^2) for each compound. These analyses gave R^2 values starting from 0.997, showing good linearity (Table 5.3). In addition, the “Limit of Detection (LOD)” and “Limit of Quantification (LOQ)” were also determined for each compound, offering a deeper understanding of the sensitivity and accuracy of the methods used for detection. Table 5.3 displays the excellent detectability that can be stretched by GC-EI-MS. The detection limits range between 0.003 to 0.13 $\mu\text{g}/\text{mL}$ (ppm).

Table 5.3: Synthetic Pyrethroid with R^2 , LOD and LOQ values using GC-EI-MS

Peak No	Component Name	tR (min)	R^2	LOD	LOQ
				ppm	ppm
1	Tefluthrin	14.43	0.997	0.011	0.035
2	Transfluthrin	15.38	0.998	0.009	0.028
3	Anthraquinone	16.26	0.998	0.012	0.037
4	Bioallethrin	17.37	0.999	0.034	0.103
5	Resmethrin 1	20.64	0.998	0.198	0.601
6	Resmethrin 2	20.76	0.998	0.01	0.029
7	Tetramethrin 1	21.22	0.996	0.131	0.395
8	Tetramethrin 2	21.35	0.999	0.003	0.01
9	Bifenthrin	21.37	0.999	0.003	0.01
10	Phenothrin 1	21.81	0.998	0.131	0.395
11	Phenothrin 2	21.93	0.997	0.011	0.034
12	Cyhalothrin, lambda-	22.52	0.999	0.008	0.024
13	Acrinathrin	22.72	0.998	0.01	0.032
14	Permethrin, cis-	23.36	0.998	0.008	0.023
15	Permethrin, trans-	23.51	0.998	0.008	0.024
16	Cyfluthrin 1	24.04	0.991	0.065	0.198
17	Cyfluthrin 2	24.14	0.991	0.065	0.198
18	Cyfluthrin 3	24.24	0.991	0.065	0.198
19	Cyfluthrin 4	24.28	0.991	0.065	0.198
20	Cypermethrin 1	24.4	0.996	0.062	0.187
21	Cypermethrin 2	24.51	0.996	0.062	0.187
22	Cypermethrin 3	24.6	0.996	0.062	0.187
23	Cypermethrin 4	24.64	0.996	0.062	0.187
24	Flucythrinate 1	24.64	0.998	0.012	0.037
25	Flucythrinate 2	24.86	0.998	0.012	0.037
26	Fenvalerate 1	25.46	0.997	0.011	0.034
27	tau-Fluvalinate 1	25.68	0.997	0.01	0.032
28	Fenvalerate 2	25.69	0.997	0.011	0.034
29	tau-Fluvalinate 2	25.74	0.997	0.01	0.032
30	Deltamethrin	29.3	0.998	0.009	0.028

5.5 Linearity, LOD and LOQ for GC-SICRIT-MS

Table 5.4 offers some insight into the analytical performance as well as characteristics of different compounds analysed through GC-SICRIT-MS. However, the key metrics here consist of linearity “(R²), LOD and LOQ”. From the table, it has can be seen that all the linearity values (R²) are above 0.990, which demonstrates an effective linearity in the calibration curve. This demonstrates that this method is reliable for quantifying compounds which are tested at the concentration ranges from 0.001 to 0.5 µg/mL. Of note, LOD and LOQ values vary depending upon the compounds, which reflect the sensitivity of the method for each analyte. It is important to keep in mind that lower LOD and LOQ values show increased sensitivity, meaning that the method is robust enough to detect as well as quantify only a small proportion of the compounds in the pesticide standard.

Table 5.4: Synthetic Pyrethroid with R 2, LOD and LOQ values using GC-SICRIT-MS

No	Component Name	Formula	R ²	LOD ppm	LOQ ppm
1	Tefluthrin	C ₁₇ H ₁₄ ClF ₇ O ₂	0.999	0.002	0.007
2	Transfluthrin	C ₁₅ H ₁₂ Cl ₂ F ₄ O ₂	0.999	0.003	0.009
3	Anthraquinone	C ₁₄ H ₈ O ₂	0.999	0.004	0.013
4	Bioallethrin	C ₁₉ H ₂₆ O ₃	0.998	0.008	0.026
5	Resmethrin 1	C ₂₂ H ₂₆ O ₃	0.993	0.098	0.297
6	Resmethrin 2	C ₂₂ H ₂₆ O ₃	0.998	0.010	0.031
7	Tetramethrin 1	C ₁₉ H ₂₅ NO ₄	0.998	0.101	0.305
8	Tetramethrin 2	C ₁₉ H ₂₅ NO ₄	0.999	0.013	0.038
9	Bifenthrin	C ₂₃ H ₂₂ ClF ₃ O ₂	0.999	0.005	0.015
10	Phenothrin 1	C ₂₃ H ₂₆ O ₃	0.997	0.127	0.384
11	Phenothrin 2	C ₂₃ H ₂₆ O ₃	0.998	0.045	0.138
12	Cyhalothrin, lambda-	C ₂₃ H ₁₉ ClF ₃ NO ₃	0.997	0.052	0.156
13	Acrinathrin	C ₂₆ H ₂₁ F ₆ NO ₅	0.998	0.087	0.264
14	Permethrin, cis-	C ₂₁ H ₂₀ Cl ₂ O ₃	0.997	0.055	0.168
15	Permethrin, trans-	C ₂₁ H ₂₀ Cl ₂ O ₃	0.998	0.087	0.265

The analytical description is an important step before beginning an ANOVA (Analysis of Variance) analysis for the LOD variable for understanding the data and hypothesis analysis. The table 5.5 provides a statistical description of the results of the LOD analysis.

Table 5.5: Descriptive statistics for LOQ of ITQMS and LTQMS

	N	Mean	Std. Deviation	Std. Error	95% Confidence Interval for Mean		Minimum	Maximum
					Lower Bound	Upper Bound		
GC-EI-MS	15	.0391	.06129	.01582	.0052	.0731	.00	.20
GC-SICRIT-MS	15	.0465	.04377	.01130	.0222	.0707	.00	.13
Total	30	.0428	.05246	.00958	.0232	.0624	.00	.20

The descriptive statistics for GC-EI-MS show equal detection limits with the average at 0.0391 and GC-SICRIT-MS has a 0.0465 average limit. Both methods demonstrate significant variation through their standard deviations which approach 0.061 and 0.044. The data ranges span from 0.00 to 0.20 for GC-EI-MS and from 0.00 to 0.13 for GC-SICRIT-MS indicating the methods detect low rates and high rates separately. The analysis using ANOVA would probably suggest that the detection limits of both GC-EI-MS and GC-SICRIT-MS are equivalent for this specific analyte since the mean values and confidence zones are parallel without any significant statistical variations.

Levene's test is a statistical test used to assess the homogeneity of variances between two or more sets of data as shown in table 5.6. This test relies on the basic assumption of analysis of variance (ANOVA).

Table 5.6: test of homogeneity of variances for LOD.

Levene Statistic	df1	df2	Sig.
.513	1	28	.480

The Levene's test results for homogeneity of variances from the LOD data appear in this table 5.6. The Levene statistic equals 0.513 while using degrees of freedom 1 and 28 to reach a p-value of 0.480. The test results indicate equal variances between the LOD method measurements since the obtained p-value exceeds 0.05. ANOVA parametric tests can be used acceptably to examine group mean differences because of this finding. After presenting Levene's test results for variable LOD, ANOVA results are provided to determine whether there are statistically differences between means. Table 5.7 shows the ANOVA result for two different systems.

Table 5.7: ANOVA results for LOD.

	Sum of Squares	df	Mean Square	F	Sig.
Between Groups	.000	1	.000	.142	.709
Within Groups	.079	28	.003		
Total	.080	29			

This ANOVA results show that there is no statistically significant difference in the LOD between the two methods, as indicated by a very high p-value of 0.709 (Sig.), which is well above the typical threshold of 0.05. The F-value of 0.142 is also very low, reinforcing that the variation between the groups (methods) is minimal compared to the variation within the groups. Specifically, the Sum of Squares for Between Groups is zero, indicating almost no difference in mean LOD, while the Within Groups sum of squares reflects variability among individual samples. Overall, this suggests that both methods have similar detection limits, and any observed differences are likely due to random variation rather than a true difference in performance.

After statistical analysis of the LOD, statistical analysis is also performed for the LOQ. It is a fundamental criterion in analytical chemistry. Assessing The LOQ and understanding this criterion are essential to ensuring the reliability of analytical results.

Descriptive analysis of the LOQ provides a solid foundation for understanding analytical performance and helps ensure that the result obtained are accurate and reliable. Table 5.8 provides a statistical description of the LOQ variable for ITQMS and LTQMS

Table 5.8: Descriptive statistics for LOQ of ITQMS, and LTQMS

	N	Mean	Std. Deviation	Std. Error	95% Confidence Interval for Mean		Minimum	Maximum
					Lower Bound	Upper Bound		
GC-EI-MS	15	.1187	.18534	.04785	.0160	.2213	.01	.60
GC-SICRIT-MS	15	.1411	.13237	.03418	.0678	.2144	.01	.38
Total	30	.1299	.15866	.02897	.0706	.1891	.01	.60

Two analytical methods GC-EI-MS and GC-SICRIT-MS produced comparable LOQ values as their measurements matched closely in average with 0.1187 and 0.1411 respectively and shared overlapping confidence range therefore their qualitative performance levels were similar. Each analytical method possesses high standard deviations that represent individual measurement variation across both GC-EI-MS and GC-SICRIT-MS. GC-EI-MS exhibits a marginally increased variability. The ANOVA analysis would show no important variation between LOQ values from both methods because the obtained confidence intervals and comparable means suggest analogous detection sensitivity for the analyte.

Levene’s test used before conducting an ANOVA to determine whether this analysis can be used correctly. Table 5.9 contains test of homogeneity of variances

Table 5.9: test of homogeneity of variances for LOQ.

Levene Statistic	df1	df2	Sig.
.508	1	28	.482

Levene's test results for homogeneity of variances appear in this table regarding the LOQ data. The Levene statistic reaches 0.508 while its degrees of freedom equate to 1 and 28 and its resulting p-value equals 0.482. The p-value of 0.482 exceeds 0.05 so the LOQ variances between methods show no significant difference thus satisfying the requirement for equal variances. A valid parametric analysis through ANOVA is possible to establish mean LOQ comparisons between methods because the data variances show homogeneity.

Using analysis of variance (ANOVA) allows to compare the means of two groups to determine if there are significant differences between them, as shown in table 5.10.

Table 5.10: ANOVA results for LOQ.

	Sum of Squares	df	Mean Square	F	Sig.
Between Groups	.004	1	.004	.145	.706
Within Groups	.726	28	.026		
Total	.730	29			

The ANOVA results indicate that LOQ measurements between methods lack statistical significance. The F-value measurement of 0.145 together with the p-value (Sig.) value of 0.706 shows that LOQ variations between the procedures are unimportant for statistical analyses. A very small difference exists between group mean LOQ values because the between-group sum of squares (.004) is low; most variance stems from individual sample variations hence the higher within-group sum of squares (.726) shows. The sensitivity levels between the two methods remain similar since they produce equivalent results for their limits of quantification values.

5.6 Ionisation and Fragmentation Behavior of Pyrethroids EI and SICRIT

It has been found that pyrethroids presented in EI spectra are highly fragmented where the molecular ion is lacking and ions correspond towards lower mass fragments of the molecules where most often seen; these fragments tended to be common to other pyrethroids. The effective use of non-specific fragment ions can act to make identification of the compound more complex but can be a useful feature for quantification should a triple quadrupole be available. As an example, Bifenthrin, $C_{23}H_{22}ClF_3O_2$ (MW=422.8); Cyhalothrin, lambda, $C_{23}H_{19}ClF_3NO_3$ (MW=449.85); Acrinathrin, $C_{26}H_{21}F_6NO_5$ (MW=541.44); Cypermethrin, $C_{22}H_{19}Cl_2NO_3$ (MW=416.3); Deltamethrin, $C_{22}H_{19}Br_2NO_3$ (MW=505.2) are different pyrethroids but all show the same dominant fragment ion at m/z 181($C_{13}H_9O$)⁺ in their GC-MS spectra.

SICRIT is a softer ionization method that can produce the molecular radical ion ($M^{+\bullet}$) and protonated molecule ($[M + H]^+$) this is the opposite of what happens with a traditional method where the molecular radical ion ($M^{+\bullet}$) is often absent such as in Electron Impact ionization (EI). This behavior, when using N_2 as makeup gas, is rationalized by the formation of nitrogen plasma by the dielectric barrier discharge (DBD); the plasma then ionizes the analyte without excessive fragmentation. The majority of pyrethroids detected using SICRIT ionization, transfluthrin, anthraquinone, bioallethrin, resmethrin1, resmethrin2, tetramethrin1, tetramethrin 2, bifenthrin, phenothrin 1, phenothrin 2, cyhalothrin, lambda-, acrinathrin, permethrin, *cis*- and permethrin, *trans*- showed $[M + H]^+$ ions. The prevalence for the protonation could be due to the presence of water vapor in the source which would encourage the development of protonated molecule rather than molecular ion. Table 5.5 summarize the ionization results of the pyrethroids detected using GC-EI-MS and GC-SICRIT-MS.

Table 5.11: Ionisation Mechanism and Mass Spectrometry Results

Component Name	GC-EI-MS	GC-SICRIT-MS
Tefluthrin	177-197-141-127	419.0690
Transfluthrin	163-91-127-334	371.0252
Anthraquinone	152-180-208	209.0617
Bioallethrin	123-81-136-91-93	303.1985
Resmethrin 1	143-123-171-81-115-128	339.1986
Resmethrin 2	128-143-171-123-115-81	339.1978
Tetramethrin 1	164-77-107-135	332.1883
Tetramethrin 2	164-135-107-81	332.1880
Bifenthrin	181-166	422.1288
Phenothrin 1	183-123-165-81	351.1995
Phenothrin 2	183-123-165-81	351.1990
Cyhalothrin, lambda-	141-181-197-161-208	450.1134
Acrinathrin	181-93-208-289-152-541	541.1373
Permethrin, cis-	183-165-127-391	390.0822
Permethrin, trans-	183-165-127-391	390.0784
Cyfluthrin 1	206-199-91-163-127-226	N/A
Cyfluthrin 2	206-91-127-163-199-165-226-434	N/A
Cyfluthrin 3	206-91-127-199-163-165-226-435	N/A
Cyfluthrin 4	206-127-91-163-165-226	N/A
Cypermethrin 1	181-127-91-163-209-152-415	N/A
Cypermethrin 2	181-127-163-91-209	N/A
Cypermethrin 3	91-127-163-209	N/A
Cypermethrin 4	91-127-163-209	N/A
Flucythrinate 1	157-199-107-451	N/A
Flucythrinate 2	157-199-107-451	N/A
Fenvalerate 1	225-125-167-119-419	N/A
tau-Fluvalinate 1	250-252-502-55	N/A
Fenvalerate 2	225-125-167-119-419	N/A
tau-Fluvalinate 2	250-252-502-55	N/A
Deltamethrin	181-252.8-172-152-93	N/A

Table 5.5 offered an effective comparison of the ionisation mechanism and ion forms for different types of pyrethroid compounds, which have been analysed with the help of different mass spectrometry techniques such as GC-EI-MS and GC-SICRIT-MS. From the table, it can be seen that GC-EI-MS favours significant ion fragments, which offered detailed information about different molecular structures, as it is helped to identify the different compounds depending upon fragmentation patterns. For instance, Anthraquinone (Exact Mass 208.0524 Da) produces ion fragments with m/z values of 152, 180, and 208. Conversely, GC-SICRIT-MS shows a single protonated molecular ion (m/z 209.0617). Thus, SICRIT ionisation is beneficial for accurate mass detection and determination of different molecular ion, Figure 5.7.

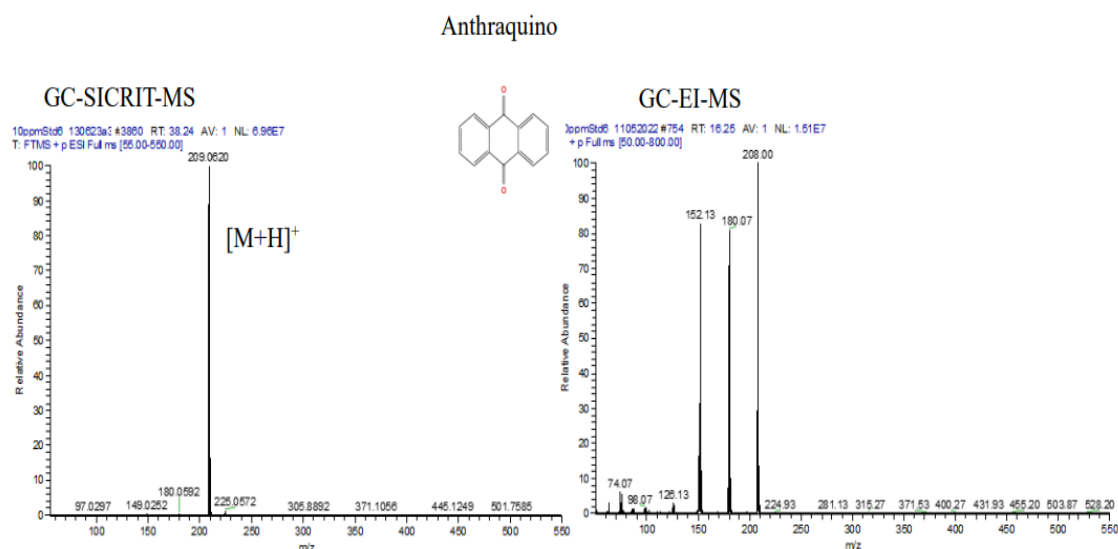


Figure 5.7: EI-MS and SICRIT-MS spectra (positive ionization mode) anthraquinone (m/z 208.22) (see table 5.5) at 10ppm, analyzed by GC-SICRIT- LTQ Orbitrap mass spectrometer and GC-EI-ITQMS

It is generally true that SICRIT ionisation showed mainly molecular or pseudo-molecular ions, but for a few compounds significant fragmentation was seen, Figure 5.8.

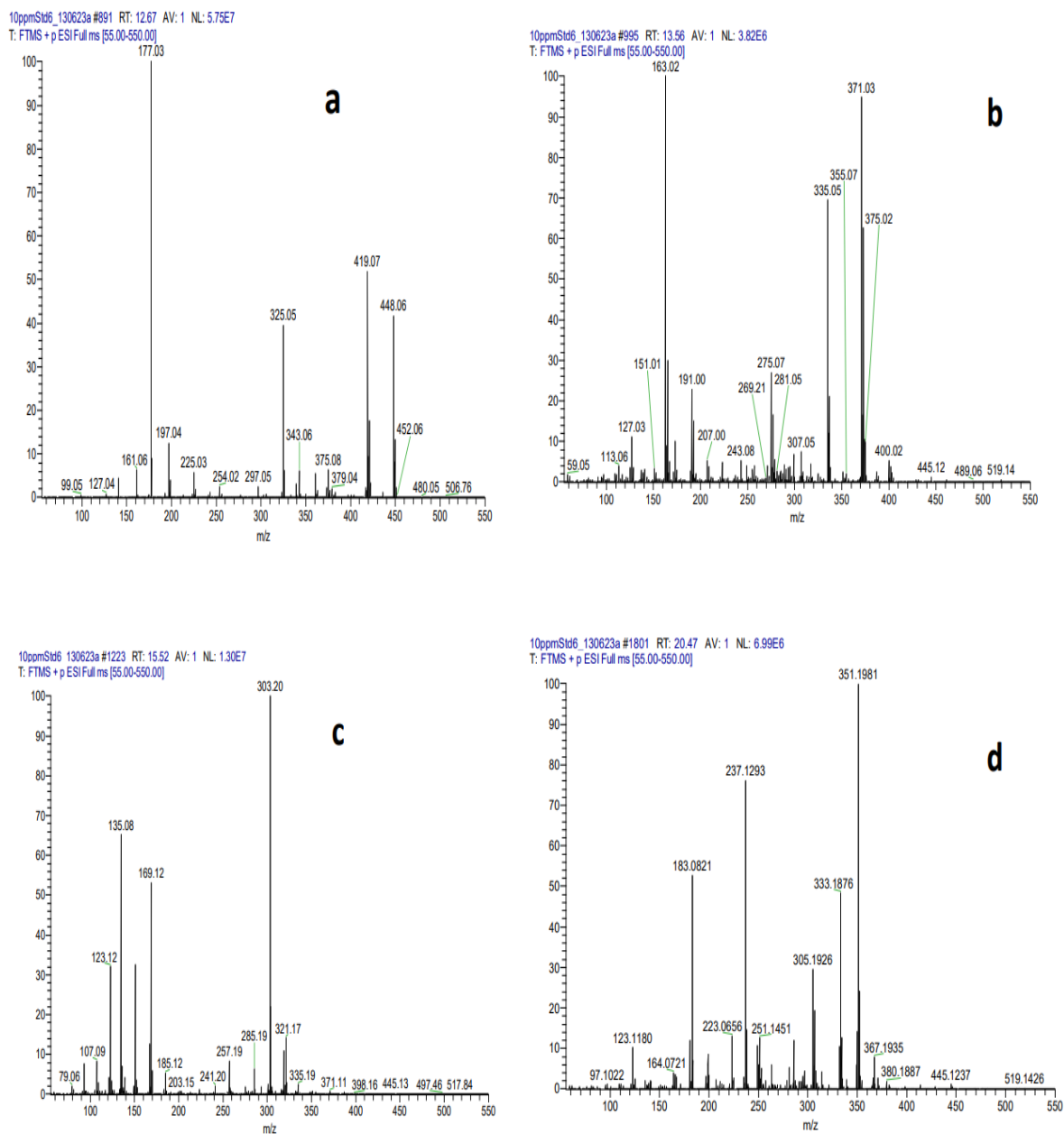


Figure 5.8: Examples of ionization of some pyrethroid pesticides using GC-SICRIT-MS. where: (a) Tefluthrin, (b) Transfluthrin, (c) Bioallethrin, and (d) Phenothrin (see table 5.5) at 10ppm, analyzed by GC-SICRIT- LTQ Orbitrap mass spectrometer.

5.7 Matrix Effect evaluation of multiple Pyrethroids pesticide residues in selected baby food matrices (milk, rice and cereal)

Table 5.12: Matrix effect on baby food samples based on GC-SICRIT-LTQMS and GC-ITQMS.Matrix

Component Name	GC-EI-MS			GC-DBDI-MS		
	Milk	Rice	Cereal	Milk	Rice	Cereal
Tefluthrin	300%	178%	347%	-90%	-76%	-80%
Transfluthrin	390%	145%	404%	-87%	-77%	-82%
Anthraquinone	271%	98%	348%	-99%	-70%	-79%
Bioallethrin	397%	189%	378%	-90%	-80%	-89%
Resmethrin	578%	282%	349%	-94%	-71%	-83%
Tetramethrin	397%	225%	270%	-91%	-79%	-82%
Bifenthrin	376%	278%	371%	-94%	-81%	-82%
Phenothrin	649%	338%	295%	-94%	-71%	-79%
Cyhalothrin, lambda-	377%	140%	292%	-88%	-70%	-78%
Acrinathrin	496%	189%	180%	-88%	-72%	-83%
Permethrin, cis-	478%	140%	225%	-90%	-77%	-75%
Permethrin, trans-	434%	278%	278%	-90%	-80%	-90%
Cyfluthrin	225%	180%	238%	N/A	N/A	N/A
Cypermethrin	580%	225%	411%	N/A	N/A	N/A
Flucythrinate	496%	278%	334%	N/A	N/A	N/A
Fenvalerate	434%	271%	390%	N/A	N/A	N/A
tau-Fluvalinate	404%	282%	397%	N/A	N/A	N/A
Deltamethrin	409%	178%	376%	N/A	N/A	N/A

Through the measured data as shown in table 5.12 that the three examined food materials (milk along with rice and cereal) bring significant changes to the detection results obtained by GC-EI-MS and GC-DBDI-MS instruments. The positive matrix effects measured in GC-EI-MS vary from 98% to greater than 649%. The results from actual experiments show strong enhancement effects caused by fats and sugars and proteins existing within samples to create false signal amplitude readouts. The effects of milk in this experiment are particularly poor because its ionization values rise above 600% which indicates how significantly matrix ingredients impact ionization during the process. The enhancement poses a risk of inaccurate analyte quantification so matrix-matched calibration or internal standard methods should be used to achieve accurate results. Within GC-DBDI-MS operations the impact of matrix components appears mainly negative and ranges between -70% to -99%. The major suppression of ion signals through matrix components creates significant problems for detecting analytes in these conditions. The signal measurement in milk shows a substantial decrease of -90% which makes analyte level measurement inaccurate because it falls significantly below a clean system signal. The two analytical techniques behave differently for sample matrices because GC-EI-MS enhances signals but GC-DBDI-MS produces signal suppression. The measurement accuracy depends on matrix effects which show different responses between different matrices thus validating methods must include matrix-effect correction protocols. Specified bias during analysis demands strict awareness to minimize bias using methods including matrix-matched standards and internal standards as well as sample dilution. Mass spectrometric processes show high sensitivity to experimental matrices so researchers must develop strict correction protocols because they aim to achieve reliable and reproducible results for difficult food analysis.

5.8 Comparison of Compounds Preferred for Analysis Using EI or SICRIT

The methodology was applied to 18 parent compounds and their isomers, including the Type I and Type II of pyrethroid pesticides. Figure 5.10 illustrates the sensitivity of these techniques for detecting the selected pyrethroids with their isomers, while GC-SICRIT-MS offers improved sensitivity for many pyrethroid pesticides, it has limitations in detecting compounds that eluted late in GC-EI-MS. The choice between these techniques would depend on the specific compounds of interest and the required sensitivity.

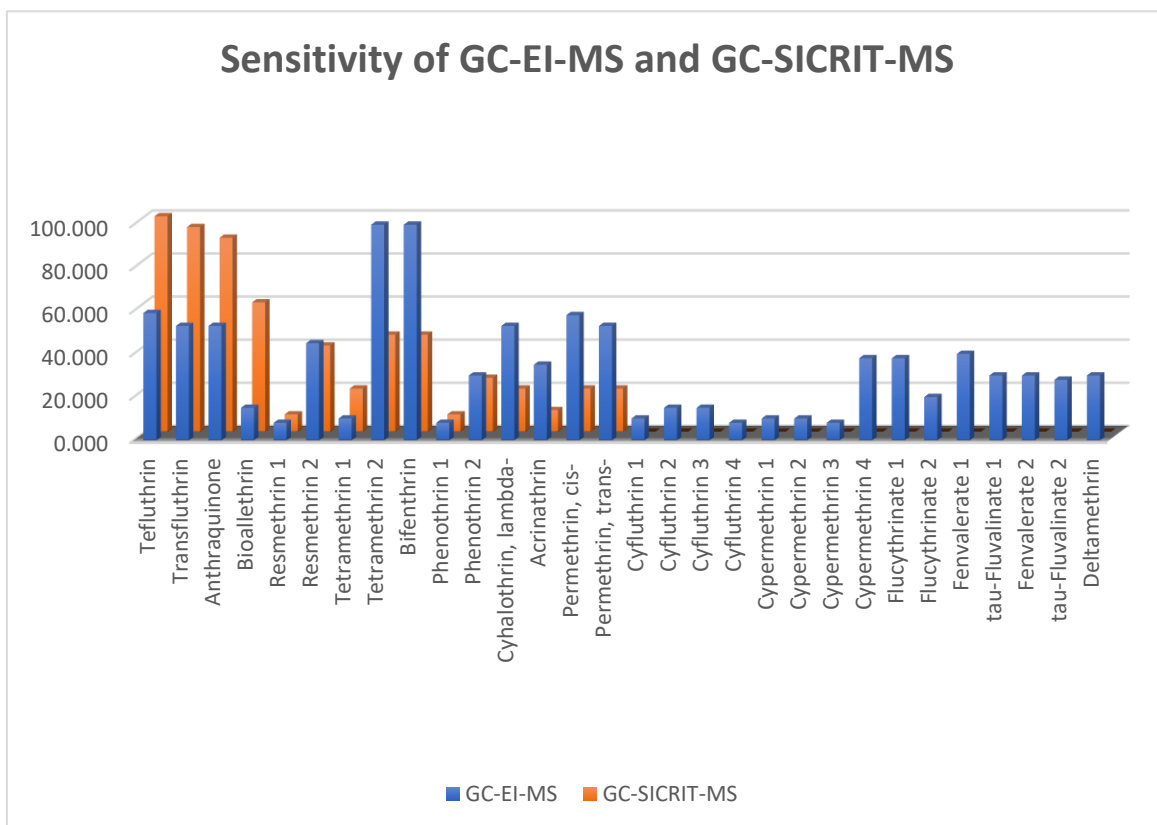


Figure 5.9: Summary of Sensitivity for GC-EI-MS and GC-SICRIT-MS

6. Determination of Organochlorin Pesticide Residues in Baby Food and Infant Formula using GC-MSD

6.1 Introduction

Organochlorine pesticides (OCPs) are classified as persistent pollutants because of their long-lasting presence in the environment. Such types of pesticides not only affect the hormonal and reproductive systems of humans and animals but also lead to other adverse health effects.^{150,151} Despite significant restrictions imposed by the Stockholm Convention on Persistent Organic Pollutants in 2004, OCPs are still found in food samples.^{152,153} OCPs have been detected in cereal crops such as wheat, corn, and cowpea, which are used to produce cereal-based complementary foods.^{154,155} Dietary intake is a major route of exposure to these pesticides, especially for children.^{156,157} Due to their higher metabolic rate and energy needs, children consume more food per kilogram of body weight than adults, making them more vulnerable to contaminated foods.^{158,159}

To evaluate the amounts of major and trace elements, as well as various chemical compounds in baby food and formula, many techniques have been employed. Due to their chemical stability, which results in them persisting and bioaccumulating in the environment and animal tissues, their presence raises the risk of health problems for humans. Exposure to OCPs in children has been linked to various adverse health outcomes, including Parkinson's-like symptoms, delayed puberty, childhood cancer, and neurological and endocrine disorders.¹⁶⁰

In this study, a mixture of 40 organochlorine pesticides (OCPs) was purchased (see table 6.1) with a concentration of 100 µg/mL in toluene, which was diluted to 10 µg/mL in acetonitrile for analysis. This analytical method consists of a gas chromatography, for separation and Mass Spectrometry for detection. Development of a GC method was complicated due to the use of a number of different GC instruments supplied by two different manufacturers, the methods for the analysis of organochlorine pesticides were developed using GC-FID, GC-EI-ITQMS, GC-EI-MSD, and GC-SICRIT-LTQMS, by making adjustments to the GC parameters such as run time, temperature settings, column type and liner type, etc, as mentioned in the methodology chapter.

Table 6.1: Compounds obtained through chromatography separation in GC-ITQMS, and GC-MSD.

Peaks no	COMPONENT NAME	Formula
1	Chloroneb	C ₈ H ₈ Cl ₂ O ₂
2	Pentachlorobenzene	C ₆ HCl ₅
3	BHC, alpha-	C ₆ H ₆ Cl ₆
4	Hexachlorobenzene	C ₆ Cl ₆
5	Pentachloroanisole	C ₇ H ₃ Cl ₅ O
6	BHC, beta-	C ₆ H ₆ Cl ₆
7	BHC, gamma-	C ₆ H ₆ Cl ₆
8	BHC, delta-	C ₆ H ₆ Cl ₆
9	Endosulfan ether	C ₉ H ₆ Cl ₆ O
10	Heptachlor	C ₁₀ H ₅ Cl ₇
11	Pentachlorothioanisole	C ₇ H ₃ Cl ₅ S
12	Aldrin	C ₁₂ H ₈ Cl ₆
13	Dichlorobenzophenone, 4,4'-	C ₁₃ H ₈ Cl ₂ O
14	Fenson	C ₁₂ H ₉ ClO ₃ S
15	Isodrin	C ₁₂ H ₈ Cl ₆
16	Heptachlor epoxide	C ₁₀ H ₅ Cl ₇ O
17	Chlorbenside	C ₁₃ H ₁₀ Cl ₂ S
18	Chlordane, trans-	C ₁₀ H ₆ Cl ₈
19	DDE, o, p'-	C ₁₄ H ₈ Cl ₄
20	Endosulfan I	C ₉ H ₆ Cl ₆ O ₃ S
21	Chlordane, cis-	C ₁₀ H ₆ Cl ₈
22	Nonachlor, trans-	C ₁₀ H ₅ Cl ₉
23	Chlorfenson	C ₁₂ H ₈ Cl ₂ O ₃ S
24	DDE, p,p'-	C ₁₄ H ₈ Cl ₄
25	Dieldrin	C ₁₂ H ₈ Cl ₆ O
26	DDD, o,p'-	C ₁₂ H ₈ Cl ₆ O
27	Ethylan	C ₁₈ H ₂₀ C ₁₂
28	Endrin	C ₁₂ H ₈ C ₁₆ O
29	Endosulfan II	C ₉ H ₆ Cl ₆ O ₃ S
30	DDD, p,p'-	C ₁₄ H ₁₀ Cl ₄
31	DDT, o,p'-	C ₁₄ H ₉ Cl ₅
32	Nonachlor, cis-	C ₁₀ H ₅ Cl ₉
33	Endrin aldehyde	C ₁₂ H ₈ Cl ₆ O

34	4,4'-Methoxychlor olefin	C ₁₆ H ₁₄ Cl ₂ O ₂
35	Endosulfan sulfate	C ₉ H ₆ Cl ₆ O ₄ S
36	DDT, p,p'-	C ₁₄ H ₉ Cl ₅
37	2,4'-Methoxychlor	C ₁₆ H ₁₅ Cl ₃ O ₂
38	Endrin ketone	C ₁₂ H ₈ Cl ₆ O
39	Tetradifon	C ₁₂ H ₆ Cl ₄ O ₂ S
40	Mirex	C ₁₀ Cl ₁₂

6.2 Chromatographic separation in GC-FID, GC-EI-ITQMS, GC-EI-MSD and GC-SICRIT-LTQMS.

The chromatographic separation helps to resolve a mixture of substances through different interactions with a stationary material. In this study, chromatographic separation was carried out using a number of different devices to enable a comparison of ionization sources and chromatographic efficiency as the main aims and objectives of this research.

Gas Chromatography-Flame Ionization Detection (GC-FID) is one of the many analytical approaches which is routinely used for analysing mixtures of different volatile components. The FID detector is known as being a good detector for a wide range of different compounds and is sensitive enough for detection and quantification of organic compounds like pesticides in food with the sensitivity required for this study. However, it is important to keep in mind that FID detection says nothing about the identity of the molecule being detected and as a result a mass spectrometer is needed if structural verification of compounds is a requirement. Both an FID and a mass spectrometer are able to detect OCPs at a concentration of 10 ppm. Initial experiments began with an evaluation of in-house GC-FID system for the detection organochlorine pesticides. This is complicated somewhat by the inability to identify the individual compounds leading to a tentative assignment based on the manufacturer's elution profile.

Figure 6.2 represents the chromatographic conditions using a ThermoFisher Gas Chromatography-Flame Ionization Detector (GC-FID) system for the 40 targeted OCPs. The peaks represented by numbers point to the different pesticides as shown in table 6.1. Although the pesticides are well separated with almost all the compound's peaks baseline resolved. There are some overlapping peaks, which is normally expected in the case of compound mixtures. For example, peaks 28 and 29 correspond to endrin ($C_{12}H_8Cl_6O$) and endosulfan II ($C_9H_6Cl_6O_3S$), respectively. Figure 6.1 shows the structure of both compounds, the difference being the presence of sulfur in endosulfan II, which is absent in endrin, their retention times are close enough to cause overlapping peaks.

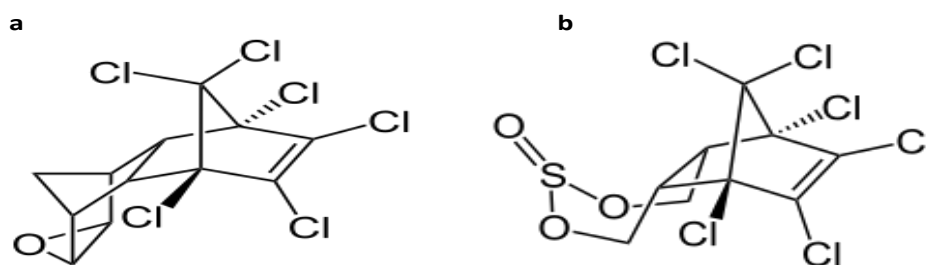


Figure 6.1: Structures of (a)endrin and (b)endosulfan II

The optimised GC-FID protocol showed baseline resolution of almost all of 40 pesticides in the mixture at a concentration of 10 ppm as shown in figure 6.2, which offered reproducible and sensitive results. However, whilst the GC-FID could efficiently separate and detect the pesticides in this mixture it cannot offer detailed structural information or differentiate between isomers; an exception would arise if individual samples of all 40 compounds were available to perform matching based on retention times. Hence, mass spectrometry (GC-MS) is needed to assign names to the detected compounds on the basis of the recorded m/z and any identified fragments. This additional information does allow structural assignment in most cases, but assignment of structures to isobaric isomers can still prove to be a difficult challenge for accurate determination.

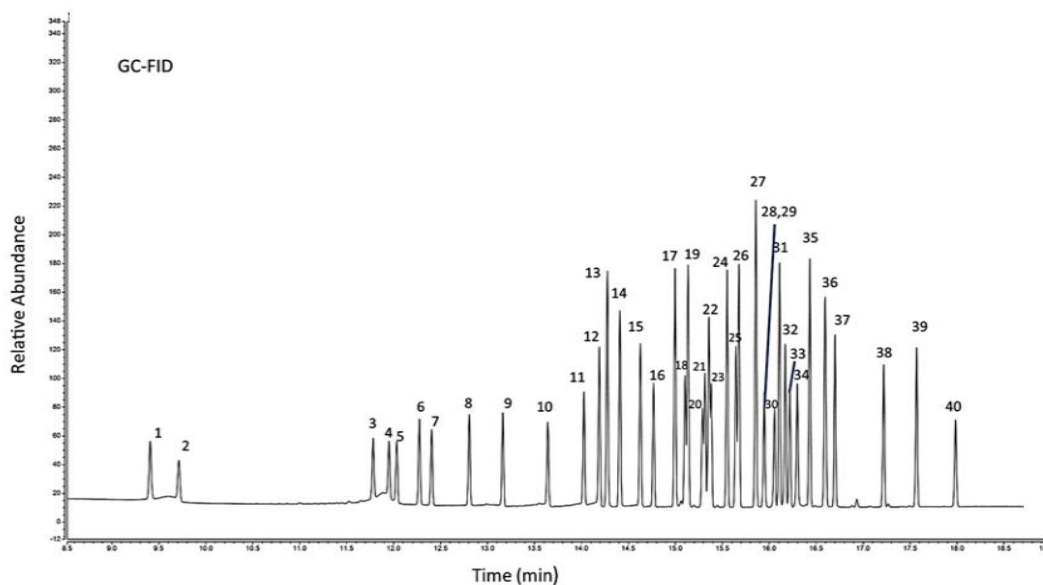


Figure 6.2: GC-FID Chromatogram of a mixture of 40 organochlorine pesticides (compounds identity in table 6.1) at 10ppm.

The chromatogram in figure 6.3 was obtained using a GC-EI-ITQMS instrument and demonstrates good chromatographic separation where each peak corresponds to an organochlorine pesticide. Using mass spectrometer, the compounds were identified by reporting the mass spectrum for each compound. Although GC-EI-ITQMS was used, it gave the same chromatogram. Peak 27, which represents ethylan ($C_{18}H_{20}Cl_2$) in both instruments, is the highest peak, indicating that both detectors have high sensitivity to ethylan. In addition to the presence of some overlapping peaks as in GC-FID chromatogram. In general, the separation using GC-ITQMS is better than GC-FID, although the retention time of pesticides in GC-FID is less than GC-ITQMS. The chromatography of peaks 1 and 2 representing chloroneb ($C_8H_8Cl_2O_2$) and pentachlorobenzene (C_6HCl_5) respectively, are very good separation with sharp peaks in GC-ITQMS, but in GC-FID the chromatography of these compounds shows broader peaks. Also, for the following compounds: BHC, alpha-, Hexachlorobenzene, Pentachloroanisole, BHC, beta-, BHC, gamma-, BHC, delta-, Endosulfan ether, Heptachlor, and Pentachlorothioanisole, representing peaks 3 to 11 respectively.

The main aspect of using mass spectrometry is that it offers valuable information regarding the molecular structure of compounds including the molecular weight (from the m/z reported by the MS detector) as well as fragmentation patterns. This data is effective in confirming the identity of detected pesticides. The above GC/MS trace were confirmed through the analysis of standards of pesticides (10 ppm) using GC/EI-MS, which provide the same peaks.

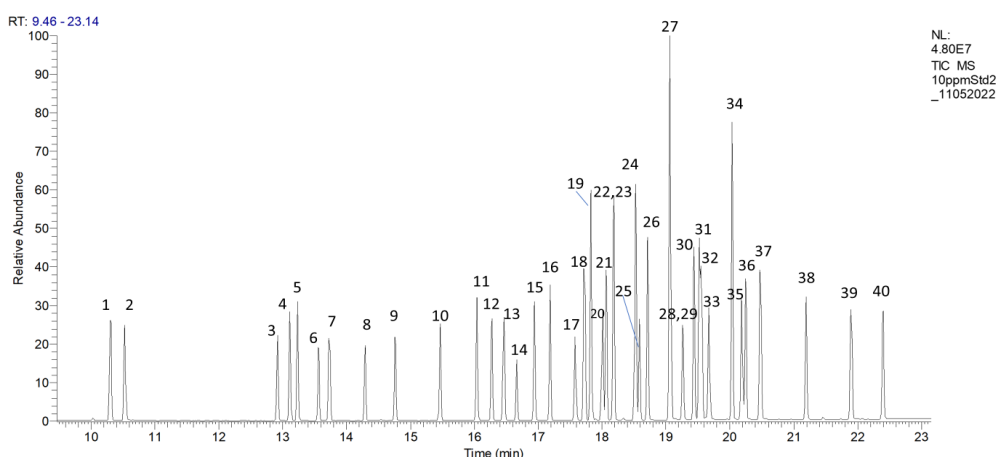


Figure 6.3: GC-EI-ITQ TIC-MS Chromatogram of a mixture of 40 organochlorin pesticides (compounds identity in table 6.1) at 10ppm

Gas chromatography with mass selective detection (GC-MSD) is a variation on the routine GCMS mode of operation where the quad allows all ions to pass through in scanning mode. GC-MSD has the GC elution time broken up into multiple time segments where, in each segment, the quad is programmed to allow only ions of a certain mass to pass through to the detector. This would essentially produce a different chromatogram, largely similar to that of a full scan acquisition, but with the possibility enhanced sensitivity/selectivity. The chromatograms obtained from GC-MSD can be found in figure 6.4. The chromatogram obtained from OCPs analysis using GC-MSD is clearly different from GC-FID and GC-ITQMS, as they differed in terms of the intensity of the peaks, indicating the difference in the sensitivity of the GC-MSD detector to these pesticides for example, peaks 1, 2, 4, and 5 represent chloroneb, pentachlorobenzene, hexachlorobenzene, and pentachloroanisole respectively, appear as very high and sharp peaks, unlike what appears in GC-FID and GC-ITQMS. Although the peaks of pesticides

are appearing in the same order in the GC-FID and GC-ITQMS chromatography, their order is slightly different using GC-MSD such as hexachlorobenzene, pentachloroanisole, and BHC, beta- representing peaks 4,5, and 6 as shown in figure 6.1, 6.2, and 6.3. The total running time in GC-MSD appears to be longer than GC-ITQMS, hence the difference in retention time for each compound. This is due the difference in type of column used for both and the type of liner which are mentioned in the methodology chapter. Table 6. 1 summarizes pesticides studied with their quantification.

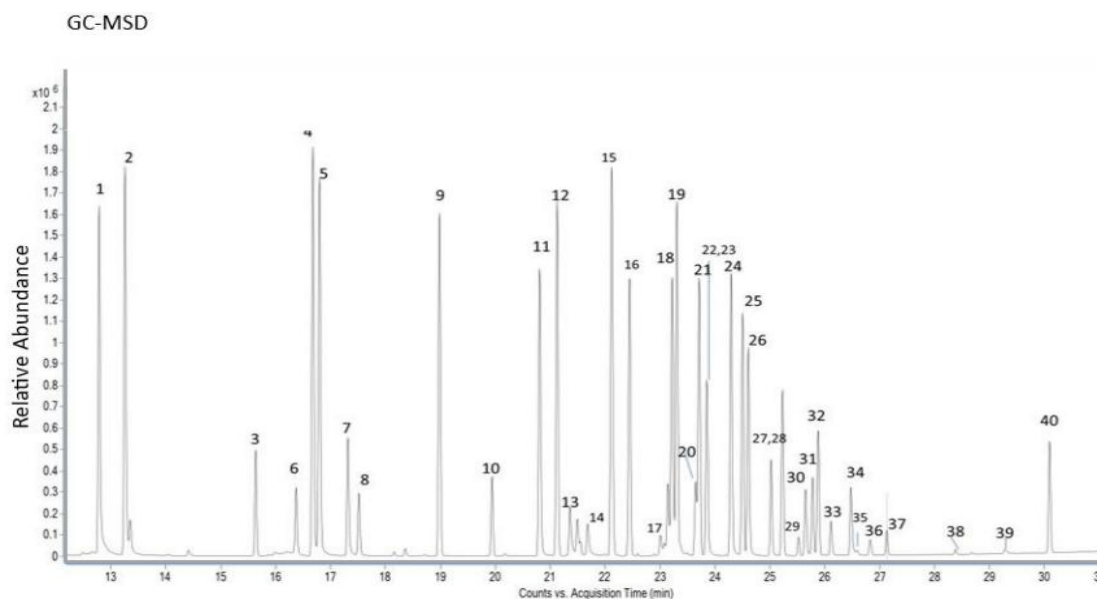


Figure 6.4: GC-EI-MSD Chromatogram of a mixture of 40 organochlorin pesticides (compounds identity in table 6.1) at 10ppm.

When comparing GC chromatograms from different systems, the results of the separation may differ and some compounds may be absent for several reasons, the most important of which is the efficiency of ionization of a particular pesticide when ionised using EI, which is what is shown in this study. Using the same standards previously analysed by GC-EI-MS, the OCPs were also analysed using a GC-SICRIT-MS setup in positive mode (Figure 6.6), 10 compounds were absent as shown in table 6.2. Analysis using negative mode was used but none of the compounds missing from the positive mode ionisation were seen when the polarity was switched (Figure 8-3 of the Appendix). The need for method development of the SICRIT MS in negative mode remains to be explored. The lack of detection may be due to the structural type of the organochlorine pesticides as all lindane compounds were observed to be absent using SICRIT as ion source, in addition all chlordane compounds as well as pentachlorobenzene and mirex were absent. (figure 6.5). Lindane is the gamma enantiomer of hexachlorocyclohexane, Different isomers of

lindane (BHC, alpha-, BHC, beta-, BHC, gamma- and BHC, delta-) are formed during photochemical chlorination of benzene using UV light.¹⁶¹

Chlordane has 140 isomers, the three isomers of chlordane that are commercially available are *cis*-chlordane, *trans*-chlordane, and *trans*-norchlordane.¹⁶²

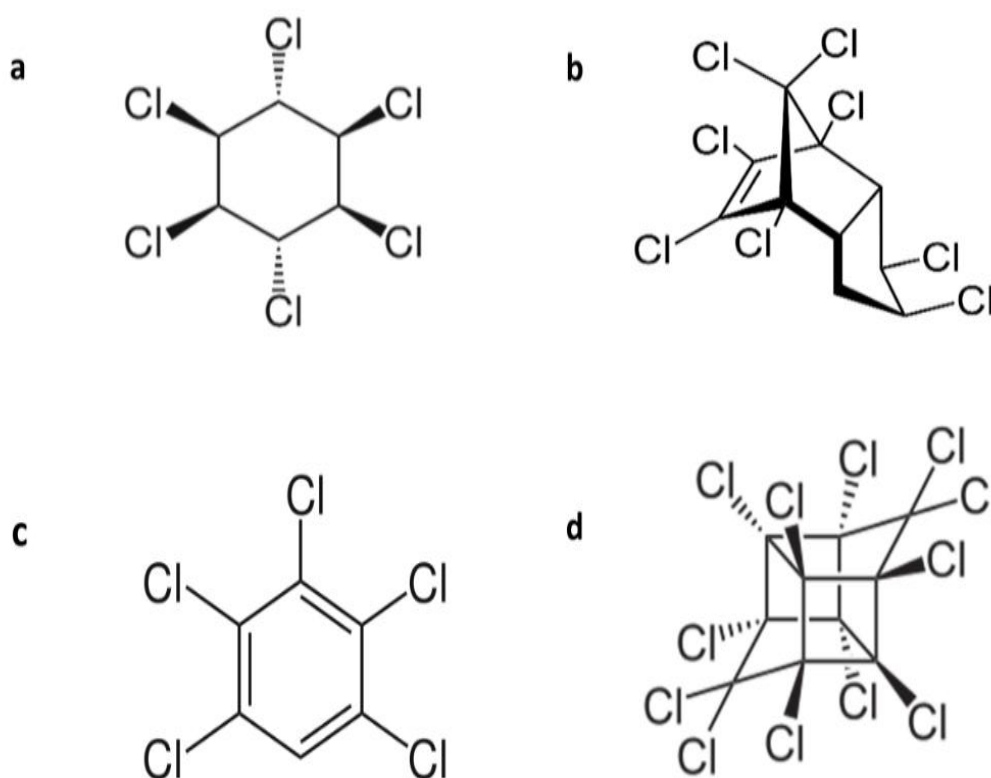


Figure 6.5: Chemical structure of different organochlorine pesticide (a) Lindane, (b) Chlordane, (c) Pentachlorobenzene and (d) Mirex.

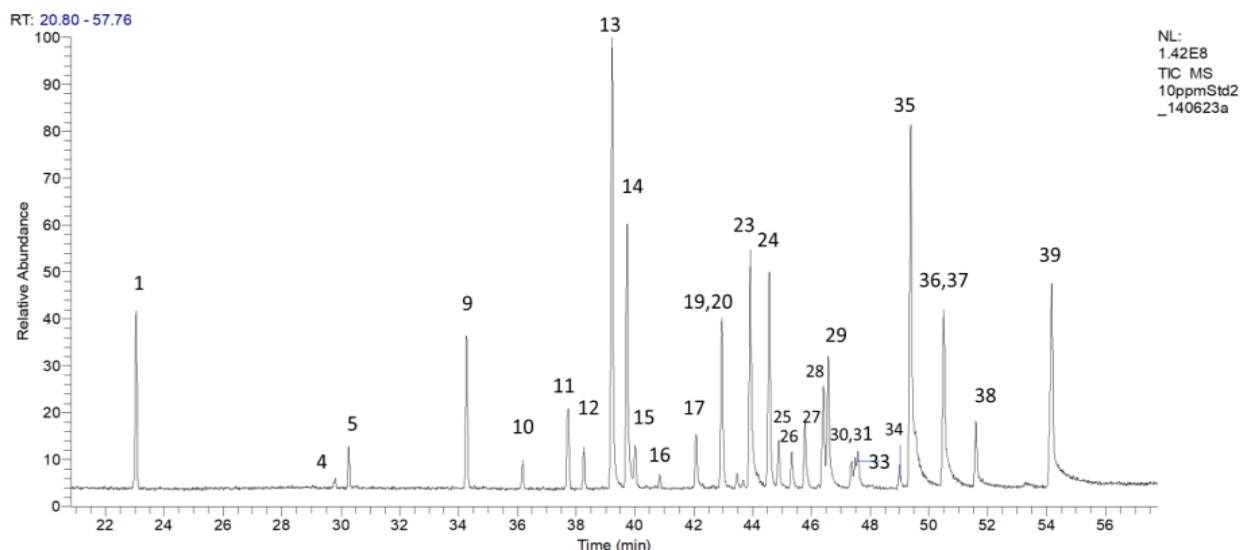


Figure 6.6: GC-SICRIT-LTQMS Chromatogram of organochlorin pesticides (compounds identity in table 6.1) at 10ppm.

Figure 6.6 shows the chromatogram obtained from a ThermoScientific GC coupled to a Plasmion SICRIT ionization source with MS analysis from a ThermoScientific Orbitrap XL (GC-SICRIT-LTQMS) in positive mode. The separation as well as detection of different compounds took significantly longer ~50 minutes compared to GC-FID, GC-ITQMS and GC-MSD studies, due to the chromatographic conditions. Not all OCPs compounds were resolved, with 30 out of 40 compounds detected, Peaks 2, 3, 6, 7, 8, 18, 21, 22, 32, and 40 were detected in GC-EI-MS instruments and numbered in their chromatogram, but with SICRIT these peaks were not detected as shown in chromatogram (Figure 6.6). Many of the compounds detected using GC-SICRIT-LTQMS have a lower response than those detected using previous GC instruments, in addition to the later eluting compounds (13-39) show broader, tailing chromatography.

6.3 Mass Spectrometry Results.

After confirming the separation capabilities, we focused on understanding the ionization mechanisms, particularly comparing SICRIT (Soft Ionization by Chemical Reaction in Transfer) with conventional Electron Impact (EI) ionization. Table 3.2 provides a comprehensive comparison of the ions observed in the GC-EI-MS and GC-SICRIT-MS spectra for detected pesticide. It details molecular formula, and the primary ions observed in each method. A key finding is that most compounds analysed using SICRIT ionised predominantly as $[M+H]^+$ ions and M^+ . In contrast, EI typically results in more extensive fragmentation.

Table 6.2: List of OCP compounds analyzed, by GC-EI-MS and GC-SICRIT-MS

Peaks	Component Name	Exact Mass	Formula	ion form	GC-EI-MS	Ion form	GC-SICRIT-MS
1	Chloroneb	205.9901	C ₈ H ₈ Cl ₂ O ₂	frg	191,206,113,141	M+	205.9918
2	Pentachlorobenzene	249.8491	C ₆ HCl ₅	frg	250,215,179,142		N/A
3	BHC, alpha-	289.8571	C ₆ H ₆ Cl ₆	frg	181,183,219,145		N/A
4	Hexachlorobenzene	283.8101	C ₆ Cl ₆	frg	284,249,214	M+	283.8123
5	Pentachloroanisole	279.8597	C ₇ H ₃ Cl ₅ O	frg	265,267,280,237,239	M+	279.8618
6	BHC, beta-	289.8571	C ₆ H ₆ Cl ₆	frg	181,183,219,145,109		N/A
7	BHC, gamma-	289.8571	C ₆ H ₆ Cl ₆	frg	183,181,219,145,109		N/A
8	BHC, delta-	289.8571	C ₆ H ₆ Cl ₆	frg	183,181,219,145,109		N/A
9	Endosulfan ether	341.8520	C ₉ H ₆ Cl ₆ O	frg	241,272	M+H	342.8627
10	Heptachlor	371.818	C ₁₀ H ₅ Cl ₇	frg	274,100,65,237,235,270,272	frg	337,339,335,371
11	Pentachlorothioanisole	295.8368	C ₇ H ₃ Cl ₅ S	frg	263,298,193,191,66	M+H	296.8484
12	Aldrin	363.8727	C ₁₂ H ₈ Cl ₆	frg	263,298,193,191	frg	293,291,295,328
13	Dichlorobenzophenone, 4,4'-	249.995	C ₁₃ H ₈ Cl ₂ O	frg	139,111,75	M+H	251.0051
14	Fenson	267.9960	C ₁₂ H ₉ ClO ₃ S	frg	77,141,268	M+H	269.0069
15	Isodrin	363.8727	C ₁₂ H ₈ Cl ₆	frg	193,261,123	M+	363.8774
16	Heptachlor epoxide	387.8130	C ₁₀ H ₅ Cl ₇ O	frg	353,351,263,193	frg	353,355,389
17	Chlorbenside	267.9880	C ₁₃ H ₁₀ Cl ₂ S	frg	125,89,268	frg	125,127,268.00
18	Chlordane, trans-	409.7918	C ₁₀ H ₆ Cl ₈	frg	373,375,264,272		N/A
19	DDE, o, p'-	317.9350	C ₁₄ H ₈ Cl ₄	frg	246,316,318,176	M+	317.9383
20	Endosulfan I	405.8139	C ₉ H ₆ Cl ₆ O ₃ S	frg	241,195,159	M+H	406.7830

21	Chlordane, cis-	409.7918	C ₁₀ H ₆ Cl ₈	frg	375,377,266,237		N/A
22	Nonachlor, trans-	443.7528	C ₁₀ H ₅ Cl ₉	frg	409,300		N/A
23	Chlorfenson	301.9571	C ₁₂ H ₈ Cl ₂ O ₃ S	frg	111,175,113	M+H	302.9966
24	DDE, p,p'-	317.9350	C ₁₄ H ₈ Cl ₄	frg	246,316,318,176	M+	317.9420
25	Dieldrin	379.8676	C ₁₂ H ₈ Cl ₆ O	frg	139,263,277,279,243	M+H	380.8799
26	DDD, o,p'-	319.9507	C ₁₄ H ₁₀ Cl ₄	frg	235,237,200	frg	235,237
27	Ethylan	306.0942	C ₁₈ H ₂₀ Cl ₂	frg	223,167,179	M+H	307.0873
28	Endrin	379.8676	C ₁₂ H ₈ Cl ₆ O	frg	223,167,179,195,224	M+H	380.8462
29	Endosulfan II	405.8139	C ₉ H ₆ Cl ₆ O ₃ S	frg	243,160,195,241,265	frg	201,223
30	DDD, p,p'-	319.9507	C ₁₄ H ₁₀ Cl ₄	frg	235,237,165,199	frg	235,237
31	DDT, o,p'-	353.9117	C ₁₄ H ₉ Cl ₅	frg	235,237,165,199	frg	235,237
32	Nonachlor, cis-	443.7528	C ₁₀ H ₅ Cl ₉	frg	409,272,237,300		N/A
33	Endrin aldehyde	379.8676	C ₁₂ H ₈ Cl ₆ O	frg	281,243,245,279,345	M+H	380,883
34	4,4'-Methoxychlor olefin	308.0370	C ₁₆ H ₁₄ Cl ₂ O ₂	frg	238,308,310,223,195	M+H	309.0367
35	Endosulfan sulfate	421.8088	C ₉ H ₆ Cl ₆ O ₄ S	frg	272,274,239,237,241	M+	421.8126
36	DDT, p,p'-	353.9117	C ₁₄ H ₉ Cl ₅	frg	235,237,165,199,212	frg	237,165,200,227
37	2,4'-Methoxychlor	344.0137	C ₁₆ H ₁₅ Cl ₃ O ₂	frg	121,227,152,197,165	frg	227,165,121
38	Endrin ketone	379.8676	C ₁₂ H ₈ Cl ₆ O	frg	245,209,139,281,317	M+H	380.8802
39	Tetradifon	355.8813	C ₁₂ H ₆ Cl ₄ O ₂ S	frg	159,229,111,75,356,161	M+H	356.8914
40	Mirex	545.6173	C ₁₀ Cl ₁₂	frg	272,274,237,239		N/A

Chloroneb

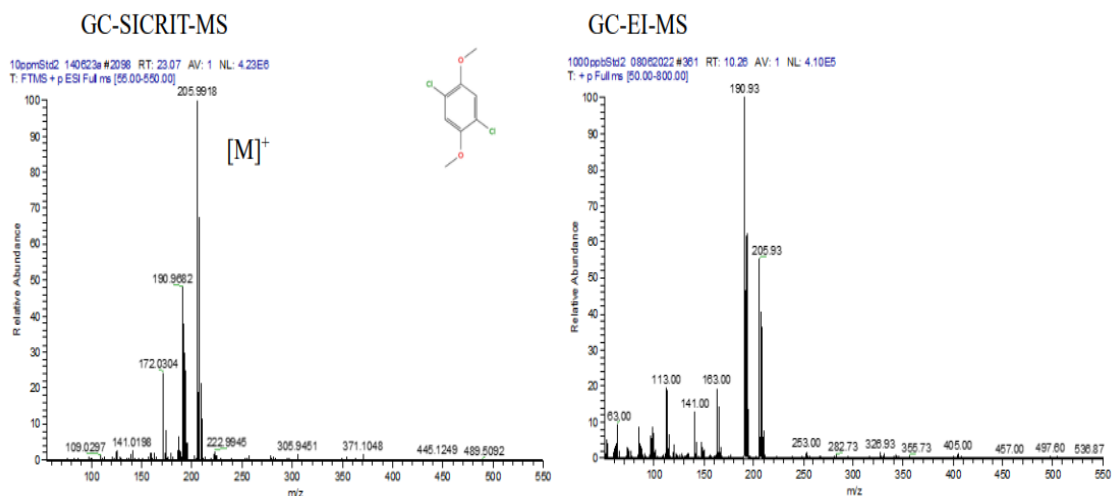


Figure 6.7: EI-MS and SICRIT-MS spectra (positive ionization mode) of chloroneb (m/z 205.9901) (see table 6.2) at 10ppm, analyzed by GC-SICRIT- LTQ Orbitrap mass spectrometer and GC-EI-ITQMS.

Figure 6.7 shows the mass spectra of the first peak, which represents chloroneb obtained using GC-SICRIT-MS on the left figure and GC-EI-MS on the right figure. The SICRIT mass spectrum shows mainly a m/z of 305.9918, which corresponds to the $[M]^+$ ion for this pesticide with a few fragments that appear at m/z 190.9682 that indicates the loss of a methyl group (CH_3) and at m/z 172.0304 that suggests the loss of a chlorine atom (Cl). The EI spectrum shows the same ions obtained using SICRIT but the mass spectrum at m/z 190.93 represents the base peak which represents the ion after losing a methyl group (CH_3). The peak at m/z 250.93 represents the $[M]^+$ of Chloroneb. The peak at m/z 170 represents the loss of (Cl), while m/z 113 may represent a large fragment ion resulting from cleavage of molecule from compound at specific bond.

Dichlorobenzophenone, 4,4'-

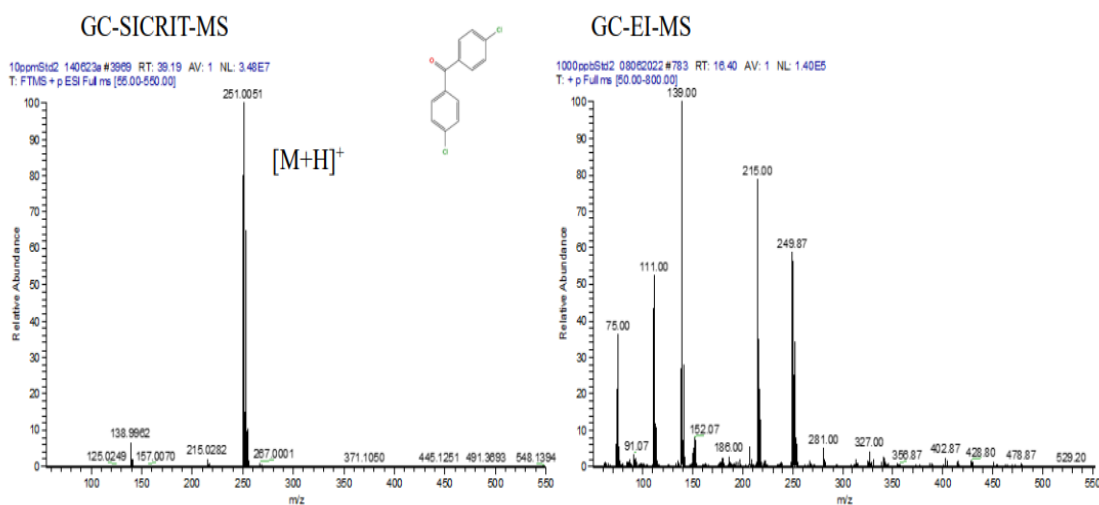


Figure 6.8: EI-MS and SICRIT-MS spectra (positive ionization mode) of Dichlorobenzophenone, 4,4'- (m/z 249.995) (see table 6.2) at 10ppm, analyzed by GC-SICRIT- LTQ Orbitrap mass spectrometer and GC-EI-ITQMS.

Figure 6.8 shows the spectra of dichlorobenzophenone, 4,4'- in both GC-SICRIT-MS and GC-EI-MS. The SICRIT mass spectrum shows mainly a m/z of 251.0052, which corresponds to the $[M+H]^+$ ion for this pesticide. This shows that SICRIT has the capacity for soft ionization without extensive fragmentation. At m/z 138.9962 a small fragment peak appears that may represent the cleavage of one of the benzene rings with the chlorine atom (Cl) as shown in figure 6.9.

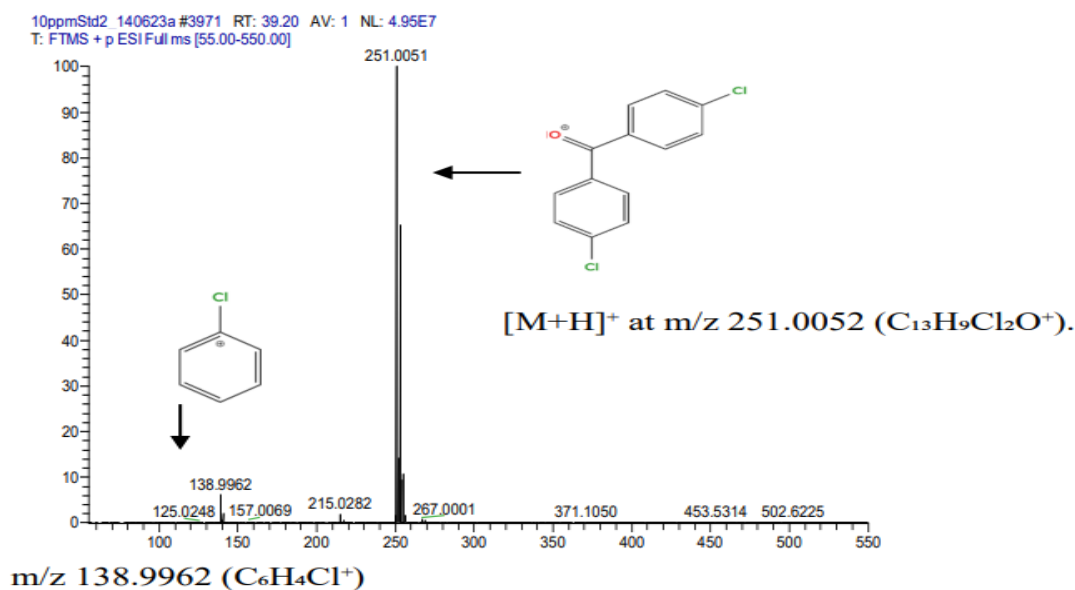


Figure 6.9: SICRIT-MS spectra (positive ionization mode) of Dichlorobenzophenone, 4,4'- (m/z 249.995) at 10ppm, analyzed by GC-SICRIT- LTQ Orbitrap mass spectrometer

In the GC-EI-MS spectrum for dichlorobenzophenone, 4,4'-, the base peak at m/z 139 is the most intense, signifying a highly stable fragment, this may indicate the loss of one of the benzene rings with chlorine atom (Cl). Additionally, the presence of peaks at m/z 215, resulting from further fragmentation. It could represent loss of a chlorine atom (Cl). The molecular ion of dichlorobenzophenone, 4,4'- at m/z 249.87 may not be the highest peak due to the extensive fragmentation associated with EI. The peak at m/z 111 represents fragment ion, perhaps resulting from cleavage of specific bonds, while at m/z 75 could represent a smaller fragment, perhaps a phenyl group.

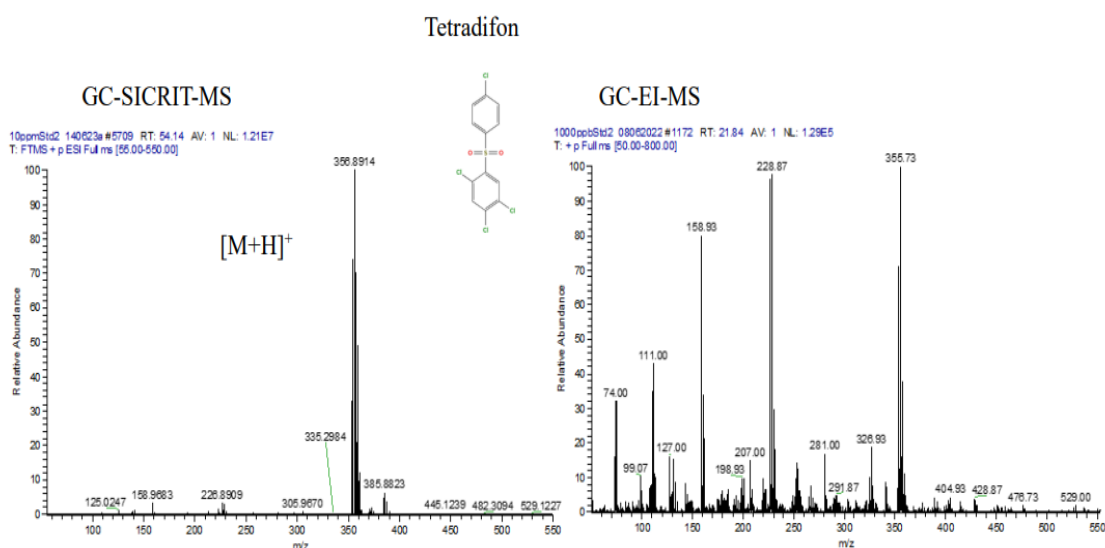


Figure 6.10: Ionisation Mechanism for Tetradifon EI-MS and SICRIT-MS spectra (positive ionization mode) of Tetradifon (m/z 355.8813) (see table 6.2) at 10ppm, analyzed by GC-SICRIT- LTQ Orbitrap mass spectrometer and GC-EI-ITQMS.

Figure 6.10 shows the spectra of tetradifon in both GC-SICRIT-MS and GC-EI-MS. In the GC-EI-MS spectrum for tetradifon, the base peak at m/z 355.73 is the most intense, this indicates the $[M]^+$ representing the intact molecule of tetradifon. Additionally, the presence of peaks at m/z 228.87, resulting from further fragmentation. It possibly formed by the loss of a dichlorophenyl group. The peak observed at m/z 158.93 likely results from cleavage of the molecule at distinct bond. The peak at m/z 111 may represents a phenyl group. The peak at m/z 281 is a fragment ion resulting from the loss of a chlorine atom (Cl).

The presence of the molecular ion at m/z 356.8914 is a key advantage of SICRIT-MS, as it allows for more confident identification of the compound and the molecular ion often appears as a protonated molecule, so this peak likely represents $[Tetradifon + H]^+$.

6.4 Method validation

6.4.1 Linearity for GC-EI-ITQMS, GC-EI-MSD and GC-SICRIT-LTQMS

The study began with preparation of calibration curves for analytes, using six calibration levels for each compound. The concentration ranges varied based on the pesticide response. Calibration was performed in the range 1–500 µg /L for three different instruments GC-EI-ITQMS, GC-EI-MSD and GC-SICRIT-LTQMS. The calibration curves were constructed by plotting the obtained pesticide signal versus the concentration. Responses were considered linear when the correlation coefficient was equal to or greater than 0.999, this was found to be true for most of the OCPs studied across all three instrumental setups used. The correlation coefficients (R^2) are summarized in table 6.3.

Linearity was assessed by repeated injections ($n=6$) of calibration standard solutions prepared in solvent (Figure 6.11). For GC-ITQMS with Endosulfan I, Chlordane, *cis*- and Endosulfan sulfate that resulted in a determination of coefficients (R^2) of 0.997, 0.998 and 0.998 respectively, below the threshold of 0.999 that had been defined as ideal linearity. All the evaluated OCPs showed R^2 values greater than 0.999. For GC-MSD, all the analytes showed linearity coefficients greater than 0.999 except for Endrin and 2,4'-Methoxychlor where R^2 values were calculated at 0.996 and 0.998 respectively. The determined R^2 coefficient values differ when using GC-SICRIT-LTQMS, many compounds are absent, up to 25%, and therefore there is no R^2 for these compounds. For the OCPs that could be reliably detected, the coefficients were found to range between 0.999 and 0.996 as shown in figure 6.11.

Table 6.3: Limit of detection (LOD), Limit of quantification (LOQ), and Linearity (R²) of organochlorine pesticides in baby food samples.

Component Name	GC-EI-MSD			GC-EI-ITQMS			GC-SICRIT-LTQMS		
	LOD µg/mL	LOQ µg/mL	R ²	LOD µg/mL	LOQ µg/mL	R ²	LOD µg/mL	LOQ µg/mL	R ²
Chloroneb	0.002	0.005	0.9998	0.007	0.021	0.9994	0.0048	0.0146	0.9996
Pentachlorobenzene	0.003	0.005	0.9994	0.007	0.021	0.9996	N/A	N/A	N/A
BHC, alpha-	0.004	0.011	0.9998	0.007	0.022	0.9991	N/A	N/A	N/A
Hexachlorobenzene	0.002	0.007	0.9994	0.006	0.020	0.9998	0.0138	0.0420	0.9974
Pentachloroanisole	0.002	0.007	0.9995	0.060	0.180	0.9998	0.0093	0.0283	0.9983
BHC, beta-	0.002	0.005	0.9998	0.083	0.253	0.9995	N/A	N/A	N/A
BHC, gamma-	0.002	0.007	0.9995	0.007	0.022	0.9994	N/A	N/A	N/A
BHC, delta-	0.002	0.005	0.9997	0.007	0.022	0.9995	N/A	N/A	N/A
Endosulfan ether	0.003	0.01	0.999	0.007	0.022	0.9992	0.0048	0.0146	0.9996
Heptachlor	0.002	0.006	0.9991	0.007	0.021	0.9990	0.0093	0.0283	0.9983
Pentachlorothioanisole	0.003	0.01	0.9991	0.060	0.180	0.9998	0.0068	0.0206	0.9996
Aldrin	0.004	0.01	0.9996	0.006	0.020	0.9996	0.0083	0.0252	0.9994
Dichlorobenzophenone, 4,4'-	0.003	0.008	0.9994	0.007	0.021	0.9997	0.0020	0.0050	0.9998
Fenson	0.002	0.005	0.9997	0.010	0.029	0.9998	0.0035	0.0105	0.9996
Isodrin	0.003	0.01	0.999	0.006	0.020	0.9996	0.0093	0.0283	0.9983
Heptachlor epoxide	0.003	0.01	0.9991	0.060	0.180	0.9993	0.0115	0.0348	0.9974
Chlorbenside	0.003	0.009	0.9994	0.007	0.020	0.9997	0.0073	0.0222	0.9996
Chlordane, trans-	0.002	0.005	0.9999	0.007	0.021	0.9993	N/A	N/A	N/A

DDE, o, p'-	0.003	0.01	0.9997	0.004	0.010	0.9995	0.0048	0.0146	0.9996
Endosulfan I	0.002	0.0061	0.9997	0.007	0.021	0.9976	0.0048	0.0146	0.9996
Chlordane, cis-	0.003	0.01	0.9997	0.007	0.021	0.9983	N/A	N/A	N/A
Nonachlor, trans-	0.004	0.01	0.9994	0.004	0.010	0.9996	N/A	N/A	N/A
Chlorfenson	0.002	0.006	0.9996	0.004	0.010	0.9996	0.0035	0.0105	0.9997
DDE, p,p'-	0.004	0.01	0.999	0.004	0.010	0.9997	0.0035	0.0105	0.9997
Dieldrin	0.004	0.01	0.9997	0.006	0.020	0.9998	0.0093	0.0283	0.9983
DDD, o,p'-	0.004	0.01	0.9996	0.005	0.015	0.9994	0.0093	0.0283	0.9983
Ethylan	0.0035	0.01	0.999	0.002	0.005	0.9998	0.0083	0.0252	0.9994
Endrin	0.014	0.043	0.9965	0.007	0.020	0.9993	0.0595	0.1804	0.9995
Endosulfan II	0.003	0.01	0.9997	0.007	0.020	0.9991	0.0052	0.0159	0.9994
DDD, p,p'-	0.004	0.01	0.9995	0.005	0.015	0.9993	0.0103	0.0311	0.9965
DDT, o,p'-	0.002	0.007	0.9997	0.005	0.015	0.9995	0.0103	0.0311	0.9965
Nonachlor, cis-	0.002	0.006	0.9996	0.005	0.015	0.9993	N/A	N/A	N/A
Endrin aldehyde	0.002	0.005	0.9998	0.007	0.022	0.9995	0.0099	0.0300	0.9976
4,4'-Methoxychlor olefin	0.003	0.009	0.9992	0.003	0.010	0.9991	0.0099	0.0300	0.9976
Endosulfan sulfate	0.003	0.01	0.999	0.007	0.022	0.9985	0.0030	0.0050	0.9994
DDT, p,p'-	0.003	0.009	0.9993	0.006	0.020	0.9994	0.0043	0.0131	0.9996
2,4'-Methoxychlor	0.004	0.011	0.9989	0.006	0.020	0.9993	0.0043	0.0131	0.9996
Endrin ketone	0.002	0.007	0.9995	0.007	0.021	0.9995	0.0073	0.0222	0.9996
Tetradifon	0.003	0.009	0.9993	0.006	0.020	0.9998	0.0035	0.0105	0.9997
Mirex	0.002	0.007	0.9997	0.007	0.021	0.9997	N/A	N/A	N/A

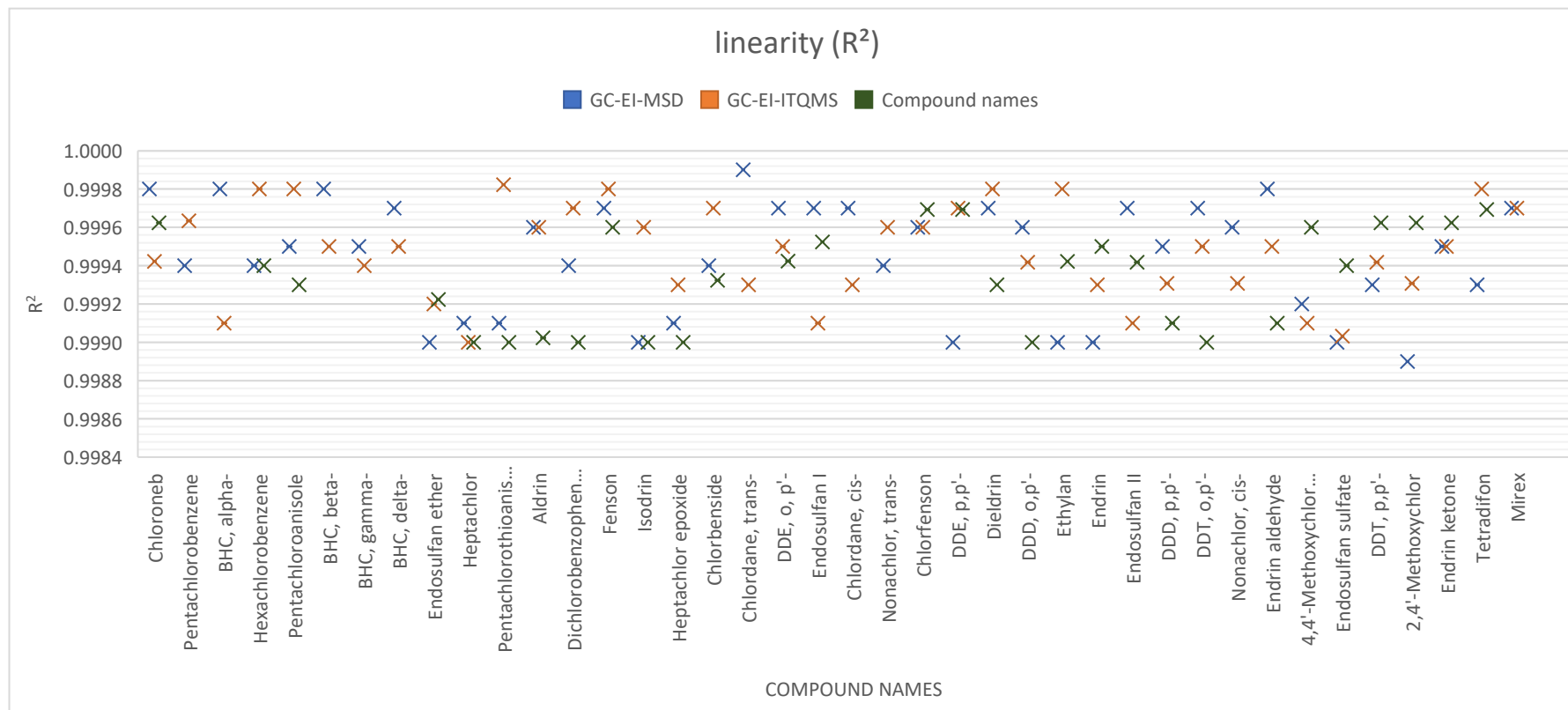


Figure 6.11: Linearity of organochlorine pesticides in baby food samples when detected by GC-EI-MS.

To determine whether there are statistically significant differences between LOD and LOQ methods, ANOVA can be used. Descriptive analysis provides information about the baseline values of LOD and LOQ, such as the mean, standard deviation and standard error, which helps understand the data as shown in table 6.4.

Table 6.4: Descriptive statistics for LOD of ITQMS, SQMS, and LTQMS

	N	Mean	Std. Deviation	Std. Error	95% Confidence Interval for Mean		Minimum	Maximum
					Lower Bound	Upper Bound		
GC-EI-MSD	40	.0031	.00193	.00030	.0025	.0037	.00	.01
GC-EI-ITQMS	40	.0121	.01846	.00292	.0061	.0180	.00	.08
GC-SICRIT-LTQMS	39	.0067	.00954	.00153	.0036	.0098	.00	.06
33.00	1	.000000	.00
Total	120	.0072	.01249	.00114	.0050	.0095	.00	.08

The LOD descriptive statistics appear in this table where four methods including GC-EI-MSD, GC-EI-ITQMS, GC-SICRIT-LTQMS along with a value of "33.00" are presented. The experimental data for LOD displays means ranging from 0.0031 to 0.0121 and displays substantial standard deviation particularly in ITQMS method data. The 95% confidence intervals show the estimated range of the true mean LOD for each method. The overall total mean LOD across all samples is 0.0072. The wide range of maximum values, especially in ITQMS, suggests some samples have much higher detection limits, but overall, the groups seem fairly comparable. To determine if the differences among the means are statistically significant, an ANOVA test would be conducted next.

Table 6.5: test of homogeneity of variances for LOD.

Levene Statistic	df1	df2	Sig.
9.988 ^a	2	116	.000

a. Groups with only one case are ignored in computing the test of homogeneity of variance for LOD.

The Levene's test produces as shown in table 6.5 significant results regarding homogeneity of variances in three LOD data groups with a statistic value of 9.988 supported by a p-value of 0.000. Since the p-value is below 0.05 this demonstrates the variances are not consistent between the three groups. The p-value significance demonstrates that the groups show heterogeneity in variability although groups with single cases were excluded from analysis. Therefore, this factor should influence interpretation of ANOVA findings. The choice of subsequent tests and potential adjustments could be affected by this non-compliance with homogeneity assumptions.

Table 6.6: ANOVA results for LOD.

	Sum of Squares	df	Mean Square	F	Sig.
Between Groups	.002	3	.001	3.842	.012
Within Groups	.017	116	.000		
Total	.019	119			

The summary of ANOVA results in table 6.6 reveals $F(3,116) = 3.842$, $p = 0.012$, showing that differences in LOD between the methods were statistically significant, indicating at least two of them likely GC-SICRIT-LTQMS as having different detection limits of less than 10.5% of the total variance accounted for or $\eta^2 \approx 0.105$ - although significant this was not a large effect size, thus requiring some post-hoc tests (such as Tukey's HSD) to find out which exact differences of method pairs could be reflected in terms of practical detection limit requirements within your application.

The LOQ helps to determine the lowest concentration that can be accurately measured, and its descriptive analysis provides a solid foundation for understanding analytical performance. The statistical description of the LOQ values begins with all systems used as shown in table 6.7.

Table 6.7: Descriptive statistics for LOQ of ITQMS, SQMS, and LTQMS.

	N	Mean	Std. Deviation	Std. Error	95% Confidence Interval for Mean		Minimum	Maximum
					Lower Bound	Upper Bound		
GC-EI-MSD	40	.0090	.00589	.00093	.0071	.0109	.01	.04
GC-EI-ITQMS	40	.0364	.05575	.00881	.0186	.0543	.01	.25
GC-SICRIT-LTQMS	39	.0202	.02898	.00464	.0108	.0296	.00	.18
33.00	1	.000000	.00
Total	120	.0217	.03782	.00345	.0149	.0286	.00	.25

The table listed above gives indications of significant LOQ performance differences for the various methods; GC-EI-MSD showed highest sensitivity and precision (mean LOQ=0.0090, tight 95% CI 0.0071-0.0109, low SD=0.00589), hence, would be best for trace-level quantification, while GC-EI-ITQMS exhibited LOQs much higher and more variable (mean=0.0364, wide CI 0.0186-0.0543, SD=0.05575), which raises the question of a possible calibration or sensitivity problem. GC-SICRIT-LTQMS lies somewhere in between (mean=0.0202, SD=0.02898), and the sole outlier (LOQ=0.0000) merits investigation. From these findings, it can be argued that whenever detection limits are very low, preference should be accorded to GC-EI-MSD. However, in its choice, considerable weight should be given to the requirements of the specific analyses and the matrix effects seen in the study.

To verify the hypothesis of data equality, Levene's test is used before conducting the analysis of variance test (ANOVA).

Table 6.8: test of homogeneity of variances for LOQ.

Levene Statistic	df1	df2	Sig.
9.983 ^a	2	116	.000

a. Groups with only one case are ignored in computing the test of homogeneity of variance for LOQ.

The significant Levene Statistic result as shown in table 6.8, which is 9.983 together with a p-value of .000 proves the violation of equal variances across groups. The measurement differences in LOQ variability between study groups become evident because the obtained significance level remains below 0.05.

Table 6.9: ANOVA results for LOQ.

	Sum of Squares	df	Mean Square	F	Sig.
Between Groups	.016	3	.005	3.932	.010
Within Groups	.154	116	.001		
Total	.170	119			

The ANOVA analysis result as shown in table 6.9 supports statistical significance between groups because the F-value reaches 3.932 and the p-value falls to 0.010 which stays beneath the alpha threshold of 0.05. The LOQ mean values between at least one group show a substantial distinction from the rest of the groups. The between-groups sum of squares equals 0.016 using three degrees of freedom whereas the within-groups sum of squares amounts to 0.154 at 116 degrees of freedom creating a total of 0.170. The analysis demonstrates that group differences (0.005) contribute more to the data variability than within-group variability (0.001) through examination of mean square values. Post hoc analysis becomes necessary because ANOVA results show the group factor creates significant effects on LOQ levels.

6.4.2 LOD and LOQ determination for GC-EI-ITQMS, GC-EI-MSD and GC-SICRIT-LTQMS

Using data obtained from the linearity study for each analysed pesticide, the estimated limit of detection (LOD) as well as estimated limit of quantification (LOQ) were calculated. LOD and LOQ results are summarized in table 6.3.

For GC-EI-MSD, 39 of the 40 studied pesticides showed LOD values ranging from 0.002 to 0.004 $\mu\text{g/mL}$. For Endrin an LOD of 0.014 $\mu\text{g/mL}$ was measured which was markedly higher than other results.

For GC-EI-ITQMS, BHC, beta-, Pentachlorothioanisole, Fenson and Heptachlor epoxide showed LODs of 0.08, 0.06, 0.01 and 0.06 $\mu\text{g/mL}$ respectively. The LOD given indicates that these compounds have lower sensitivity in this instrument compared to the 36 compounds that show LOD in the range of 0.002 to 0.007 $\mu\text{g/mL}$.

For GC-SICRIT-LTQMS, in addition to instrument not being able to detect about 10 organochlorine compounds, there were four compounds with a LOD of 0.01 $\mu\text{g/mL}$, giving the impression that this instrument is less sensitive to these compounds. The other compounds that were characterised showed LODs in the range of 0.002 to 0.009 $\mu\text{g/mL}$.

According to the LOD values of 40 organochlorine pesticides across three instruments, it was observed that GC-MSD is the most sensitive for all 40 OCPs tested followed by GC-ITQMS as shown in figure 6.12.

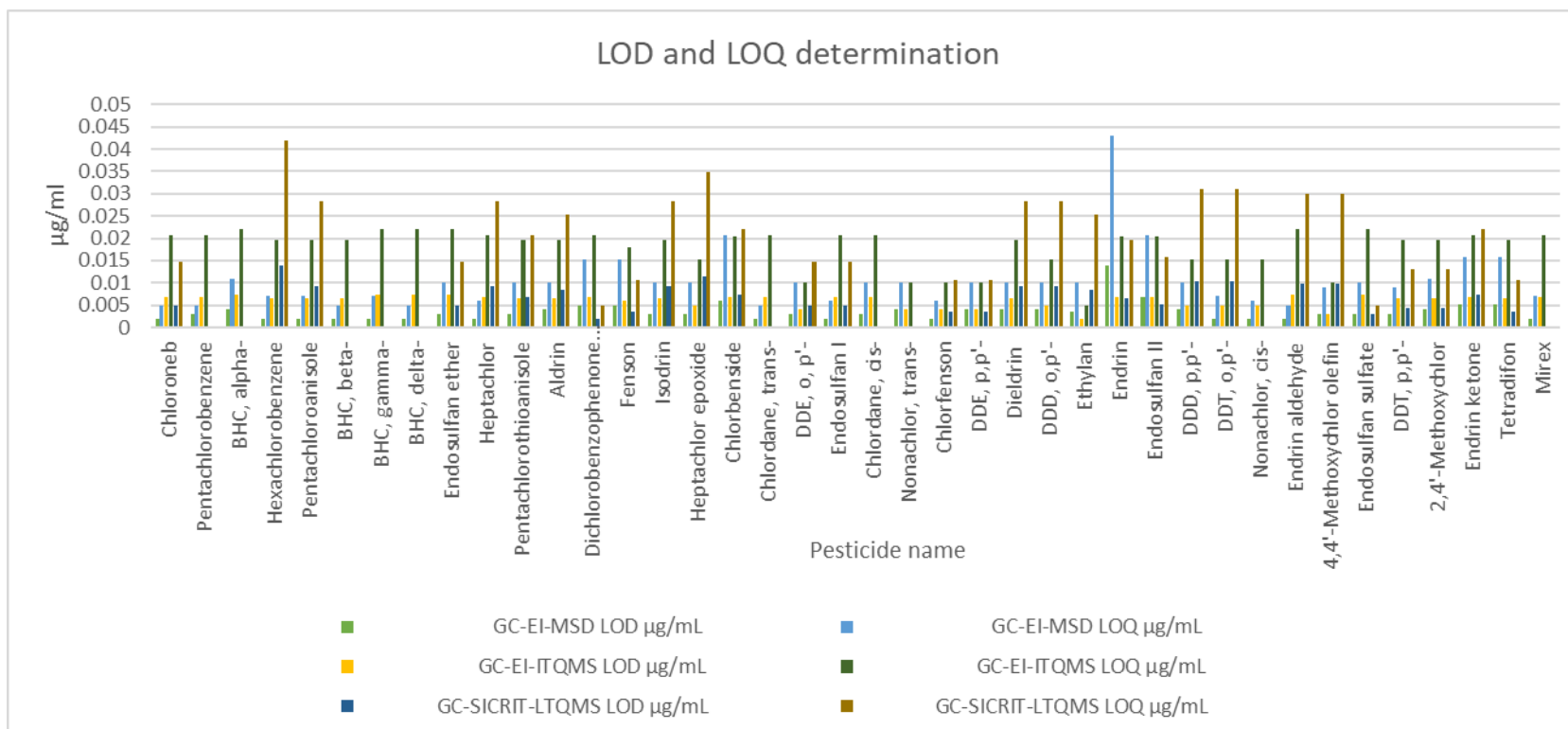


Figure 6.12: LOD and LOQ in determination of organochlorine pesticides detected by GC-EI-MSD, GC-EI-ITQMS and GC-SICRIT-MS.

6.5 Matrix effect by GC-EI-MSD

Matrix interferences are one of the major factors that must be taken into account in pesticide residue analysis as different matrices can suppress or enhance the chromatographic detection.¹⁶³ These effects may result in under or over measurement of analyte recovery.

In this study the task is to estimate the matrix effect for the set of OCPs in or standard mixture in three different samples (milk, rice and cereal) using the QuEChERS technique followed by a d-SPE clean-up process.

The matrix effect was calculated by comparing the peak area of a pesticide in the stock standard prepared in the matrix to the peak area of the same pesticide in the standard prepared in the solvent diluent. That is,

$$\text{ME}\% = ((\text{Area (Standard in matrix)}) / (\text{Area (Standard in solvent)}) - 1) * 100$$

Matrix effect results for organochlorine pesticides are summarized in Table 6.10. This table displays the matrix effect values for all organochlorine pesticides extracted from milk, rice, and cereal samples analysed using Gas Chromatography coupled with Electron Impact Mass Spectrometric Detection (GC-EI-MSD). Matrix effect (ME) refers to the influence of the sample matrix on the analytical signal of a particular analyte, which can lead to inaccurate quantification or identification of target compounds. Positive values indicate enhancement of the analyte signal due to the matrix, while negative values suggest suppression. To calculate these matrix effects, the blank samples for each matrix (milk, rice, and cereal) were analysed as shown in figures 8.1, 8.2, and 8.3 (see the Appendix) to ensure no pesticide contamination was present in the base matrix. This allows for an accurate determination of how each matrix affects the detection of the added pesticides.¹⁶⁴

Overall, it is observed from figure 6.13 that there is a significant difference in the ME among the three samples (milk, rice, and cereal) as well as variability in ME of each sample within itself. This provides a comprehensive view that the composition of pesticides plays a major role in its interaction with matrix, and the components of the matrix also have an important role in determining the effect of the matrix.

Milk is a complex matrix rich in fats, while rice and cereal are carbohydrate-rich. This provides a preliminary explanation for the difference in values. For instance,

pentachlorobenzene exhibits a higher ME% in milk (24%) compared to rice (19%) and cereal (18%), indicating that the matrix components in milk have a greater influence on the ionization efficiency of pentachlorobenzene.¹⁶⁵ Similarly, BHC, delta-, DDE, o,p'-, chlordane, trans-, chlordane, cis-, dieldrin, DDD, o,p'-, endrin, endosulfan II, endosulfan sulfate, tetradifon, and mirex. also display higher ME% in milk compared to rice and cereal, suggesting that these pesticides may interact more strongly with the matrix components present in milk. A positive matrix effect (+Ve) indicates that the presence of milk enhances the detection signal of pesticides.¹⁶⁶

Furthermore, there are variations in matrix effects among pesticides within the same matrix. For example, in milk, 2,4'-methoxychlor shows a higher ME% (727%) compared to other pesticides like chlordane, trans- (110%) and endosulfan ether (-8%). This discrepancy may be attributed to differences in the chemical properties of these pesticides and their interactions with the milk matrix components. Similarly, in rice, chlorbenseide exhibits a higher ME% (647%) compared to DDE, p,p'-(95%) and BHC, gamma- (-4%), indicating differential matrix effects among these pesticides within the rice matrix. And also in cereal, endrin aldehyde exhibits a higher ME% (659%) compared to DDD, p,p'-(111%) and isodrin (-8%), this indicates that there is a difference in the same matrix based on the pesticide.¹⁶⁷

Pentachloroanisole showed the highest suppression response for all types of matrices studied, but they still remained at less than -100% for all evaluated matrices. Chlorbenseide, chlorfenson, endrin and 2,4'-methoxychlor showed the highest enhancement response across all matrices.¹⁴⁶ Fenson, nonachlor, *trans*-, ethylan and endrin aldehyde showed the highest enhancement response for rice and cereal samples but the enhancement response was lower from the milk matrix.¹⁴⁷

Isodrin showed a response enhancement for the milk matrix. Furthermore, opposite matrix effects were observed for isodrin, 8% for rice and -8% for cereal. Rice and cereal are both carbohydrate rich matrices, but for isodrin they showed opposite matrix effects. This behaviour shows that some matrices, even though they are grossly similar, affect some analytes with unpredictable outcomes as evidenced for isodrin.

Table 6.10: Matrix effect of organochlorine pesticides in baby food samples using GC-MSD

GC-EI-MSD	Milk	Rice	Cereal
Component Name	ME%	ME%	ME%
Chloroneb	25	11	31
Pentachlorobenzene	24	19	18
BHC, alpha-	15	-26	-56
Hexachlorobenzene	8	18	12
Pentachloroanisole	-99	-83	-68
BHC, beta-	44	65	37
BHC, gamma-	10	-4	-14
BHC, delta-	29	20	12
Endosulfan ether	-8	7	7
Heptachlor	11	-3	-19
Pentachlorothioanisole	10	-19	-9
Aldrin	5	-24	-15
Dichlorobenzophenone, 4,4'-	30	92	96
Fenson	186	323	317
Isodrin	33	8	-8
Heptachlor epoxide	9	-7	-21
Chlorbenside	821	647	684
DDE, o,p'-	31	3	4
Chlordane, trans-	110	88	79
Chlordane, cis-	110	88	79
Endosulfan I	68	91	81
Nonachlor, trans-	195	512	471
Chlorfenson	430	613	649
DDE, p,p'-	51	95	75
Dieldrin	41	8	13
DDD, o,p'-	116	98	81
Ethylan	147	239	223
Endrin	686	473	465

Endosulfan II	103	88	71
DDD, p,p'-	103	101	111
Nonachlor, cis-	103	89	70
Endrin aldehyde	390	707	659
4,4'-Methoxychlor olefin	107	169	142
DDT, p,p'-	69	139	104
Endosulfan sulfate	121	97	70
2,4'-Methoxychlor	727	395	395
Endrin ketone	106	182	159
Tetradifon	128	91	77
Mirex	46	36	30

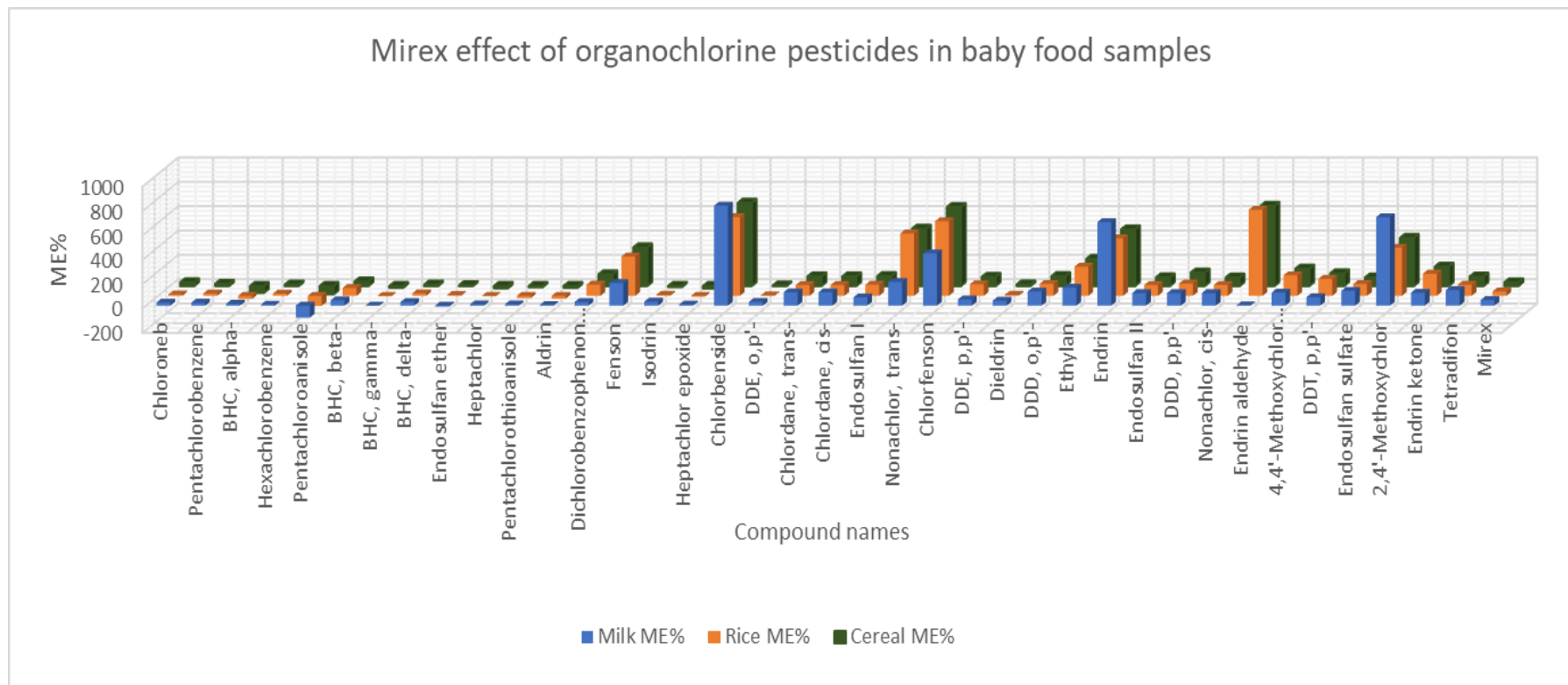


Figure 6.13: Matrix effect of organochlorine pesticides in baby food samples.

6.6 Method Precision and Accuracy by GC-EI-MSD

Accuracy, this parameter is specifically measured by spiking the sample matrix of interest specifically with a known concentration of analyte standard. It analyses the sample specifically by using a validation method. The procedure and calculation for Accuracy are different from matrix to matrix.

Precision is a measure of how close repeated measurement agree with each other experimentally. it is expressed as the percentage of relative standard deviation (% RSD)

$$\% \text{Relative standard deviation} = \text{Standard deviation} \div \text{Mean} \times 100$$

Relative standard deviation (RSD) is a statistical measure that is commonly used in Chemistry. The replicate injections range approximately lie between 4 to 6 particularly used to determine the RSD. The selected number of replicates enables an accurate assessment of the method precision without requiring unnecessary resource investment. The method's variability and reproducibility can be properly reflected when replicates are done with standard conditions and matching instrument setups to the sample. Method precision requires at least three replicate tests but additional tests over six can exceed necessary levels unless precision demands are high. It is accepted that a low relative standard deviation indicates high precision, on the other hand, a high relative standard deviation indicates low precision. The relative standard deviation (RSD) signifies the exactness of the method as it gives variability with respect to the mean as percentage values. Thus, low RSD (%) denotes a tight clustering of the replicate measurements (high precision), whereas high RSD (%) indicates larger scatter (low precision). For instance, in GC-MS replicate analyses of a pesticide sample, an RSD of 1% (low) would indicate a reliable instrument performance, while an RSD of 15% would indicate that method or technical problems are present. It can thus be understood that precision and RSD are related in an inverse relation, as RSD is a normalized parameter of dispersion-more RSD represents more relative variation and therefore poor reproducibility.

Recovery is a value that describes how close the value calculated for analytes post the analytical protocol matches to the true concentration of the analyte in a sample. Poor recovery produces negative results that affect accuracy and reliability of the analysis and lead to false results.¹⁴⁸⁻¹⁵⁰

The recovery parameter was determined in this experimental analysis as it helped in evaluating the effectiveness of a quantitative analytical workflow. Two levels of pre-spiked quality controls (QCs) were used that were used to judge the recovery of analytes for the three matrices used in this study. These matrices were spiked at two concentration levels of 0.1 and 0.05 $\mu\text{g}/\text{mL}$. each test was done in six replicates. Recovery was calculated based on the ratio of analyte responses for two different matrix calibration levels. The recovery studies were conducted using pre-spiked quality controls at 0.05 and 0.1 $\mu\text{g}/\text{mL}$ (equivalent to 50 and 100 $\mu\text{g}/\text{kg}$ in the original sample) to ensure reliable detection above the method's LODs (0.001–0.009 $\mu\text{g}/\text{mL}$) while aligning with SANTE guidelines for validation. Samples (15 g of milk, rice, or cereal) were spiked with pesticide standards in acetonitrile, equilibrated for 30 minutes, and extracted via QuEChERS (AOAC 2007.01) with d-SPE cleanup, yielding recoveries of 70–120% for organophosphorus pesticides—the primary focus due to their acute toxicity and regulatory relevance in baby foods. While these levels exceeded the typical 10 $\mu\text{g}/\text{kg}$ MRLs, they were chosen to ensure robust method performance; recovery studies for other pesticide classes were deferred due to structural similarities and resource constraints, though future validation across all classes is planned to address this limitation.

According to guidelines specifically SANTE, mean recoveries are acceptable particularly when the range is approximately between 70 to 120% and the relative standard deviation is less than approximately 20%

Table 6.11: Recovery and relative standard deviation of organochlorine pesticides in baby food samples

Component Name	Milk				Rice				Cereal			
	0.05µg/ml		0.1µg/ml		0.05µg/ml		0.1µg/ml		0.05µg/ml		0.1µg/ml	
	Recovery %	RSD %										
Chloroneb	103	5%	73	2%	110	3%	105	18%	114.0	6%	109.2	4%
Pentachlorobenzene	90	17%	87	5%	84	14%	116	8%	100.5	10%	100.2	11%
BHC, alpha-	89	19%	99	19%	115	13%	93	18%	72.5	3%	70.7	19%
Hexachlorobenzene	70	13%	72	8%	118	13%	94	4%	76.0	12%	102.9	12%
Pentachloroanisole	103	5%	93	14%	103	5%	90	14%	112.1	14%	104.4	14%
BHC, beta-	72	8%	90	2%	96	11%	104	5%	84.5	12%	98.5	2%
BHC, gamma-	88	14%	106	1%	106	15%	84	18%	91.6	6%	96.8	2%
BHC, delta-	81	17%	90	4%	95	10%	90	16%	99.7	2%	82.8	5%
Endosulfan ether	71	11%	73	2%	105	5%	103	19%	81.8	3%	74.1	10%
Heptachlor	70	2%	97	8%	70	2%	97	8%	114.1	7%	104.8	4%
Pentachlorothioanisoe	73	13%	93	2%	70	2%	72	3%	107.2	16%	105.3	11%
Aldrin	73	7%	76	2%	99	17%	97	7%	99.7	1%	116.4	8%
Dichlorobenzophenone, 4,4'-	99	2%	118	14%	72	7%	95	14%	77.1	12%	120.3	11%
Fenson	101	1%	105	11%	83	15%	70	8%	89.8	14%	89.6	3%
Isodrin	101	2%	95	5%	96	4%	106	7%	85.8	7%	87.6	7%
Heptachlor epoxide	76	8%	105	2%	85	16%	101	13%	107	2%	70.1	7%
Chlorbenside	131	22%	125	21%	67	25%	64	23%	68	23%	68	27%

Chlordane, trans-	72	6%	85	2%	72	4%	84	12%	73.4	16%	76.7	7%
DDE, o,p'-	116	3%	97	1%	92	16%	92	2%	105.1	14%	79.1	4%
Endosulfan I	107	4%	105	1%	93	3%	82	3%	91.7	19%	85.0	16%
Chlordane, cis-	71	12%	81	15%	94	19%	84	16%	93.2	8%	72.5	3%
Nonachlor, trans-	78	15%	97	9%	107	4%	112	16%	82.7	6%	102.7	19%
Chlorfenson	122	22%	115	8%	69	24%	126	29%	68	22%	129	26%
DDE, p,p'-	116	7%	95	18%	104	12%	104	6%	98.6	14%	104.4	12%
Dieldrin	81	12%	93	2%	102	3%	99	2%	97.3	2%	97.2	1%
DDD, o,p'-	73	6%	72	4%	87	10%	104	19%	72.5	4%	70.7	6%
Ethylan	95	19%	101	4%	83	7%	81	2%	108.5	5%	103.6	5%
Endrin	122	21%	124	21%	67	24%	74	8%	60	29%	98	2%
Endosulfan II	109	9%	104	10%	115	4%	105	7%	97.6	9%	101.3	3%
DDD, p,p'-	74	8%	72	6%	73	6%	83	5%	74.9	5%	73.4	6%
DDT, o,p'-	101	8%	97	3%	92	4%	99	2%	81.8	5%	116.4	4%
Nonachlor, cis-	92	19%	101	6%	117	16%	84	8%	102.0	14%	94.8	3%
Endrin aldehyde	84	7%	83	3%	60	25%	69	22%	124	21%	128	22%
4,4'-Methoxychlorolefin	105	9%	87	12%	107	4%	119	10%	107.0	10%	116.4	6%
Endosulfan sulfate	85	5%	73	9%	83	13%	103	5%	89.6	7%	83.3	13%
DDT, p,p'-	117	7%	70	5%	101	5%	104	12%	87.8	18%	93.7	14%
2,4'-Methoxychlor	141	29%	67	23%	102	10%	87	4%	89.2	20%	96.6	16%
Endrin ketone	111	20%	100	8%	106	6%	91	15%	107.9	8%	99.8	2%
Tetradifon	109	1%	99	1%	109	1%	100	1%	94.2	4%	89.6	7%
Mirex	74	8%	104	10%	103	5%	104	12%	73.4	6%	74.2	8%

There are various alarming outliers from the recovery data, which fall well outside the validation criteria of SANTE/12682/2019 of 70%-120% recovery with RSD \leq 20%. The most alarming outlier was chlorbense showing high recoveries ranging between 125 and 131% for milk, but with poor precision, RSD 21-27%, whereas chlorfenson exhibited erratic behavior across all the matrices (69-129% recovery, RSD up to 29%). Endrin showed very worrying recovery in cereal (60-124%) with a variability measure (RSD) as high as 29% and 2,4'-methoxychlor showed extreme recovery of 141% in milk. Matrices-specific interactions could be the cause of these outliers; for example, the high-fat milk matrix appears to be one that may interfere with chlorinated compounds through either enhancement phenomena or just incomplete cleanup; also, it has been shown that some cereal components may adsorb some pesticides like endrin during extraction. The explanation for this is consistent: high RSDs (>20%) with these problematic compounds, suggesting fundamental methodological problems rather than random variation, indicating that these analytes might require either method re-optimization (e.g., modified cleanup protocols) or exclusion from the final analytical scope if performance is not consistent.

Baby food samples were subjected to two analyte concentrations of 0.1 and 0.05 $\mu\text{g/mL}$, followed by extraction with 10 mL of acetonitrile for a QuEChERS extraction and clean up protocol in six replicates. The detected amounts of the two analytes were calculated based on the corresponding calibration curves. The spike recoveries were calculated using following equation:

$$\text{Recovery (\%)} = \frac{(\text{Total amount detected} - \text{Original amount})}{\text{Amount spiked}} \times 100\%$$

The results of the spike recovery experiments are listed in Table 6.11. It was found that the overall spike recoveries of the two selected analytes from different samples were between 70.00 to 120 % with the RSD less than 20% for many organochlorine pesticides in milk, rice and cereal samples which are acceptable values.

As can be seen in Figure 6.14, from the 40 studied pesticides, 35 compounds had an acceptable recovery percentage in the range from 70 to 120% for spike levels 0.1 and 0.05 µg/mL, respectively.

One of the pesticides, chlorbenside, showed unacceptable recovery for both concentrations for all three matrix types, resulting RSD values >20% as shown in figure 6.15.

Chlorfenson showed unacceptable recovery at levels 0.1 and 0.05 µg/mL for rice and cereal samples and it showed 122% recovery at 0.05 µg/mL in milk samples, but at 0.1 µg/mL showed 115%. In contrast, unacceptable recovery was found at both levels for endrin for the milk sample, while for the rice and cereal samples unacceptable recoveries were found at the lower level evaluated.¹⁵¹⁻¹⁵⁴

In the milk matrix, the recovery of endrin aldehyde was better at both spike levels, which is the opposite of what is seen for endrin aldehyde recovery from the rice and cereal samples as shown in figure 6.14. As for 2,4'-Methoxychlor, it showed a 141% recovery at 0.05 µg /mL and 67% at 0.1 µg /mL for milk matrix, but the recovery values were around 87% to 102% for the rice and cereal matrices which are acceptable values.¹⁵⁵

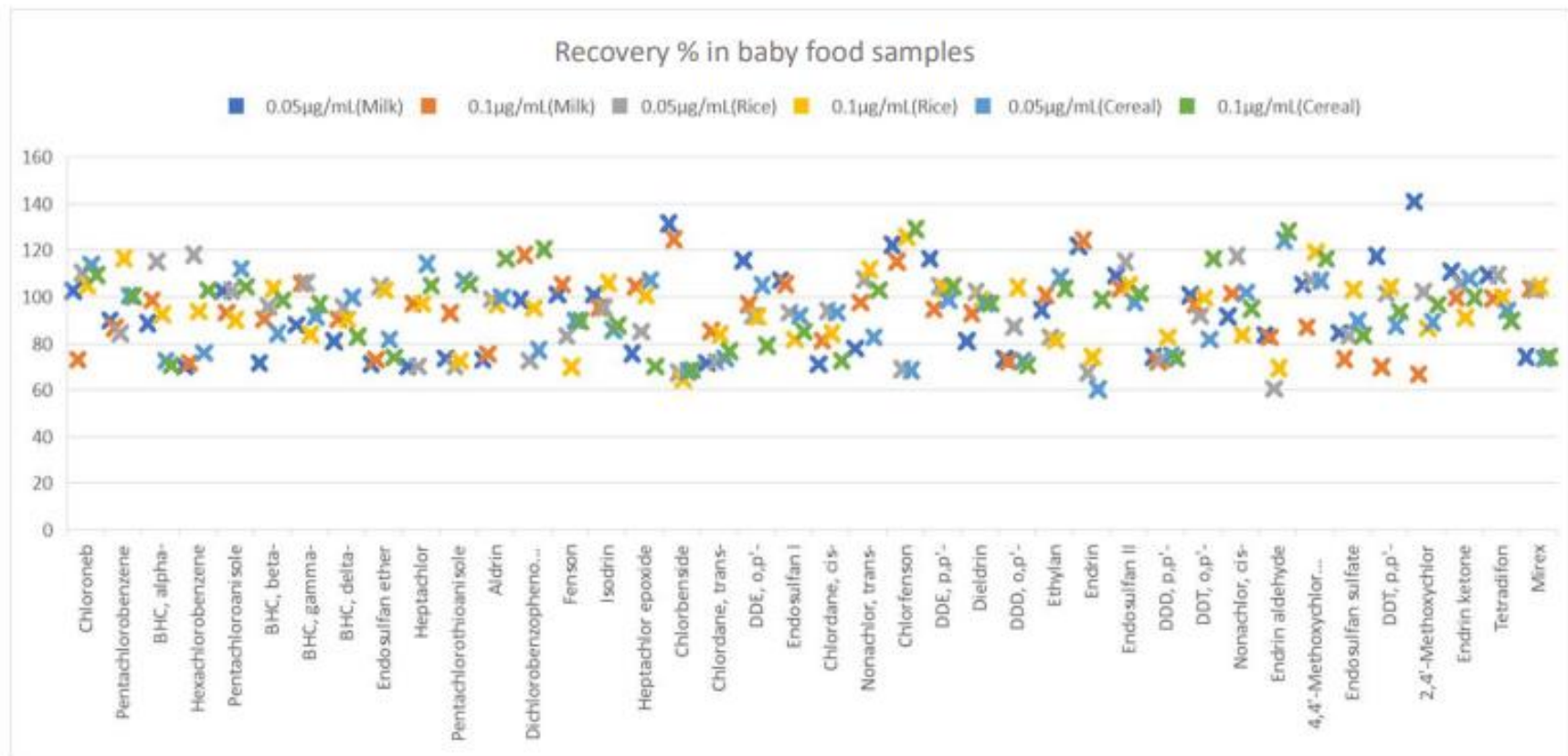


Figure 6.14: Recovery percentage of organochlorine pesticides in baby milk, rice and cereal.

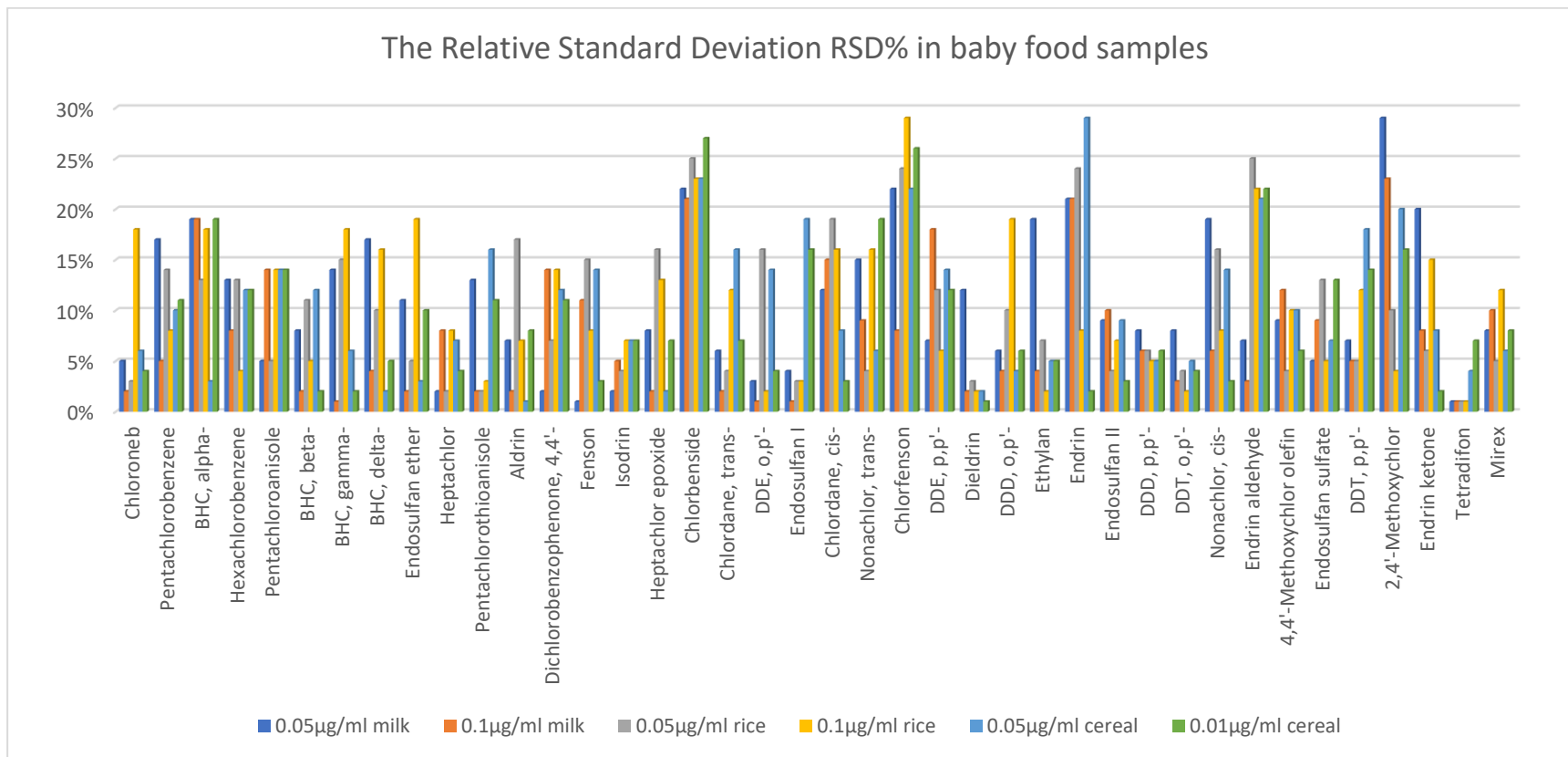


Figure 6.15: RSD percentage of organochlorine pesticides in baby milk, rice and cereal

Although the compounds of both organonitrogen (ONP) and organophosphate (OPP) were detected and separated using both SICRIT and EI techniques, not all organochlorine compounds were detected using SICRIT technique, but were detected and separated using only EI technique.¹⁵⁶⁻¹⁵⁸

The GC-EI-MS method was developed to study a mixture of 40 organochlorine pesticides (OCPs). The results showed by single quadrupole GCMSD; it can analyze 40 organochlorine pesticides. The method had a suitable linearity ($R^2 \geq 0.999$). Limit of detection (LOD) and limit of quantification (LOQ) were ranged from 0.002 to 0.01 $\mu\text{g}/\text{mL}$ and 0.005 to 0.04 $\mu\text{g}/\text{mL}$ respectively.¹⁵⁹ Average recoveries varied from 70% to 120% for most selected compounds, with RSD lower than 20%. The matrix effect was calculated based on the changing of chromatographic response of the analyte. The effect of the matrix on the response of the analyte varied according to the type of matrix.¹⁶⁰

7. Conclusion and Future Directions

This research presents the first documented application of a GC-SICRIT-MS multi-residue approach for pesticide analysis in baby food matrices. A total of 115 pesticides from different classes (Organophosphate, Organochlorine, Organonitrogen, and Pyrethroid) were analyzed and separated using four different analytical instruments (GC-FID, GC-EI-ITQMS, GC-SICRIT-LTQMS, and GC-EI-MSD). The method was verified by studying the linearity, Limit of detection (LOD), and Limit of quantification (LOQ) assessments, utilizing ANOVA analysis of variance to verify data consistency and analytical accuracy.

key Findings

1. GC-SICRIT-MS was applied as the first multi-residue method for pesticide analysis in infant food samples, marking a new advance in the field of chemical analysis. Although this technique has shown good success in detecting pesticides from the organophosphate and organonitrogen classes, it failed to detect several organochlorine compounds. Moreover, the performance in pyrethroid is not satisfactory as multiple compounds are absent, and the isomers detected using GC-EI-MS are not identified.
2. The matrix effect assessment showed that GC-SICRIT-MS exhibited a significant inhibitory effect, as evidenced by negative matrix effect values in all infant food samples (baby formula, rice and cereal). In contrast, GC-EI-MS exhibited positive matrix effects, enhancing pesticide detection in all studied matrix.

Comparison of Ionization Mechanisms: EI vs. SICRIT

The study revealed the key differences between SICRIT (soft ionization) and EI (hard ionization).

GC-EI-MS produced board from fragmentation patterns, detecting major peaks for organophosphorus compounds such as 84, 199,137,179 (Diazinon) and organochlorine pesticides (e.g., Isodrin 193,261,123).

GC-SICRIT-MS preserved molecular ions, allowing for the detection of compounds in their native state. Protonated molecular ion peak (+) was recorded for compounds such as isazophos (314.0511) and diazinon (305.1102).

Some compounds were not detected in negative ionization mode, indicating a need for methodological improvements, particularly in tuning the transfer line between the GC and the SICRIT source, along with adjusting the nitrogen makeup gas composition (e.g., methanol, isopropanol or acetonitrile).

Future Recommendations

1. Improving Ionization Conditions for GC-SICRIT-MS

Evidence indicates that carrier gas composition significantly affects ionization efficiency. Future methods should develop alternatives to water vapor, such as methanol, acetonitrile, or isopropanol, to improve the ionization environment and increase detection sensitivity.

2. Expanded Study of Pyrethroid Pesticides

The chromatogram resulting from the analysis of pyrethroids showed poor performance using GC-SICRIT-MS, with many compounds missing. In addition to its inefficiency in detecting isomers of these compounds. This requires expanding future studies to explore alternative calibration strategies and develop tools and instruments setting as well to improve detection rate for this class of pesticides.

3. Optimizing GC-SICRIT-MS Ionization for Organochlorine Pesticides

To improve and enhance the detection of all organochlorine compounds, a method for modifying the SICRIT ionization parameters, including alternative solvents in the nitrogen makeup gas, is required. SICRIT has the option to use a number of solvents in the nitrogen makeup gas (water is the default) and an effect on the ionization of compounds has been noted when different solvents are used. Vincent et al. studied the effect of solvent type on the ionization of the compound during the analysis of lubricants. It was found that when water vapor was used, both antioxidant and hydrocarbons were easily analysed. While replacing water in the bubbler with organic solvent such as methanol, isopropanol or acetonitrile gave greater efficacy to aminic antioxidants and yielding $[M + H]^+$ ion in positive mode, in negative ion mode, anionic species were produced for hydrocarbon base oil similar to water vapor.¹⁵⁹

4. Revising GC-SICRIT Transfer Line Configuration

Observations indicate that the GC transfer line in SICRIT-MS significantly impacts chromatographic performance and ionization of compounds as observed. Therefore, improvements in line transfer in GC-SICRIT-MS may improve detection reliability and reduce signal fluctuation.

8. Appendix

8.1 Studied pesticides.

Table 8.1. GC multi-residue pesticide kits GC Multiresidue Pesticide Standards Kit (Restek 32562-100 µg/mL each in toluene, 1 mL/ampul)

Component Name	CAS #	Molecular weight	Formula	group
Diazinon	333-41-5	304.3455	C ₁₂ H ₂₁ N ₂ O ₃ PS	OPP
Isazophos	42509-80-8	313.7413	C ₉ H ₁₇ ClN ₃ O ₃ PS	OPP
Chlorpyrifos-methyl	5598-13-0	322.533	C ₇ H ₇ Cl ₃ N ₃ O ₃ PS	OPP
Fenitrothion	122-14-5	277.234	C ₉ H ₁₂ N ₂ O ₅ PS	OPP
Pirimiphos-methyl	29232-93-7	305.3336	C ₁₁ H ₂₀ N ₃ O ₃ PS	OPP
Chlorpyrifos	2921-88-2	350.5863	C ₉ H ₁₁ Cl ₃ N ₃ O ₃ PS	OPP
Pirimiphos-ethyl	23505-41-1	333.3867	C ₁₃ H ₂₄ N ₃ O ₃ PS	OPP
Quinalphos	13593-03-8	298.2979	C ₁₂ H ₁₅ N ₂ O ₃ PS	OPP
Pyridaphenthion	119-12-0	340.335	C ₁₄ H ₁₇ N ₂ O ₄ PS	OPP
Phosmet	732-11-6	317.321	C ₁₁ H ₁₂ N ₂ O ₄ PS ₂	OPP
EPN	2104-64-5	323.304	C ₁₄ H ₁₄ N ₂ O ₄ PS	OPP
Phosalone	2310-17-0	367.8086	C ₁₂ H ₁₅ ClNO ₄ PS ₂	OPP
Azinphos-methyl	86-50-0	317.3243	C ₁₀ H ₁₂ N ₃ O ₃ PS ₂	OPP
Pyrazophos	13457-18-6	373.3645	C ₁₄ H ₂₀ N ₃ O ₅ PS	OPP
Azinphos-ethyl	2642-71-9	345.3775	C ₁₂ H ₁₆ N ₃ O ₃ PS ₂	OPP
Pyraclufos	77458-01-6	360.7961	C ₁₄ H ₁₈ ClN ₂ O ₃ PS	OPP
Chloroneb	2675-77-6	207.0539	C ₈ H ₈ Cl ₂ O ₂	OCP
Pentachlorobenzene	608-93-5	250.3371	C ₆ HCl ₅	OCP
BHC, alpha-	319-84-6	290.8298	C ₆ H ₆ Cl ₆	OCP
Hexachlorobenzene	118-74-1	284.7822	C ₆ Cl ₆	OCP
Pentachloroanisole	1825-21-4	280.3631	C ₇ H ₃ Cl ₅ O	OCP
BHC, beta-	319-85-7	290.8298	C ₆ H ₆ Cl ₆	OCP
BHC, gamma-	58-89-9	290.8298	C ₆ H ₆ Cl ₆	OCP
BHC, delta-	319-86-8	290.8298	C ₆ H ₆ Cl ₆	OCP
Endosulfan ether	3369-52-6	342.9	C ₉ H ₆ Cl ₆ O	OCP
Heptachlor	76-44-8	373.3177	C ₁₀ H ₅ Cl ₇	OCP
Pentachlorothioanisole	1825-19-0	296.4287	C ₇ H ₃ Cl ₅ S	OCP
Aldrin	309-00-2	364.9099	C ₁₂ H ₈ Cl ₆	OCP
Dichlorobenzophenone, 4,4'-	90-98-2	251.108	C ₁₃ H ₈ Cl ₂ O	OCP
Fenson	80-38-6	268.7161	C ₁₂ H ₉ ClO ₃ S	OCP
Isodrin	465-73-6	364.9099	C ₁₂ H ₈ Cl ₆	OCP
Heptachlor epoxide	1024-57-3	389.3171	C ₁₀ H ₅ Cl ₇ O	OCP
Chlorbenside	103-17-3	269.1895	C ₁₃ H ₁₀ Cl ₂ S	OCP
Chlordane, trans-	5103-74-2	409.7786	C ₁₀ H ₆ Cl ₈	OCP
DDE, o,p'-	3424-82-6	318.0253	C ₁₄ H ₈ Cl ₄	OCP
Endosulfan I	959-98-8	406.9251	C ₉ H ₆ Cl ₆ O ₃ S	OCP
Chlordane, cis-	5103-71-9	409.7786	C ₁₀ H ₆ Cl ₈	OCP

Nonachlor, trans-	39765-80-5	444.2237	C10H5Cl9	OCP
Chlorfenson	80-33-1	303.1611	C12H8Cl2O3S	OCP
DDE, p,p'-	72-55-9	318.0253	C14H8Cl4	OCP
Dieldrin	60-57-1	380.9093	C12H8Cl6O	OCP
DDD, o,p'-	53-19-0	380.9093	C12H8Cl6O	OCP
Ethylan	72-56-0	320.0412	C14H10Cl4	OCP
Endrin	72-20-8	307.2574	C18H20Cl2	OCP
Endosulfan II	33213-65-9	406.9251	C9H6Cl6O3S	OCP
DDD, p,p'-	72-54-8	320	C14H10Cl4	OCP
DDT, o,p'-	789-02-6	354.4863	C14H9Cl5	OCP
Nonachlor, cis-	5103-73-1	444.2237	C10H5Cl9	OCP
Endrin aldehyde	7421-93-4	380.9093	C12H8Cl6O	OCP
4,4'-Methoxychlor olefin	2132-70-9	309.1872	C16H14Cl2O2	OCP
Endosulfan sulfate	1031-07-8	422.9245	C9H6Cl6O4S	OCP
DDT, p,p'-	50-29-3	354.4863	C14H9Cl5	OCP
2,4'-Methoxychlor	30667-99-3	345.6481	C16H15Cl3O2	OCP
Endrin ketone	53494-70-5	380.9093	C12H8Cl6O	OCP
Tetradifon	116-29-0	356.0518	C12H6Cl4O2S	OCP
Mirex	2385-85-5	545.543	C10Cl12	OCP
Allidochlor	93-71-0	173.64	C8H12ClNO	ONP
Pebulate	1114-71-2	203.3448	C10H21NOS	ONP
N-(2;4-Dimethylphenyl)formamide	60397-77-5	149.1897	C9H11NO	ONP
Propachlor	1918-16-7	211.688	C11H14ClNO	ONP
Cycloate	1134-23-2	215.3555	C11H21NOS	ONP
Diallate 1⁺⁺	2303-16-4	270.2191	C10H17Cl2NOS	ONP
Diallate 2⁺⁺	2303-16-4	270.2191	C10H17Cl2NOS	ONP
Clomazone	81777-89-1	239.6981	C12H14ClNO2	ONP
Propyzamide	23950-58-5	256.1278	C12H11Cl2NO	ONP
Triallate	2303-17-5	304.6641	C10H16Cl3NOS	ONP
Propanil	709-98-8	218.0799	C9H9Cl2NO	ONP
Dimethachlor	50563-36-5	255.7405	C13H18ClNO2	ONP
Acetochlor	34256-82-1	269.7671	C14H20ClNO2	ONP
Alachlor•	15972-60-8	269.7671	C14H20ClNO2	ONP
Propisochlor	86763-47-5	283.7937	C15H22ClNO2	ONP
Linuron	330-55-2	249.0939	C9H10Cl2N2O2	ONP
Metolachlor	51218-45-2	283.7937	C15H22ClNO2	ONP
Diphenamid	957-51-7	239.3123	C16H17NO	ONP
Metazachlor	67129-08-2	277.7493	C14H16ClN3O	ONP
Flutolanil	66332-96-5	323.3096	C17H16F3NO2	ONP
Pretilachlor	51218-49-6	311.8468	C17H26ClNO2	ONP
Oxadiazon	19666-30-9	345.221	C15H18Cl2N2O3	ONP
Norflurazon	27314-13-2	303.6676	C12H9ClF3N3O	ONP
Methoxychlor	72-43-5	345.6481	C16H15Cl3O2	ONP
Fenpropathrin	39515-41-8	349.4229	C22H23NO3	ONP
Tebufenpyrad	119168-77-3	333.8557	C18H24ClN3O	ONP
Pyridaben	96489-71-3	364.9326	C19H25ClN2OS	ONP
Fluquinconazole	136426-54-5	376.172	C16H8Cl2FN5O	ONP

Prochloraz	67747-09-5	376.6654	C15H16Cl3N3O2	ONP
Tefluthrin	79538-32-2	418.7	C17H14ClF7O2	SPP
Transfluthrin	118712-89-3	371.1542	C15H12Cl2F4O2	SPP
Anthraquinone	84-65-1	208.2121	C14H8O2	SPP
Bioallethrin**	584-79-2	302.4079	C19H26O3	SPP
Resmethrin 1^{††}	10453-86-8	338.44	C22H26O3	SPP
Resmethrin 2^{††}	10453-86-8	338.44	C22H26O3	SPP
Tetramethrin 1^{††}	7696-12-0	331.4	C19H25NO4	SPP
Tetramethrin 2^{††}	7696-12-0	331.4	C19H25NO4	SPP
Bifenthrin	82657-04-3	422.8	C23H22ClF3O2	SPP
Phenothrin 1^{††}	26002-80-2	350.4	C23H26O3	SPP
Phenothrin 2^{††}	26002-80-2	350.4	C23H26O3	SPP
Cyhalothrin, lambda-	91465-08-6	449.8501	C23H19ClF3NO3	SPP
Acrinathrin	101007-06-1	541.4391	C26H21F6NO5	SPP
Permethrin, cis- ***	61949-76-6	391.2877	C21H20Cl2O3	SPP
Permethrin, trans-	61949-77-7	391.2877	C21H20Cl2O3	SPP
Cyfluthrin 1^{††}	68359-37-5	434.2876	C22H18Cl2FNO3	SPP
Cyfluthrin 2^{††}	68359-37-5	434.2876	C22H18Cl2FNO3	SPP
Cyfluthrin 3^{††}	68359-37-5	434.2876	C22H18Cl2FNO3	SPP
Cyfluthrin 4^{††}	68359-37-5	434.2876	C22H18Cl2FNO3	SPP
Cypermethrin 1^{††}	52315-07-8 (mixture)	416.2972	C22H19Cl2NO3	SPP
Cypermethrin 2^{††}	52315-07-8 (mixture)	416.2972	C22H19Cl2NO3	SPP
Cypermethrin 3^{††}	52315-07-8 (mixture)	416.2972	C22H19Cl2NO3	SPP
Cypermethrin 4^{††}●	52315-07-8 (mixture)	416.2972	C22H19Cl2NO3	SPP
Flucythrinate 1^{††}	70124-77-5	451.4619	C26H23F2NO4	SPP
Flucythrinate 2^{††}	70124-77-5	451.4619	C26H23F2NO4	SPP
Fenvalerate 1^{††}	51630-58-1	419.9001	C25H22ClNO3	SPP
tau-Fluvalinate 1^{††}	102851-06-9	502.9127	C26H22ClF3N2O3	SPP
Fenvalerate 2^{††}	51630-58-1	419.9001	C25H22ClNO3	SPP
tau-Fluvalinate 2^{††}	102851-06-9	502.9127	C26H22ClF3N2O3	SPP
Deltamethrin	52918-63-5	505.1992	C22H19Br2NO3	SPP

8.2: Examples of total ion chromatogram (TIC) of a sample blank obtained from QuEChERS extraction method and d-SPE as clean-up method

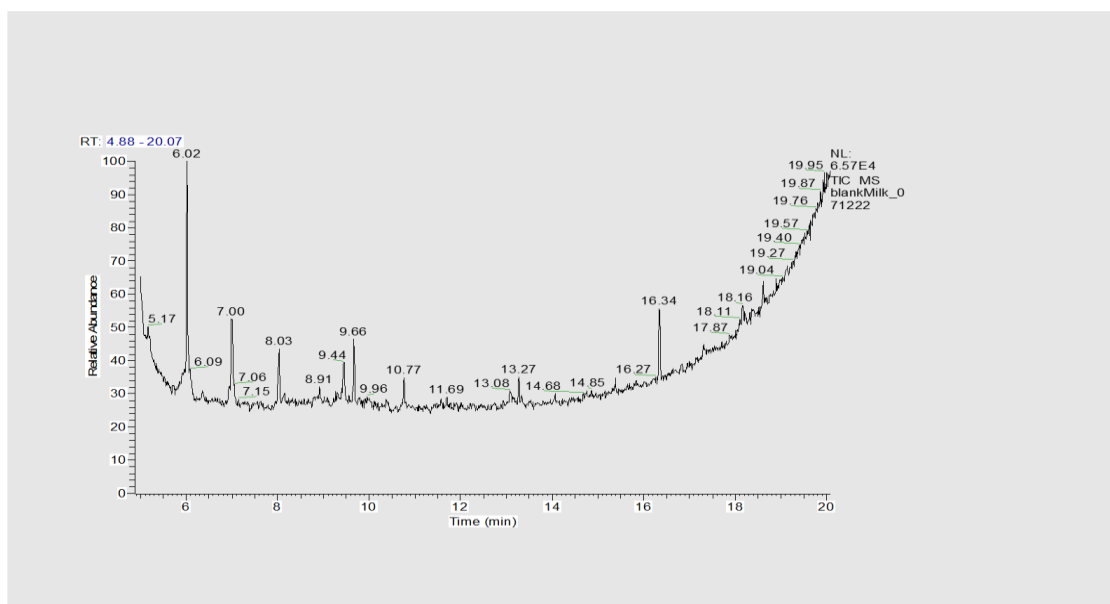


Figure 8.1: Example of total ion chromatogram (TIC) of a cereal blank obtained from QuEChERS extraction method and d-SPE as clean-up method

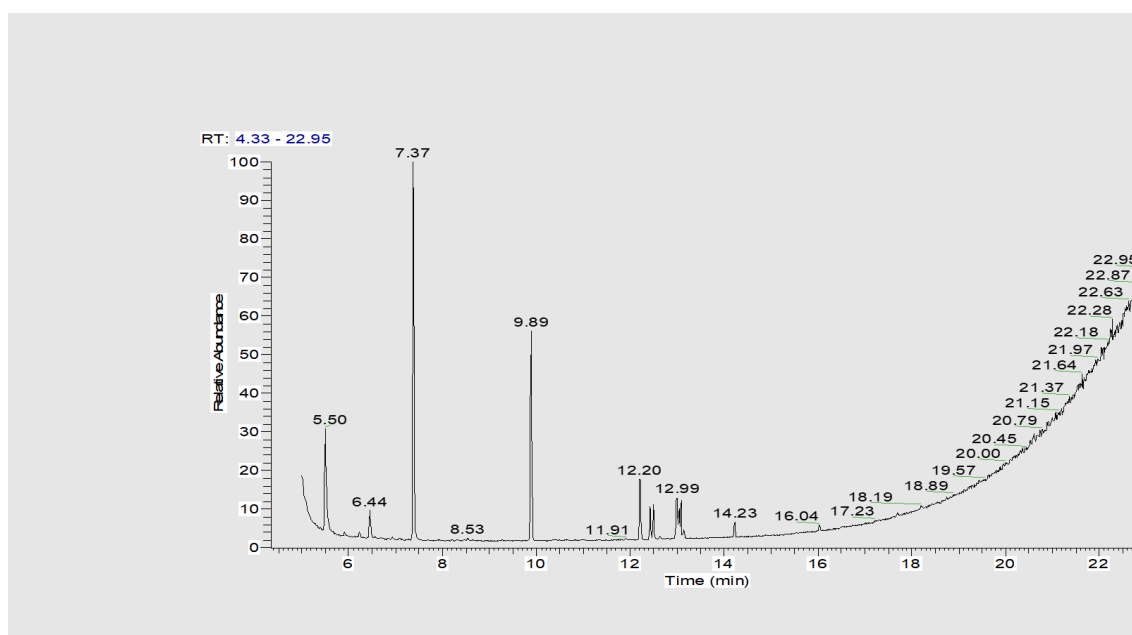


Figure 8.2: Example of total ion chromatogram (TIC) of a baby rice blank obtained from QuEChERS extraction method and d-SPE as clean-up method

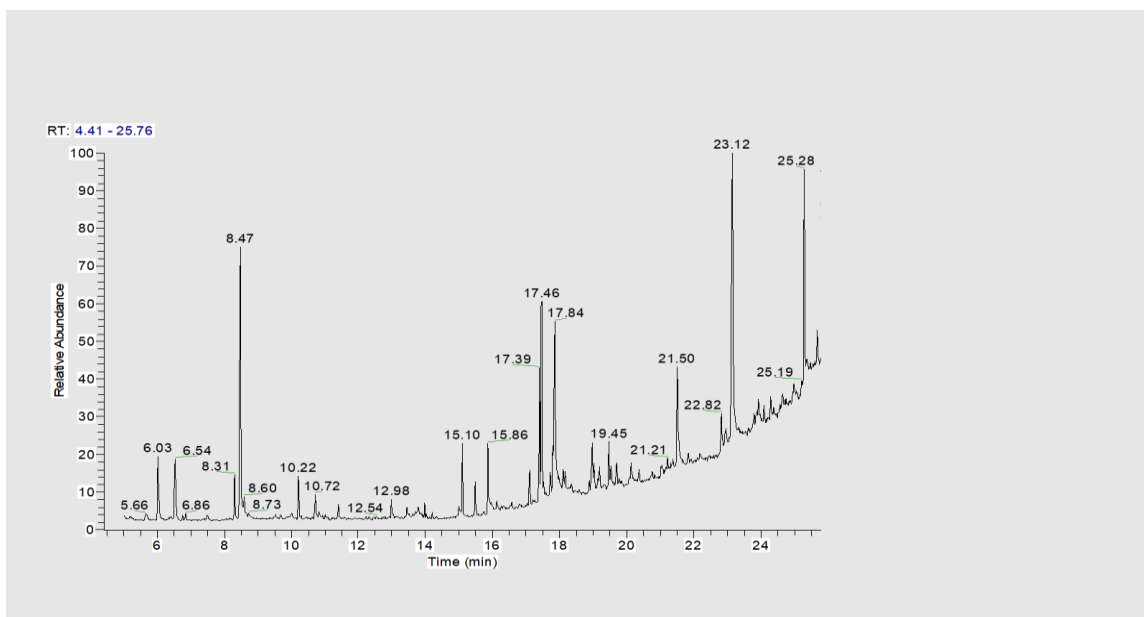


Figure 8.3: Example of total ion chromatogram (TIC) of a baby milk blank obtained from *QuEChERS* extraction method and *d-SPE* as clean-up method

8.3 Analysis of organochlorine pesticides in negative mode using GSICRIT-LTQMS

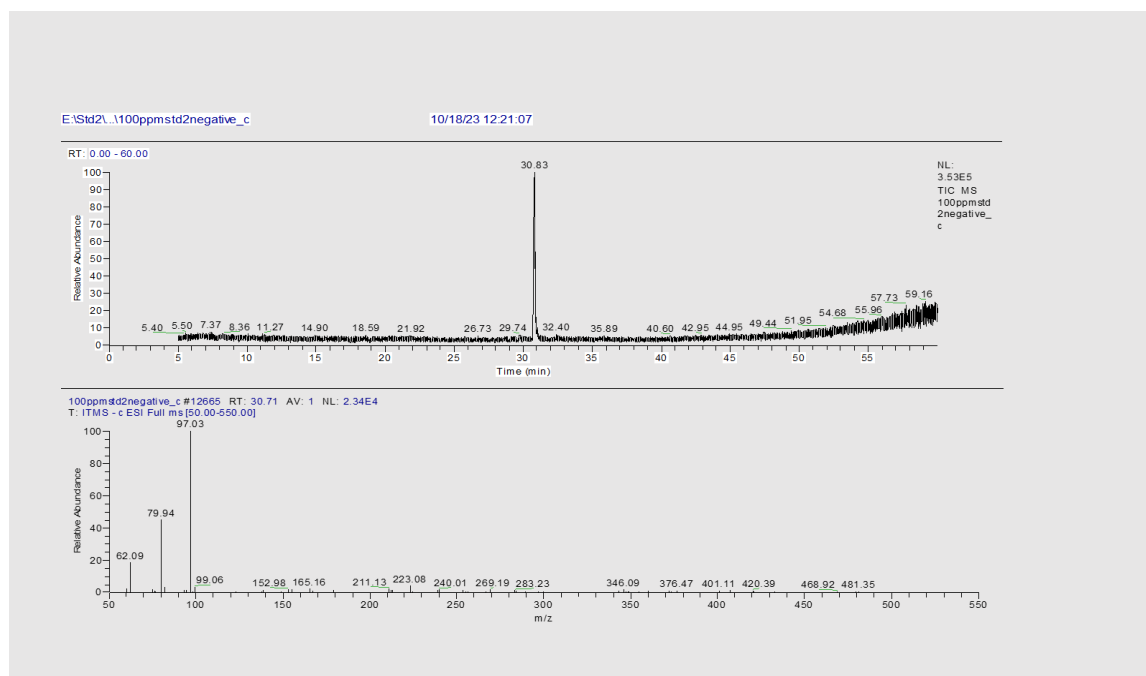


Figure 8.4: GC-SICRIT-LTQMS Chromatogram of organochlorine pesticides in negative mode

8.4 Selecting the appropriate column for pesticide analysis by GC-FID, GC-EI-ITQMS, and GC-SICRIT-LTQMS

Before finalising the pesticide analysis methods in the methodology chapter, two types of columns were evaluated:

1. Rxi-5HT GC Capillary Column, 15 m, 0.25 mm ID, 0.25 μm
2. Rxi-5ms GC Capillary Column, 30 m, 0.53 mm ID, 1.5 μm

The studied pesticides were not detected using Rxi-5HT but they were detected using Rxi-5ms as shown in figures A.5, A.6, A.7, and A.8. even though these two types have the same chemical composition and both are Low-polarity phase, 5% diphenyl / 95% dimethyl polysiloxane. Therefore, Rxi-5ms column was chosen as part the method development based on the results obtained because it has a low bleeding phase and high inert, in addition it is good for trace analysis and MS work.

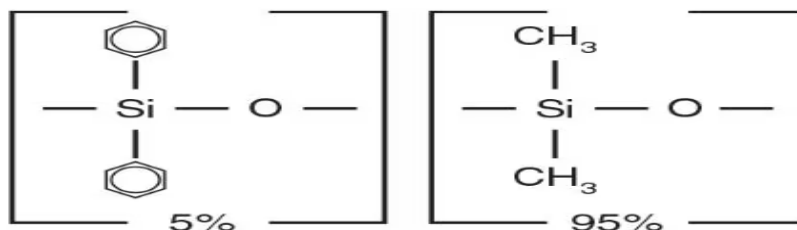


Figure 8.5: GC Capillary Column

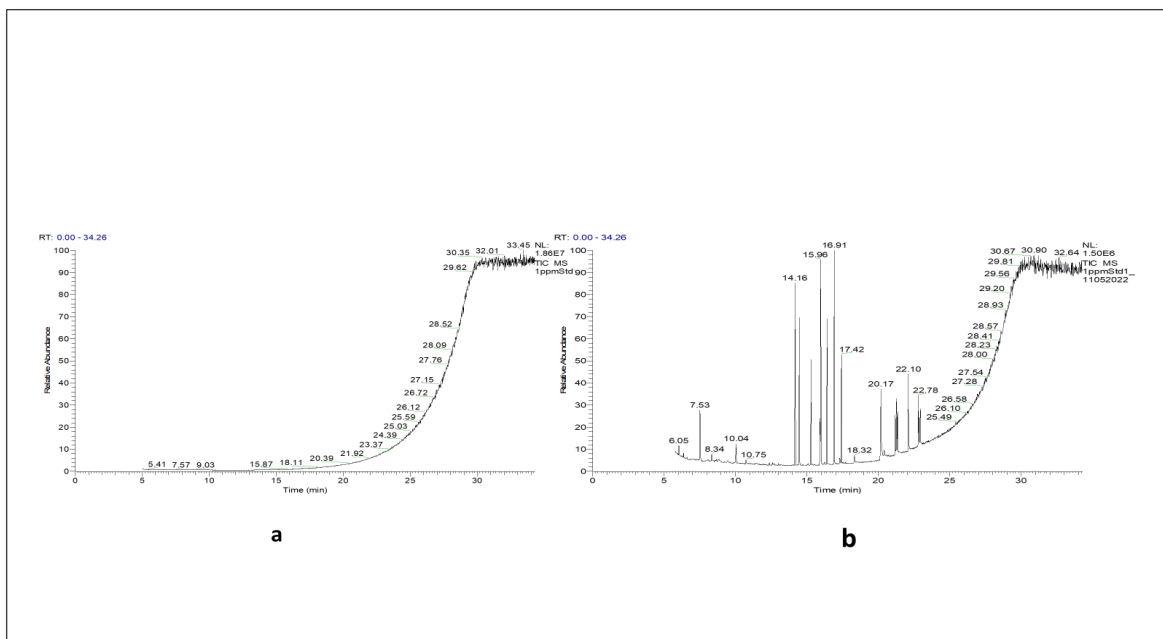


Figure 8.6: GC-EI-ITQMS Chromatogram of organophosphorus pesticides (a) the standard chromatogram using Column RXI-5HT (b) the standard chromatogram using Column RXI-5MS

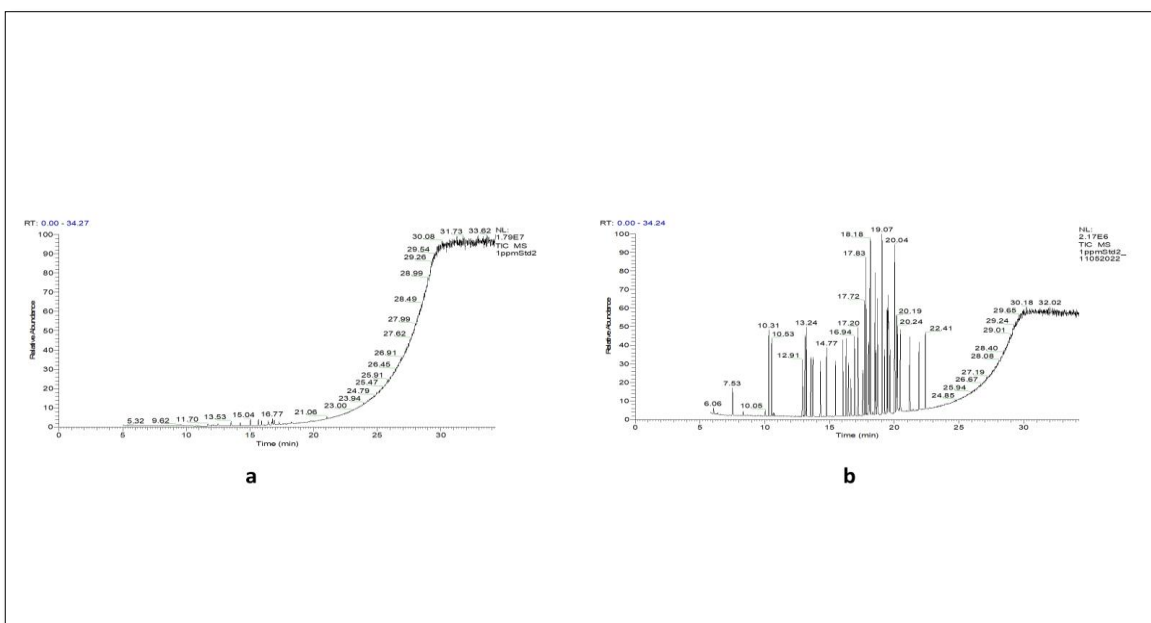


Figure 8.7: GC-EI-ITQMS Chromatogram of organochlorine pesticides (a) the standard chromatogram using Column RXI-5HT (b) the standard chromatogram using Column RXI-5MS

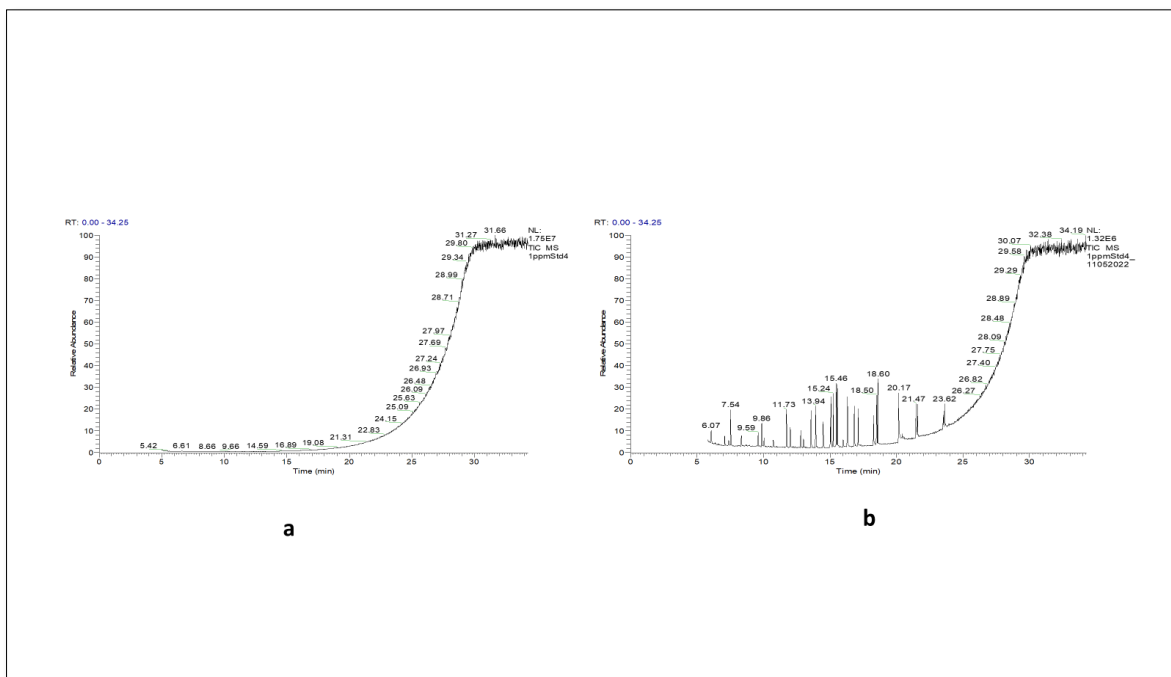


Figure 8.8: GC-EI-ITQMS Chromatogram of organonitrogen pesticides (a) the standard chromatogram using Column RXI-5HT (b) the standard chromatogram using Column RXI-5MS

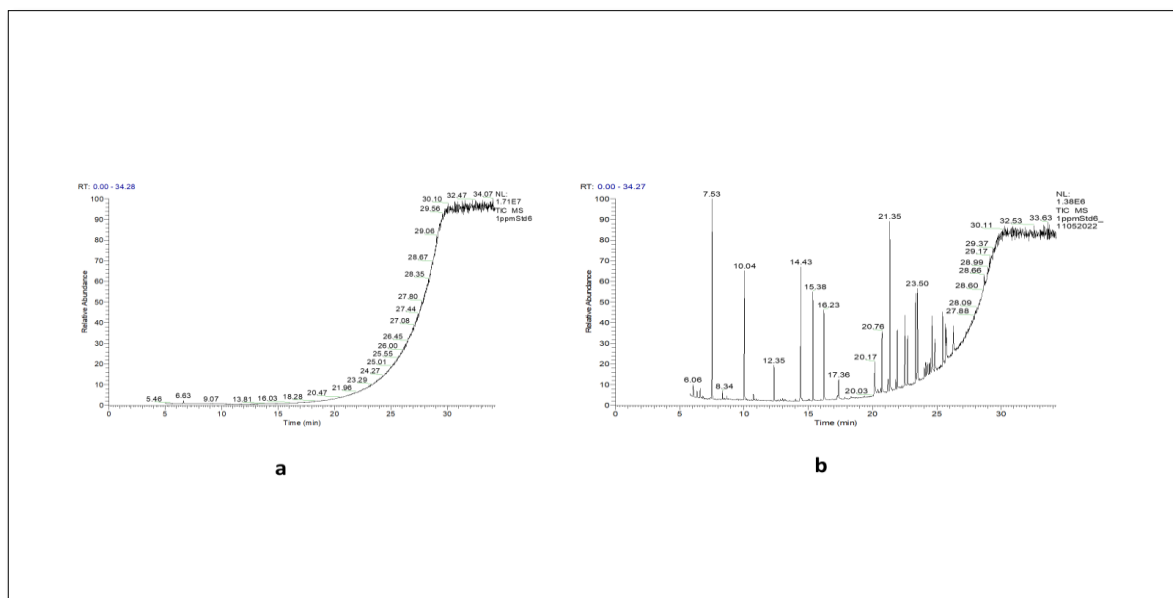


Figure 8.9: GC-EI-ITQMS Chromatogram of pyrethroid pesticides (a) the standard chromatogram using Column RXI-5HT (b) the standard chromatogram using Column RXI-5MS

8.5 Choosing the appropriate QuEChERS extraction method

There are three variations of the QuEChERS procedure in common use: ORIGINAL UNBUFFERED, EN, and AOAC 2007.01.

ORIGINAL UNBUFFERED, and AOAC 2007.01 are commonly used with pesticides analysis.

As part of the development of the method, these procedures were tested in the baby milk matrix to a comparison of effectiveness.

In fact, the end result showed little difference for our desired analysis as shown in figure 8.10, but AOAC 2007.01 was chosen because it has buffering agents to control pH. Since the study will be using a number of pesticide classes with different classifications, we must take into account that some of these pesticides are sensitive to pH.

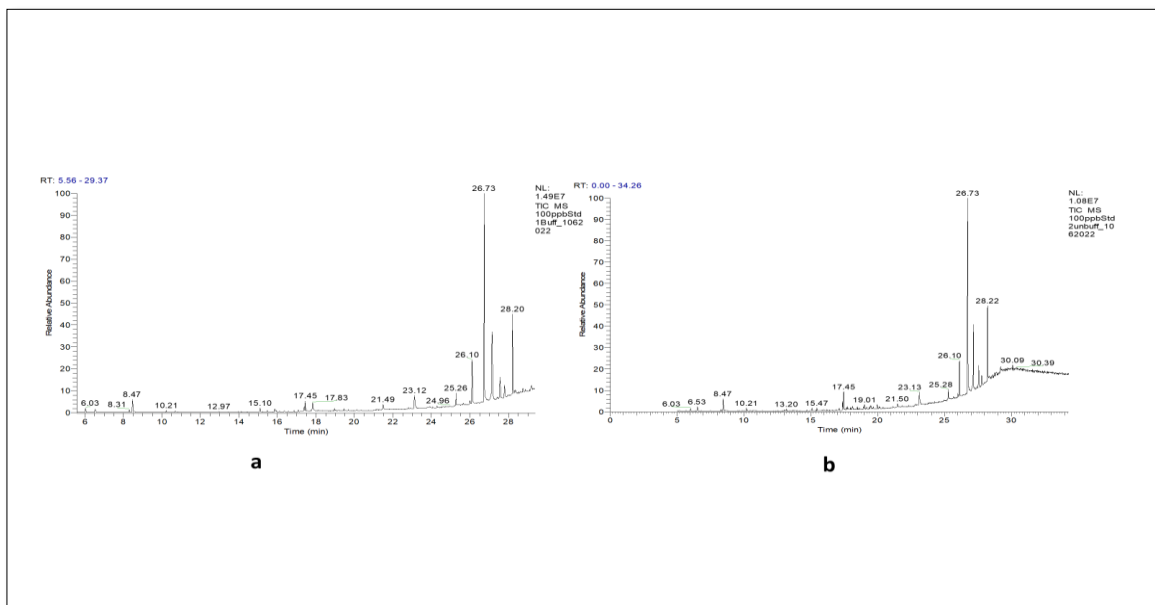


Figure 8.10: Example of total ion chromatogram (TIC) of blank baby milk (a) obtained from AOAC2007 QuEChERS extraction method (b) obtained from original unbuffered QuEChERS extraction method

8.6 Use dry N₂ when analysis of pesticides using GC-SICRIT-LTQMS

‘Wet’ nitrogen was used in the ionization process using the GC-SICRIT-LTQMS instrument, but through the results obtained, it was shown that the presence of water affects the sensitivity and accuracy of the measurements. Comparison with the use of ‘dry’ nitrogen in our experiments showed that more reliable results are obtained, figure 8.11.

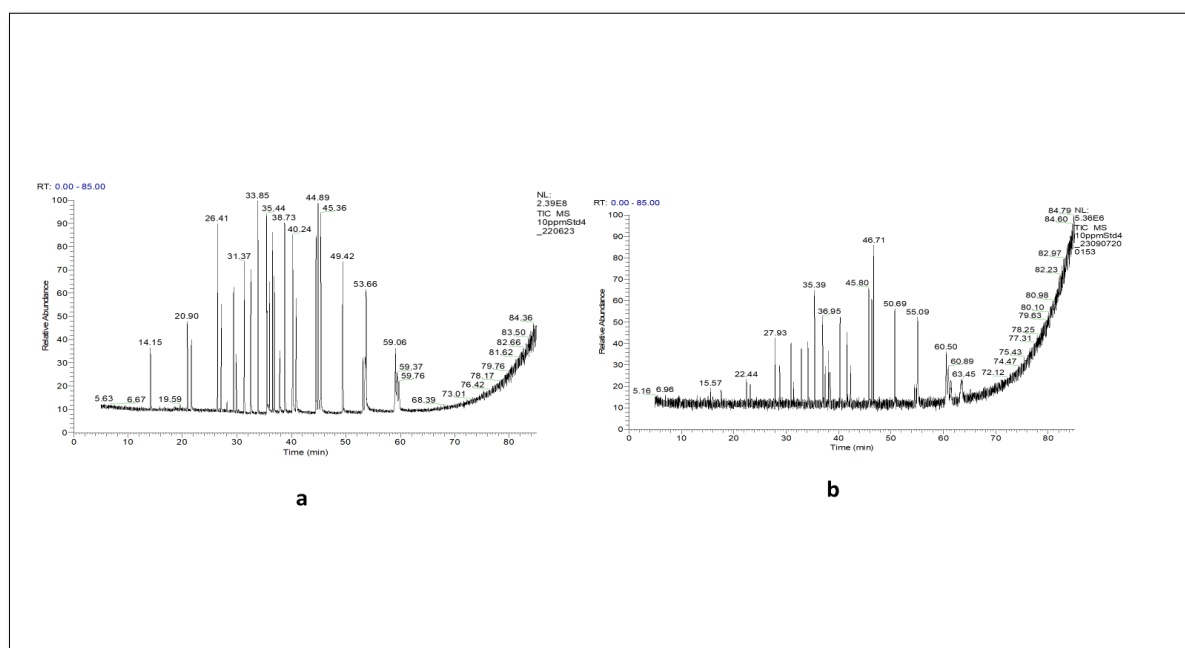


Figure 8.11: Gas Chromatography of organonitrogen pesticides Using GC-SICRIT-LTQMS (a) using dry N₂ (b) using wet N₂

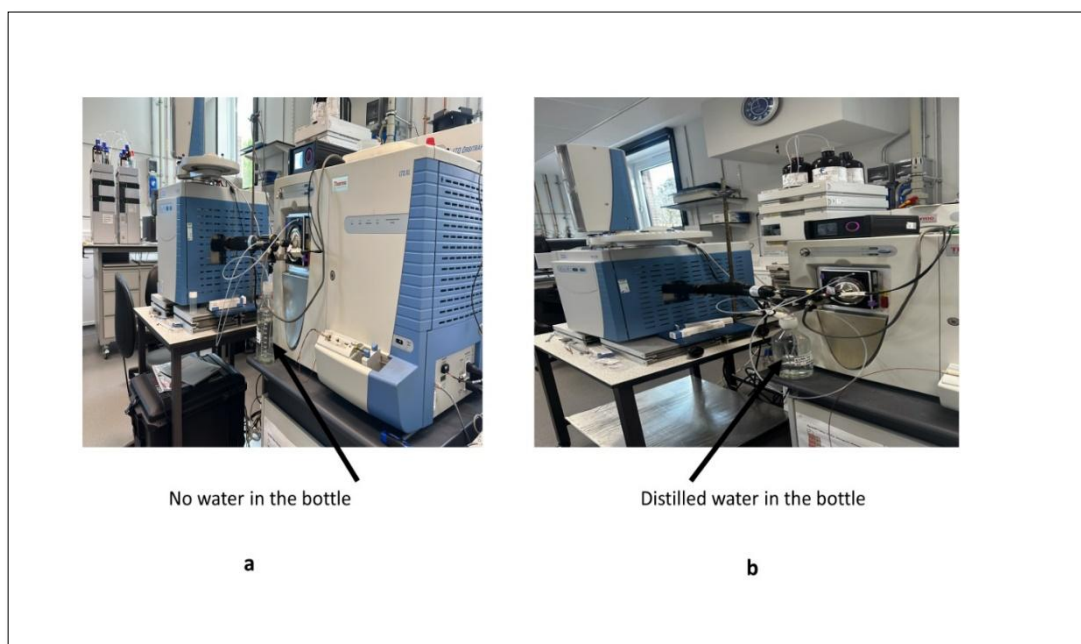


Figure 8.12: photograph of SICRIT setup (a) using dry N₂ (b) using wet N₂



Figure 8.13: Photograph of SICRIT connected to GC and LTQMS.

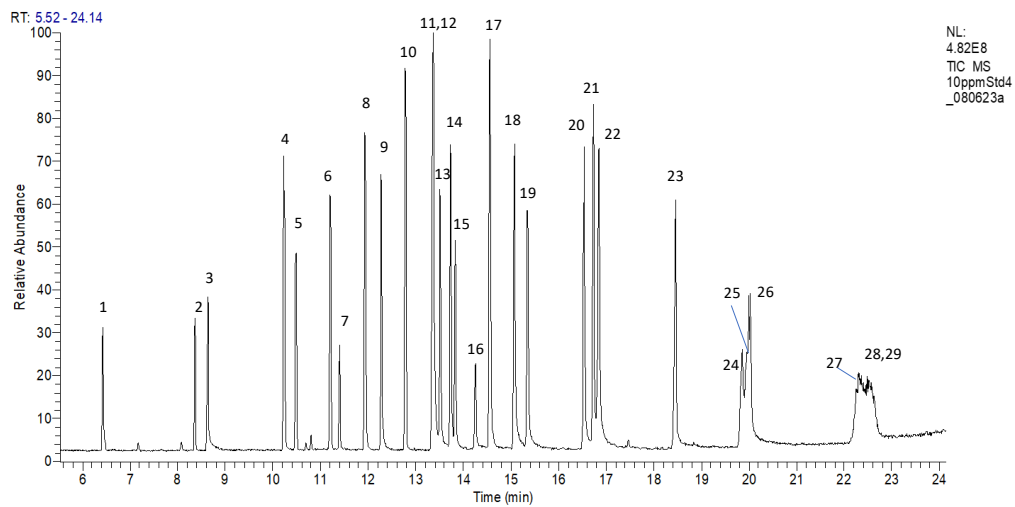


Figure 8.14: GC-MS-TIC separation chromatogram of organonitrogen pesticides (29Compound), method 1.

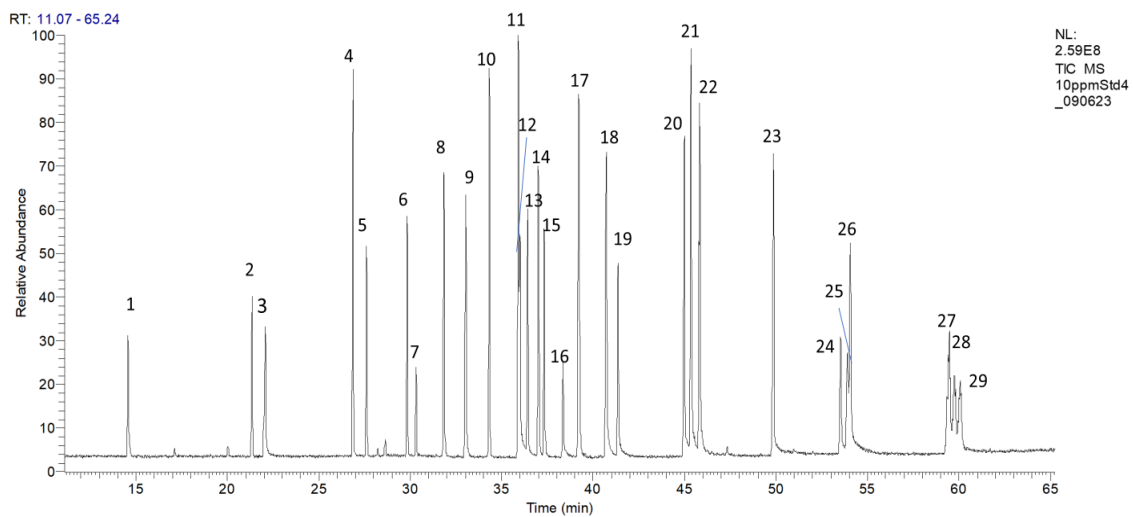


Figure 8.15 :GC-MS-TIC separation chromatogram of organonitrogen pesticides (92Compound), method 2.

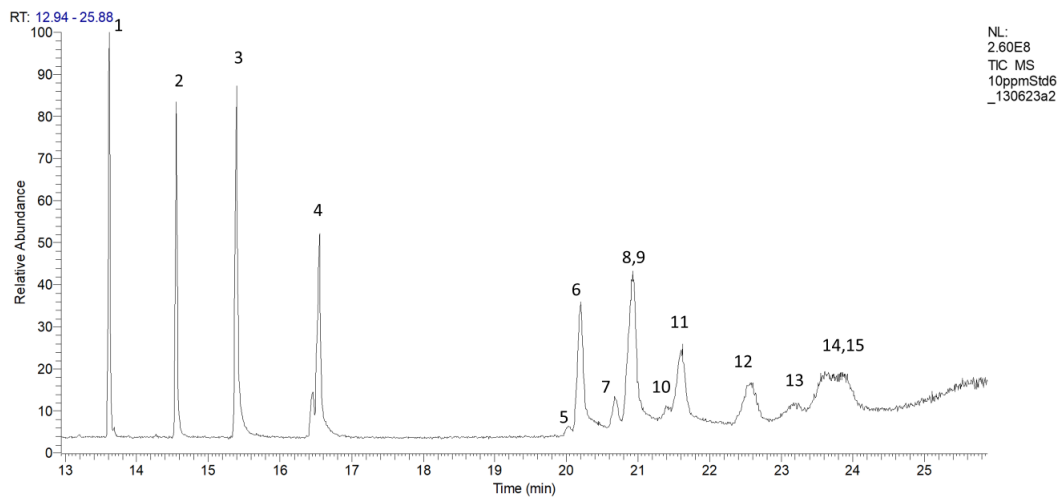


Figure 8.16: GC-MS-TIC separation chromatogram of pyrethroid pesticides (30 parent Compounds and their isomers), method 1.

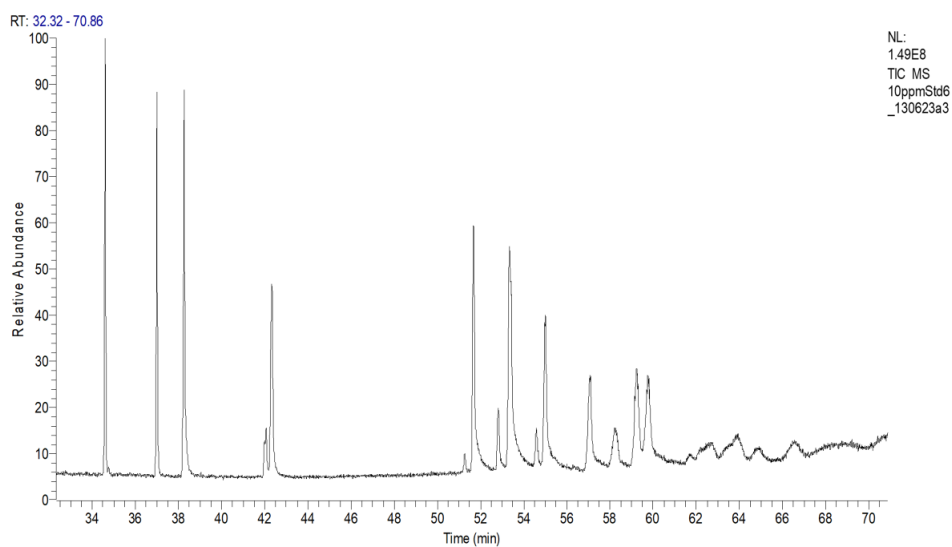


Figure 8.17: GC-MS-TIC separation chromatogram of pyrethroid pesticides (30 parent Compounds and their isomers), method 2.

9. References

1. Sandra P, Tienpont B, David F. Multi-residue screening of pesticides in vegetables, fruits and baby food by stir bar sorptive extraction–thermal desorption–capillary gas chromatography–mass spectrometry. *J Chromatogr A*. 2003;1000:299-309.
2. Klerks M, Román S, Haro-Vicente JF, Bernal MJ, Sanchez-Siles LM. Healthier and more natural reformulated baby food pouches: Will toddlers and their parents sensory accept them? *Food Qual Prefer*. 2022;99:104577.
3. Prata R, Petrarca MH, Filho JT, Godoy HT. Simultaneous determination of furfural, 5-hydroxymethylfurfural and 4-hydroxy-2,5-dimethyl-3(2H)-furanone in baby foods available in the Brazilian market. *J Food Compos Anal*. 2021;99:103874. doi:10.1016/j.jfca.2021.103874
4. Eyring P, Tienstra M, Mol H, Herrmann SS, Rasmussen PH, Frandsen HL, Poulsen ME. Development of a new generic extraction method for the analysis of pesticides, mycotoxins, and polycyclic aromatic hydrocarbons in representative animal feed and food samples. *Food Chem*. 2021;356:129653. doi:10.1016/j.foodchem.2021.129653
5. Notardonato I, Russo MV, Vitali M, Protano C, Avino P. Analytical method validation for determining organophosphorus pesticides in baby foods by a modified liquid–liquid microextraction method and gas chromatography–ion trap/mass spectrometry analysis. *Food Anal Methods*. 2019;12(1):41-50. doi:10.1007/s12161-018-1335-6
6. Petrarca MH, Fernandes JO, Godoy HT, Cunha SC. Multiclass pesticide analysis in fruit-based baby food: A comparative study of sample preparation techniques previous to gas chromatography-mass spectrometry. *Food Chem*. 2016;212:528-536. doi:10.1016/j.foodchem.2016.06.010
7. Global Market Insights Inc. Baby Food Market Analysis. Retrieved from <https://www.gminsights.com/industry-analysis/baby-food-market>.
8. Alghamdi BA, Alshumrani ES, Saeed MSB, Rawas GM, Alharthi NT, Baeshen MN, et al. Analysis of sugar composition and pesticides using HPLC and GC–MS techniques in honey samples collected from Saudi Arabian markets. *Saudi J Biol Sci*. 2020;27(12):3720-3726.
9. Hassaan MA, El Nemr A. Pesticides pollution: Classifications, human health impact, extraction and treatment techniques. *Egypt J Aquat Res*. 2020;46(3):207-220.
10. Kaur R, Mavi GK, Raghav S, Khan I. Pesticides classification and its impact on environment. *Int J Curr Microbiol Appl Sci*. 2019;8(3):1889-1897.
11. Buchel KH. *Chemistry of pesticides*. Wiley; 1983.
12. Yadav IC, Devi NL. Pesticides classification and its impact on human and environment. *Environ Sci Eng*. 2017;6:140-158.
13. U.S. Environmental Protection Agency. Pesticide Registration. 2024. Retrieved from <https://www.epa.gov/pesticide-registration>

14. Racke KD. Degradation of organophosphorus insecticides in environmental matrices. In: *Organophosphates Chemistry, Fate, and Effects*. Academic Press; 1992. p. 47-78.
15. Mileson BE, Chambers JE, Chen WL, Dettbarn W, Ehrich M, Eldefrawi AT, et al. Common mechanism of toxicity: a case study of organophosphorus pesticides. *Toxicol Sci*. 1998;41(1):8-20.
16. Sikka SC, Gurbuz N. Reproductive toxicity of organophosphate and carbamate pesticides. In: *Toxicology of organophosphate & carbamate compounds*. Academic Press; 2006. p. 447-62.
17. Costa LG. Current issues in organophosphate toxicology. *Clin Chim Acta*. 2006;366(1-2):1-13.
18. Zhou M, Wang J, Yang H, Ji X, Qian M, Li Z. Organophosphate ester concentrations in infant food and dietary risk assessment for the infant population in China. *Food Control*. 2022;139:109107.
19. Stepán R, Tichá J, Hajslová J, Kovalczuk T, Kocourek V. Baby food production chain: Pesticide residues in fresh apples and products. *Food Addit Contam*. 2005;22(12):1231-42.
20. Araújo MF, Castanheira EMS, Sousa SF. The Buzz on Insecticides: A Review of Uses, Molecular Structures, Targets, Adverse Effects, and Alternatives. *Molecules*. 2023;28(8):3641.
21. Christ L, Dreesmann DC. SAD but True: Species Awareness Disparity in Bees Is a Result of Bee-Less Biology Lessons in Germany. *Sustainability*. 2022;14(5):2604.
22. Sannino A, Bolzoni L, Bandini M. *J Chromatogr A*. 2004;1036:161-9.
23. Nassar AMK, Salim YM, Malhat FM. Assessment of Pesticide Residues in Human Blood and Effects of Occupational Exposure on Hematological and Hormonal Qualities. *Pak J Biol Sci*. 2016;19:95-105.
24. Rusiecki JA, Baccarelli A, Bollati V, Tarantini L, Moore LE, Bonefeld-Jorgensen EC. Global DNA hypomethylation is associated with high serum-persistent organic pollutants in Greenlandic Inuit. *Environ Health Perspect*. 2008;116(11):1547-52.
25. Jeong Y, Lee S, Kim S, Choi S-D, Park J, Kim H-J, et al. Occurrence and exposure assessment of polychlorinated biphenyls and organochlorine pesticides from homemade baby food in Korea. *Sci Total Environ*. 2014;470-471:1370-5.
26. Kaiser, J. (2000). ENDOCRINE DISRUPTERS: Panel Cautiously Confirms Low-Dose Effects. *Science*, 290(5492), 695–697. <https://doi.org/10.1126/science.290.5492.695>
27. Briz V, Molina-Molina JM, Sánchez-Redondo S, Fernández MF, Grimalt JO, Olea N, et al. Differential estrogenic effects of the persistent organochlorine pesticides dieldrin, endosulfan, and lindane in primary neuronal cultures. *Toxicol Sci*. 2011;120(2):413-27.

28. USEPA. Endosulfan. The Health Effects Division's Human Health Risk Assessment. 2010. EPA DP Barcode: D372569. Docket No.: EPA-HQ-OPP-2002-0262-0178; <http://www.regulations.gov>.
29. Damale RD, Dutta A, Shaikh N, Pardeshi A, Shinde R, Babu KD, et al. Multiresidue analysis of pesticides in four different pomegranate cultivars: Investigating matrix effect variability by GC-MS/MS and LC-MS/MS. *Food Chem.* 2023;407:135179.
30. Nasser S, Dehghani M, Amin S, Naddafi K, Zamanian Z. Fate of Atrazine in the agricultural soil of corn fields in Fars province of Iran. *Iran J Environ Health Sci Eng.* 2009;6(4):223-32.
31. El Bouraie MM, El Barbary AA, Yehia MM. Examining the concentration of organonitrogen pesticides in water at Nile Delta, Egypt. *Iran J Energy Environ.* 2011;2(4):331-8. <https://doi.org/10.5829/idosi.ijee.2011.02.04.2558>
32. Kandil H, Ibrahim SA. Influence of some selective herbicides on growth, yield and nutrients content of wheat (*Triticum aestivum* L.) plants. *J Basic Appl Sci Res.* 2011;1(1):201-7.
33. Donley N. The USA lags behind other agricultural nations in banning harmful pesticides. *Environ Health.* 2019;18:44. <https://doi.org/10.1186/s12940-019-0488-0>
34. Reigert JR, Roberts JR. Organophosphate Insecticides. Recognition and Management of Pesticide Poisonings. U.S. Environmental Protection Agency, Office of Prevention, Pesticides and Toxic Substances, Office of Pesticide Programs, U.S. Government Printing Office. 5th ed. 1999;5:34-40.
35. Valmorbidia I, Hohenstein JD, Coates BS, Bevilaqua JG, Menger J, Hodgson EW, et al. Association of voltage-gated sodium channel mutations with field-evolved pyrethroid resistant phenotypes in soybean aphid and genetic markers for their detection. *Sci Rep.* 2022;12(1):1-14.
36. Li H, Cheng F, Wei Y, Lydy MJ, You J. Global occurrence of pyrethroid insecticides in sediment and the associated toxicological effects on benthic invertebrates: An overview. *J Hazard Mater.* 2016;324:258-71. <https://doi.org/10.1016/j.jhazmat.2016.10.024>
37. Goel A, Aggarwal P. Pesticide poisoning. *Natl Med J India.* 2007;20(4):182.
38. Feo ML, Eljarrat E, Barcelo D. Determination of pyrethroid insecticides in environmental samples. *TrAC Trends Anal Chem.* 2010;29(7):692-705. doi: 10.1016/j.trac.2010.03.011
39. Damalas CA, Eleftherohorinos IG. Pesticide exposure, safety issues, and risk assessment indicators. *Int J Environ Res Public Health.* 2011;8(5):1402-19.
40. Harrison JL. Pesticide drift and the pursuit of environmental justice. Cambridge, Mass: MIT Press; 2011.
41. American College of Obstetricians and Gynecologists. Reducing Prenatal Exposure to Toxic Environmental Agents: Committee Opinion Number 832 (Replaces Committee Opinion Number 575, October 2013. Reaffirmed 2024). Committee on Obstetric Practice. Endorsed by the American College of Nurse-Midwives. 2021.

42. Peshin R, Dhawan AK. Integrated pest management: innovation-development process. Dordrecht: Springer; 2009.
43. Kanthasamy A, Jin H, Anantharam V, Sondarva G, Rangasamy V, Rana A. Fyn kinase regulates misfolded α -synuclein uptake and NLRP3 inflammasome activation in microglia. *J Neuroinflammation*. 2019;16(1):1-15.
44. Damalas CA, Koutroubas SD. Farmers' exposure to pesticides: Toxicity types and ways of prevention. *Toxics*. 2016;4(1):1-10.
45. Repetto R, Baliga SS. Pesticides and Immunosuppression: The Risks to Public Health. *Health Policy Plan*. 1997;12(2):97-106. doi: 10.1093/heapol/12.2.97.
46. Beyond Pesticides. Breakdown products (metabolites) from pesticides may be more toxic than parent compound, study finds. 2021 May 6. Available from: <https://beyondpesticides.org/dailynewsblog/2021/05/breakdown-products-metabolites-from-pesticides-may-be-more-toxic-than-parent-compound-study-finds/>
47. Christensen, N. L., Bartuska, A. M., Brown, J. H., Carpenter, S., D'Antonio, C., Francis, R., Franklin, J. F., MacMahon, J. A., Noss, R. F., Parsons, D. J., Peterson, C. H., Turner, M. G., & Woodmansee, R. G. (1996). The Report of the Ecological Society of America Committee on the Scientific Basis for Ecosystem Management. *Ecological Applications*, 6(3), 665–691. <https://doi.org/10.2307/2269460>
48. Available from: www.epa.gov/ocfo
49. Statutory Interpretation. Federal Food, Drug, and Cosmetic Act. Fourth Circuit Holds That FDA Lacks Jurisdiction to Regulate Tobacco. *Brown & Williamson Tobacco Corp. v. Food & Drug Administration*, 153 F.3d 155 (4th Cir.), reh'g en banc Denied, 1998 U. S. App. LEXIS 28409 (4th Cir. Nov. 10, 1998). (1998). *Harvard Law Review*, 112(2), 572. <https://doi.org/10.2307/1342430>
50. Saviola, J. F., Hilmantel, G., & Rosenthal, A. R. (2003). The U. S. Food and Drug Administration's Role in Contact Lens Development and Safety. *Eye & Contact Lens: Science & Clinical Practice*, S160–S165. <https://doi.org/10.1097/00140068-200301001-00044>
51. Levin TM. The Infant Formula Act of 1980: A Case Study of Congressional Delegation to the Food and Drug Administration. *Food Drug Cosmet Law J*. 1987;42(1):101-154.
52. EUR-Lex. Regulation (EU) No 609/2013 of the European Parliament and of the Council. 2013. Available from: EUR-Lex website.
53. EUR-Lex. Commission Delegated Regulation (EU) 2016/127. 2016. Available from: EUR-Lex website.
54. Government of Canada. Safe Food for Canadians Act (SFCA). Available from: Justice Laws website.
55. Justice Laws Website - Site Web de la législation (Justice). *Laws-Lois.justice.gc.ca*. Retrieved July 7, 2021, from <http://laws-lois.justice.gc.ca/>
56. Wahab S, Muzammil K, Nasir N, Khan MS, Ahmad MF, Khalid M, Ahmad W, Dawria A, Reddy LKV, Busayli AM. Advancement and New Trends in Analysis of Pesticide Residues in Food: A Comprehensive Review. *Plants*

- (Basel). 2022 Apr 19;11(9):1106. doi: 10.3390/plants11091106. PMID: 35567107; PMCID: PMC9105315.
57. Umapathi R, Park B, Sonwal S, Rani GM, Cho Y, Huh YS. Advances in optical-sensing strategies for the on-site detection of pesticides in agricultural foods. *Trends Food Sci Technol*. 2022;119:69-89.
 58. Wasik A, Kot-Wasik A, Namiesnik J. New trends in sample preparation techniques for the analysis of the residues of pharmaceuticals in environmental samples. *Curr Anal Chem*. 2016;12(4):280-302.
 59. Ribeiro C, Ribeiro AR, Maia AS, Goncalves VM, Tiritan ME. New trends in sample preparation techniques for environmental analysis. *Crit Rev Anal Chem*. 2014;44(2):142-185.
 60. Alsharif AMA, Tan GH, Choo YM, Lawal A. Efficiency of hollow fiber liquid-phase microextraction chromatography methods in the separation of organic compounds: a review. *J Chromatogr Sci*. 2017;55(3):378-391.
 61. Mohebbi A, Farajzadeh MA, Mahmoudzadeh A, Etemady A. Combination of poly (ϵ -caprolactone) grafted graphene quantum dots-based dispersive solid phase extraction followed by dispersive liquid-liquid microextraction for extraction of some pesticides from fruit juices prior to their quantification by gas chromatography. *Microchem J*. 2020;153:104328.
 62. Samsidar A, Siddiquee S, Shaarani SM. A review of extraction, analytical and advanced methods for determination of pesticides in environment and foodstuffs. *Trends Food Sci Technol*. 2018;71:188-201.
 63. Lambropoulou DA, Albanis TA. Methods of sample preparation for determination of pesticide residues in food matrices by chromatography-mass spectrometry-based techniques: a review. *Anal Bioanal Chem*. 2007;389:1663-1683.
 64. Syrgabek Y, Alimzhanova M. Modern Analytical Methods for the Analysis of Pesticides in Grapes: A Review. *Foods*. 2022;11(11):1623.
 65. Harvey D. Modern analytical chemistry. Boston: McGraw-Hill; 2000. ISBN: 0-07-237547-7.
 66. Pavia L, Lampman GM, Kriz GS, Engel RG. Introduction to Organic Laboratory Techniques. 4th ed. Thomson Brooks/Cole; 2006. p. 797-817. ISBN: 978-0-495-28069-9.
 67. El-Naggar AY. Factors affecting selection of mobile phase in gas chromatography. *Am J Res Commun*. 2013;1(3):219-228. ISSN: 2325-4076. Available from: www.usa-journals.com.
 68. Harris DC. Quantitative chemical analysis. 9th ed. New York: Charles A. Lucy; 2016. ISBN: 978-1-4641-3538-5.
 69. Kazar Soydan D, Turgut N, Yalçın M, Turgut C, Karakuş PBK. Evaluation of pesticide residues in fruits and vegetables from the Aegean region of Turkey and assessment of risk to consumers. *Environ Sci Pollut Res Int*. 2021;28:27511-27519.

70. Cámara MA, Cermeño S, Martínez G, Oliva J. Removal residues of pesticides in apricot, peach and orange processed and dietary exposure assessment. *Food Chem.* 2020;325:126936.
71. Horning EC, Horning MG, Carroll DI, Dzidic I, Stillwell RN. New picogram detection system based on a mass spectrometer with an external ionization source at atmospheric pressure. *Anal Chem.* 1973;45:936-943. doi: 10.1021/ac60328a035.
72. Ayala-Cabrera JF, Turkowski J, Uteschil F, Schmitz OJ. Development of a Tube Plasma Ion Source for Gas Chromatography–Mass Spectrometry Analysis and Comparison with Other Atmospheric Pressure Ionization Techniques. *Anal Chem.* 2022;94(27):9595-602. doi: 10.1021/acs.analchem.2c00582.
73. Kersten, H., Kroll, K., Haberer, K., Brockmann, K. J., Benter, T., Peterson, A., & Makarov, A. (2016). Design Study of an Atmospheric Pressure Photoionization Interface for GC-MS. *Journal of the American Society for Mass Spectrometry*, 27(4), 607–614. <https://doi.org/10.1007/s13361-015-1320-x>
74. Rüter CP, Neumann A, Sklorz M, Zimmermann R. Atmospheric Pressure Single Photon Laser Ionization (APSPLI) Mass Spectrometry Using a 157 nm Fluorine Excimer Laser for Sensitive and Selective Detection of Non- to Semipolar Hydrocarbons. *Anal Chem.* 2021;93(8):3691-3697. doi: 10.1021/acs.analchem.0c04740.
75. Ayala-Cabrera JF, Lipok C, Moyano E, Schmitz OJ, Santos FJ. Atmospheric pressure ionization for gas chromatography-high resolution mass spectrometry determination of polychlorinated naphthalenes in marine sediments. *Chemosphere.* 2021;263:127963.
76. Portolés T, Mol JG, Sancho JV, Hernández F. Use of electron ionization and atmospheric pressure chemical ionization in gas chromatography coupled to time-of-flight mass spectrometry for screening and identification of organic pollutants in waters. *J Chromatogr A.* 2014 Apr 25;1339:145-53. doi: 10.1016/j.chroma.2014.03.001. Epub 2014 Mar 11. PMID: 24674644.
77. Schiewek R, Schellenträger M, Mönnikes R, Lorenz M, Giese R, Brockmann KJ, Gäb S, Benter T, Schmitz OJ. Ultrasensitive determination of polycyclic aromatic compounds with atmospheric-pressure laser ionization as an interface for GC/MS. *Anal Chem.* 2007 Jun 1;79(11):4135-40. doi: 10.1021/ac0700631. Epub 2007 May 2. PMID: 17472342.
78. Makarov A, Denisov E, Lange O, Horning S. Dynamic range of mass accuracy in LTQ Orbitrap hybrid mass spectrometer. *J Am Soc Mass Spectrom.* 2006;17:977-82.
79. Harper JD, Charipar NA, Mulligan CC, Zhang X, Cooks RG, Ouyang Z. Low-temperature plasma probe for ambient desorption ionization. *Anal Chem.* 2008;80:9097-104.
80. Dass C. *Fundamentals of Contemporary Mass Spectrometry.* John Wiley & Sons; 2007.
81. Awad H, Khamis MM, El-Aneed A. Mass spectrometry, review of the basics: ionization. *Appl Spectrosc Rev.* 2015 Feb 7;50(2):158-75.

82. Undergraduate Instrumental Analysis, Sixth Edition. (2004). CRC Press. <https://doi.org/10.1201/b15940>
83. Guo C, Tang F, Chen J, Wang X, Zhang S, Zhang X. Development of dielectric-barrier-discharge ionization. *Anal Bioanal Chem.* 2015;407(9):2345-2364. doi:10.1007/s00216-014-8281-y
84. Eliasson B, Hirth M, Kogelschatz U. Ozone synthesis from oxygen in dielectric barrier discharges. *J Phys D Appl Phys.* 1987;20(11):1421-1437. doi:10.1088/0022-3727/20/11/010
85. Adamovich I, Baalrud SD, Bogaerts A, et al. The 2017 Plasma Roadmap: Low temperature plasma science and technology. *J Phys D Appl Phys.* 2017;50(32):323001. doi:10.1088/1361-6463/aa76f5
86. Müller S, Krähling T, Veza D, Horvatic V, Vadla C, Franzke J. Operation modes of the helium dielectric barrier discharge for soft ionization. *Spectrochim Acta - Part B At Spectrosc.* 2013;85:104-111. doi:10.1016/j.sab.2013.04.005
87. Mirabelli MF, Wolf JC, Zenobi R. Direct Coupling of Solid-Phase Microextraction with Mass Spectrometry: Sub-pg/g Sensitivity Achieved Using a Dielectric Barrier Discharge Ionization Source. *Anal Chem.* 2016;88(14):7252-7258. doi:10.1021/acs.analchem.6b01507
88. Meyer C, Müller S, Gurevich EL, Franzke J. Dielectric barrier discharges in analytical chemistry. *Analyst.* 2011;136(17):3846-57. doi:10.1039/c0an00994f.
89. Beneito-Cambra M, Gilbert-López B, Moreno-González D, Bouza M, Franzke J, García-Reyes JF, Molina-Díaz A. Ambient (desorption/ionization) mass spectrometry methods for pesticide testing in food: a review. *Anal Methods.* 2020;12(40):4831-52. doi:10.1039/D0AY01474E.
90. Mirabelli MF, Wolf JC, Zenobi R. Atmospheric pressure soft ionization for gas chromatography with dielectric barrier discharge ionization-mass spectrometry (GC-DBDI-MS). *Analyst.* 2017;142(11):1909-16. doi:10.1039/C7AN00345A.
91. Sakhale A, Sankar PR, Taheera S, Vidhate MN, Gude S, Babu PS. Advancements in Mass Analyzers: A Comprehensive Overview of Cutting-Edge Technologies in Mass Spectrometry. *IOSR J Pharm.* 2023;13(6):16-31. Available from: www.iosrphr.org.
92. Domingues P, Garcia A, Skrzydlewska E, Łuczaj W. AACLifeSci Course Companion Manual: Advanced Analytical Chemistry for Life Sciences. University of Aveiro, University Foundation San Pablo CEU, Medical University of Bialystok; 2018. ISBN: 978-83-951534-7-1.
93. McMahon G. Types of Ion Detector for Mass Spectrometry. *Technology Networks.* 2021. Retrieved from Technology Networks.
94. Shabir GA. Validation of high-performance liquid chromatography methods for pharmaceutical analysis. Understanding the differences and similarities between validation requirements of the US Food and Drug Administration, the US Pharmacopeia and the International Conf. *J Chromatogr A.* 2003;987:57-66.
95. Mekonnen B, Siraj J, Negash S. Determination of Pesticide Residues in Food Premises Using QuEChERS Method in Bench-Sheko Zone, Southwest Ethiopia. *BioMed Res Int.* 2021;2021(1):6612096.
96. Araujo P. Key aspects of analytical method validation and linearity evaluation. *J Chromatogr B Anal Technol Biomed Life Sci.* 2009;877:2224-34.

97. Khan N, Yaqub G, Hafeez T, Tariq M. Assessment of health risk due to pesticide residues in fruits, vegetables, soil, and water. *J Chem.* 2020;2020(1):5497952.
98. Nemati M, Tuzen M, Farazajdeh MA, Kaya S, Mogaddam MRA. Development of dispersive solid-liquid extraction method based on organic polymers followed by deep eutectic solvents elution; application in extraction of some pesticides from milk samples prior to their determination by HPLC-MS/MS. *Anal Chim Acta.* 2022;1199:339570.
99. Taverniers I, De Loose M, Van Bockstaele E. Trends in quality in the analytical laboratory. II. Analytical method validation and quality assurance. *TrAC Trends Anal Chem.* 2004;23:535-52.
100. Bulaić Nevistić M, Kovač Tomas M. Matrix Effect Evaluation in GC/MS-MS Analysis of Multiple Pesticide Residues in Selected Food Matrices. *Foods.* 2023;12:3991. <https://doi.org/10.3390/foods12213991>.
101. Green J. Peer Reviewed: A Practical Guide to Analytical Method Validation. *Anal Chem.* 1996;68:305A-309A.
102. Hrvat, N. M., & Kovarik, Z. (2020). Counteracting poisoning with chemical warfare nerve agents. *Archives of Industrial Hygiene and Toxicology*, 71(4), 266–284. <https://doi.org/10.2478/aiht-2020-71-3459>
103. Ballantyne B, Marrs TC. *Overview of the Biological and Clinical Aspects of Organophosphates and Carbamates.* Butterworth-Heinemann Ltd; 1992.
104. Jaleel CA, Gopi R, Manivannan P, Panneerselvam R. Exogenous application of triadimefon affects the antioxidant defense system of *Withania somnifera* Dunal. *Pestic Biochem Physiol.* 2008;91:170-4.
105. Xiong J, Hu B. Comparison of hollow fiber liquid phase microextraction and dispersive liquid-liquid microextraction for the determination of organosulfur pesticides in environmental and beverage samples by gas chromatography with flame photometric detection. *J Chromatogr A.* 2008;1193:7-18.
106. Palanivelu J, Chidambaram R. Acetylcholinesterase with mesoporous silica: Covalent immobilization, physiochemical characterization, and its application in food for pesticide detection. *J Cell Biochem.* 2019;120:10777-86.
107. Claeys WL, Schmit JF, Bragard C, Maghuin-Rogister G, Pussemier L, Schiffers B. Exposure of several Belgian consumer groups to pesticide residues through fresh fruit and vegetable consumption. *Food Control.* 2011;22:508-16.
108. Villaverde JJ, Sevilla-Morán B, Sandín-España P, López-Goti C, Alonso-Prados JL. Challenges of biopesticides under the European regulation (EC) No. 1107/2009: An overview of new trends in residue analysis. *Stud Nat Prod Chem.* 2014;43:437-82.
109. Nougadère A, Sirot V, Cravedi JP, Vasseur P, Feidt C, Fussell RJ, et al. Dietary exposure to pesticide residues and associated health risks in infants and young children—results of the French infant total diet study. *Environ Int.* 2020;137:105529.
110. Environmental Working Group. New EWG study: Pesticides still found in baby food but most-toxic threats eliminated through advocacy, regulation. [Internet]. 2023. Available from: <https://www.ewg.org/news-insights/news->

release/2023/11/new-ewg-study-pesticides-still-found-baby-food-most-toxic#:~:text=EWG%20sampled%2073%20products%20from [Accessed 12 Aug. 2024].

111. Pascale A, Laborde A. Impact of pesticide exposure in childhood. *Rev Environ Health*. 2020;35(3):221-227.
112. Shukla A, Malhotra S, Kumar M, Singla N. Pesticides and human health: The noxious impact on maternal system and fetal development. In: *Pesticides in the Natural Environment*. 2022. p. 209-226.
113. Bhattu M, Kathuria D, Billing BK, Verma M. Chromatographic techniques for the analysis of organophosphate pesticides with their extraction approach: a review (2015-2020). *Anal Methods*. 2022;14(4):322-358. doi: 10.1039/d1ay01404h. PMID: 34994766.
114. European Commission. Guidance Document on Analytical Quality Control and Method Validation Procedures for Pesticides Residues Analysis in Food and Feed, SANTE/11813/2017. 2017.
115. Shrivastava A, Gupta V. Methods for the determination of limit of detection and limit of quantitation of the analytical methods. *Chron Young Sci*. 2011;2:21. doi: 10.4103/2229-5186.79345.
116. Fernández-Alba AR. Chromatographic-Mass Spectrometric Food Analysis for Trace Determination of Pesticide Residues. In: *Wilson & Wilson's comprehensive analytical chemistry*. 1st ed. Amsterdam: Elsevier; 2005.
117. Pizzutti, I. R., Dias, J. V., Kok, A. de, Cardoso, C. D., & Vela, E. (2016). Pesticide Residues Method Validation by UPLC-MS/MS for Accreditation Purposes. *Journal of the Brazilian Chemical Society*. <https://doi.org/10.5935/0103-5053.20160012>
118. Rutkowska, E., Łozowicka, B., & Kaczyński, P. (2017). Modification of Multiresidue QuEChERS Protocol to Minimize Matrix Effect and Improve Recoveries for Determination of Pesticide Residues in Dried Herbs Followed by GC-MS/MS. *Food Analytical Methods*, 11(3), 709–724. <https://doi.org/10.1007/s12161-017-1047-3>
119. Pizzutti IR, Kok A, Hiemstra M, Wickert C, Prestes OD. *J Chromatogr A*. 2009;1216:4539.
120. Wolf JC, Gyr L, Mirabelli MF, Schaer M, Siegenthaler P, Zenobi R. A Radical-Mediated Pathway for the Formation of $[M + H]^+$ in Dielectric Barrier Discharge Ionization. *J Am Soc Mass Spectrom*. 2016;27(9):1468-1475. doi: 10.1007/s13361-016-1420-2.
121. Barceló D. Environmental Protection Agency and Other Methods for the Determination of Priority Pesticides and Their Transformation Products in Water. *J Chromatogr*. 1993;643:117-143.
122. Boyd-Boland A, Pawliszyn JB. Determination of Triazines and Amides in Water Using Solid Phase Microextraction Coupled with GC-MS. *J Chromatogr A*. 1995;704:163-172.
123. Tronczynski J, Munsch C, Durand G, Barceló D. GCMS Determination, Occurrence and Distribution of Trace-Levels of Herbicides and Their

- Degradation Products in the Rhone River, France. *Sci Total Environ.* 1993;132:327-334.
124. Pereira WE, Rostad CE, Leiker TJ. Determination of trace levels of herbicides and their degradation products in surface and ground waters by gas chromatography/ion-trap mass spectrometry. *Anal Chim Acta.* 1990;228:69-75.
 125. Soniassy R, Sandra P, Schlett C. *Water analysis: organic micropollutants. A practical guide.* Hewlett-Packard Publication No. 5962-6216E. 1994. p. 225-41.
 126. Brugard DJ, Dowdy RH, Koskinen WC, Cheng HH. Movement of metribuzin in a loamy sand soil under irrigated potato production. *Weed Sci.* 1994;42:462-8.
 127. Peterson HG, Boutin C, Martin PA, Freemark KE, Moody MM. Toxicity of hexazinone and diquat to green algae, diatoms, cyanobacteria and duckweed. *Aquat Toxicol.* 1994;28:275-81.
 128. Hileman B. Concerns broaden over chlorine and chlorinated hydrocarbons. *Chem Eng News.* 1993;71:11-7.
 129. Johnson RM, Pepperman AB. Analysis of pesticides in water using liquid chromatography. *J Liq Chromatogr.* 1995;18:739-53.
 130. Anyakudo F, Adams E, Van Schepdael A. Thin-layer chromatography–flame ionization detection. *Chromatographia.* 2020;83(2):149-57.
 131. Gautam A, Kumar U, Yadav A, Boadh R, Aggarwal M, Khandal RK. Nutritional aspects of ready-to-eat and homemade food products with emphasis on fatty acid profiling of ready-to-eat food using GC-FID technique—a comparative study. *J Pharm Negat Results.* 2022;2825-46.
 132. Martinez G, Niu J, Takser L, Bellenger JP, Zhu J. A review on the analytical procedures of halogenated flame retardants by gas chromatography coupled with single quadrupole mass spectrometry and their levels in human samples. *Environ Pollut.* 2021;285:117476.
 133. Pico Y, Alfarhan AH, Barcelo D. How recent innovations in gas chromatography-mass spectrometry have improved pesticide residue determination: an alternative technique to be in your radar. *TrAC Trends Anal Chem.* 2020;122:115720.
 134. Arsene C, Vione D, Grinberg N, Olariu RI. GC×GC-MS hyphenated techniques for the analysis of volatile organic compounds in air. *J Liq Chromatogr Relat Technol.* 2011;34(13):1077-111.
 135. Wen HC, Wilczek T, Neudörfl JM, Wagener F, Piper T, Thevis M, Schäfer M. A comprehensive gas chromatography electron ionization high resolution mass spectrometry study of a new steroidal selective androgen receptor modulator (SARM) compound S42. *J Mass Spectrom.* 2024;59(8):e5077.
 136. Gosselin RE. *Clinic toxicological of commercial products.* Baltimore, MD: Williams and Wilkins; 1984.
 137. Ding, G., Shi, R., Gao, Y., Zhang, Y., Michihiro Kamijima, Sakai, K., Wang, G., Feng, C., & Tian, Y. (2012). Pyrethroid Pesticide Exposure and Risk of Childhood Acute Lymphocytic Leukemia in Shanghai. *Environmental Science & Technology*, 46(24), 13480–13487. <https://doi.org/10.1021/es303362a>

138. Zhang, Q., Zhang, W., Wang, X., & Li, P. (2010). Immunoassay Development for the Class-Specific Assay for Types I and II Pyrethroid Insecticides in Water Samples. *Molecules*, 15(1), 164–177.
<https://doi.org/10.3390/molecules15010164>
139. Roberts JR, Karr CJ, Paulson JA, Brock-Utne AC, Brumberg HL, Campbell CC, et al. Pesticide exposure in children. *Pediatrics*. 2012;130(6):e1757-63.
140. Garry VF. Pesticides and children. *Toxicol Appl Pharmacol*. 2004;198(2):152-63.
141. Soderlund DM. Molecular mechanisms of pyrethroid insecticide neurotoxicity: recent advances. *Arch Toxicol*. 2012;86(2):165-81.
142. Ahamad A, Kumar J. Pyrethroid pesticides: An overview on classification, toxicological assessment and monitoring. *J Hazard Mater Adv*. 2023;10:100284.
143. Corcellas C, Eljarrat E, Barceló D. Enantiomeric-selective determination of pyrethroids: application to human samples. *Anal Bioanal Chem*. 2015;407:779-86. doi: 10.1007/s00216-014-7905-6.
144. Ayala-Cabrera JF, Montero L, Meckelmann SW, Uteschil F, Schmitz OJ. Review on atmospheric pressure ionization sources for gas chromatography-mass spectrometry. Part I: Current ion source developments and improvements in ionization strategies. *Anal Chim Acta*. 2023;1238:340353.
145. Golden RJ, Noller KL, Titus-Ernstoff L, Kaufman RH, Mittendorf R, Stillman R, Reese EA. Environmental endocrine modulators and human health: an assessment of the biological evidence. *Crit Rev Toxicol*. 1998;28:109-227.
146. Hosie S, Loff S, Witt K, Niessen K, Waag KL. Is there a correlation between organochlorine compounds and undescended testis? *Eur J Pediatr Surg*. 2000;10:304-9.
147. Tiemann U. In vivo and in vitro effects of the organochlorine pesticides DDT, TCPM, methoxychlor, and lindane on the female reproductive tract of mammals: A review. *Reprod Toxicol*. 2008;25(3):316-26.
148. Waliszewski SM, Villalobos-Pietrini R, Gómez-Arroyo S, Infanzón RM. Persistent organochlorine pesticides in Mexican butter. *Food Addit Contam*. 2003;20(4):361-7.
149. Da Silva RL, Da Silva CP, Navickiene S. Multiresidue determination of carbamate, organochlorine organophosphorus, and dicarboximide pesticides in lettuce by GC/MS. *J Environ Sci Health B*. 2010;45:589-94.
150. Toteja GS, Mukherjee A, Diwakar S, Singh P, Saxena BN. Residues of DDT and HCH pesticides in rice samples from different geographical regions of India: a multicentre study. *Food Addit Contam*. 2003;20(10):933-9.
151. Bakore N, John PJ, Bhatnagar P. Organochlorine pesticide residues in wheat and drinking water samples from Jaipur, Rajasthan, India. *Environ Monit Assess*. 2004;98(1-3):381-9.
152. Fenske RA, Kedan G, Lu C, Fisker-Anderson JA, Curl CL. Assessment of organophosphorous pesticide exposures in the diets of preschool children in Washington State. *J Expo Anal Environ Epidemiol*. 2002;12:21-8.

153. Clayton AC, Pellizzari ED, Whitmore RW, Quackenboss JJ, Adgate J, Sefton K. Distributions, associations, and partial aggregate exposure of pesticides and polynuclear aromatic hydrocarbons in the Minnesota Children's Pesticide Exposure Study (MNCPEs). *J Expo Anal Environ Epidemiol*. 2003;13:100-11.
154. IPCS. IPCS risk assessment terminology, Part 1&2. World Health Organization, International Programme on Chemical Safety (Harmonization Project Document, No.1). 2004. Available from: http://www.who.int/ipcs/methods/harmonization/areas/ipcsterminologyparts1a_d2.pdf. Accessed 15 May 2014.
155. FSA. Risk assessment of mixtures of pesticides and similar substances. Committee on Toxicity, Food Standards Agency, FSA/0691/0902. 2012. Available from: <http://cot.food.gov.uk/pdfs/reportindexed.pdf>. Accessed 15 May 2014.
156. Bhatia R, Shiao R, Petreas M, Weintraub JM, Farhang L, Eskenazi B. Organochlorine pesticides and male genital anomalies in the child health and development studies. *Environ Health Perspect*. 2005;113(2):220-4.
157. Vega M, Romano D, Uotila E. Lindane (persistent organic pollutant) in the EU. Directorate General for Internal Policies. Policy Department C: Citizens' Rights and Constitutional Affairs. Petitions. 2016. PE 571.398. Available from: [https://www.europarl.europa.eu/RegData/etudes/STUD/2016/571398/IPOL_STU\(2016\)571398_EN.pdf](https://www.europarl.europa.eu/RegData/etudes/STUD/2016/571398/IPOL_STU(2016)571398_EN.pdf). Accessed 16 Aug 2019.
158. Martins FA, Daré JK, Freitas MP. Theoretical study of fluorinated bioisosteres of organochlorine compounds as effective and eco-friendly pesticides. *Ecotoxicol Environ Saf*. 2020;199:110679.
159. Elobeid T, Ganji V, Al-Saeedi S, Mohamed AA, Dahir HM, Hassan H, et al. Pesticide residues in foods and water in Qatar and their impact on food exposure risk assessment. *Br Food J*. 2021;123:4082-96. doi: 10.1108/BFJ-01-2021-0040.
160. Lozowicka B, Kaczynski P, Paritova AE, Kuzembekova GB, Abzhalieva AB, Sarsembayeva NB, et al. Pesticide residues in grain from Kazakhstan and potential health risks associated with exposure to detected pesticides. *Food Chem Toxicol*. 2014;64:238-48. doi: 10.1016/j.fct.2013.11.038.
161. Krueve A, Künnapas A, Herodes K, Leito I. Matrix effects in pesticide multi-residue analysis by liquid chromatography-mass spectrometry. *J Chromatogr A*. 2008;1187(1-2):58-66. doi: 10.1016/j.chroma.2008.01.077.
162. Zhang K, Wong JW, Yang P, Tech K, Dibenedetto AL, Lee NS, et al. Multiresidue pesticide analysis of agricultural commodities using acetonitrile salt-out extraction, dispersive solid-phase sample clean-up, and high-performance liquid chromatography-tandem mass spectrometry. *J Agric Food Chem*. 2011;59(14):7636-46. doi: 10.1021/jf2010723.
163. Taverniers I, De Loose M, Van Bockstaele E. Trends in quality in the analytical laboratory. II. Analytical method validation and quality assurance. *TrAC Trends Anal Chem*. 2004;23:535-52. doi: 10.1016/j.trac.2004.04.001.
164. Basham V, Hancock T, McKendrick J, Tessarolo N, Wicking C. Detailed chemical analysis of a fully formulated oil using dielectric barrier discharge

- ionisation–mass spectrometry. *Rapid Commun Mass Spectrom.* 2022;36(14):e9320. doi: 10.1002/rcm.9320.
165. Hecht ES, Scigelova M, Eliuk S, Makarov A. Fundamentals and Advances of Orbitrap Mass Spectrometry. In: Meyers RA, editor. *Encyclopedia of Analytical Chemistry*. 2024. doi: 10.1002/9780470027318.a9309.pub2.
166. Shimadzu. Introduction to LC-MS Part 6. 2014. Available from: <http://www.shimadzu.com/an/lcms/support/intro/lib/lctalk/61/61intro.html>. Accessed 26 Mar 2014.
167. Weber M, Wolf JC, Haisch C. Gas Chromatography–Atmospheric Pressure Inlet–Mass Spectrometer Utilizing Plasma-Based Soft Ionization for the Analysis of Saturated, Aliphatic Hydrocarbons. *J Am Soc Mass Spectrom.* 2021;32(9):1707-15.